Hybrid Dynamic Modelling of Engine Emissions on Multi-Physics Simulation Platform

A Framework Combining Dynamic and Statistical Modelling to Develop Surrogate Models of System of Internal Combustion Engine for Emission Modelling

Gaurav PANT

Submitted for the degree of

Doctor of Philosophy

Faculty of Engineering and Informatics

University of Bradford

2018

Abstract

Gaurav Pant

Hybrid Dynamic Modelling of Engine Emission on a Multi-Physics Simulation Platform

A Framework Combining Dynamic and Statistical Modelling to Develop Surrogate Models of Systems of Internal combustion Engine for Emission Modelling

Keywords: Engine Modelling, System identification, Internal combustion engine, Dynamic modelling, Neural-Network models, Local model networks, LOLIMOT, Emissions Modelling

The data-driven models used for the design of powertrain controllers are typically based on the data obtained from steady-state experiments. However, they are only valid under stable conditions and do not provide any information on the dynamic behaviour of the system. In order to capture this behaviour, dynamic modelling techniques are intensively studied to generate alternative solutions for engine mapping and calibration problem, aiming to address the need to increase productivity (reduce development time) and to develop better models for the actual behaviour of the engine under real-world conditions.

In this thesis, a dynamic modelling approach is presented undertaken for the prediction of NOx emissions for a 2.0 litre Diesel engine, based on a coupled pre-validated virtual Diesel engine model (GT- Suite ® 1-D air path model)

and in-cylinder combustion model (CMCL ® Stochastic Reactor Model Engine Suite). In the context of the considered Engine Simulation Framework, GT Suite + Stochastic Reactor Model (SRM), one fundamental problem is to establish a real time stochastic simulation capability. This problem can be addressed by replacing the slow combustion chemistry solver (SRM) with an appropriate NOx surrogate model. The approach taken in this research for the development of this surrogate model was based on a combination of design of dynamic experiments run on the virtual diesel engine model (GT- Suite), with a dynamic model fitted for the parameters required as input to the SRM, with a zonal design of experiments (DoEs), using Optimal Latin Hypercubes (OLH), run on the SRM model. A response surface model was fitted on the predicted NOx from the SRM OLH DoE data. This surrogate NOx model was then used to replace the computationally expensive SRM simulation, enabling real-time simulations of transient drive cycles to be executed.

The performance of the approach was validated on a simulated NEDC drive cycle, against experimental data collected for the engine case study. The capability of methodology to capture the transient trends of the system shows promising results and will be used for the development of global surrogate prediction models for engine-out emissions.

Dedicated to the memory of my sister, Aastha Pant.

Acknowledgement

First of all, I would like to thank my supervisor, Prof. Felician Campean for his excellent guidance, care, and patience. This thesis would not have been possible without his invaluable support. I would like to extend my gratitude to my co-supervisor, Prof. Daniel Neagu, for his creative ideas, technical discussion, and critical review during the research.

I would like to thank Dr Oscar Garcia Afonso, from Jaguar Land Rover Company, for all his assistance and technical input. Also, special thanks to Efe Tunc and Zhihang Chen, from Jaguar Land Rover Company, who reviewed my work periodically and provided their suggestions and engaged in technical discussions.

I would also like to thank Dr Byron Mason, from Loughborough University, who introduced me to the field of research and was a mentor to me since the beginning of my higher education journey. Also, thanks to Aleksandr Korsunovs, who as a colleague and a friend was always willing to help and give his best suggestions. Whenever I was in a doubt, he was always ready to join me to peaks of the UK to clear my head.

Finally, I would like to express my deepest gratitude to my parents and family for their unconditional love and support. They have always believed in me and supported me in all ventures of my life. Special thanks to my wife carmen for her love, support, and constant encouragement. I could only imagine how difficult it must have been for her, but she was always believed in me, even when I struggled to do it myself.

Table of Contents

List of Figures

List of Tables

Nomenclature

Chapter 1

NOx	Nitrous Oxides
HC	Hydrocarbons
CO	Carbon Oxides
ECU	Electronic/Engine Control Unit
MBC	Model-Based Calibration
SS	Steady State
DoE	Design of Experiment
MPES	Multi-Physics Engine Simulation
CFD	Computational Fluid Dynamics
GT	Gamma Technologies

Chapter 2

LH	Latin Hypercube
SDO	Sequential Design for Optimisation
IVS	Input Variable Selection
PCA	Principal Component Analysis
ICA	Independent Component Analysis
LOLIMOT	Local Order Lolimot Tree
PRBS	Pseudo Random Binary Sequence

APRBS	Amplitude Modulated Pseudo Random Binary Sequence
T_h	Hold Time

Chapter 3

1-D	One dimensional
NARX	Nonlinear Autoregressive with Exogenous Input
NARMAX	Nonlinear Autoregressive Moving Average with Exogenous Input
OLS	Orthogonal Least Squares
EA	Evolutionary Algorithms
ASMOD	Additive Spline Modelling
RMSE	Root Mean Square Error
PRESS	Prediction Error Sum of Squares
ANN	Artificial Neural Network
RBF	Radial Basis Function
MLP	Multi-Layer Perceptron
LLNF	Local Linear Neuro Fuzzy
LMN	Local Model Network
LM	Local Model
HILOMOT	Hierarchical Local Model Tree

Chapter 4

NEDC	New European Drive Cycle
NARX	Nonlinear Autoregressive with Exogenous Input
RPM	Revolution Per Minute
N-m	Newton-meter
SRM	Stochastic Reactor Model
CMCL	Computational Modelling Cambridge Ltd.
EGR	Exhaust Gas Recirculation
IVC	Inlet Valve Closing
mf	Mass Fraction
OLH	Optimal Latin Hypercube
MSE	Mean Square Error
NRMSE	Normalised Root Mean Square Error
MB-MV	Model Building-Model Validation
MATLAB MBC	Model-Based Calibration Toolbox
NN	Neural Network

Chapter 5

MAF	Mass Air Flow
FFT	Fast Fourier Transformation

N	Engine Speed
T_q	Torque
P(inl)	Inlet Pressure
T(inl)	Inlet Temperature
SYSID	System Identification Toolbox
MISO	Multiple Input Single Output
r	Correlation Coefficient
GPM	Gaussian Process Model
MSE	Mean Square Error
NRMSE	Normalised Root Mean Square Error
MB-MV	Model Building-Model Validation
MATLAB MBC	Model-Based Calibration Toolbox
NN	Neural Network

Chapter 1 Introduction

1.1 Background

Internal combustion engines have improved over time and transformed from being mechanically controlled using flyweight mechanisms in the 1960s to having 35% electronification and electrification in 2012 (Grondin *et al.*, 2004; Isermann, 2014). Modern engines have gone through technological developments such as variable valve timing, multiple injections, exhaust gas recirculation, and turbocharging. These changes were led by the increasing demands that engines are expected to meet not only to satisfy customer requirements but also to comply with the stringent legislation. These regulations are generally focused on fuel consumption and emissions, such as NOx, HC, CO. As these changes delivered improvement, they also contributed to increment the complexity of the system. The inclusion of emerging technology, more actuators and controls on the engine, increased the calibration requirements for the engine electronic control unit (ECU). This increment in the complexity of mapping and calibration of the internal combustion engine created the need in industry for new and improved methodologies to be able to model and understand the new and better engine.

To overcome this calibration challenge with satisfactory expenditure of cost and time, strategies such as model-based calibration (MBC) or simulation-based calibration (Singh *et al.*, 2007; Röpke, 2009; Kruse *et al.*, 2010) have been widely used as a way to empower calibration engineers to optimise all

the engine control parameters simultaneously. The model-based calibration process is illustrated in Figure 1.1.

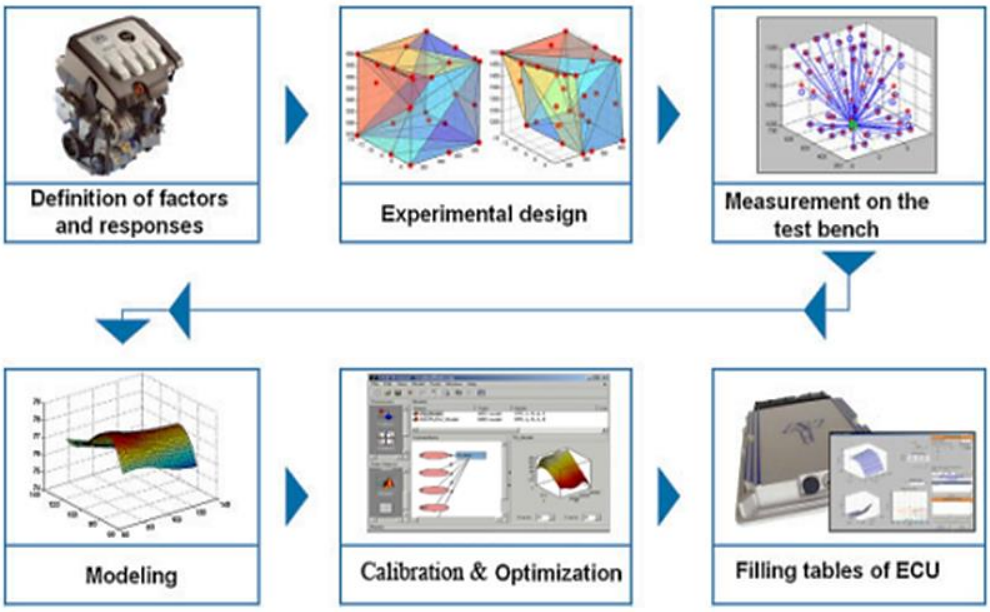

Figure 1.1: Steps of Model-Based Calibration (MBC) (Khan, 2011).

In the MBC process, a substantial amount of time is spent on the engine testing, which could be considered as a starting step, of many operating points required to produce calibration maps (Gautier *et al.*, 2008). To align with the goal of the industry, to optimise trade-off between quality, cost, and time (Atkinson and Mott, 2005; Röpke *et al.*, 2012; Ostrowski *et al.*, 2017), virtual engine simulation frameworks have been proposed in the literature (Neumeister *et al.*, 2007; Gautier *et al.*, 2008; Di Gioia *et al.*, 2012; Korsunovs, 2017). The virtual engine framework replaces engine testing as the basis for mapping and calibration experiments. The incorporation of simulation concept in the engine development process has been illustrated in Figure 1.3, this figure depicts the possibility to reduce cost and time effort by inclusion of the simulation-based model at different stages of engine development, and the

quality aspect of the requirement could be satisfied by adopting high-fidelity models as a choice for system modelling task.

Although this concept is not new, with the availability of new tools it might be possible to apply it to full engine simulation (air path + combustion process) to satisfy the industry needs. However, the primary challenge with the development of virtual simulation framework for the Internal combustion engines is associated with the amount of time required by computationally intensive high-fidelity models (2 or 3-dimensional Computational Fluid Dynamics models) to converge. Thus, making it impossible to run transient drive cycle simulations.

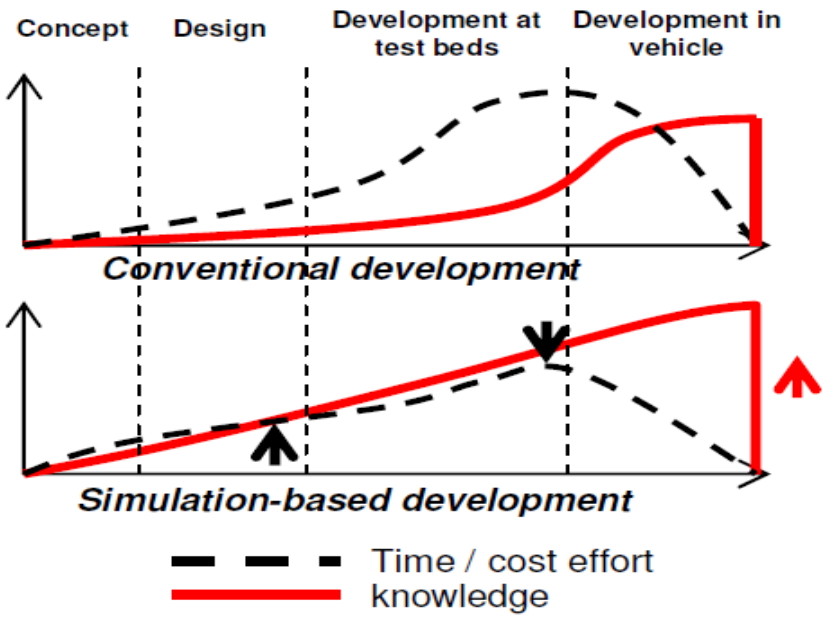

Figure 1.2: Concept of simulation in engine development to reduce cost and save time (Gautier *et al.*, 2008).

A preferable strategy is to replace expensive simulation models with approximation models that are more efficient to run and are referred to as

metamodels or surrogate models. The metamodel or surrogate model is a “model of a model” (Kleijnen, 1987) and metamodeling (technique of developing metamodel) is based on response surface modelling techniques (Box *et al.*, 1978) initially introduced to develop prediction models for expensive physical experimental responses (Simpson *et al.*, 2001).

Metamodeling techniques can be classified into parametric and non-parametric models, where parametric models (such as polynomials (Myers *et al.*, 1989)) are dependent on model structure (Khan, 2011) . On the other hand, non-parametric models such as radial basis function (Morton and Knott, 2002), Neural Network (Hagan *et al.*, 2006) and Kriging models (Sacks *et al.*, 1989), do not require explicit model assumptions and use experimental data to define the functional relationship (Åström and Eykhoff, 1971).

Metamodeling is frequently and increasingly used in various fields as an alternative to expensive simulation models (Jin *et al.*, 2001). (Simpson *et al.*, 1998) have evaluated the performance of Kriging methods against the polynomials for a optimisation problem of aerospike nozzle design based on finite element analysis and CFD simulation codes. (Jin *et al.*, 2001) have proposed a procedure to compare metamodels based on comparing various metamodeling techniques across different problems and concluded radial basis function (RBF) with Gaussian kernels performs the best, among the considered case studies. (Fang *et al.*, 2005) compared RBF and polynomials for crashworthiness application and they found that both techniques perform equally well but RBF outperforms polynomial for smaller sampling sizes. (Seabrook *et al.*, 2003) investigated different metamodeling techniques, RBF

neural networks (NN) and Kriging, for engine calibration experiments and they established that Kriging offered a robust solution in cases where results are affected by experimental noise.

Metamodeling techniques have proven to be effective and efficient approach from both theoretical and practical perspective. They could provide a viable solution to overcome the challenge of prohibitive computational and time cost associated with high-fidelity simulation models and enable real-time (transient drive cycle) simulation of an engine during initial stages of product development. In alignment with this goal, (Korsunovs, 2017) proposed an integrated multi-physics simulation platform.

1.2 Multi-Physics Engine Simulation

This research was conducted as a part of the ongoing collaboration between the University of Bradford and industrial partner, *Jaguar Land Rover*, hereafter referred to as the Sponsor Company. The role of the University of Bradford was to investigate a Multi-Physics Engine Simulation (MPES) platform, to facilitate the development of high-fidelity engine modelling process at the product development stage, in relation to the capability for real-world prediction of engine emissions. The MPES platform combines two primary systems of the compression ignition engine: air path (labelled as 1 in Figure 1.3) and combustion process model (marked as 2 Figure 1.3).

There are detailed models of airpath available, which are based on design geometry (Unver *et al.*, 2016) such as GT Power (Gamma Technologies Inc, 2016) and Wave (Ricardo Plc). Although detailed models provide high fidelity

and are used during engine development phase (Wu *et al.*, 2011), their computation time is slower than real time (Winterbone and Yoshitomi, 1990; Tietze, 2015). Similarly, detailed combustion models, such as three-dimensional Computational Fluid Dynamics (CFD), can provide high fidelity results, but they require high computational effort both in terms of development and simulations. On the other hand, the dynamic data based models presented in literature for emission prediction (Burke *et al.*, 2013; Sakushima *et al.*, 2013; Sequenz, 2013; Cheng *et al.*, 2017) which are extremely fast and robust, rely on engine data for their intensive training requirements and cannot be used during early engine development phase.

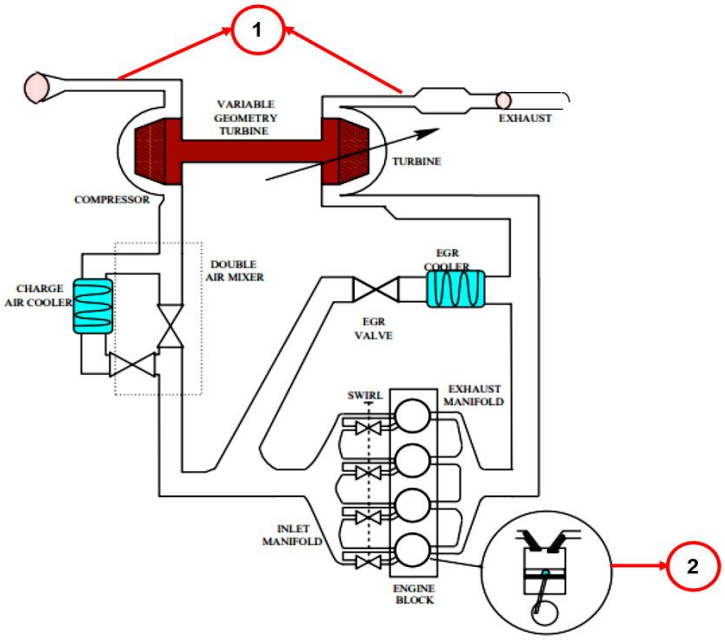

Figure 1.3: Illustration of modern compression ignition engine with two main areas of interest labelled as, 1) air-path, 2) combustion (Ahmed, 2013).

While detailed models of both air path and combustion process are available in the literature, there are only few which combine all of them to present a

complete engine simulation. The studies which do, such as (Unver *et al.*, 2016) and (Smallbone *et al.*, 2011), either do not include complex physical phenomena of combustion process or do not address the transient capability.

The MPES platform utilised here combines mean value model of detailed air path model capable of simulating in real time with the detailed model of the combustion process, developed using probability density function (PDF) based Stochastic reactor thermodynamic model (SRM). The combustion process model developed using combustion chemistry solver package, CMCL SRM (CMCL Innovations, 2016), provides good prediction capabilities with significantly less time for one cycle simulation (Etheridge *et al.*, 2009; Smallbone and Coble, 2011; Parry *et al.*, 2017), when compared to three-dimensional CFD models. However, the SRM model is not fast enough to simulate in real time. To support real-time simulation capability based on MPES, Korsunovs (2017) proposed developing a local surrogate model (using steady-state procedure) for SRM and replacing SRM with the look-up table for real-time simulation (transient drive cycle).

1.3 Research Objectives

This research aims to develop a framework for Hybrid Dynamic Modelling of engine emissions based on the MPES platform. The proposed framework develops surrogate models for two principal components of MPES, air path model and combustion process model, by coupling two distinct metamodeling approaches. The aim can be divided into two main aspects:

- Implementation of dynamic modelling techniques to develop a surrogate model for GT-Suite Diesel engine air path (MPES), aiming for high fidelity air path states models and fast estimation of mean values of air path inputs to combustion process model.
- Applying design of experiments (DoE) strategies to assist in the development of a surrogate model of engine-out emissions (focusing on NOx), based on the SRM model (MPES).

The experimental work to validate the research framework was carried on a 2.0 litre Diesel engine, with the target of modelling nitrous oxide (NOx) emissions in real time.

The specific research objectives defined for this thesis include:

- To explore a strategy for implementing an efficient dynamic experiment in conjunction with non-linear dynamic models on the MPES platform, to obtain accurate and fast estimating surrogate models.
- To demonstrate, for the first time, the application of a developed strategy for the Diesel engine case study.
- To apply established design of experiments approach for the first time, in the context of proposed framework, to develop a surrogate model (model of a model) of engine-out emissions (NOx emissions) based on SRM combustion process model.
- To integrate two metamodeling strategies, dynamic (for GT-Suite air path model) and statistical (for SRM combustion process model) and

demonstrate the application of the developed framework on the Diesel engine case study.

- To compare the developed framework with the steady state approach.

1.4 Research Contribution

The main contributions of the research conducted for this thesis can be summarised as follow:

- Evaluation and implementation of a novel modelling framework, hybrid dynamic modelling framework, which integrates dynamic modelling and a global exploration-based DoE. It was demonstrated that the proposed framework was both effective and efficient for developing engine emissions model with transient drive-cycle simulation capability.

- Implementation of dynamic modelling techniques on virtual engine framework (MPES), to reduce the simulation time associated with running GT-Suite Diesel engine model to provide mean value estimates for inputs to the combustion process model and at the same time being able to accurately predict the transient behaviour of the system. This includes, for the first time, design and implementation of a co-modelling strategy to select an appropriate signal and modelling technique combination for the system modelling task.

- Contribution to the field of emission modelling, in particular to NOx emission modelling, with development of surrogate model (model of a model) of NOx emission capable of predicting transient drive cycle

behaviour during early stages of development. This includes, for the first time, exploring emission modelling by integrating combination of the dynamic modelling deployed on the real-time GT airpath model with the statistical models fitted on data collected by running global exploration based optimal Latin hypercube (OLH) DoE test runs on the PDF-based stochastic reactor thermodynamic models (known to have high prediction capability with fast response time).

1.5 Thesis Outline

The thesis commences by analysing the design of experiments (DoEs) approach for both steady state engine model-based calibration process and dynamic calibration in Chapter 2. This chapter is presented in two main categories: Design of Experiments and Design OF Dynamic Experiments.

Chapter 3 reviews the existing methods for identification of dynamic systems, including broad discussion on the process of modelling dynamic systems and the sound evaluation of current modelling techniques used for generating dynamic models, such as Neural Networks, Local Order Linear Model Tree, and Volterra series.

Chapter 4 presents the research methodology planned to accomplish the research objectives. This chapter also provides the details of the engine case study, and the commercial software packages used for this research.

Chapter 5 presents a novel application of dynamic modelling approach implemented on Multi-Physics Engine Simulation (MPES) platform, to reduce the cost associated with testbed operation and to allow faster basic calibration

during the engine development phase while achieving the target accuracy. The developed strategy presents the method for selection of an efficient dynamic experiment and modelling technique based on statistical and trend analysis criterion. Thereafter, the developed strategy is applied for a Diesel engine case study, to fit the appropriate models to identify the dynamic air path model the engine responses of interest.

Chapter 6 utilises the dynamic models generated in chapter 5 to provide inputs to the combustion model and describe the application of developed hybrid dynamic modelling to create surrogate combustion model capable of predicting engine emissions in real time. The developed approach is further validated by evaluating its performance on legislative transient drive cycle. After that, the performance of the developed framework is compared with the steady-state approach.

Finally, Chapter 7 and 8 summarises the presented methods and the findings, discusses the conclusions, original research contributions, and provides an outlook for future work.

An outlook of how to read this thesis is given in Figure 1.4.

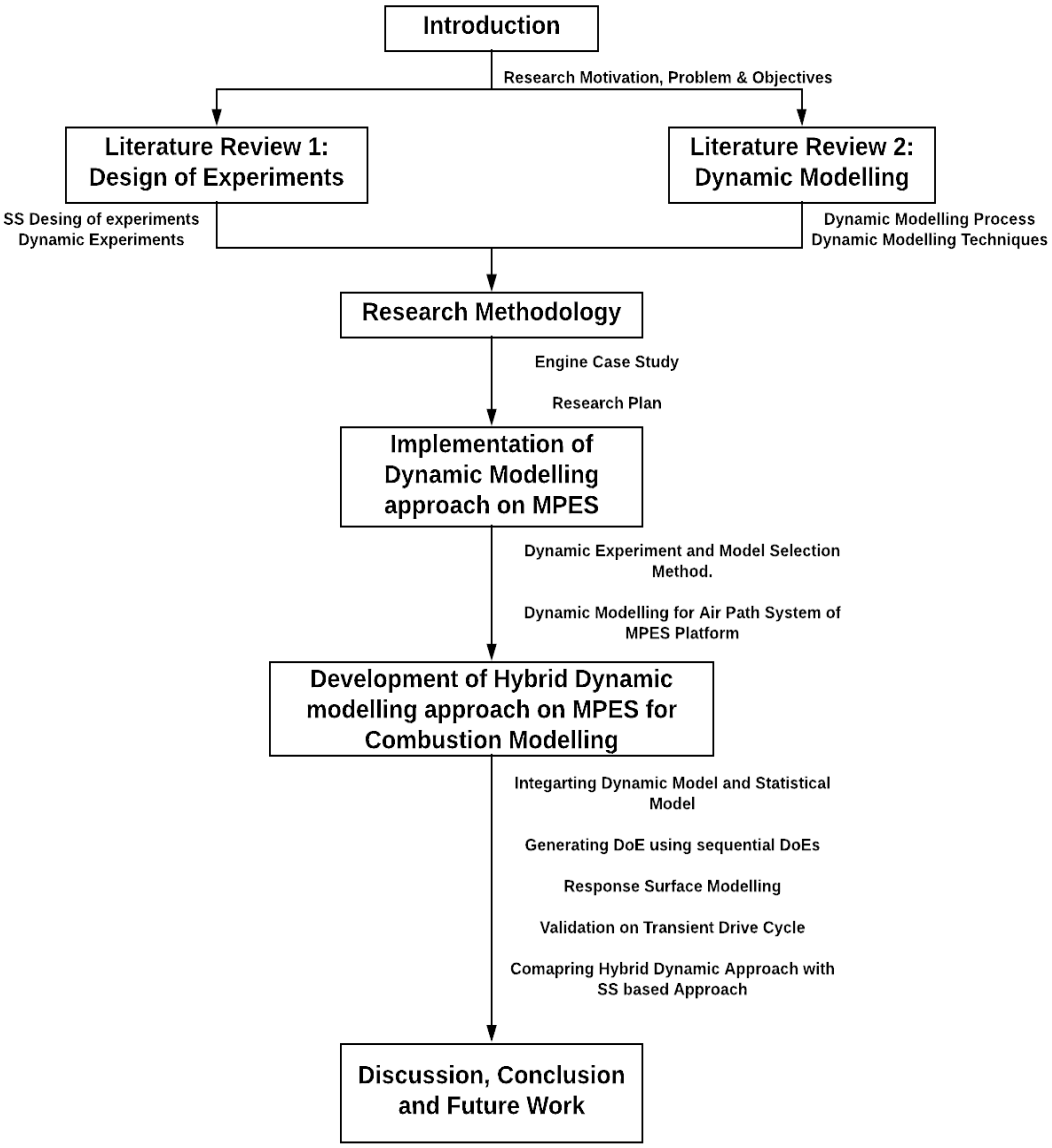

Figure 1.4: Flow chart illustrating the presentation of the thesis.

Chapter 2 Review of Design of Experiments

In this chapter, a broad survey of literature is carried out on the existing design of experiments strategies with a focus on the dynamic design of experiments. This overview is presented in the following sections:

- Section 2.1 describes the design of experiments for steady-state applications
- Section 2.2 introduces the dynamic design of experiments and compares the commonly used excitation signals
- Section 2.3 Summary

2.1 Design of Experiment (DoE)

This section presents the traditional Design of Experiment (DoE) methods available in the literature. The primary purpose of DoE methods is to collect maximum possible information with least measurement effort (Kruse *et al.*, 2010). This is achieved by determining a set of minimum test points which are used to extract enough information to describe the behaviour of response over whole operating space (Gorissen *et al.*, 2007). The application of DoE techniques has become a common practice in the automotive industry, regarding engine development, and have become an essential tool for engineers for little more than a decade (Khan, 2011). The application of DoE methods has allowed enhancement of the steady-state testing effectiveness (Röpke, 2009), as they enable modelling of engine response with enough fidelity and accuracy to support engine calibration process.

The adaptation of DoE approaches in the automotive industry was quite late, when compared with the fact that DoE was initially introduced in the 1920s for agricultural experiments by Sir Ronald A. Fischer (Yates, 1964). Since the introduction in the early 1920s, there have been many other subsequent DoE developments. The main reason behind the interest and popularity of DoE techniques in the automotive industry as stated in (Kianifar, 2014) are the development of response surface methodology by Box and Wilson (Box and Wilson, 1951), and further development of advanced statistical DoE techniques such as work of Taguchi (Charteris, 1992).

There are numerous DoE approaches available in literature and the most commonly used methods in automotive industry for steady state engine mapping experiments include Optimal DoEs (e.g. D-Optimal and V-Optimal) and space-filling DoEs (McKay *et al.*, 1979; Sacks *et al.*, 1989; Cary, 2003; Seabrook *et al.*, 2003; Grove *et al.*, 2004). The existing DoE approaches in literature have been categorised in two main categories in (Kianifar, 2014) and are presented below:

- **Single level DoE strategies**: in this category of DoE methods all DoE test points are collected in a single attempt. These strategies can be further classified into three subcategories:
  - Classical designs
  - Optimal designs
  - Space-filling designs

- **Sequential DoE strategies**: they are also known as adaptive DoEs, and in this category, DoE test points are collected iteratively. Sequential DoE strategies can be further divided into two main categories:

  - Optimal sequential designs
  - Evolutionary sequential designs

In the proceeding subsections of this section, a brief overview of these strategies will be presented.

2.1.1 Single Level DoE Strategies: Classical Design of Experiments

Classical designs are thoroughly investigated for simple regions, e.g. hypercube, and are generally chosen for responses which can be defined by low order polynomials (Kianifar, 2014). The focal point of these designs is the planning of experiments to minimise the influence of random errors present in physical experiments on the acceptance of the model hypothesis (Khan, 2011).

- **Full Factorial Design:** These are one of the primary DoE methods and full factorial designs based on polynomial models were widely used for engine testing (Grove and Davis, 1992). In this design, all level-combinations of the variables are equally important (Montgomery *et al.*, 2001). The number of required test points for this design depends on a number of variables (n) and levels (k); and is defined by a function $\mathbf{(k)^n}$ (Guerrier and Cawsey, 2004). Some examples of full factorial DoE and variation in number of test points with number of variables are presented in Figure 2.1.

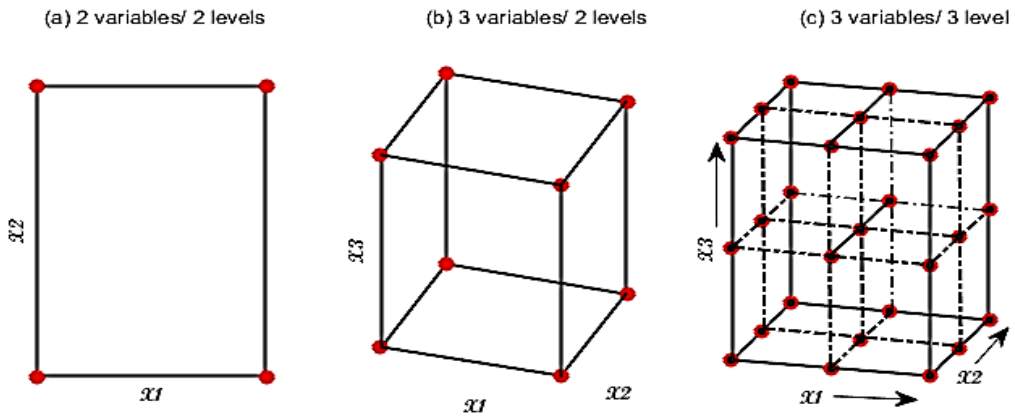

Figure 2.1: Examples of Full Factorial Design

- **Fractional Factorial Design:** These designs are a subset of full factorial design. These designs can reduce the number of tests required, given prior knowledge is available regarding the necessary combinations of variables and insignificance of higher order interactions (Montgomery *et al.*, 2001; Yin, 2012). Two of the broadly used fractional factorials design in automotive industry (Kianifar, 2014), are central composite designs (CCD) and Box-Behnken designs (BBD). (Dimopoulos *et al.*, 1999) used the CCD design of experiments approach for optimising fuel consumption and emissions, leading to reduced number of test points in comparison with full-factorial design (for certain cases- models with pilot injection). An illustration of both central composite designs and Box-Behnken designs is depicted in Figure 2.2.

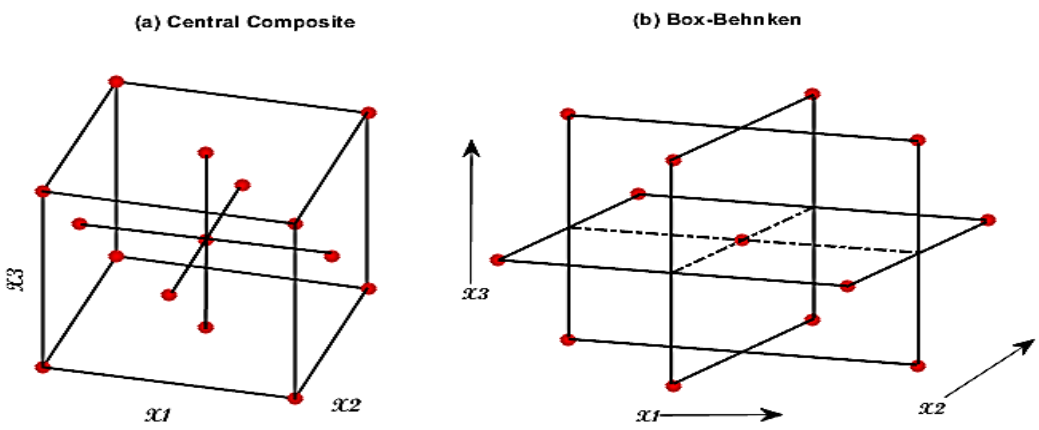

Figure 2.2: An example of fractional designs for 3 Variables / 3 levels

In summary, classical DoE methods perform extremely well for simple problems, i.e. a small number of variables and levels. However, they have some drawbacks:

- For full factorial design as per relation stated in (Guerrier and Cawsey, 2004), as the number of variables and variables levels increases, the number of design points for complete experimental domain increases exponentially (Forrester *et al.*, 2008; Yin, 2012).

- The fractional factorial design does provide the solution for the full factorial design drawback by neglecting the insignificant higher interactions but requires prior knowledge regarding response surface (Grove and Davis, 1992; Yin, 2012). However, in engine mapping process availability of prior knowledge is limited.

- Classical designs cannot be implemented for variables with asymmetric boundary limits (Guerrier and Cawsey, 2004).

Considering these drawbacks classical DoE methods might not be adequate for complicated design space, such as engine applications (Cary, 2003).

2.1.2 Single Level DoE Strategies: Optimal Design of Experiments

In most of the criterion for the optimal design of experiments, optimality of design is associated with the mathematical model of the process (Alvarez, 2000; Kianifar, 2014). The implementation of optimal designs in the automotive industry can be found in (Steidten *et al.*, 2005; Chang *et al.*, 2007; Singh *et al.*, 2007) and many other examples are available in the literature.

In (Alvarez, 2000), the author defines the objective of optimal design is to select the best set of points from a larger set of candidate points to achieve an adequate level of response. The mathematical form of optimal criteria is expressed in (Kianifar, 2014) and (Yin, 2012) as:

$$\mathrm{Y} = \mathrm{X} * \mathrm{B} + \mathrm{e} \qquad \text{Equation 2.1}$$

Where Y is the vector of observation, e is a vector of errors, X is the matrix of design variable at DoE test points, and B is the vector of tuning parameters. B can be estimated using the least-squares method and is presented in (Yin, 2012) as:

$$\mathrm{B} = (\mathrm{X}^{\mathrm{T}} * \mathrm{X})^{-1}\mathrm{X}^{\mathrm{T}}\mathrm{Y} \qquad \text{Equation 2.2}$$

In the equation above, $(X^T * X)^{-1}$ is defined by the inverse of the information matrix and is known as the variance matrix (Atkinson, 1996). There exist different optimal designs in literature and are obtained by optimising some

variable quantity of Equation 2.2. An example of optimal DoE design is illustrated in Figure 2.3 and some of the commonly implemented optimal designs with their optimality criterion are summarised in Figure 2.4.

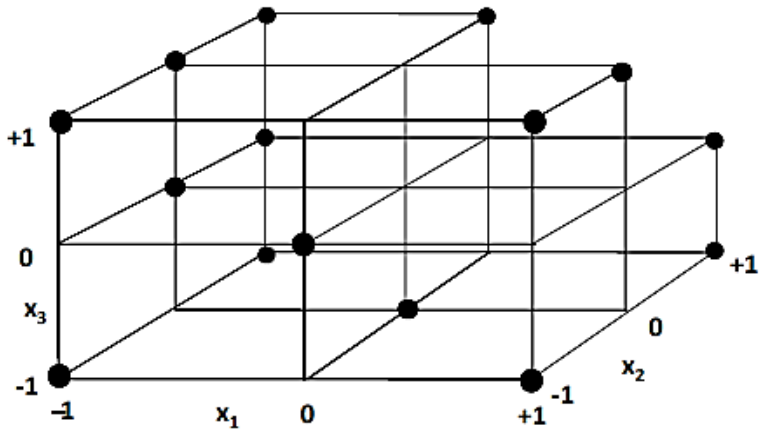

Figure 2.3: D-Optimal design for 3 variables with 3 levels.

Optimal Design	Optimisation Criteria	Statistical Meaning	Advantages
A-Optimal	Maximising trace of the IM	Minimising the average variance of the estimates of the regression coefficients	(Marseille *et al.*, 1994) chose A-optimum sampling pattern and obtained a 30% reduction in scan time for magnetic resonance imaging (MRI)
D-Optimal	Maximising the determinant of the IM	Minimising the covariance of the parameter estimates	(Chang *et al.*, 2007) applied online D-optimal design for minimising emission deviation due to injectors.
G-Optimal	Minimising the maximum entry in the diagonal of hat matrix or $X(\mathrm{X}^{\mathrm{T}} * \mathrm{X})^{-1}\mathrm{X}^{\mathrm{T}}$	Minimising the maximum variance of the predicted values	(Deese *et al.*, 2017) implemented G-optimal design for optimisation of system and controller design of airborne wind turbine which lead to 99% reduction in the system design space.
V-Optimal	Minimising the average of diagonal entries of hat matrix	Minimising the average prediction variance over the design points	(Singh *et al.*, 2007) used V-Optimal design for optimisation of camshaft control and reported fuel consumptions improvement varying from 7.3 % to 2.5 %

Figure 2.4: Optimal designs with their respective optimality criterion.

Optimal design method offers several advantages over classical design such as they require a smaller number of experimental runs(Atkinson, 1996), and the possibility to use an irregular shape (Yin, 2012) or constrained design space (Atkinson *et al.*, 2007). However, they do have their disadvantages, and their efficiency can be affected for complex designs (Seabrook *et al.*, 2003; Grove *et al.*, 2004). Optimal designs require prior knowledge of both model type and number of test points, which can make them infeasible for problems where these are unknown.

2.1.3 Single Level DoE Strategies: Space-Filling Design of Experiments

Space-filling designs aim to uniformly distribute data points in the design space to be measured (Bates *et al.*, 2003, 2004; Toropov *et al.*, 2005; Yin, 2012; Kianifar, 2014). Space-filling designs do not require prior knowledge of system behaviour (Bates *et al.*, 2003; Toropov *et al.*, 2005; Yin, 2012) and as of which they have been an attractive option for steady state engine mapping problems.

There have been many variations of space filling design methods introduced in the literature such as Uniform design, Minimum Potential, and Latin Hypercube. However, among them, Latin Hypercube (LH) design introduced by (McKay *et al.*, 1979) has been used quite frequently in steady state engine mapping area (Cary, 2003; Seabrook *et al.*, 2003; Grove *et al.*, 2004). One of the variations of the LH design method is Optimal Latin Hypercube (OLH), which is an alternative idea to improve LH design. The idea is based on using some optimality criteria for the generation of LH design (Khan, 2011), to

optimise the uniformity of distribution of a set of test points (Yin, 2012). There are several optimality criterion proposed in literature to generate an OLH design such as Manhattan (Ye *et al.*, 2000; Van-Dam *et al.*, 2007), Maximin (Johnson *et al.*, 1990; Ye *et al.*, 2000; Van-Dam *et al.*, 2007; Joseph *et al.*, 2008), and Audze Eglais (Narayanan *et al.*, 2007).

Space-filling designs offer advantages over both classical and optimal designs such as they are more flexible (Kianifar, 2014), removing the infeasible test points does not degrade the entire design (Stinstra *et al.*, 2003), and allows the use of advanced modelling techniques (Kianifar, 2014). Palmer (cited in (Simpson *et al.*, 2001)) and Simpson (Simpson *et al.*, 1998) recommended the use of these designs at early stages of modelling when prior knowledge of model type is not available. An example of space-filling Latin hypercube is depicted in Figure 2.5.

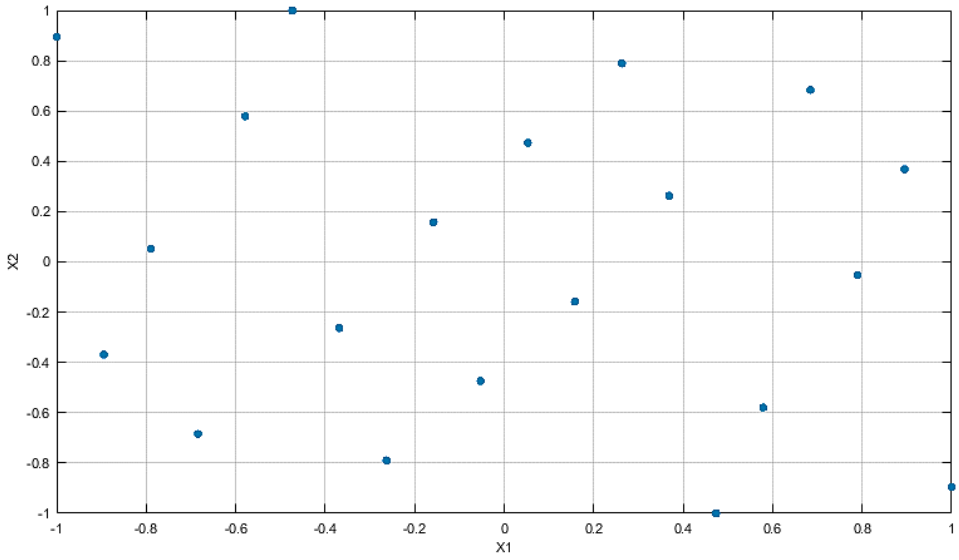

Figure 2.5: An example of Space-filling strategy with 2 variable/ 20 points.

There are several other advantages which vary with the choice of design. Along with the advantages, there are also disadvantages associated with choices of design such as the major drawback of LH design either optimised or non-optimised is the incapability of accurately predicting the response outside the region where data is collected, resulting in high prediction error values at the boundaries of design space (Guerrier and Cawsey, 2004).

2.1.4 Summary of Single level DoEs

Single level DoE strategies allow collection of required data at one time in advance to response model fitting stage. However, this not always desired or the best course of action, especially when prior knowledge of system behaviour is unavailable (Hartmann and Nelles, 2013). Implementation of single-level DoE strategies for unknown system increases the risk of either over-sampling or under-sampling, which will either result in loss of time and efforts by a collection of unnecessary tests than required or inadequate model accuracy due to lack of enough information (Kianifar, 2014).

These shortcomings of single-level DoEs were addressed by the development of adaptive DoEs (Lehmensiek *et al.*, 2002) or sequential DoEs. The idea behind sequential DoE is an iterative augmentation of initial smaller DoE with additional test points until desired model quality is achieved (Crombecq *et al.*, 2009). In consideration, this approach could reduce the number of test points while still delivering adequate models and have been reviewed in the next section.

2.1.5 Sequential DoE Strategies: Optimal Sequential design

In section 2.1, sequential DoE strategies were sub-categorised in two main categories, Optimal and Evolutionary sequential design. The first category optimal sequential design is presented here, and the other follows this section.

In optimal sequential design, knowledge of model type and its parameters are known in advance (Kianifar, 2014). In this category, algorithms aim to locate an optimum by utilising properties of a known metamodel for allocation of design points close to an estimated optimum (Aute, 2009). An example of such is cited in (Kianifar, 2014) which states that D-optimal designs aim to minimise the covariance of the model parameters estimates.

A few examples methods which adopt the use of estimation of optima includes Sequential Design for Optimisation (SDO) by Cox and John (Cox and John, 1997), the method by Sasena *et al.* (2000, 2002).

As the allocation of sample points is based on prior knowledge of the response model and if the pre-selected model type is not suitable for the response, the DoE plan will not be efficient. Hence, improvement in model accuracy with additional iterations is not certain.

The optimal sequential design discussed here required knowledge of model type in advance and given that it might not be a possibility for many engineering problems, a sequential design which does not require prior knowledge such as model type, a number of sample points or system behaviour would be beneficial. An evolutionary sequential design, which is presented in next section, does not require such information and utilises the

information from previous iterations to guide the allocation of new test points (Crombecq *et al.*, 2009).

2.1.6 Sequential DoE Strategies: Evolutionary Sequential design

Evolutionary sequential design or also referred as generic sequential design in [39], have a major advantage over optimal sequential design strategies when little knowledge is available regarding the model type or black box setting (Crombecq *et al.*, 2009). Evolutionary sequential designs can be further classified into two sub-categories, Exploration-based sequential design and exploitation-based sequential design.

- **Exploration-based sequential design**: These designs as described by (Provost *et al.*, 1999; Kianifar, 2014), Gherke et al. (1999) (cited in (Crombecq *et al.*, 2009)), aim to assign equal importance to all the regions of design space and populate these regions as evenly as possible during each iteration. The even distribution is achieved by defining a density measure, which assigns ranks to the region in a domain based on their sampling density. This method provides an advantage over single-level DoE strategies by ensuring neither too many nor too few samples are generated for same regions of design space, and this is attained by using feedback from previous test point location for generating new test points. These DoEs have the capability to generate evenly distributed points throughout the design space while not being tailored to any specific response model (Crombecq *et al.*, 2009; Kianifar, 2014).

- **Exploitation-based sequential designs**: These DoE methods use an error measure from previous steps to guide the sampling process to the specific areas of design space. The definition of the specific or interesting area depends on the definition of the error measure, some examples of the interesting area are highly non-linear areas (Crombecq *et al.*, 2009), areas with discontinuous system behaviour, or areas containing optima (Kianifar, 2014). The examples of exploitation-based sequence methods can be found in (Geest *et al.*, 1999; Couckuyt *et al.*, 2009), Glassner (1995) (cited in(Crombecq *et al.*, 2009)). The major drawback of these designs is the tendency to over-focus on specific locations, which could result in under-sampling of other areas of design space.

2.1.7 Summary of Sequential DoEs

As it has been described above, sequential DoE strategies provide certain advantages over single-level DoE strategies such as reduced number of sample points, in case of evolutionary sequential design methods generation of sample points in design space without prior knowledge of system behaviour.

In regard to optimal sequential design methods, these methods can be highly efficient given the model it has been developed for is suitable for the system response behaviour. However, this might not be possible in every case as prior knowledge of system behaviour is not always available. In contrast to optimal sequential designs, evolutionary sequential designs do not require prior knowledge of the system response behaviour and sampling points are

allocated based on information acquired from previous iterations either via density measure or error measure.

The evolutionary sequential design methods were categorised into two methods exploration and exploitation-based design. In (Crombecq *et al.*, 2011), the trade-off between exploration and exploitation for the augmentation design of evolutionary sequential DoE methods has been suggested. The argument proposed in (Kianifar, 2014) states that if the exploration-based algorithm is used solely for augmentation design, the sampling points are allocated evenly through design space regardless of the nonlinearity present in the design space. On the other hand, exploitation-based algorithm focuses solely on the nonlinearity in one area while neglecting the other areas (where different nonlinearity could also be present) of the design space. This would result in inefficient DoE plan, so (Kianifar, 2014) and (Crombecq *et al.*, 2009) stated that sequential experimental design should consider exploration to a certain degree.

There has been extensive work carried out in the field of sequential DoEs such as hybrid sequential DoE by (Crombecq *et al.*, 2009), OLH based sequential DoE by (Kianifar *et al.*, 2013), and sequential methods using low-discrepancy strategy (Rafajłowicz and Schwabe, 2006; Lam, 2008).

2.2 Design of Dynamic Experiments

The design of experiment methods described in the preceding section have been widely recognised and been successfully implemented for steady state model-based calibration (Cary, 2003; Grove *et al.*, 2004; Guerrier and

Cawsey, 2004; Lumsden *et al.*, 2004; Schlosser *et al.*, 2006; Brahma *et al.*, 2008; Khan, 2011; Kianifar, 2014). In these DoE methods, the test plan is designed for the design space in which input variables are varied over their expected range to estimate the system behaviour in a statistically sound way. However, the input variables in these methods are not time-dependent (Georgakis, 2013). Also, in (Brahma *et al.*, 2009; Brahma and Chi, 2012a, 2012b) researchers found that the practices of the steady-state process do not transfer to dynamic process.

Design of Dynamic experiments or dynamic design of experiments (dynamic DoE) can be categorised into two sub-categories (Deflorian and Klöpper, 2009):

- **Model-Based Approaches**: This category of dynamic experiments design requires prior knowledge of model structure (Deflorian and Zaglauer, 2011). In these approaches, measurement effort is reduced, if statistical criterions such as D-optimal are used to define an optimal dynamic DoE plan (Deflorian and Zaglauer, 2011; Tietze, 2015). Fedorov (1972) and Fedorov & Hackl (1997) have been cited in (Tietze, 2015) as a source which provided a detailed description of mathematical introductions for these approaches.

- **Model-Free Approaches**: In model free DoE, prior knowledge of model structure is not necessary, the aim is to distribute the design points throughout the input space as uniformly as possible (Deflorian and Zaglauer, 2011). This leads to space filing design, which provides even coverage of input space by maximising the minimal distance between design points

(Hametner *et al.*, 2013; Tietze, 2015). In this thesis, these approaches have been implemented due to lack of prior knowledge.

The main task of dynamic DoE is to define the dynamic boundaries in which system can be excited and to design appropriate excitation signals. In the dynamic modelling process, a sequence of time variant excitation signals is employed to generate a test design for modelling system behaviour (Sakushima *et al.*, 2013). Excitation signals also known as dynamic experiments (Burke *et al.*, 2013), influence the process to gather information regarding its behaviour (Nelles, 2001). Thus, the design of excitation signal is crucial in the process of dynamic system identification as it should effectively excite the dynamic behaviour of the system of interest (Fang and Shenton, 2010; Deflorian and Zaglauer, 2011; Fang, 2012; Hametner *et al.*, 2013; Sakushima *et al.*, 2013).

The steps involved in dynamic DoE can be summarised as follow and are discussed in detail in the proceeding sub-sections:

- selection of model inputs
- design of excitation signals

2.2.1 Model Inputs

The first stage in the development of dynamic DoE for the identification of dynamic systems is to determine the relevant model inputs which influence the system of interest (Nelles, 2001; Tietze, 2015). In mechanical processes, the influence of the different variables is clear and relevant inputs are chosen based on prior knowledge of the system (Nelles, 2001). However, in dynamic

processes even though the system inputs are known, they differ in their properties for identification (Tietze, 2015). An overview of automotive system inputs was presented in (Tietze, 2015) and is depicted in Figure 2.6. The automotive system in this figure is categorised into the dynamical system to be identified, the vehicle, the ECU and the environment.

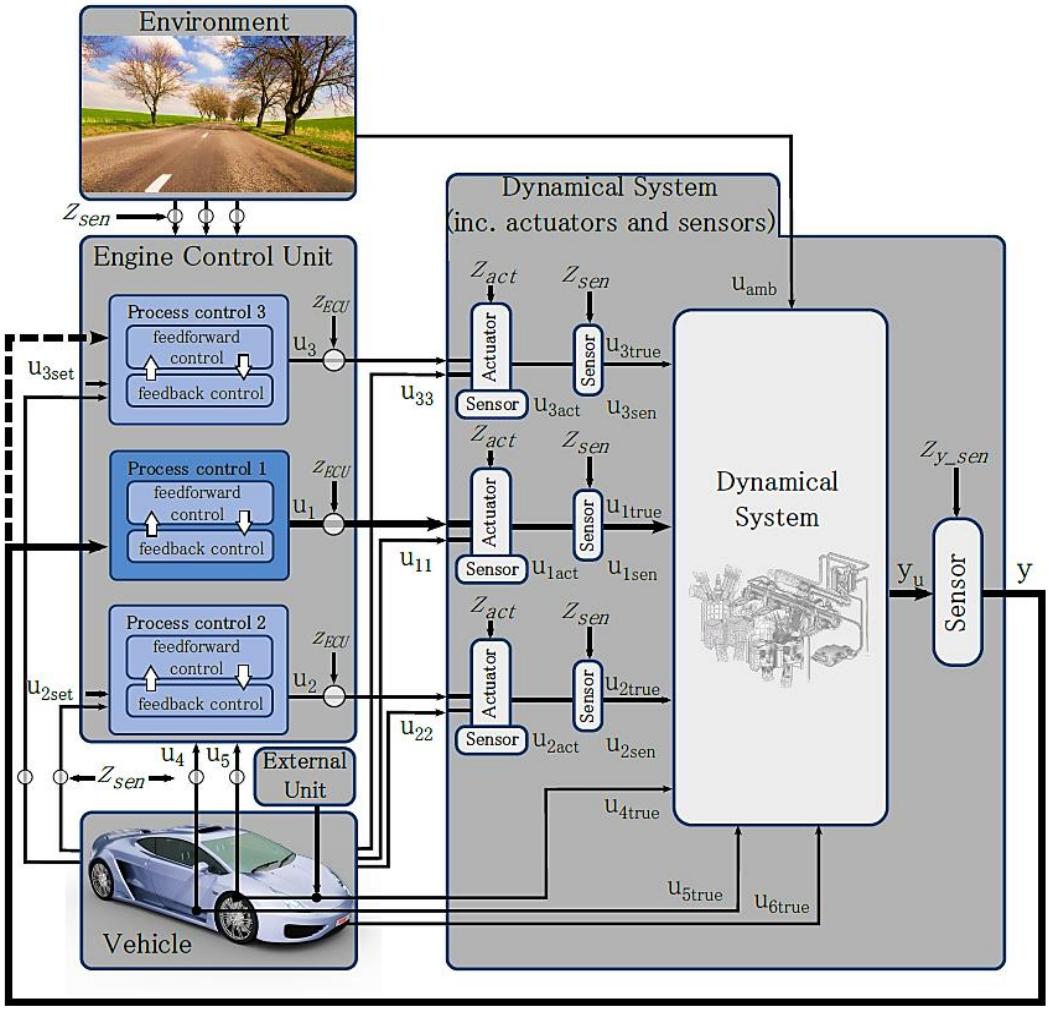

Figure 2.6: Categorised system inputs in an automotive system (Tietze, 2015).

In (Tietze, 2015), author categorised input signals into six categories based on the origin of the signals and properties for identification. These can be

broadly categorised into three sub-categories, ECU actuated inputs, External Inputs, and Environmental inputs.

- **ECU Actuated Inputs**: As the name suggests, they are actuated by ECU and are suitable for identification of dynamic system. These signals can be identified in Figure 2.6 as control signal $\mathbf{u_1}$, $\mathbf{u_2}$ and $\mathbf{u_3}$. Also, the sub-signals such as an actuator, sensor, and true are also included in this category. However, their suitability for the identification of system differs and is presented in detail in (Tietze, 2015).

- **External Inputs**: External signals are the signals which influence the dynamic system but cannot be actuated by ECU. In context to Figure 2.6, these signals are labelled $\mathbf{u_4}$, $\mathbf{u_{4\text{-}true}}$, $\mathbf{u_5}$ *and* $\mathbf{u_{5\text{-}true}}$. As these signals are the not directly actuated by ECU, they need to be actuated via external unit. The actuation can be costly, and thus the effect of the signal on a dynamic system should be analysed to decide whether to use it as real input or disturbance (Tietze, 2015).

- **Environmental Inputs**: These inputs, labelled as $\mathbf{u_{amb}}$ in Figure 2.6, describe the environmental conditions such as ambient temperature, air pressure, and air humidity. In the real world, excitation of such inputs is extremely difficult and are treated as disturbances.

There is another input, depicted as $\mathbf{u_6}$ in Figure 2.6 and cannot be classified in the above categories, as it is neither measured by ECU nor by an external unit. This should be treated as a disturbance unless it strongly affects the

system where it can be transformed into external inputs by installing an additional sensor.

As stated previously, the selection of relevant inputs is the first stage in the process of identification of a dynamic system, and it also is a key step as it influences all the following stages of identification. The number of inputs should be kept to the minimum, as an increase in inputs number exponentially increases the measurement time of excitation signals (Tietze, 2015). Also, with the increasing number of inputs the insight into the influence of variables on system decreases (May *et al.*, 2011). The relevant inputs for stationary problems can be identified using trial and error approach (Nelles, 2001; Tietze, 2015). However, in the context of dynamic modelling a trial and error approach can be difficult to implement, as the number of inputs besides physical inputs further increase depending on the choice of dynamical modelling structure (Nelles, 2001; Tietze, 2015). In dynamic modelling, this extension in input space beside physical input is due to the delayed inputs which are fed into the system. For example, if external dynamic approach is chosen for identification of system of n^{th} order with input ***u (k)*** and output ***y(k)***, the input space, in this case, will be defined as ***u(k-1) ...u (k-n)*** and ***y(k-1) …y(k-n)*** (Nelles, 2001). Although there is only u(k) defined as an input, all the other delayed inputs and outputs follow. An example of the external dynamic structure is illustrated in Figure 2.7.

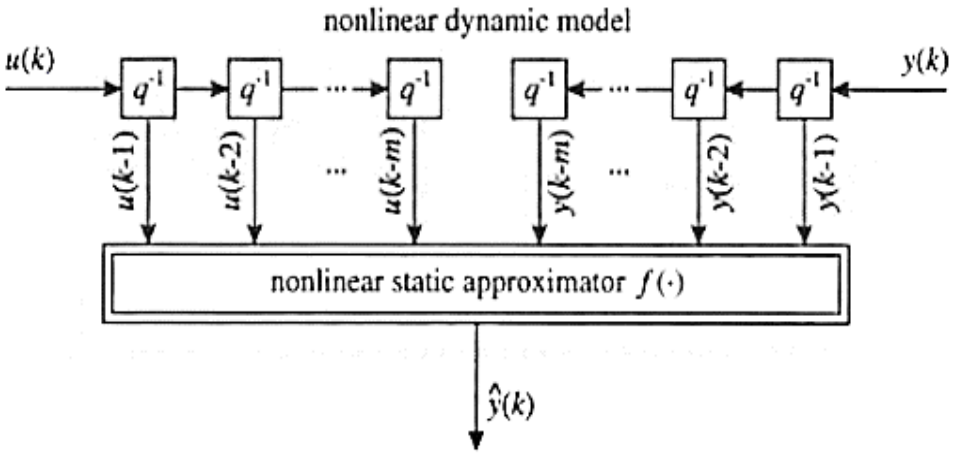

Figure 2.7: External Dynamic Approach (Nelles, 2001).

In (Nelles, 2001) and (May *et al.*, 2011), Input Variable Selection (IVS) strategies have been categorised into four different strategies and are presented below.

a) **Strategy I**: Initial approach could be using all the inputs as relevant inputs; it can be practical if the number of relevant inputs is small. However, if the number is large, this approach will be infeasible as it will require a vast amount of data and longer training times, which will lead to an increase in measurement and identification cost.

b) **Strategy II**: Another approach suggests trying all possible input combinations. Although this approach might lead to the best combination of input, it is practically infeasible as the number of combinations would increase with the increase in the number of relevant inputs.

c) **Strategy III**: In this strategy, inputs are selected using tools such as Principal Component Analysis (PCA), Independent Component Analysis (ICA), or other similar techniques. This approach is also referred to as

unsupervised input selection or dimension reduction strategy. In this strategy, a large number of inputs is reduced by discarding non-relevant inputs with low computational demand (Nelles, 2001) and the mechanism of doing this is explained in (Nelles, 2001), and (May *et al.*, 2011). In this strategy, criteria of relevance become quite important, as in PCA relevance of input is based on the distribution of input data which might lead to the removal of inputs which have a strong effect on system behaviour but lack in data distribution. Also, the combination of inputs and the relationship of the principal component with output is assumed to be linear (May *et al.*, 2011). This will result in the failure to identify any non-linear relationships within the data.

d) Strategy IV: This strategy is also known as supervised input selection (Nelles, 2001) or embedded strategy (May *et al.*, 2011). In this approach, the strategy for identifying inputs are incorporated into the learning algorithm for model identification. In this approach, the criteria for selection of the model input is based on improvement in model accuracy. In case of linear models, this can be achieved by using correlation analysis and for non-linear models, it can be accomplished by employing either evolutionary algorithms or model-specific algorithms (Nelles, 2001; May *et al.*, 2011). There are many model specific algorithms such as Local Order Linear Model Tree (LOLIMOT) (Nelles *et al.*, 1996) for neuro-fuzzy models, pruning or step-wise regression for Neural networks (May *et al.*, 2011). This strategy is extremely powerful but computationally demanding.

The next sub-section dictates the step after selection of relevant inputs, i.e. design of excitation signals.

2.2.2 Excitation Signals

Once the relevant inputs have been selected, the target of dynamic DoE is to excite system to achieve maximum information with every measurement (Deflorian and Zaglauer, 2011). To do so, highly dynamic input excitation is required to cover the operating space with the data (Tietze, 2015). Common excitation signals for dynamic identifications are multi-valued PRBS (pseudo-random binary sequence) (Isermann and Münchhof, 2011; Isermann, 2014), amplitude modulated PRBS (APRBS) (Nelles, 2001; Deflorian and Zaglauer, 2011; Isermann and Münchhof, 2011; Isermann, 2014), and chirps (Baumann *et al.*, 2008, 2009; Deflorian and Klöpper, 2009; Tietze, 2015).

The design of the excitation signal plays a key role in the process of dynamic identification. To excite the dynamic system, regarding multiple-input systems, the excitation signals for relevant individual input must be uncorrelated (Gutjahr, 2012). This allows modelling approach to distinguish the effect of various input on the system behaviour. The correlation between the two signals can be computed using cross-correlation (Tietze, 2015). In addition to this, dynamic experiments should define the dynamic boundaries of the DoE for smooth signal transition and safe excitation. Dynamic boundaries refer to the permitted frequencies and amplitude of the input; these can be evaluated by analysing the excitation signal in the frequency domain (Burke *et al.*, 2013; Tietze, 2015). For this, the signal must be transformed using Discrete Fourier Transformation (Keesman, 2011; Pintelon and Schoukens, 2012), and this can be achieved by using algorithms such as Fast Fourier Transformation (Blahut, 2010; Keesman, 2011).

All of these criterion and some more (Tietze, 2015) can be used to design the suitable excitation signals. The excitation signals can be broadly categorised into three major categories, generic signals, optimised signals, and advanced dedicated signals.

- **Generic Signal**: This category of signals is commonly used for identification of system with no prior knowledge. This kind of signal has a flat power band within the defined frequency boundaries (Ghosh, 2016). The examples of common excitation signal which fall in this category are PRBS, APRBS, Chirp, and white noise.

- **Optimised Signals**: As the name suggests, these signals are generated through an optimisation process. The optimisation can be achieved by optimising many properties of a signal, but the popular choices include minimising crest factor (Tietze, 2015), and optimising input power of spectrum [86]. Phased optimised multi-sine signals and Discrete interval binary sequence belongs to this category of input signals.

- **Advanced Dedicated Signals**: These signals are designed specifically for system behaviour, hence require insight of the system (Ghosh, 2016). The design of an input signal varies from process to process, for example, an ill-conditioned system; inputs are designed with an emphasis on acquiring a balanced response. Another example is illustrated in (Pintelon and Schoukens, 2012), a mechanical system with acceleration where input excitation needs to be designed with controlled system properties like velocity and acceleration. The popular approaches for generation of these types of

signals, as listed in (Ghosh, 2016), are simultaneous minimisation of crest factor at input and output, and simultaneous minimisation of peak values at input and output.

As mentioned earlier, generic signals do not require any prior knowledge of the system for the design of excitation signals and which has made them a common choice for identification of engine systems (Isermann and Muller, 2001; Hafner and Isermann, 2003; Guhmann and Riedel, 2011; Burke *et al.*, 2013; Isermann, 2014). As prior knowledge of system behaviour is scarcely available, only the generic excitation signals commonly used for identification of engine systems will be discussed further.

2.2.3 Comparison of Excitation Signals

The last section briefly introduced the criterion which need to be considered to create suitable excitation signals for dynamic identification and some commonly used excitation signals. In this section, these signals, a pseudo-random binary sequence (PRBS), amplitude modulated PRBS (APRBS), and chirps will be discussed.

I. Pseudo Random Binary Sequence (PRBS)

A common excitation signal and frequently applied is multi-valued PRBS (Nelles, 2001; Deflorian and Zaglauer, 2011; Fang, 2012). It is suitable for identification purposes, as it excites all frequencies uniformly by imitating white noise (Nelles, 2001). This signal can be generated using a set of shift-register circuits, and the length of the signal is determined using the digit of the register (Ljung, 1997). The amplitude of the signal can be defined using

two predetermined levels (maximum and minimum) (Fang, 2012). An example of the PRBS signal is illustrated in Figure 2.8.

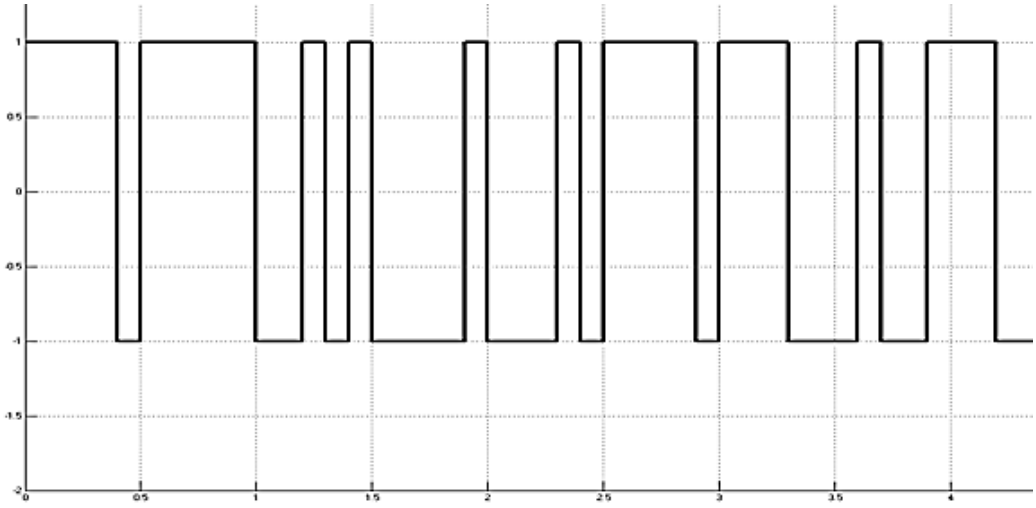

Figure 2.8; A generic pseudo-random binary signal.

The multi-valued PRBS was developed for linear system identification (Nelles, 2001; Deflorian and Zaglauer, 2011), and hence only covers a limited number of amplitude levels. Since, this signal only alternates in between the minimum and maximum value this leads to poor coverage of input space (Nelles, 2001). This makes the signal not suitable for the nonlinear system identification as no information regarding the system behaviour is gathered other than at maximum and minimum points. A case study is presented in (Nelles, 2001), illustrating the drawbacks of this type of signals.

II. Amplitude Modulated Pseudo Random Binary Signal (APRBS)

The amplitude modulated PRBS is a periodic deterministic signal with properties like Gaussian white noise (Tan and Godfrey, 2002). APRBS has been often used in system identification regarding automotive industry applications, Hafner (2003) and Zimmerschied (2005) (cited in (Deflorian and

Zaglauer, 2011)), (Isermann and Muller, 2001; Hafner and Isermann, 2003; Deflorian and Klöpper, 2009). An example of APRBS signals is illustrated in Figure 2.9. APRBS cover a wide amplitude range which is essential for capturing the nonlinearities and this has been depicted in Figure 2.10 (Hafner and Isermann, 2003; Baumann *et al.*, 2008; Deflorian and Zaglauer, 2011; Schmiechen *et al.*, 2013). In (Heinz and Nelles, 2017), it has been illustrated that APRBS shows the best data coverage and step transition between two amplitudes provides high dynamic excitation. Also, APRBS has a combination of both low-frequency component (piecewise constant) and a high-frequency component (step amplitude) which enhances its capability to cover both high and low-frequency areas of input space.

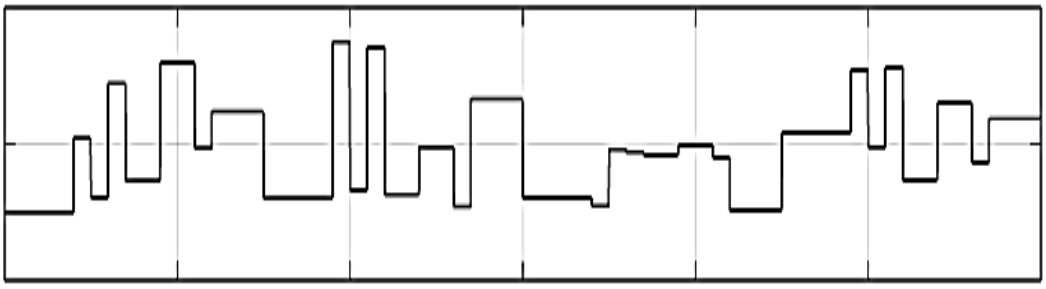

Figure 2.9: An example of the amplitude modulated PRBS (APRBS) signal.

APRBS signals can be defined as the composition of N design points, d_i, which vary in their maximum and minimum amplitude values and have a certain hold time, T_h (Deflorian and Zaglauer, 2011). A pictorial illustration of this concept is present in Figure 2.11.

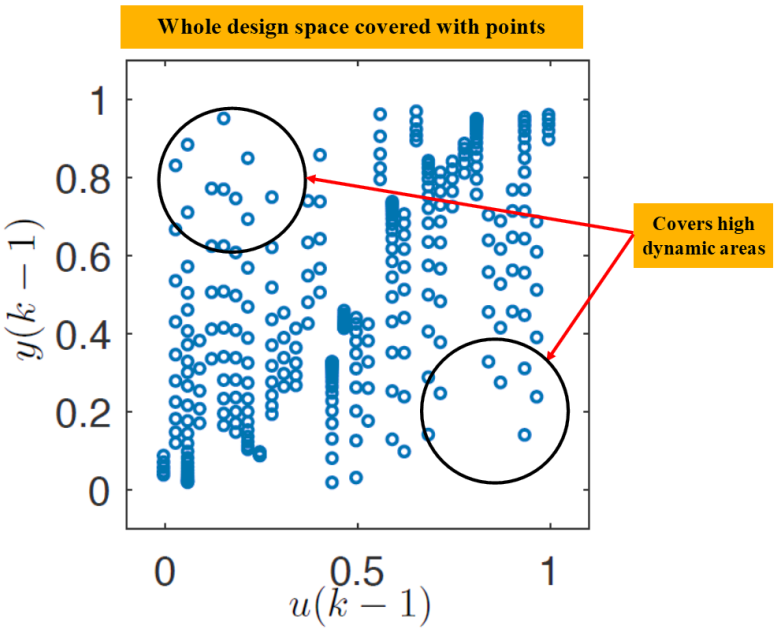

Figure 2.10: Data distribution of APRBS in pseudo input space (Heinz and Nelles, 2017).

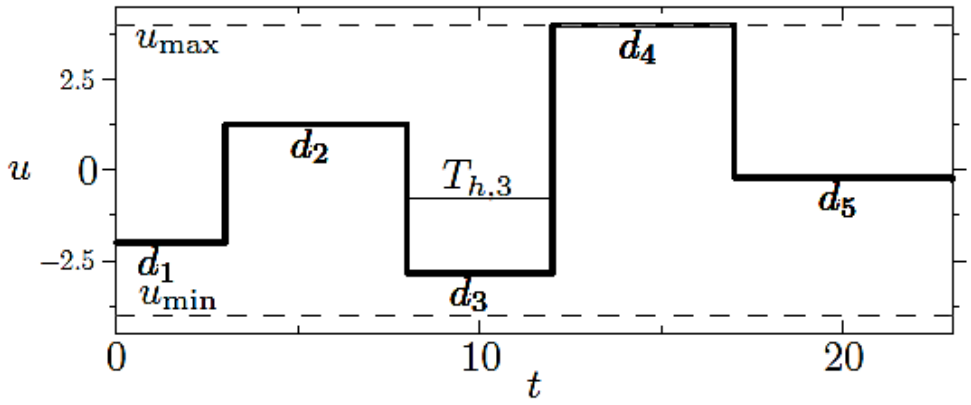

Figure 2.11: A conceptual view of APRBS Design in the time domain (Deflorian and Zaglauer, 2011).

The major drawback of APRBS is in regards of the step excitation, which might lead to unsafe excitation, such as drastic step change from one design point to another (Deflorian and Zaglauer, 2011; Tietze, 2015). However, this drawback can be overcome by the careful selection of steps, such as discrete

steps with fixed step length (Fang, 2012). Another attribute of APRBS which might not be desirable in some application is, decrease in amplitude with increasing frequencies (Tietze, 2015).

III. Chirp Signals

In chirp signals, or also known as swept sine, the frequency either increasing (swept up) or decreasing (swept down) in one measurement period (Tietze, 2015). These signals belong to the category of sinus signals and are slow-varying dynamic signals with less significant step change (Baumann *et al.*, 2008). An example of a chirp signal is presented in Figure 2.12. Chirp signals can be defined as a sinusoidal signal with a time-variant frequency and can be represented as follow:

$$x(t) = A sin(2\pi f t^2) \qquad \text{Equation 2.3}$$

Where f is the frequency component and t being the period.

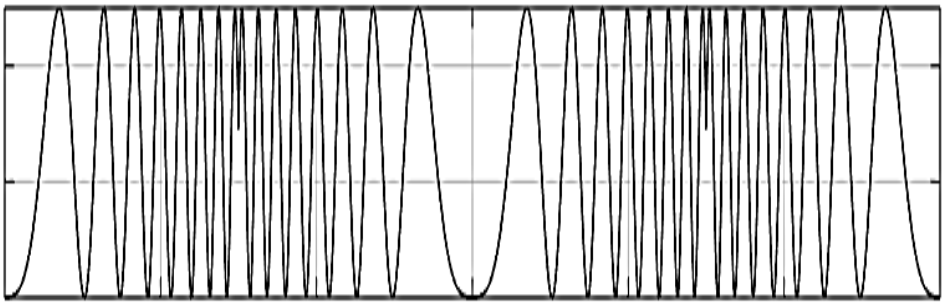

Figure 2.12: Chirp Signal

The advantage of chirp signals over APRBS is a uniform distribution of amplitude over the user selected frequency, and it has been illustrated in (Tietze, 2015). The disadvantage of the chirp signal is the scarce coverage of

the centre of the input space (Heinz and Nelles, 2017) and had been depicted in Figure 2.13. Another main disadvantage of chirp signals is that they require a long measurement time in order to cover the whole input space and this increases with the number of relevant inputs.

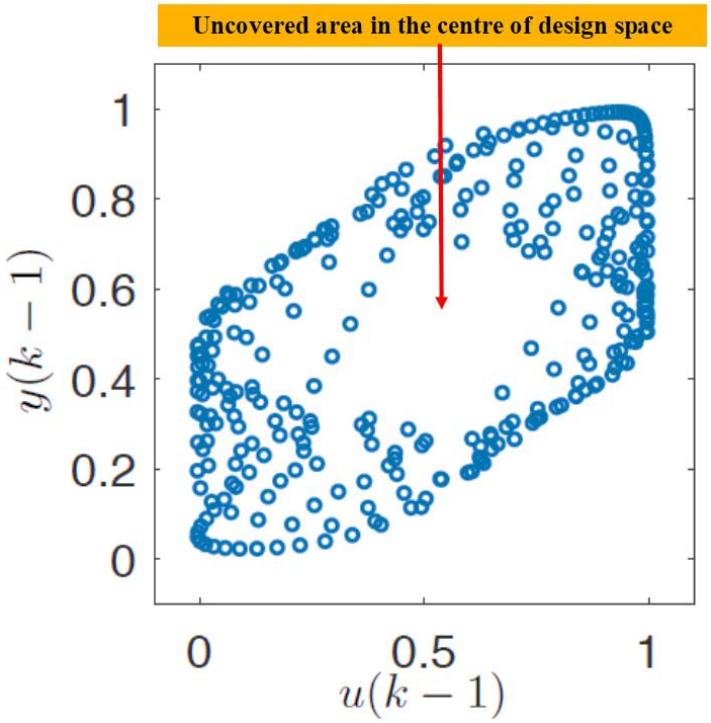

Figure 2.13: Data distribution of chirp signal in pseudo input space (Heinz and Nelles, 2017).

There are other signals available in the literature which have been discussed for identification purpose such as ramps (Nelles, 2001; Deflorian and Zaglauer, 2011; Heinz and Nelles, 2017), and multi sine (Tietze, 2015; Heinz and Nelles, 2017).

2.2.4 Summary of Dynamic DoE

In the section, Dynamic design of experiments, a theoretical analysis of the input selection, design of excitation signals, and comparison of common excitation signal was presented. The advantages and disadvantages of the methods and approaches were presented. The APRBS signals provide good coverage of the input space but suffer the challenge of safe excitation, while chirp provides safe excitation environment but require longer measurement time. In Table 2.1, an overview of some of the applications of the excitation signal along with the respective modelling structure is presented.

Table 2.1: Overview of excitation signals and their applications in literature.

Excitation Signal	Modelling Approach	Application	Reference
Chirps	Volterra series	Engine Emissions	(Burke et al., 2013)
APRBS	LOLIMOT	NOx Emission	(Isermann, 2014)
Chirps	Volterra Series	Exhaust Temperatures	(Baumann et al., 2008)
APRBS	LOLIMOT	NOx Emissions	(Hafner and Isermann, 2003)
APRBS	LOLIMOT	NOx Emissions	(Isermann and Muller, 2001)
Chirps	Volterra series/ MLP/ Hammerstein-wiener Model/ RBF/ NARX Model	Engine Emissions	(Guhmann and Riedel, 2011)
Multi-sine/ Chirp/ Ramps	Gaussian Process Regression	Fuel Supply control system	(Tietze, 2015)

2.3 Summary

In this chapter, Design of Experiments, a review of existing literature on both steady state and dynamic design of experiments were presented. The steady state DoEs are well established and provide an elegant solution for steady state engine mapping. The techniques such as single-level DoE and

sequential DoE strategies were described for steady state DoE. It was found that single level DoE strategies generate test plans with all points in one iteration. This might not be a desirable attribute, if no prior knowledge of system behaviour is available, as it might lead to under-sampling or over-sampling. While sequential DoEs generates test plans in an iterative manner, where initial design can have a small number of points and additional points can be added with each iteration until desired model accuracy is achieved.

It was found that the practices of steady-state processes do not transfer to dynamic processes, so the dynamic design of experiments was introduced. In Dynamic DoE, two approaches were introduced model-based or model-free DoEs. In the model-based DoE, prior knowledge of system response is required to guide the test plan to reach an optimum. However, prior knowledge is seldom available. Thus, a model-free approach would become more suitable. Model-free approaches are similar as space filling designs, which emphasises on the uniform distribution of test point over the input space. Additional aspects related to dynamic design such as selection of relevant inputs, the design of excitation signals, and comparison of commonly used excitation signals was also presented in this chapter. Overall it becomes clear that the dynamic DoE is not a straightforward step and will not lead to perfect system measurement, covering all dynamical system states. Also, due to the lack of prior knowledge regarding the system response, an optimal test plan cannot be implemented. Hence, this raises the need for a flexible modelling approach for handling specific system measurements. These modelling techniques and steps will be discussed in the next chapter.

Chapter 3 Review of Identification methods for Dynamic Nonlinear system

In the preceding chapter, techniques regarding the design of experiments were introduced. These techniques are employed to collect the observations data, and once the data is collected, the next step is to develop a mathematical model which describes the relationship in between inputs and outputs.

In this chapter, first the concept of modelling is introduced, and a brief introduction to the physical modelling and their applications in engine development has been provided. Thereafter, the chapter focuses on the overview of modelling nonlinear dynamic systems and establishes the process involved in the identification of such models. The criterion for selection of an appropriate modelling technique are introduced, and modelling techniques are compared based on these criterions. This review is presented in the following sections:

- Section 3.1: Introduction
- Section 3.2: Modelling of Dynamic Systems
- Section 3.3: Nonlinear Dynamic Model Identification
- Section 3.4: Summary

3.1 Introduction

Modelling has become essential in the automotive industry due to engine technologies being developed and implemented, such as electronic throttle/ active body control / electronic stability control/ Exhaust gas recirculation, to

improve the performance, fuel economy and drivability while meeting increasingly stringent emissions legislation. Although, all these sub-systems provide further flexibility to the engine but at the cost of increasing system complexity (Burke *et al.*, 2013). This has resulted in the increased complexity of powertrain calibration with considerable time and cost implications. To overcome these challenges with the satisfactory expenditure of cost and time, strategies such as model-based calibration (MBC) have been introduced (Röpke, 2009; Kruse *et al.*, 2010).

In model-based calibration, mathematical models are derived either by the phenomenological way (physical / theoretical) or behavioural way (experimental) (Isermann, 2014). A pictorial presentation of a breakdown of theoretical and experimental modelling is presented in Figure 3.1. A model described fully by the physical laws is termed white box, and in contrast, a model described based on experiments or data-driven model is termed black box model (Bekey, 1970; Isermann, 2014). In addition to these approaches, there exists an approach named grey box modelling (Bekey, 1970) which combines theoretical as well as experimental knowledge to model a system and more information can be found in (Guzzella and Amstutz, 1998; Nelles, 2001).

Theoretical models are a valuable tool used by researchers to understand the basic principles and underlying concepts of the engine. A detailed review of physical models can be found in literature in (Heywood, 1998; Chow and Wyszynski, 1999; Grondin *et al.*, 2004; Pezouvanis, 2009) and many others. They have been successfully implemented for simulating engine systems and

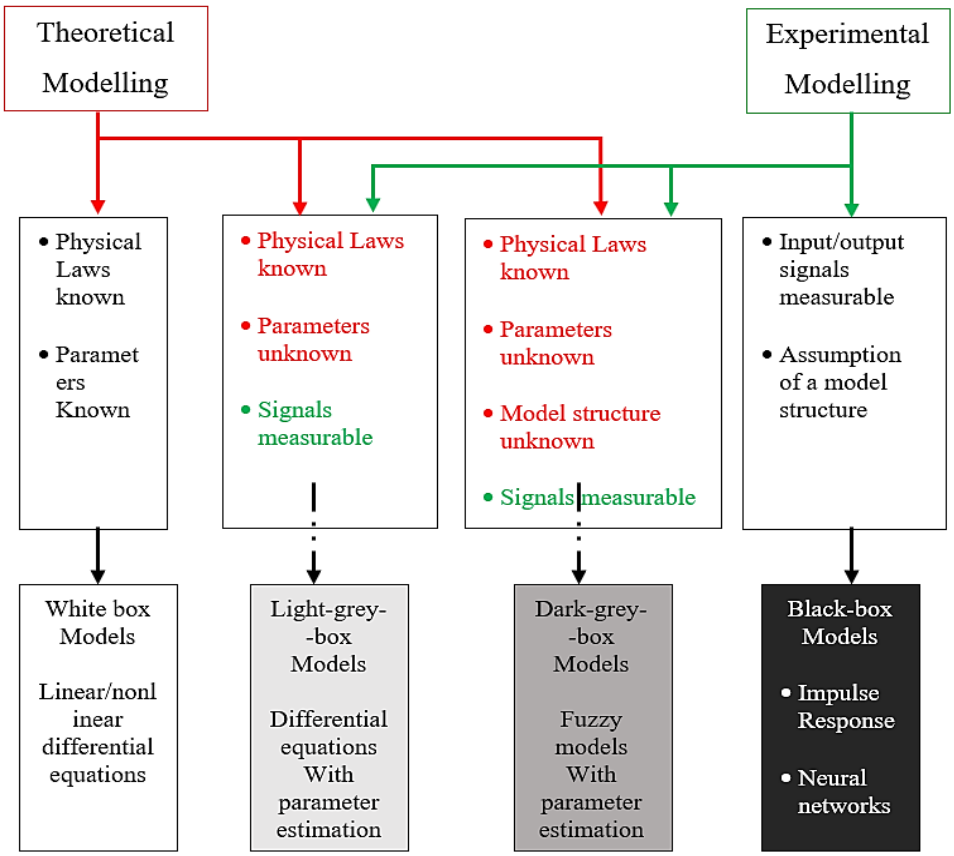

Figure 3.1: Sub-categories of theoretical and experimental modelling (Isermann, 2014).

concepts such as power prediction, fuel consumption, and prediction of emissions when combined with chemistry-based sub model (Heywood, 1998; Chow and Wyszynski, 1999). Furthermore, applications of physical models, such as thermodynamic models, fluid dynamic models can be found in (Roselló *et al.*, 2002; Arsie *et al.*, 2004; Jia *et al.*, 2008; Schögl *et al.*, 2009; Verhelst and Sheppard, 2009; Bernard *et al.*, 2011; Fridriksson *et al.*, 2011; Jajčević, 2011; Zheng and Caton, 2012; Aziz Hairuddin *et al.*, 2016; Ngwaka *et al.*, 2016). One-dimensional (1D) models are widely used at early stages of engine development because of their fast simulations speeds and robust prediction capabilities (Schögl *et al.*, 2009; Jajčević, 2011).

Although physical modelling can provide high precision when implemented accurately, it has associated drawbacks such as high complexity and computational efforts. This makes this modelling unsuitable for real-time applications (Nelles, 2001; Tietze, 2015). Also, automotive processes such as emission formation, turbocharger, are only partially known or require an unreasonable effort to be modelled physically (Nelles, 2001; Tietze, 2015). Due to the disadvantage of complex physical models and high computation cost, the trend in engine modelling has shifted from physical modelling to experimental modelling over the past years (Pezouvanis, 2009).

An alternative to physical models is so-called experimental or data-driven models (black-box). Experimental models do not require any a-priori-knowledge and can incorporate unknown non-linearities encoded in the sampled data. The complex physical models were unsuitable for controller design, thus simple experimentally (input-output data based) derived engine models were the first kind of models used for control purposes. The linear discrete engine model was first developed by Hazell and flower (Hazell and Flower, 1971a) based on sampled-data theory (Flower and Hazell, 1971; Hazell and Flower, 1971b). Thereafter, (Flower and Windett, 1976a, 1976b) incorporated PRBS techniques to identify dynamic characteristics of a large diesel engine. (Wellstead *et al.*, 1978) employed a non-parametric identification technique (frequency response estimation) to characterise the diesel engine dynamics. There have been many further advancements in the field of data-based modelling since the development of linear experimental

models, such as development of nonlinear models like neural network, neuro-fuzzy models and many others.

Data-based models have the advantage of fast simulation speeds and can be applied in real-time applications, such as model-based calibration of ECU (Tietze *et al.*, 2014). An overview of linear and non-linear experimental modelling for the reader's interest can be found in (Sjöberg *et al.*, 1995; Ljung, 1997, 2006; Nelles, 2001; Keesman, 2011), along with their applications. Furthermore, for the identification of engines using dynamic modelling is also presented in (Isermann and Münchhof, 2011) and (Isermann, 2014).

Hereafter, the chapter will focus on data-based dynamic modelling techniques, which are later implemented in this thesis for modelling purposes. The most commonly used modelling techniques namely, Neural network and Local Linear-Fuzzy models will be analysed and compared.

3.2 Modelling of Dynamic Systems

Modelling and identification of nonlinear dynamic systems is a challenging task because nonlinear processes are unique in the sense that they do not share many properties. System Identification estimates mathematical models by statistic methods with the purpose of representing real dynamic systems. A model should be adapted in such a manner that it could represent the behaviour of a process as closely as possible. The model capability to do so is typically measured in terms of a function of the error between the process output and the model input, which is later utilised to adjust the model's parameters. A general procedure and major steps involved to perform a

successful system identification loop are depicted in Figure 3.2. The first step related to data generation such as the selection of the input signal, the design of the excitation signal, was introduced in the previous chapter. In this chapter rest of the steps will be introduced with emphasis on identification dynamic modelling techniques namely, Neural network and Local Linear-Fuzzy models will be analysed and compared.

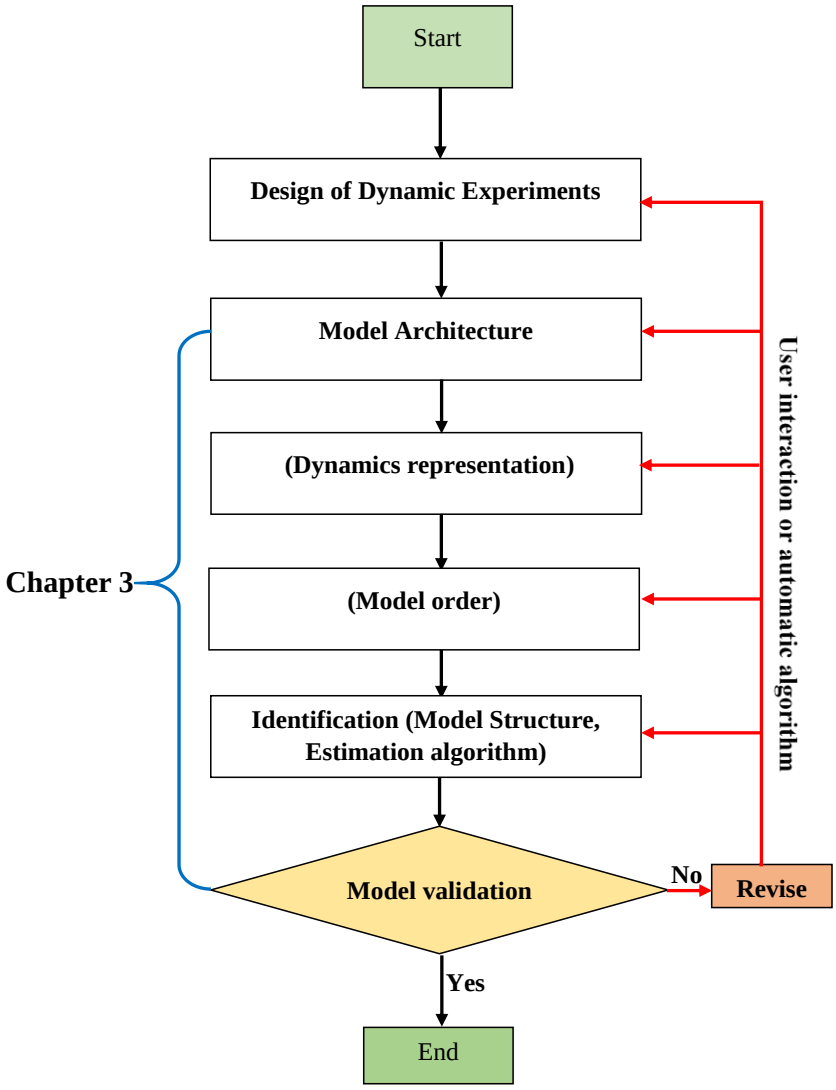

Figure 3.2: The System Identification Loop (parenthesis above indicate steps that are necessary only when dealing with dynamic systems).

3.2.1 Model Architecture

Nelles (2001), describes this step of identification to be one of the critical steps in the loop and provides criterion for the selection of appropriate model architecture. The choice of model architecture, such as polynomial, Neural Networks, and local linear neuro-fuzzy models, depends on the many factors and some of these are presented, in Table 3.1, below:

Table 3.1: Criterion for the selection of model architecture.

Criteria	Explanation
Defining the Problem	This means the classification of the problem, is it either approximation of static system or identification of dynamic systems.
Purpose of Model	This is selected based on the intended use of the model. This could vary from one-step prediction, simulation, optimisation, fault detection etc. A representation of different purposes is depicted in Figure 3.3.
Dimensionality	The number of relevant inputs and outputs plays an important role in the selection of suitable model architecture. For example, the polynomial is not suitable for high dimensional problems due to their properties which causes a rapid increase in parameters with the increase in dimensionality.
Data-sets	Availability of amount and quality of data affects the choice of model architecture. Dynamical measurements generally lead to longer measurements, which is caused by associated high dimensionality of the input space (Tietze, 2015). Hence, the choice of model should be able to cope with the training needs linked with large datasets.

	If the data is sparse and noisy, a global approach would be suitable as they average out disturbances (Nelles, 2001).
Development, Training and Evaluation time	Development time depends strongly on training time. Training and evaluation time share inverse relationship. Longer training times enables fast model evaluation while short training times imply require longer model evaluation times. Such as in the case of implementation for ECU of automotive systems chosen model should have fast evaluation time and require low resources.
Requirements of memory	Memory restriction is an important issue in the automotive industry (Nelles, 2001). Hence, the model with a smaller memory requirement will be preferred. (Tietze, 2015)
Offline or Online learning	All architectures are suitable for offline learning (Nelles, 2001). Online modelling is an interesting option and would require adaptive model architecture.
Interpretation	Model with interpretable parameters would be beneficial, as most black box models provide no physical meanings of the parameters.
Incorporation of Prior Knowledge	The possibility of incorporating physical knowledge into the model is beneficial, and the lack of this is a common drawback of black box models. Thus, a model with this capability should be considered during the selection stage.
Noise Sensitivity	Models need to consider the accurate noise level to avoid overfitting.
Accuracy	The ability to map nonlinear input-output relationships with high accuracy would also sway the choice of architecture.

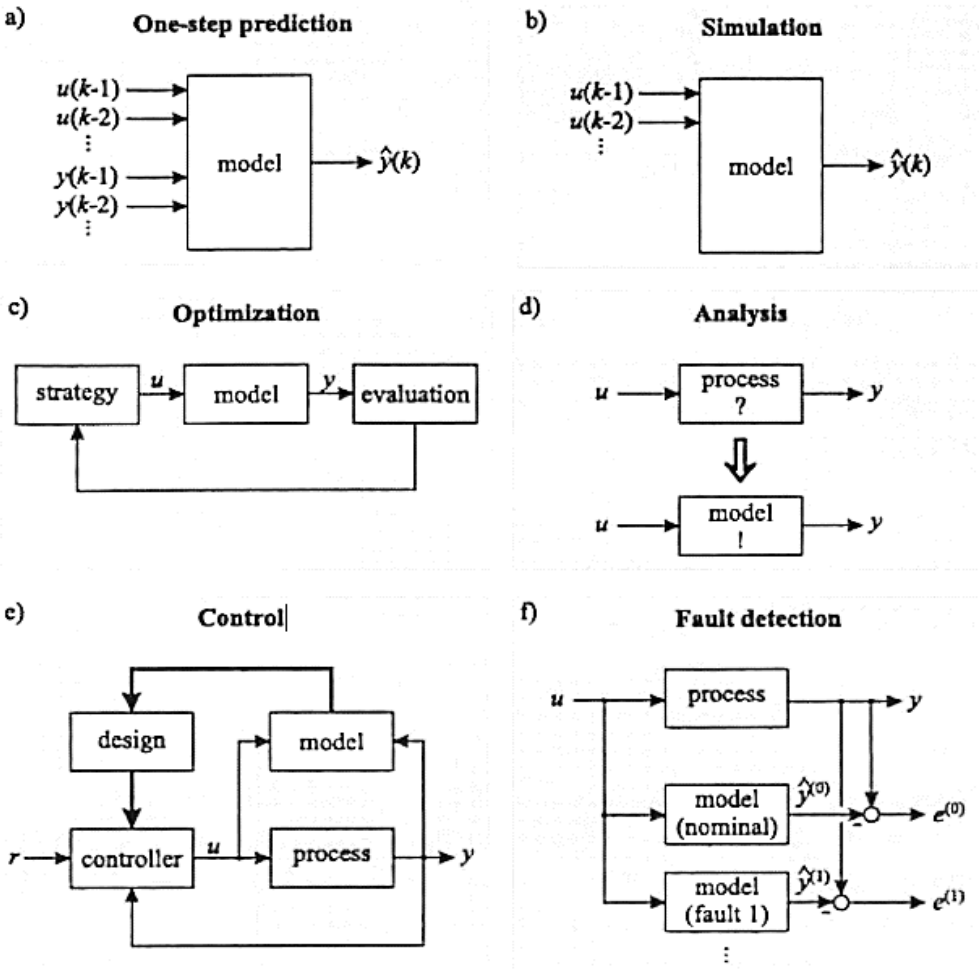

Figure 3.3: Various representation of models based on their intended use (Nelles, 2001).

The list mentioned above is certainly incomplete as there are many other factors which would influence the choice of model architecture such as customer requirement, availability of tools and software, and many more. There are further scenarios which should be considered on the basis of choice of dynamic representation and practical usage such as data distribution, extrapolation effect, local complexity etc. and can be found in details in (Nelles, 2001; Tietze, 2015). In the following section, the choice of dynamic representation is described.

3.2.2 Dynamic Representation

The choice of dynamic representation depends on the purpose of the model. The chosen model architecture and the available prior knowledge about the process also influence the decision in this stage. For example, if it is to be used for one-step prediction, a NARX (Nonlinear autoregressive with exogenous input) or NARMAX (Nonlinear autoregressive Moving Average with exogenous input) representation could prove a good choice.

Dynamic representation can be classified into two categories of internal and external dynamics. The internal dynamics strategy is based on the incorporation of dynamic elements into the model structure (Nelles *et al.*, 1996), while external dynamic approach separates the models into two parts: a nonlinear static approximator and external dynamic filter bank (Nelles, 2001). The illustration of both strategies is depicted in Figure 3.4. An external dynamic approach is the most frequently applied strategy (Nelles *et al.*, 1996; Schaffnit *et al.*, 2000; Nelles, 2001; Tietze, 2015) and will be applied in this work. In the external dynamic approach, the static nonlinear approximator is represented with different model types such as neural network, LOLIMOT and an external dynamic filter models the dynamic behaviour by tapped delay lines.

In terms of application, the external dynamic approach is divided into two cases: series-parallel model (equation error model) and parallel model (output error model) (Schaffnit *et al.*, 2000). These cases are illustrated in Figure 3.5.

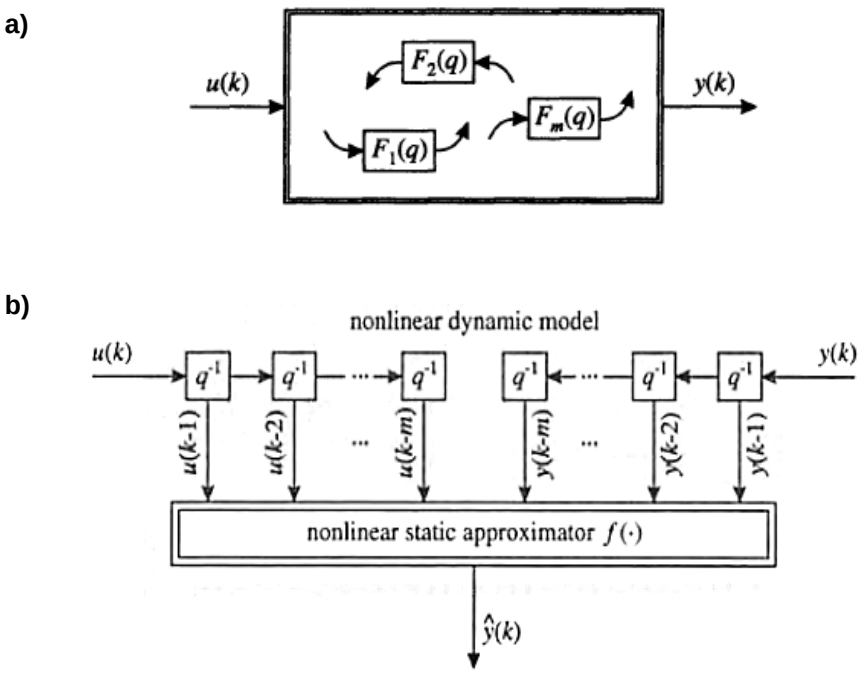

Figure 3.4: Dynamic representations: a) internal, b) external (Nelles, 2001).

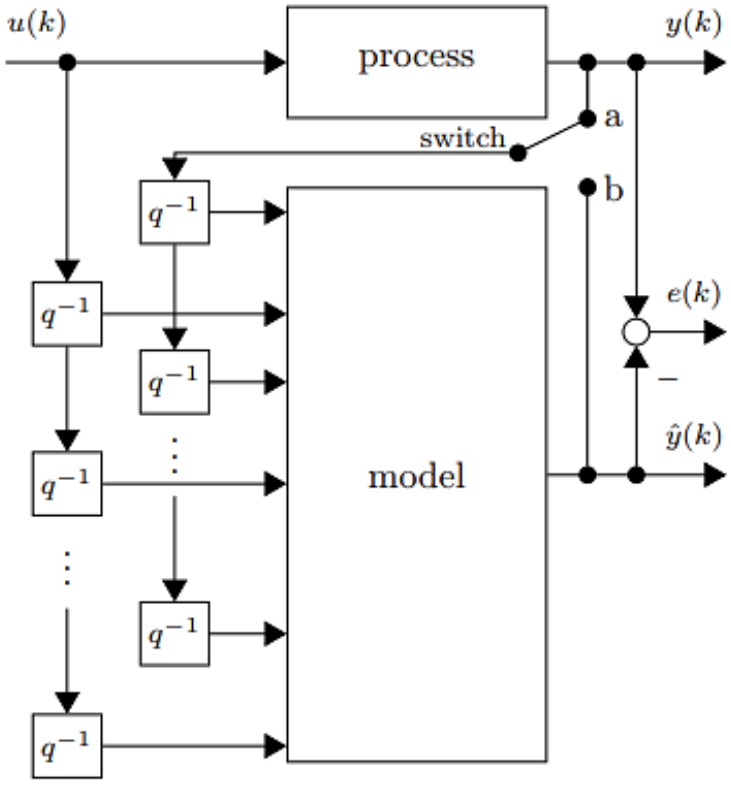

Figure 3.5: Series-parallel model (switch to **'a'**: one-step prediction) and parallel model (switch to **'b'**: simulation) (Belz *et al.*, 2017).

3.2.3 Model Order

The model order is typically determined by a combination of prior knowledge and trial and error (Nelles, 2001). However, an automatic order selection methodology has been recently proposed in (Belz *et al.*, 2017). In the external dynamic approach, higher dynamic order of the model increases the dimensionality, and delayed inputs will lead to larger regression matrix and increased number of parameters (Nelles, 2001; Tietze, 2015). Hence, the consideration of the model order is quite an important task. An example of the effect of different order on the model capability to predict is illustrated in (Nelles, 2001) and (Tietze, 2015) and is presented here in Figure 3.6. The upper plot of the figure shows a system modelled using polynomial models with a different degree of order and lower plot depicts the associated training and test error.

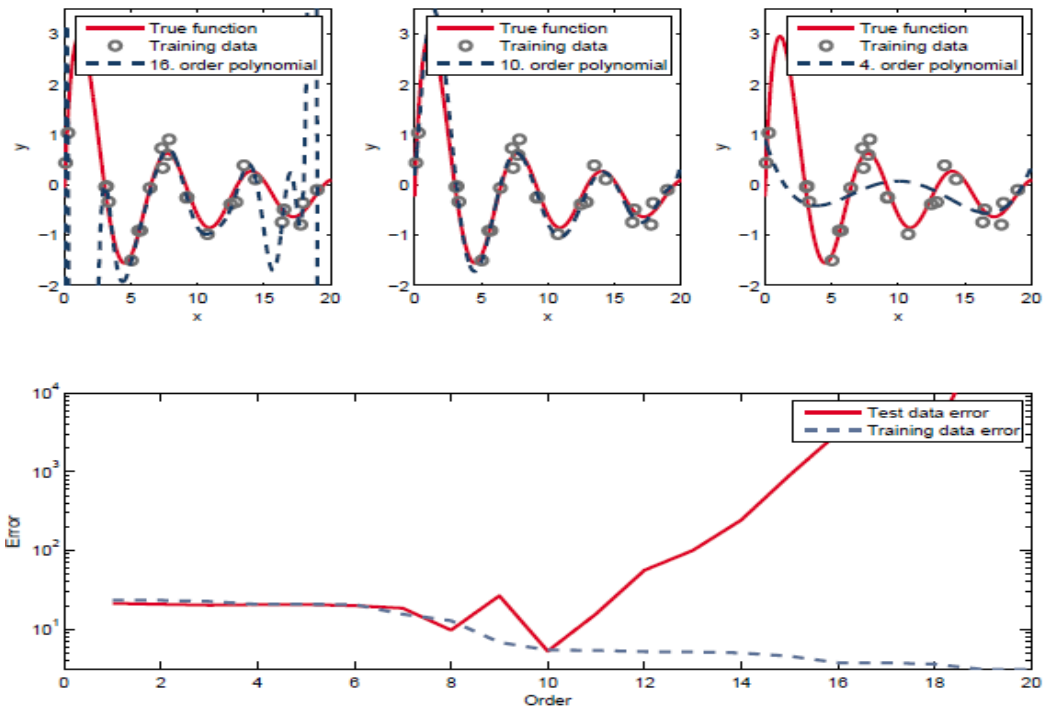

Figure 3.6: Effect of different model order on model fitting (Tietze, 2015)

The model on the left side (16th order polynomial) can fit the training points with a small error but generalises poorly for the test data. This is a scenario of overfitting, where the model is overly complex and flexible. On the contrary, the model on the right (4th order polynomial) presents low complexity and unable to fit the training points, and this is called underfitting. The model in the middle (10th order polynomial) provides a good fit for both training and test data.

This figure shed light on the concept commonly known as the bias/variance dilemma. An excessively complex model leads to a small bias but a high variance, as in the case of the 16th order model, and vice versa, as in the case of a 4th order model. The generic representation of bias/variance trade-off is presented in Figure 3.7.

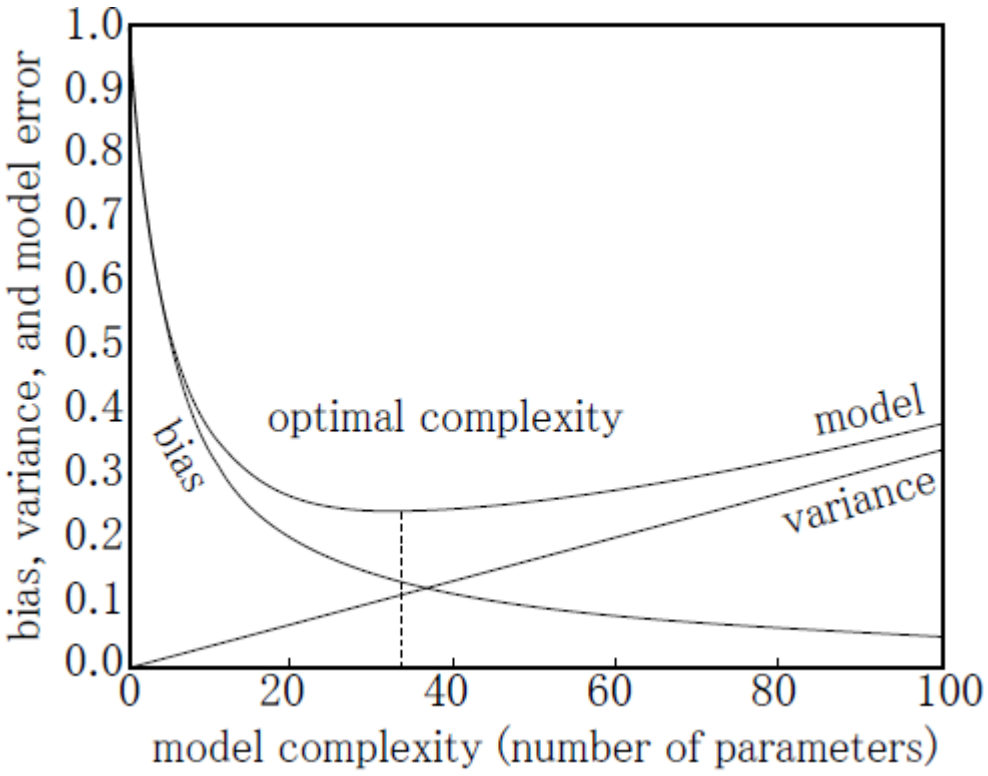

Figure 3.7: Bias/Variance Trade-off (Nelles, 2001).

3.2.4 Identification

Identification can be carried out automatically if structure optimisation techniques are applied such as orthogonal least squares (OLS) for linear parameterised models or evolutionary algorithms (EAs) for nonlinear parameterised models. An alternative to these general approaches is model specific growing and/or pruning algorithms such as Local order linear model tree for local linear neuro-fuzzy model (Nelles *et al.*, 2000), ASMOD (Additive Spline Modelling) for additive singleton neuro-fuzzy stems (Bossley *et al.*, 1997; Harris and Wu, 1997) or wide variety of algorithms available for multilayer perceptron networks (Reed, 1993; Augasta and Kathirvalavakumar, 2013).

The approach to the identification of static nonlinear approximators in external dynamic such as neural network, local linear neuro-fuzzy networks, Volterra series etc., are discussed and compared in section 3.3.

3.2.5 Model Validation

The main objective of model validation is to investigate how accurately a fitted model can predict the true behaviour of a response. There are different methods to validate the accuracy of the model:

- **Physical Behaviour:** The first option is to validate the response behaviour based on physical interactions of the input variables (Saunders, 2004). This validation method requires prior knowledge about the response behaviour to ensure that the model is not overfitting.

- **Internal Validation:** Internal validation technique is based on investigating model's statistical properties using different statistical methods, such as Root Mean Square Error (RMSE) (Röpke *et al.*, 2012; Burke *et al.*, 2013; Hartmann *et al.*, 2013), as given by Equation 3.1. RMSE is principally calculated by the discrepancy between the real value (y) of the measured sample points (n) and the corresponding prediction values ($\hat{y}$).

$$\mathrm{RMSE} = \sqrt{\frac{1}{\mathrm{n}} . \sum_{\mathrm{i}=1}^{\mathrm{n}} (\mathrm{y_i} - \hat{\mathrm{y}}_\mathrm{i})^2} \qquad \text{Equation 3.1}$$

PRESS RMSE (Prediction Error Sum of Squares) (Klein *et al.*, 2013) is also an internal validation criterion, which is useful for cross-validation technique for investigating overfitting (Grove *et al.*, 2004; Guerrier and Cawsey, 2004). PRESS RMSE is calculated by fitting the statistical model to 'n -1' of the measurements and predicting the response value for the remaining sample point. The difference between the actual and the predicted value of the remaining sample point is called prediction residual, and the sum of the squares of all the predicted residuals is PRESS (Howlett *et al.*, 1999).

- **External Validation:** This technique requires an additional set of measurements, for example, name it validation data to be used for validation of the model's predictive performance (Cary, 2003). To clarify the notations and names, data used for fitting the model can be named training data and the one used for validation could be named validation data. Training data

(Model fitting data) has ***'n'*** sample points, and validation data has a ***'v'*** sample point.

These measurements are not used for fitting the model rather is a fresh set of data. Accordingly, the fitted response model to 'n' measurements is used to calculate the response values of the 'v' validation sample points. There are different external validation criterion such as Validation RMSE (Hartmann *et al.*, 2013), given by Equation 3.2, and Relative Error (Rango *et al.*, 2013), illustrated by Equation 3.3, that can be used to investigate a model's accuracy. This validation criterion exploits the discrepancy between the predicted values and the measured values of the validation set.

$$\text{Validation RMSE} = \sqrt{\frac{1}{v} . \sum_{i=1}^{v} (y_i - \hat{y}_i)^2} \qquad \text{Equation 3.2}$$

$$\text{Relative Error } (\%) = \sqrt{\frac{\sum_{i=1}^{v} (y_i - \hat{y}_i)^2}{\sum_{i=1}^{v} (y_i)^2}} \qquad \text{Equation 3.3}$$

The use of external validation criteria allows to determine whether the fitted model (on training data set) can provide similar level of performance on new set of data (validation data set). In other words, the fitted model can generalise the relationship in the data without exhibiting overfitting or underfitting. The overfitting means that model is overcompensating by fitting all the data points (including random errors) rather than learning the underlying system. While

underfitting occurs when fitted model fails to learn the relation in the training data because of not being able to fit the training sample points.

3.3 Nonlinear Dynamic Model Identification

There is a vast number of data-based modelling techniques which can be applied to define the relationship between input and output, such as look-up tables, Hammerstein models, Wieners models, Volterra series, neural networks, and local model networks. These techniques have been widely implemented in the literature related to engine modelling such as Volterra series for prediction of emissions in (Guhmann and Riedel, 2011; Burke *et al.*, 2013), neural networks for modelling torque and lambda and fuel optimisation in (Fang *et al.*, 2015), modelling of Diesel engine with neural networks in (He and Rutland, 2004), and NOx modelling using LOLIMOT algorithm in (Hafner *et al.*, 2000) and (Isermann and Muller, 2001). Once the modelling structure is defined, the model fitting process is followed. The model fitting can be either offline or online, in this thesis offline based parameter optimisation algorithms are implemented. The model fitting process can be categorised into three main categories:

- **Parametric Models**: parametric models are explicitly dependent on the underlying model structure, thus demanding prior knowledge regarding the response behaviour (Kianifar, 2014). These models can lead to large errors in approximation If order of the model does not agree with the order of the process (Åström and Eykhoff, 1971). For these models, the unknown model parameters for the pre-defined model type are estimated based on the

experimental measurements (i.e. test points). In the following section, polynomials (Myers *et al.*, 1989; Morris and Mitchell, 1995) which are well-known parametric models, are reviewed in detail. Polynomials have been commonly used as a modelling technique for engine model-based calibration (Hartmann *et al.*, 2013; Rango *et al.*, 2013).

- **Non-Parametric Models**: non-parametric models do not require explicit model assumptions (Rango *et al.*, 2013). Therefore, these models are an attractive modelling option for engineering cases when no prior knowledge regarding the suitable model type is available. Given that non-parametric models have recently gained attraction in engine model-based calibration (Hartmann *et al.*, 2013; Rango *et al.*, 2013), one of the mostly used non-parametric modelling techniques in model-based calibration (Morton and Knott, 2002; Seabrook *et al.*, 2005),Neural Networks (Hagan and Demuth, 1999), is reviewed in this section.

- **Multi-Model Approach**: this is an approach toward modelling and identification of complex non-linear systems that rely on problem decomposition strategy. In this approach, a global system model is constructed with the set of models integrated with different degree of validity. The multi-model framework has been applied in different context with different names such as Local Model Networks (Murray-Smith, 1994), Local Linear Neuro-Fuzzy Models (Nelles *et al.*, 1996), and will be reviewed in this section.

3.3.1 Parametric Models: Polynomial Models

Polynomial models are popular in modelling context due to their simple structure which makes them easy to understand (Hartmann *et al.*, 2013) and parameters of polynomial models can be optimised easily and rapidly using least squares regression and explicit formula (Nelles, 2001; Burke *et al.*, 2013; Tietze, 2015). A polynomial of a response behaviour (y) based on the input parameters (X) by linear combination of a set of base functions (f), can be expressed as (Myers *et al.*, 1989; Morris and Mitchell, 1995; Nelles, 2001):

$$y(x) = f^{t}.a = \sum_{p=1}^{P} a_{p}.f_{p}(X) \qquad \text{Equation 3.4}$$

Where P indicates the number of base functions, and a is the parameter vector. In (Nelles, 2001), for an ***m***-dimensional polynomial of degree ***n***, base function and number of parameters are defined as:

$$P = \frac{(n+m)!}{n!\,m!} - 1 \qquad \text{Equation 3.5}$$

$$\text{Number of Parameters} = P + 1 \qquad \text{Equation 3.6}$$

The nonlinear dynamic extension for the polynomial model is achieved by utilising polynomials for the approximation of nonlinear static approximator, in one step prediction model of external dynamic approach, and is referred as

Kolmogorov- Gabor polynomial (Nelles, 2001). The representation of both static and dynamic structure is illustrated in Figure 3.8.

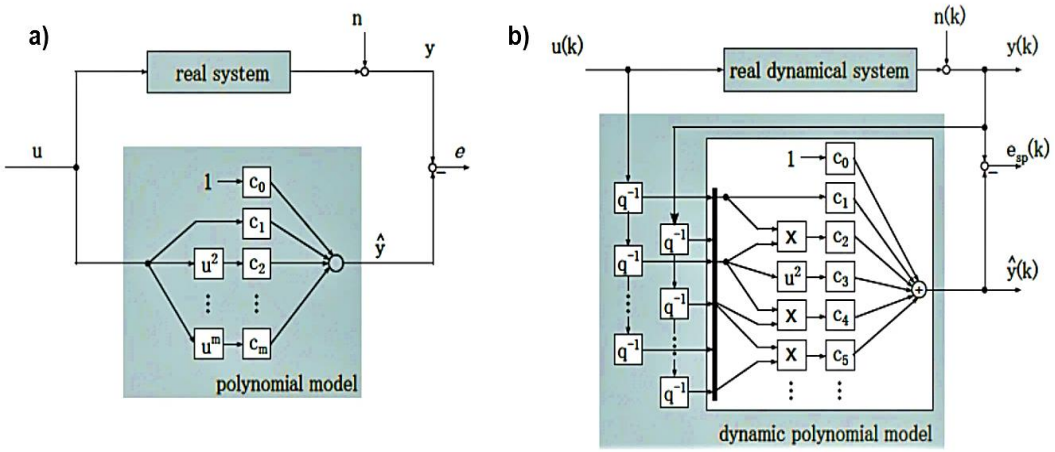

Figure 3.8: Illustration of static (3.8a) and dynamic (3.8b) polynomial model structure (Tietze, 2015).

In light of Equation 3.5 and Equation 3.6, it becomes clear that the number of parameters and thus the model complexity increases dramatically with increasing input dimensionality and degree of the polynomial (Nelles, 2001; Khan, 2011; Tietze, 2015). This attribute of polynomial models makes them unsuitable for high dimensional problems. This can be resolved by applying polynomial models in combination with a structural selection technique like orthogonal least square. These subset selection techniques can automatically select the relevant terms from full polynomial leading to reduced model and thus increasing polynomials capability (Nelles, 2001). However, if the full polynomial has a large number of terms, this would result in structure selection being computationally demanding. Also, high degree polynomials suffer from oscillatory interpolation which could lead to incorrect dynamics representation

or instability depending on the direction of oscillation (Nelles, 2001). In spite of the disadvantages of the polynomial model, their simple structure, mathematical operations in terms of multiplications and summations, allows easy implementation as an ECU function (Tietze, 2015).

3.3.2 Parametric Models: Volterra Series

A practical extension to dynamic polynomial models is the parametric Volterra series (Nelles, 2001; Burke *et al.*, 2013). In parametric Volterra series static model, one step prediction model of external dynamic approach is realised using linear feedback term and previous states of model inputs (Nelles, 2001; Burke *et al.*, 2013). The generic form of Volterra series can be expressed as in Equation 3.7 (Nelles, 2001) and its structure can be illustrated as in Figure 3.9. The structure is composed of nonlinear transformation of input quantities by polynomials with subsequent finite response filter (FIR). However, finite impulse responses tend to decay over time and to accurately represent a dynamic system with large time constant with FIR would lead to large number of parameters. Therefore, to cope with such system without accumulating large number of parameters, an infinite response filter (IIR) is used.

$$\mathbf{y(k)} = \mathbf{f}\big(\mathbf{u(k-1)}, \dots, \mathbf{u(k-m)}\big) - \mathbf{a_1 y(k-1)} - \cdots - \mathbf{a_m y(k-m)} \qquad \text{Equation 3.7}$$

The simplification of linear feedback and modelling nonlinearity only for the inputs leads to a reduced number of regressors and avoids the drawbacks of

oscillatory interpolation, which is present in dynamic polynomial models (Nelles, 2001).

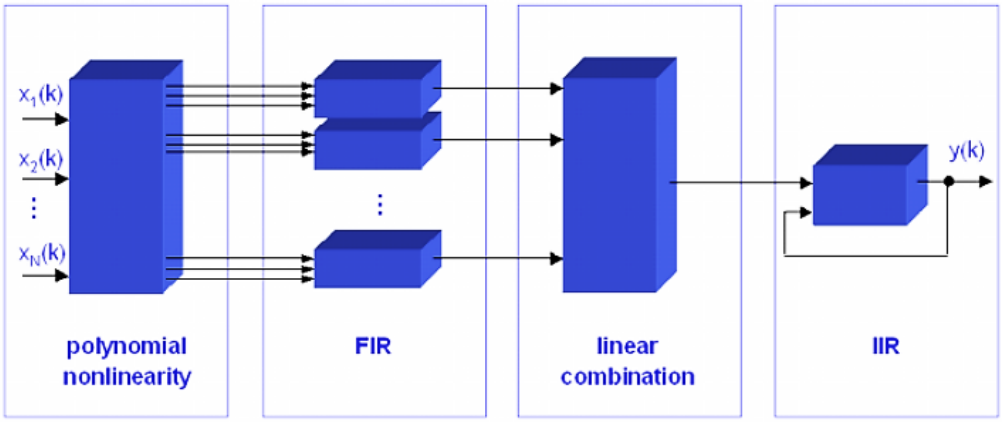

Figure 3.9: Schematic representation of the parametric Volterra series (Sakushima *et al.*, 2013)

However, they do suffer from their own disadvantage such as restriction of generality and incapability of describing a system with nonlinear dependence on output. The system whose nonlinear behaviour depends strongly on output can be represented by this choice of the model if the chosen model order is large (Nelles, 2001). However, as of the large model order, the number of parameters would increase which would lead to more complex regression process (Burke *et al.*, 2013).

The parametric Volterra series models have been often used for modelling nonlinear dynamic systems, and a detailed review of these models can be found in (Cheng *et al.*, 2017). The properties which have made them popular for application in the automotive industry are linearity of parameters, flexibility, and easily proven stability criterion using linear system theory (Nelles, 2001; Röpke, 2014) . They have been successfully applied for modelling NOx

emission in a Diesel engine by (Guhmann and Riedel, 2011; Burke *et al.*, 2013; Sakushima *et al.*, 2013) and choice of the excitation signal in all these publications have been chirp for these type of models.

3.3.3 Non-Parametric Models: Artificial Neural Network

An artificial neural network (ANN) or more commonly known, neural network is a nonparametric computational model which is composed of mathematically formulated neurons (Isermann, 2014). The ANN represents a network formed by interconnecting simple processing units (He and Rutland, 2004; Tietze, 2015) and these simple units are generally referred to as neurons. A basic representation of elements of a neuron is depicted in Figure 3.10, where weights determine the contribution of certain input towards the target and activation functions introduces the nonlinearity into the network.

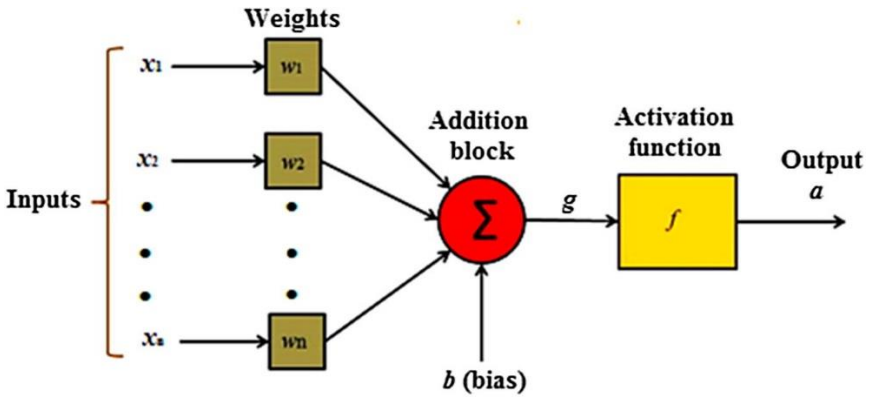

Figure 3.10: Representation of elements of neural computation (Turkson *et al.*, 2016)

The network contains three layers in general and is as follow:

- Input layer: This layer is responsible for transferring value to the next layer, i.e. a hidden layer, and does not perform any computation.

- Output layer: The layer which produces the output.

- Hidden Layer: this layer lies in between the 'Input' and 'Output' layers. These layers are arranged by neurons, and each layer may contain several numbers of neurons. Neurons only connect the adjacent layers, and signals propagate via neurons through these hidden layers.

The ANN can be viewed as an input-output mapping which provides a response for a set of inputs based on information it acquired during the learning process (He and Rutland, 2004; Isermann, 2014). The procedure of learning and testing process is well described in (Nelles, 2001; He and Rutland, 2004). There have been successful applications of neural network in automotive field such as NOx emission prediction in (Guhmann and Riedel, 2011), to predict engine system reliability by (Xu *et al.*, 2003), modelling torque in biodiesel engine by (Cirak and Demirtas, 2014), modelling engine using speed, efficiency and exhaust gases by (Serikov, 2010), neural networks for modelling torque and lambda and fuel optimisation in (Fang *et al.*, 2015), modelling of Diesel engine with neural networks in (He and Rutland, 2004), and many more. The wide implementation of ANN in the automotive industry is because they do not require specific knowledge of the process structure (Isermann, 2014) and provides a balanced approach to deal with the trade-off between model accuracy and run time (He and Rutland, 2004).

The neural networks can be broadly classified into two categories: feedforward and recurrent neural networks. The feedforward neural networks can be further classified into radial basis function (RBF) networks, single-layer and multi-layer perceptron networks. The detailed description of all these categories can be found in (Nelles, 2001; Isermann and Münchhof, 2011; Keesman, 2011; Isermann, 2014). The multi-layer perceptron (MLP) networks are widely known and popular choice of architecture for dynamic modelling applications (Nelles, 2001; He and Rutland, 2004; Tietze, 2015).The MLP networks have either one or more than one hidden layer, and a generic representation of the MLP network is depicted in Figure 3.11.

The MLP networks are generally chosen for nonlinear dynamic modelling as they are well suited for the external dynamic approach. The reason being, MLP networks ability to find the main direction of nonlinearity in the system and thus overcome the curse of dimensionality (Nelles, 2001). Also, the number of parameters has a linear relationship with the number of inputs, given a fixed number of hidden neurons, which allows for a reduced number of parameters. Furthermore, they can easily handle uneven data distribution (Nelles, 2001) which is a by-product of the optimisation of hidden layer weights. However, MLP networks suffer from disadvantages such as high training effort, the existence of many poor local optima but these can be overcome by RBF networks (Nelles, 2001). But RBF networks when applied for dynamic systems suffer from poor extrapolation behaviour and also the accuracy is lower compared to MLP networks (Nelles, 2001).

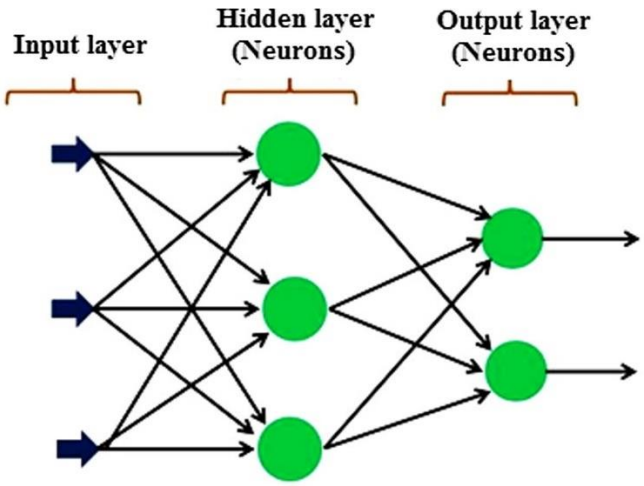

Figure 3.11: Multi-layer perceptron feedforward network structure (Turkson *et al.*, 2016).

The ANN modelling approach is useful in a scenario when the underlying function of a system is too complex to define or when it is too expensive to model it in a conventional way (He and Rutland, 2004). They are a suitable model choice for a highly nonlinear or very large problem (Khan, 2011). Artificial neural networks due to their black box nature do not allow transparent interpretation of the parameters and an alternative to this, as per (Isermann, 2014), is local linear models which will are discussed in the following section.

3.3.4 Multi-Model Approach

Multi-modelling approach is another technique for modelling and identification of complex nonlinear systems. In this method, operating space of the system is decomposed using local models, and these local models represent the dynamics of the system in their specific region of the global space (Johansen and Foss, 1997). The idea of multi-model approach has been developed in different fields with different names such as regime based models (Johansen,

1994), local model networks (Murray-Smith, 1994; Murray-Smith and Hunt, 1995), Takagi-Sugeno fuzzy models(Takagi and Sugeno, 1985) ,local linear neuro-fuzzy models (Nelles *et al.*, 2000) The multi-model framework has found its way in developments and modelling of engine processes such as hardware in loop simulation of turbocharger in (Nelles *et al.*, 1996) and (Schaffnit *et al.*, 2000), optimisation of engine variables setting in (Hafner *et al.*, 2000), NOx emission modelling in (Isermann, 2014), and model predictive control of air conditioning system using LOLIMOT for identification of neuro-fuzzy models is presented in (Rehrl *et al.*, 2014) and improvement of accuracy in real-world heating ventilation and air conditioning in (Belz *et al.*, 2017).

An illustration of a multi-model approach based on their partition strategy, validity computation (defines the transition between local models), and sub-model structure is depicted in Figure 3.12. In this review incremental partition strategy, pre-validity components such as Gaussian and sigmoid function, and soft switching, which allows a smooth transition between models, are discussed. The other strategies for partition are presented in (Adeniran and Ferik, 2016) and validity computation such as hard switching. can be found in (Billings and Zhu, 1994) along with other literature mentioned in (Nelles, 2001).

The modelling architecture chosen in this thesis for multi-model approach is local linear neuro-fuzzy networks. This modelling approach allows modelling of the nonlinear dynamic process of a system on the basis of its input-output relationship and the structure of this approach also allows incorporation of

knowledge and prior information of the system (Murray-Smith and Hunt, 1995).

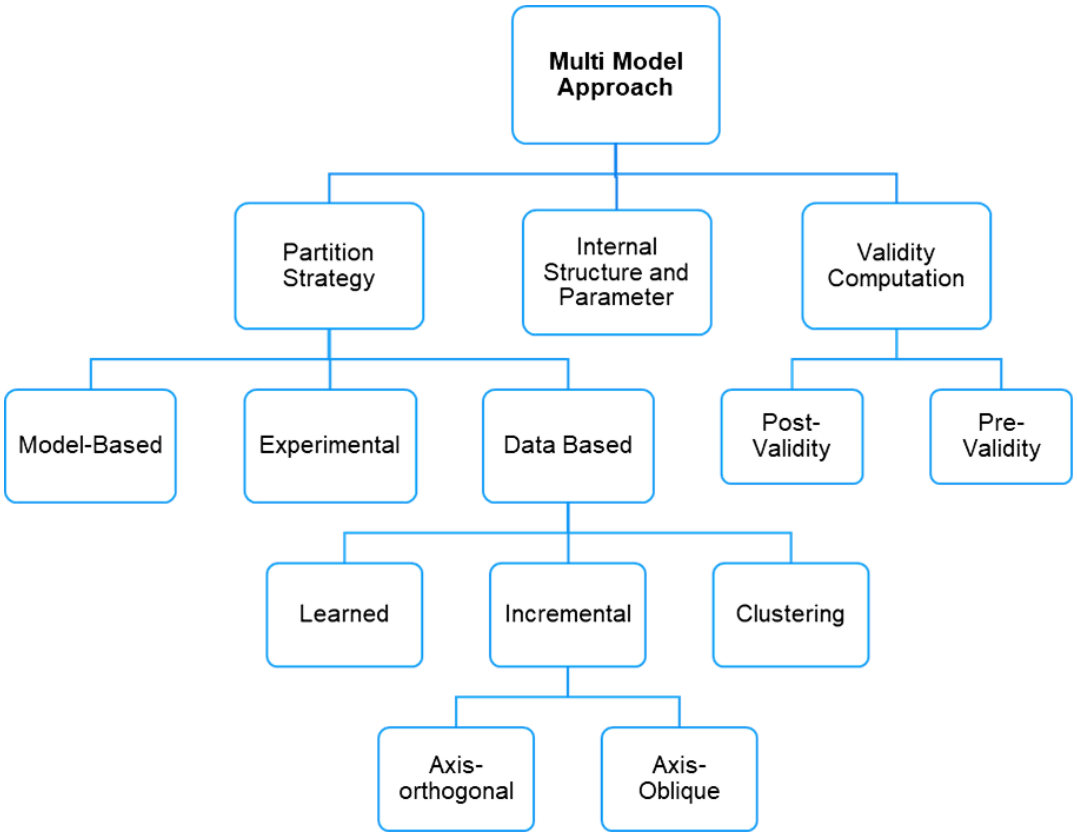

Figure 3.12: Classification of the multi-model approach adopted from (Adeniran and Ferik, 2016).

3.3.5 Local Linear Neuro Fuzzy (LLNF) Models

The local linear neuro-fuzzy models are also referred to as Takagi-Sugeno fuzzy models. The analysis of their interaction stating differences and similarities with T-S fuzzy models, LMN based on RBF networks and normalised RBF networks can be found in (Nelles, 2001) and has been mentioned in (Schaffnit *et al.*, 2000). In Figure 3.13, an illustration of the

relationship between these models is presented, and the details regarding the conditions or restriction have been reviewed in (Nelles, 2001).

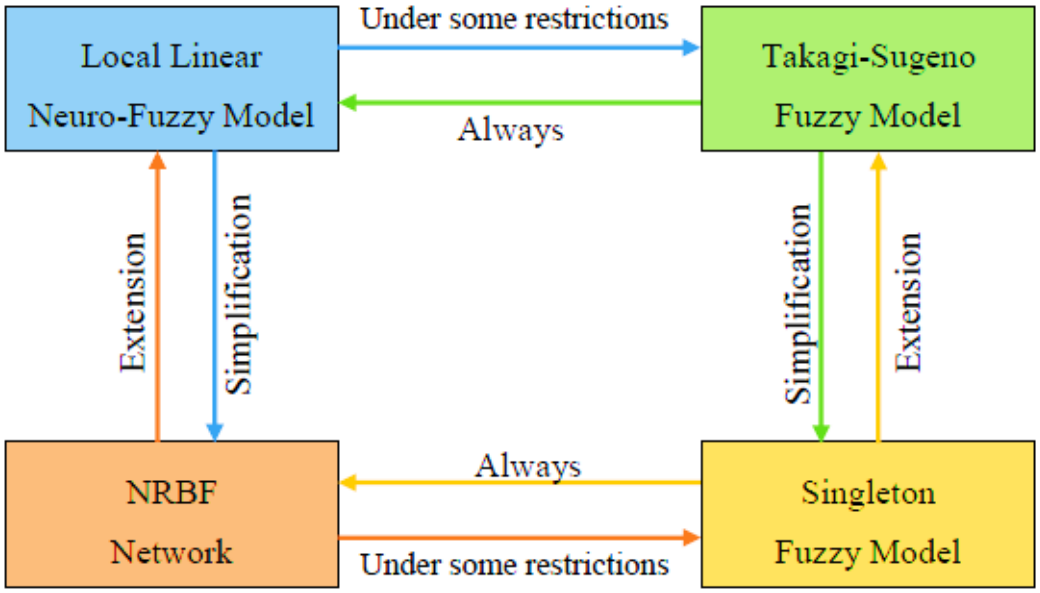

Figure 3.13: Relationship between LLNF models and other architectures

The local linear modelling approach is based on divide and conquer strategy, i.e. a complex modelling problem is divided into several smaller and simpler sub-models, such as linear models, which can be identified simply and almost independently (Nelles, 2001). A mathematical representation of dynamic LLNF models, pursuing the external dynamic approach introduced in section 3.2.2, for *p* number of inputs and *m* order is obtained by using Equation 3.8 and Equation 3.9 and is presented in Equation 3.10. A representation of Local linear modelling approach with external dynamics is depicted in Figure 3.14.

The most important factor for the success of such a modelling approach is the partition strategy for the original complex problem. Therefore, the properties

of local linear neuro-fuzzy models crucially depend on the applied construction algorithm that implements a certain division strategy. The application of such partition strategy can be found in (Fischer *et al.*, 1998; Schaffnit *et al.*, 2000; Nelles, 2006; Hartmann *et al.*, 2013) and are discussed later in this section.

$$\underline{\mathbf{x}} = \underline{\boldsymbol{\varphi}}(\mathbf{k}), \quad \underline{\mathbf{z}} = \underline{\boldsymbol{\varphi}}(\mathbf{k}) \qquad \text{Equation 3.8}$$

Where $\underline{x}$ is called rule consequents, $\underline{z}$ is rule premise and $\underline{\varphi}(k)$ being the vector containing regressors. The regressors are given as:

$$\begin{aligned}\underline{\boldsymbol{\varphi}}(\mathbf{k}) = [&\mathbf{u_1}(\mathbf{k}-\mathbf{1}) \dots \mathbf{u_1}(\mathbf{k} \\ &-\mathbf{m}) \dots \mathbf{u_p}(\mathbf{k}-\mathbf{1}) \dots \mathbf{u_p}(\mathbf{k}-\mathbf{m})\, \mathbf{y}(\mathbf{k} \\ &-\mathbf{m}) \dots \mathbf{y}(\mathbf{k}-\mathbf{m})]^{\mathbf{T}}\end{aligned} \qquad \text{Equation 3.9}$$

Incorporating information from Equation 3.8 and Equation 3.9, the dynamic local linear neuro-fuzzy models can be represented as:

$$\begin{aligned}\hat{\mathbf{y}}(\mathbf{k}) = \sum_{\mathbf{i=1}}^{\mathbf{M}} \{&\mathbf{b_{i1}}\mathbf{u}(\mathbf{k}-\mathbf{1}) + \dots + \mathbf{b_{im}}\mathbf{u}(\mathbf{k}-\mathbf{m}) \\ &-\mathbf{a_{i1}}\hat{\mathbf{y}}(\mathbf{k}-\mathbf{1}) - \dots \mathbf{a_{im}}\hat{\mathbf{y}}(\mathbf{k}-\mathbf{m}) + \boldsymbol{\zeta}_\mathbf{i}\}\boldsymbol{\Phi}_\mathbf{i}\,(\underline{\mathbf{z}})\end{aligned} \qquad \text{Equation 3.10}$$

Where b_{ij} and a_{ij} represent the numerator and denominator coefficients and ζ_i is the offset of the *i*th local linear model.

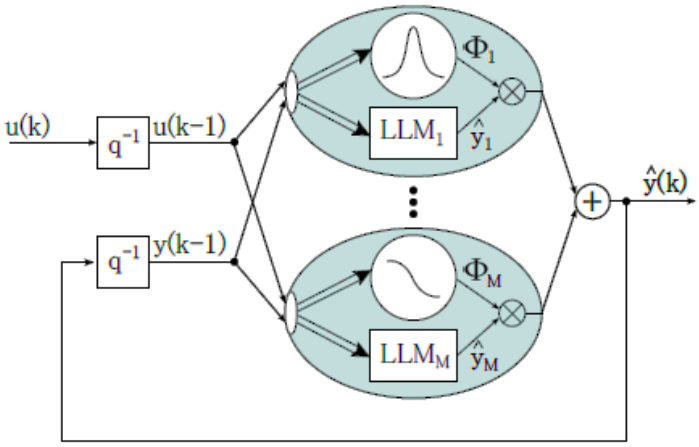

Figure 3.14: Local linear models with an external dynamic approach (Nelles, 2001)

In general case, the rule premise and consequent are well represented by Equation 3.8, but in the case of the multivariable system of high dynamic order the dimensionality of regressor space, $\underline{\varphi}(k)$, can be quite high. Therefore, for dynamic model based on external dynamic approach require algorithms which can deal with the high dimensionality and are presented hereafter.

The two well-known algorithms for identification of local linear models are LOLIMOT (Local linear model tree) and HILOMOT (Hierarchical local model tree). These algorithms are based on incremental partitioning strategy, axis orthogonal and axis oblique partitioning, mentioned in Figure 3.12.

1) Dynamic Modelling using LOLIMOT and HILOMOT algorithm:

LOLIMOT, as mentioned earlier, stands for Local Linear Model Tree and is a multi-model approach which utilises incremental partitioning strategy of axis orthogonal nature. LOLIMOT was presented in (Nelles *et al.*, 1996) and have

been adopted ever since for modelling in many research studies, (Hafner *et al.*, 2000; Nelles *et al.*, 2000; Schaffnit *et al.*, 2000; Pedram *et al.*, 2008; Rehrl *et al.*, 2014). It is an iterative modelling technique, for each iteration a new local linear model (LLM) is added (Nelles, 2001). These local models (LMs) are associated with the partition of the operating space, where they are valid, which is determined by the tree construction algorithm utilising axis orthogonal splits (Sequenz, 2013). The partitioning strategy is illustrated in Figure 3.15a). The LMs generated are of linear or affine types (if an offset is applied), and they are weighted to overall model output by means of normalised Gaussian weighting function (Tietze, 2015). Thus, allowing a smooth transition from one LM to another (Sequenz, 2013). The global output of LOLIMOT model is then calculated by weighted summation of LMs output multiplied by the weighting function (Nelles *et al.*, 1996), this is depicted in Figure 3.15b).

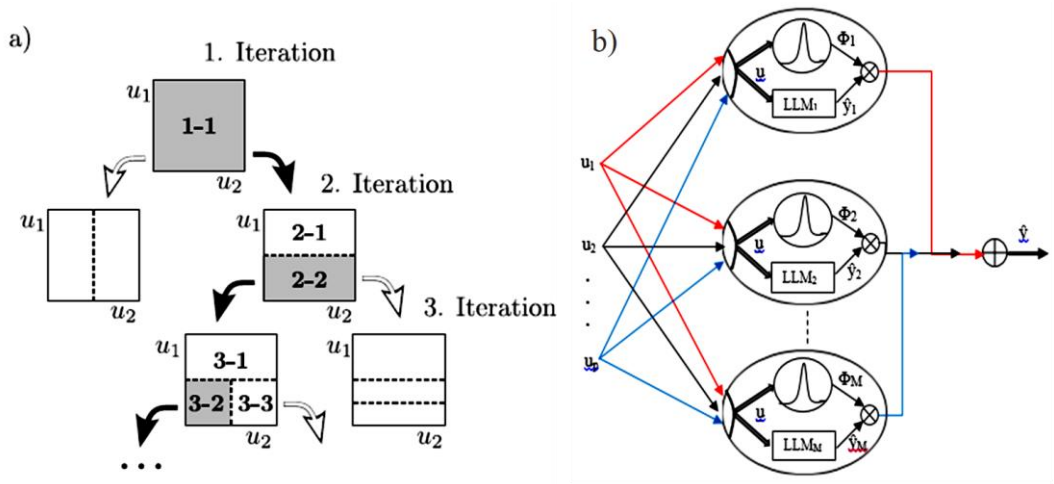

Figure 3.15: a) Tree construction algorithm and its partitioning strategy and b) model structure of LOLIMOT illustrating the contribution of LLM towards the global model output

The parameter estimation of LOLIMOT local models can be achieved either simultaneously or separately by using global or local estimation approach respectively. The choice of either global or local depends on the problem under consideration and detailed description for both approaches is provided in (Nelles, 2001). In summary, a global estimation approach is an efficient approach in terms of performance, while the local estimation approach increases flexibility and allow fast computation. A detailed comparison of the two approaches is discussed in (Nelles, 2001).

The advantage of LOLIMOT models is efficient and fast parameter estimation as a local model structure is polynomial (Tietze, 2015), thus leading to fast training speed. Also, the implementation of the heuristic approach which is generally automated provides high usability for these models. The axes-orthogonal split of the input space provides excellent interpretability (Nelles, 2001). Furthermore, LOLIMOT models, for dynamic application, allow distinction between rule premise and rule consequent inputs, i.e. distinction of the inputs to be part of the model or to be part of validity function, which leads to reduced number of regressors (Nelles, 2001). Thus, the number of effective parameters can be reduced, which counteracts the curse of dimensionality. However, in case of high dimensional problem where a reduction in premise input space cannot be exploited, the LOLIMOT models become inefficient due to sub-optimal decomposition of input space by axis orthogonal partition (Nelles, 2001; Hartmann *et al.*, 2013). The axis orthogonal partitioning decomposition strategy of LOLIMOT models also leads to a large number of

LLMs, when compared to other axis-orthogonal approaches like ANFIS (Nelles, 2001)(Tietze, 2015).

The major restriction of axes orthogonal split in LOLIMOT models could be overcome by an extension to axes-oblique partitioning (Nelles, 2006). The algorithm which allowed such incorporation is called HILOMOT and stands for Hierarchical Local Model Tree. The axes-oblique partitioning algorithm introduced by Nelles (Nelles, 2006) and is partly adopted from work of Ernst in (Ernst, 1998), which is based on the contribution of hinge functions by (Breiman, 1993) and smooth hinge functions by (Pucar and Millnert, 1995). The partitioning strategy and hierarchical structure of HILOMOT are illustrated in Figure 3.16.

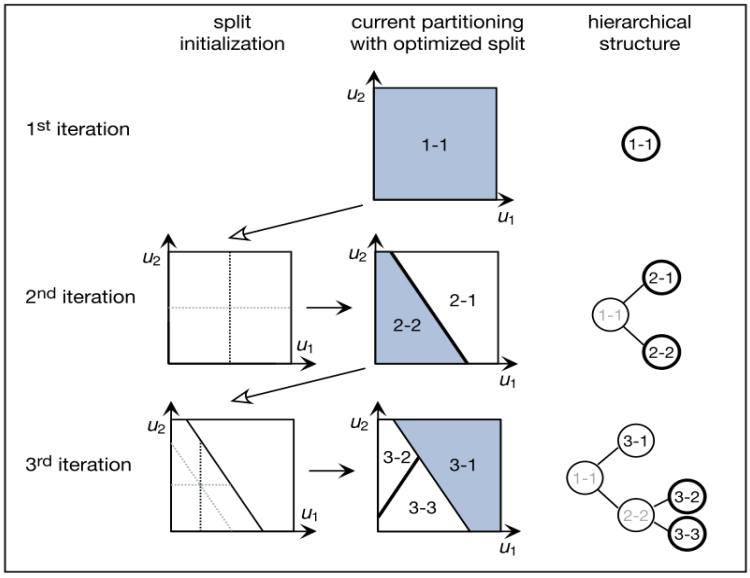

Figure 3.16: Axes oblique split partitioning and general model structure of HILOMOT(Hartmann and Nelles, 2013).

HILOMOT models like LOLIMOT models are based on incremental tree approach, and LLMs are generally polynomial in structure. Thus, leading to

fast parameter estimation. The property which sets them apart from LOLIMOT is the use of sigmoid validity functions rather than Gaussian. The sigmoid functions allow an arbitrary axes-oblique orientation of splits (Hartmann and Nelles, 2013). In contrast to the axes-orthogonal strategy of LOLIMOT, axes-oblique allows higher flexibility and are well suited for high-dimensional problems (Nelles, 2006). However, higher flexibility offered by sigmoid functions comes at the price of nonlinear optimisation of validity function parameters (Klein *et al.*, 2013). Thus, leading to a computationally expensive approach. Further details on HILOMOT model and axes oblique partitioning can be found in (Hartmann and Nelles, 2009b, 2009a; Hartmann *et al.*, 2013). A review of applications of multi-model approach is presented in Table 3.2.

Table 3.2: Review of applications of multi model approach

Application	**Partition/parameter estimation/ validity function**	**Reference**
Modelling of turbocharged gas engine power plant	axis-orthogonal/total least square/ Gaussian	(Jakubek *et al.*, 2008)
Optimise the engine's exhaust emission	axis-orthogonal/least square/ Gaussian	(Castric *et al.*, 2009)
Process optimisation	axis-orthogonal/least square/ Gaussian	(Hartmann *et al.*, 2009)
NOx emission prediction	axis-orthogonal/least square/ Gaussian	(Sequenz and Isermann, 2011)
Modelling gasoline engine emission	axis-orthogonal/least square/ Gaussian	(Martínez-Morales *et al.*, 2013)
Vehicle fuel consumption prediction	axis-orthogonal/least square/ Gaussian	(Mohammad Reza Rafimanzelat and Seyed Hossein Iranmanesh, 2012)
Reduction of measurement time for calibration of the combustion engine	axis-oblique/weighted least square/ Sigmoid	(Klein et al., 2013)
Model based ultrasonic imaging	axis-oblique/weighted least square/ Sigmoid	(Hartmann *et al.*, 2011)

3.4 Summary

The system identification loop for dynamic modelling and its steps are presented and discussed. A list of criterions for selection of model architecture is presented, followed by the model structures. The model structures, polynomials, Volterra series, Neural Networks, LOLIMOT, and HILOMOT were introduced and analysed in the light of the criterion mentioned previously. The advantages and disadvantages of modelling techniques have been discussed along with their applications in this chapter.

Polynomial models have been a popular choice as their structure is easy to understand, but they suffer from the so-called curse of dimensionality. The curse of dimensionality here refers to the increase in modelling effort due to increased number of inputs. This becomes important regarding the high dimensional problem, as the number of regressors grows with the number of input dimension leading to increasing computational efforts. Although they have a disadvantage for high dimensional mapping, their simple structure allows easy ECU implantation.

Volterra series model which is an extension of dynamic polynomial models overcome certain disadvantages of polynomial models such as oscillatory interpolation. They have reduced number of regressor due to their structure which only includes linear feedback. However, due to this structure, they struggle to map the system whose nonlinearity strongly depends on output. However, their advantages of linearity of parameters, flexibility, and easily

proven stability criterion using the linear system have made them a popular choice of model for automotive systems.

Non-parametric models are introduced with a focus on multi-layer perceptron networks, as they are suitable for modelling nonlinear dynamic system using external dynamic approach. MLP networks have the advantage of a small number of parameters and can handle uneven data distribution which is common in an external dynamic approach. But they suffer from high training effort and the existence of many poor local optima. However, neural networks are useful for highly nonlinear problems, in the scenario when the underlying function of a system is too complex to define, or when it is too expensive to model it in a conventional way.

An alternative to non-parametric models, the multi-model approach is introduced, which if prior knowledge is available functions as a grey-box model and in the absence of such knowledge functions as black-box models. In this framework, the operating space of the system is decomposed using local models, and these local models represent the dynamics of the system in their specific region of the global space. Two most common decomposition strategy, axes-orthogonal and axes-oblique are presented along with their algorithms LOLIMOT and HILOMOT. The axes-orthogonal splits lead to very fast training time but can be challenging for a high dimensional problem if prior knowledge is not available to reduce the regressor input space. An alternative to this axes-oblique partitioning strategy is introduced, which can robustly model high dimensional problem but becomes computationally expensive and thus, leading to longer training time.

The comparison of parametric models, non-parametric models, and multi-model approach is presented in a tabular form below. The properties of the models chosen here are based on the criterion for the selection of model architecture introduced in this chapter. The table is dominantly adopted from the description and review in (Nelles, 2001, 2006; Hartmann *et al.*, 2013; Tietze, 2015). The table aids in comparing the model types for identification purpose, for example, if the model is to be selected based on training speed, LOLIMOT models are very fast, HILOMOT and Polynomials are fast, but MLP models require longer time compared to the others. Thereafter, other model selection criterion could be compared to make an informed decision about the model type to be selected. This table along with the review of different modelling techniques enabled the selection of the modelling approach suitable for the surrogate modelling of virtual air path system. The influence of this review on adaptation of identification method is discussed in the following chapter and the selected methods along with the justification of choice is presented in 4.4.1.2.

Table 3.3: Summary of modelling techniques (**++/--** = property very favourable/ undesirable)

Properties	Polynomial	MLP	LOLIMOT	HILOMOT
Interpolation behaviour	**-**	**+**	**0**	**+**
Extrapolation behaviour	**--**	**0**	**++**	**+**
Local changing dynamics	**--**	**-**	**++**	**++**
Accuracy	**0**	**++**	**+**	**++**
Smoothness	**-**	**++**	**+**	**+**
Noise sensitivity	**+**	**++**	**++**	**+**
Parameter estimation	**++**	**--**	**++**	**+**
Structure optimisation	**0**	**-**	**++**	**++**
Online adaptation	**-**	**--**	**++**	**++**
Training Speed	**+**	**--**	**++**	**+**
Evaluation Speed	**0**	**+**	**+**	**0**
High Dimensional mapping	**-**	**++**	**0/+**	**+/++**
Interpretation	**0**	**--**	**++**	**+**
Incorporation of prior knowledge	**-**	**--**	**++**	**+**
Incorporation of constraints	**-**	**--**	**++**	**+**
Usability	**0**	**-**	**++**	**++**
Memory requirement	**++**	**+**	**0**	**+**
Effort for ECU implementation	**++**	**+**	**+**	**0**
Iterative modelling	**--**	**--**	**++**	**++**
Noise variations	**--**	**--**	**+**	**+**
Large data sets	**++**	**0**	**+**	**0**

Chapter 4 Research Methodology

The main aim of this research is to develop a framework for Hybrid Dynamic Modelling of engine emissions based on MPES platform and evaluate the performance of dynamic modelling techniques, for the system modelling task, based on the Multi-Physics Engine Simulation Platform (MPES) platform. Underpinned by the critical review of the related work and literature presented in Chapter 2 and Chapter 3, this chapter defines the research methodology for the work presented in this thesis. The chapter is organised as follows:

- Outline the Diesel engine case study.
- Describe the Multi-Physics Engine Simulation Platform.
- Describe the research methodology for hybrid dynamic modelling of engine emissions based on the MPES Platform.
- List of toolboxes and software packages used to conduct the research.
- Provide the implementation plan for the research methodology.

4.1 Diesel Engine Case Study

The engine case study for this research was a 2.0 litre Diesel engine and the basic information regarding this engine is tabulated in Table 4.1. Engine test data was available from the Sponsor Company, collected from hot steady state testing, based on experiments conducted at a set of 29 pre-defined engine speed-load reference points. The operational domain covered by these test points is presented in Figure 4.1.

Table 4.1: Diesel Engine Basic Information.

Parameter	Value
Bore	83 mm
Stroke	92.35 mm
Connecting Rod Length	140 mm
Compression Ratio	15.5
Emissions Standard	Euro 6c
Peak Power	130 kW @ 4000 RPM
Peak Torque	430 Nm @ 1750 – 2500 RPM

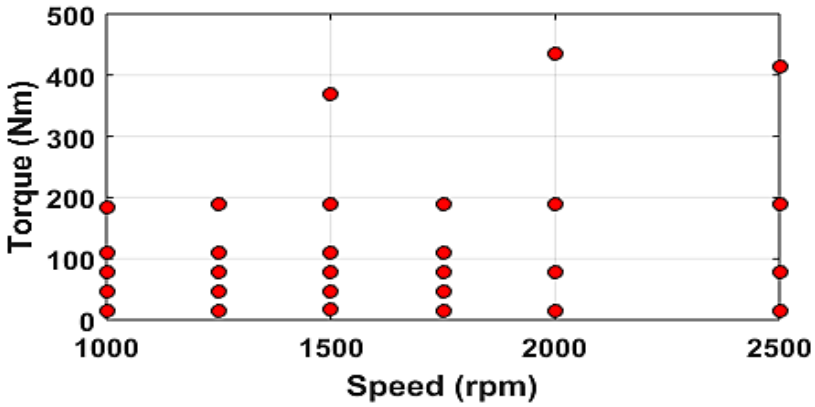

Figure 4.1: Steady State Calibration Reference Points.

In addition to this, New European Drive Cycle (NEDC) data measured on a transient engine dynamometer test facility was also available. The operational domain, in respect of speed and load, covered by the NEDC drive cycle is illustrated in Figure 4.2.

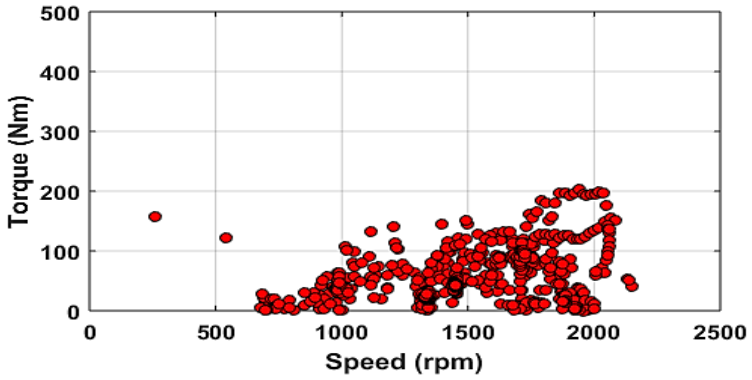

Figure 4.2: NEDC drive cycle operational domain.

As the study is carried for hot operation, therefore, engine speeds below 1000 rpm and torque below 20 Nm were not considered. The region of interest in drive cycle data of the Diesel engine is depicted by the dashed line in Figure 4.3, and the operating range is listed in Table 4.2.

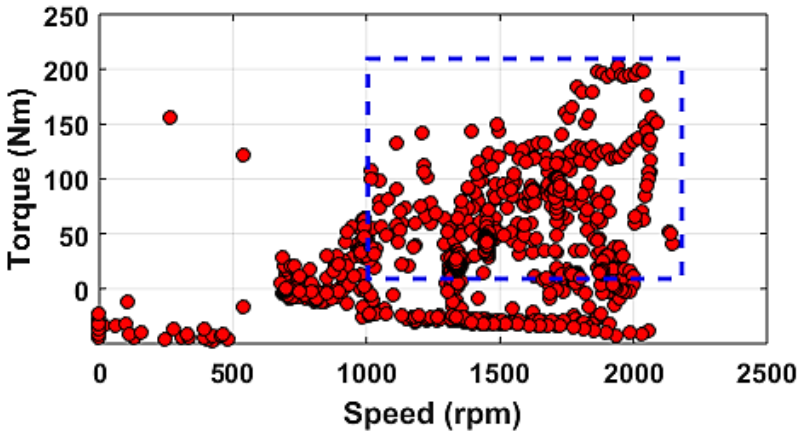

Figure 4.3: NEDC drive cycle region of interest.

Table 4.2: Operational limits of drive cycle data.

Operational Inputs	Units	Range
Speed	rpm	1000-2250
Torque	Nm	20-220

4.2 Multi-Physics Engine Simulation (MPES) Platform

The MPES Multi-Physics Engine Simulation Platform was originally developed by Korsunovs (2017) at the University of Bradford in collaboration with the Sponsor Company. The motivation behind this platform arises from the lack of complete virtual engine modelling systems, which are both efficient and cost effective to be used at early stages of engine development. The complete

engine modelling system in here refers to combined air path and combustion process.

There are many examples available in the literature regarding air path system modelling such as geometry based detailed models (Wu *et al.*, 2011; Ahmed, 2013), and mean value models (Skogtjarn, 2002; Jung, 2003; Wahlström and Eriksson, 2011) . For engine combustion model, generally, detailed modelling is adopted due to the complex dynamics resulting from the interaction of chemical processes, thermodynamics and fluid dynamics. The review of these models has been presented in (Themi, 2016; Unver *et al.*, 2016; Korsunovs, 2017).

The detailed models of air path system, generally one dimensional (1D) models, provide an accurate description for engine development phase (Wu *et al.*, 2011), but are slower than real time (Winterbone and Yoshitomi, 1990; Tietze, 2015). To obtain real-time capable mode, they are used in reduced form (Unver *et al.*, 2016), which leads to a limitation in prediction capability.

The detailed engine combustion model such as three-dimensional computational fluid dynamics can provide high fidelity results, but they require high computational effort in terms of development and simulations. The alternative to this, reduced One-dimensional fluid dynamics model, have the capability to run faster but have limited prediction capability. Furthermore, there are data-driven models (Burke *et al.*, 2013; Sakushima *et al.*, 2013; Sequenz, 2013; Cheng *et al.*, 2017) which are extremely fast and robust, but

these are not suitable during development phase due to their dependency on the engine testbed data.

To address these challenges, based on the MPES platform, a steady-state based strategy was proposed (Korsunovs, 2017) to develop a surrogate model for the SRM to enable real-time simulation of engine emissions. The framework developed is illustrated in Figure 4.4.

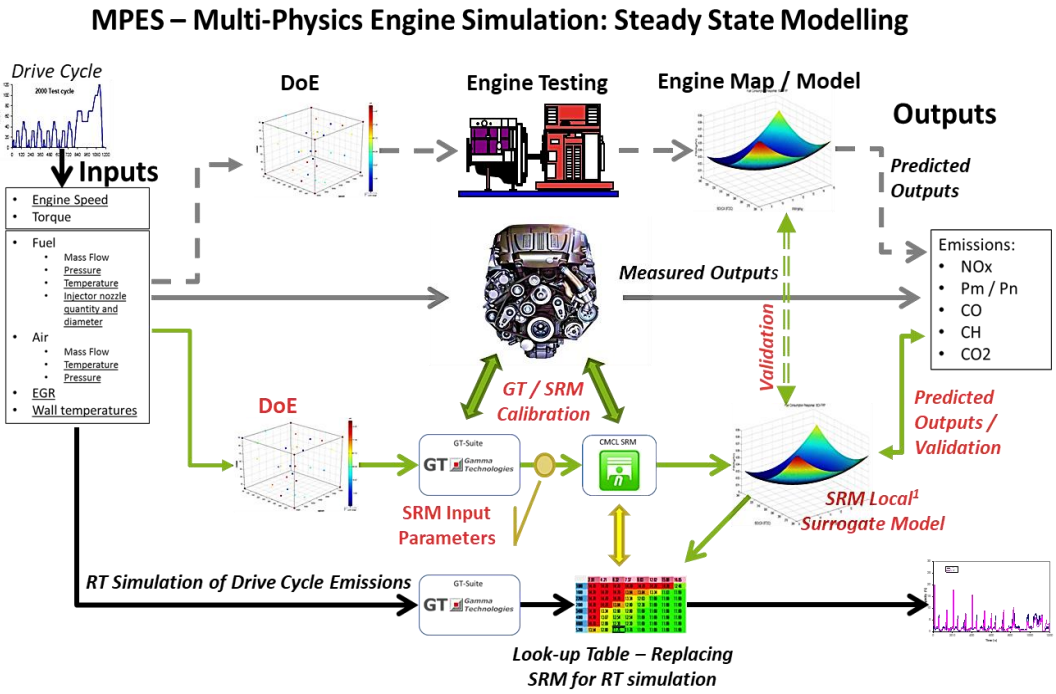

Figure 4.4: Multi-Physics Engine Simulation (MPES) Platform- Steady State approach (Korsunovs, 2017).

The principle of the approach behind the framework is to replace engine testing as the basis for mapping and calibration experiments (illustrated as a Model-Based Calibration (MBC) approach at the top of the diagram in Figure 4.4 with a virtual engine simulation framework as a multi-physics simulation platform – MPES, coupling airpath simulation modelling (based on GT) with

combustion chemistry solver (SRM). The engine mapping and calibration strategy based on the MPES platform is in principle similar to the MBC strategy of running steady-state experiments on a physical engine. In order to support real-time simulation capability based on the MPES platform, Korsunovs (2017) proposed the development of a local (in relation to the engine speed-load point tested in the steady-state procedure) surrogate model for the slower SRM solver, and the use of lookup tables for emissions (NOx in particular) replacing SRM in the real-time simulation.

The key modelling elements of the MPES framework are described in more detail in the following sections.

4.2.1 Air Path System Model

The air path system, illustrated as GT-Suite block in Figure 4.4, is modelled as 1D (one-dimensional) fluid dynamics model using GT-Suite commercial software package (developed by Gamma Technologies). This model accounts for the processes which occur outside the engine cylinder, such as turbo-compressor assembly, inlet and exhaust valves, air flow through the air path. The GT-Suite engine model represents the virtual air path system and is responsible for providing inputs to the combustion model. The GT-Suite engine model can run real-time, depending on the complexity of the model, while being able to meet the accuracy demand. The virtual air path model was calibrated against physical engine data collected at the test points illustrated in Figure 4.1.

4.2.2 SRM Combustion Process Modelling

The combustion process was modelled using the CMCL SRM environment, which describes the complex phenomena occurring inside the cylinder. The model types which are generally used to represent the combustion process such as empirical, three-dimensional CFD, one dimensional CFD either do not capture the detailed phenomena or are computationally expensive or does not provide accurate prediction. To address this, the combustion system was modelled using the Probability Density Function (PDF) based stochastic thermodynamic model (Zero-dimensional). The model was developed using a commercial software package, Kinetics and SRM Engine Suite designed by Computational Modelling Cambridge Ltd. (CMCL), and hereafter will be referred to as SRM. The SRM model, virtual combustion system, can provide reasonably fast computation using the reduced chemistry mechanism, with a computation time of 2-3 minutes per cycle, while still preserving good prediction capabilities (Coble *et al.*, 2011).

Although being relatively faster compared to the expensive three-dimensional computational fluid dynamics model, the SRM model does not have the capability to run real time. Therefore, to support real-time drive cycle engine simulation a surrogate model for SRM is developed. The initial approach for surrogate model development was based on planning and running DoE experiments with data collected from the SRM engine model at set engine speed-load points, covering the engine operation domain (domain illustrated in Figure 4.1).

Before the surrogate model could be generated, the SRM model (virtual combustion system) needed to be calibrated and validated. The model calibration goal was to derive settings for the SRM parameters, such that a good correlation can be obtained with the engine testbed measurements and SRM model outputs. One set of values for the whole domain was chosen instead of a different set of values at each set point (steady state speed-load points), as it would reduce the cost and complexity associated with the engine model building process. To proceed with the calibration task, a detailed sensitivity analysis of the SRM model outputs, engine emissions (NOx) prediction and in-cylinder condition, in relation to both external and internal SRM parameters was carried out (Korsunovs, Campean, Pant, Garcia-Afonso and Tunc, 2019).

The external parameters derived from the engine data can be categorised into two main categories: constant and speed-load specific parameters. Constant parameters, such as engine geometry/fuel/atmosphere, only need to be defined once for a specific engine, speed-load specific parameters need to be defined for every reference/set point. The external parameters, both constant and speed-load specific, are listed in Table 4.3.

The internal SRM parameters are associated with thermodynamic sub-models, such as turbulence model, injection model, evaporation model, and heat transfer model, and are listed in Table 4.4.

Table 4.3: SRM Model External Input Parameters selected for sensitivity analysis (Korsunovs *et al.*, 2019).

Engine Geometry [*constant for every engine*]	Simplified cylinder geometry, including: Bore and stroke; Length of the connecting rod; Compression ratio; Wrist pin offset; Crevice dimensions
Intake Mixture Static [*Constant for every engine/location*]	– Air chemical composition – EGR composition settings
Intake Mixture Dynamics [*Speed-load point specific*]	– Intake mixture temperature at IVC – Intake mixture pressure at IVC – EGR mass fraction
Fuel System Static [Constant for every engine and fuel]	– Fuel chemical composition – Injector nozzle diameter and number – Fuel properties (density, vaporisation enthalpy, surface tension, viscosity at 30°c, temperature)
Fuel System Dynamics [Speed-load point specific]	– Injection pressure – Injection rate profile
In-cylinder Wall Temperatures [Speed-load point specific]	– Piston, cylinder head, cylinder liner wall temperatures

Table 4.4: SRM Model Internal Input Parameters selected for sensitivity analysis (Korsunovs *et al.*, 2019).

Internal Parameters	**Symbol**	**Thermodynamic Sub-Model**	**Intended Purpose**
Evaporation Constant	(λ) - Lambda	Fuel Evaporation Model	Controls evaporation rate of fuel
Injection Alpha	α	Injection model	quantifies the charge stratification extent
End of Injection Lag	-	-	account for the turbulence induced by the combustion by adjusting the amount of crankshaft-angle degrees
Woschni Constant	C_1	Heat Transfer Model	adjusts the effect of the mean piston speed on the heat transfer
Turbulence Parameter (during injection)	$C_{\varphi(injection)}$	Turbulence Model	adjusts the intensity of turbulence in the thermodynamic model during injection events
Turbulence Parameter	C_{φ}	Turbulence Model	adjusts the intensity of turbulence in the thermodynamic model through the rest of the cycle.

In a sensitivity analysis carried out in (Korsunovs *et al.*, 2019), it was found that the inlet pressure, inlet temperature, and EGR mass fraction have a significant effect on the NOx prediction while the other external parameters did not have any effect or not significant enough.

In the case of SRM internal parameters, evaporation constant (λ) and turbulence parameter during injection $(C_{\varphi(injection)})$ had a significant effect on NOx prediction. While the other internal parameters either had a small effect

or negligible effect**.** The set of global parameters achieved from the optimisation are tabulated in Table 4.5.

Table 4.5: Global optimum solution for Internal SRM parameters (Korsunovs *et al.*, 2019).

Internal SRM Parameter	**Global Setting for SRM Internal Parameters (Optimal Solution)**
Evaporation Constant	0.207
Injection Alpha	60
End of Injection Lag	1.357
Woschni Constant	8.786
Turbulence Parameter (during injection)	6.095
Turbulence Parameter	3.024

The SRM combustion model generated using these set of parameters, presented a good correlation between simulated and experimental (measured on the test bench for steady-state test points) in-cylinder pressure traces and these are illustrated in Figure 4.5. For apparent heat release rate (aHRR) profiles, it was observed that trends in profiles are predicted well across low/medium load but at high load during main injection aHRR rises slightly asynchronously with the experimental data. Also, at some speed-load points (2000 & 2500 RPM-high load), it was observed that model does not perform very well in relation to the pilot injection; as seen in Figure 4.5, where the SRM model struggles to identify the aHRR from the pilot injection. In other words, the pilot injection does not ignite as quickly as it is required which effects combustion speed and leads to delay in combustion (in comparison to experimental). However, general trends were captured accurately and results aligned well with the experimental data (Korsunovs *et al.*, 2019).

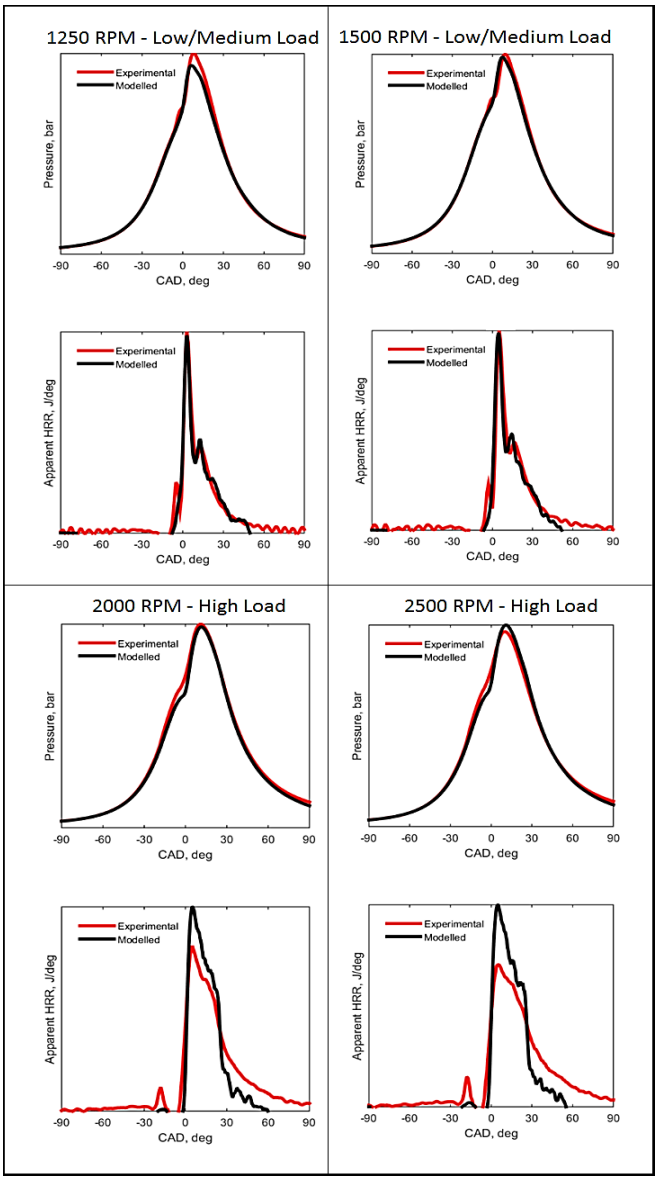

Figure 4.5: In-cylinder conditions correlation for SRM combustion model (Korsunovs, Pant *et al.*, 2019).

4.3 Proposed Methodology: MPES Hybrid Dynamic Modelling Approach

The acknowledged means of addressing the challenge of test bench costs, as outsourcing a test bed can cost > £2000 per day (Lacey, 2012; Siemens, 2012; Mohile, 2017), during the engine development is the increased use of model-based methodologies (Röpke *et al.*, 2012; Fang *et al.*, 2016) and the virtual engine simulation platform (MPES) proposed by Korsunovs (2017)

aligns well with this goal of the automotive industry. It is based on the well-established steady state approach which is widely used across the automotive industry and yields satisfactory results (Korsunovs, Pant *et al.*, 2019).

However, due to multiple engine operating modes (steady-state and transient) and challenges imposed by legislation, such as transient emission regulations/ fuel economy reduction/ optimising driveability for load changes, interest in techniques for modelling dynamic behaviour has risen. This trend was observed in Chapter 3, where literature review revealed the increasing efforts placed on investigation of dynamic calibration methodologies (Nelles, 2001; Knaak *et al.*, 2007; Röpke *et al.*, 2012; Sequenz, 2013) and application of dynamic experiments and modelling techniques for system modelling task (Baumann *et al.*, 2008, 2009; Hametner and Nebel, 2012; Burke *et al.*, 2013; Fang *et al.*, 2016; Cheng *et al.*, 2017; Heinz and Nelles, 2017). The reason for these developments was underpinned by the possible advantages of these techniques such as faster data capture as no settling time is required; improved model fidelity by capturing dynamic behaviour; inherent interpolation, and also the fact that point-based calibration process would be expensive to represent the transient behaviour, as data need to be captured at an increased number of reference point for each of the multiple control parameters.

Furthermore, the current legislative drive cycles have become stricter, for an example while NEDC drive cycle has 2 phases of urban and non-urban driving (Isermann, 2014), WLTP (Worldwide Harmonised Light Vehicle Test Procedure) has four more dynamic phases and has longer cycle time (ACEA,

2017). Also, Real Driving Emissions (RDE) test has added to the complexity, and future amendments will be more rigorous (ACEA, 2017). Therefore, to incorporate the transient behaviour into virtual engine simulation framework and still being able to meet the industrial requirement (quality, cost, and time) a hybrid dynamic modelling approach for modelling engine emissions based on MPES is proposed and is illustrated in Figure 4.6.

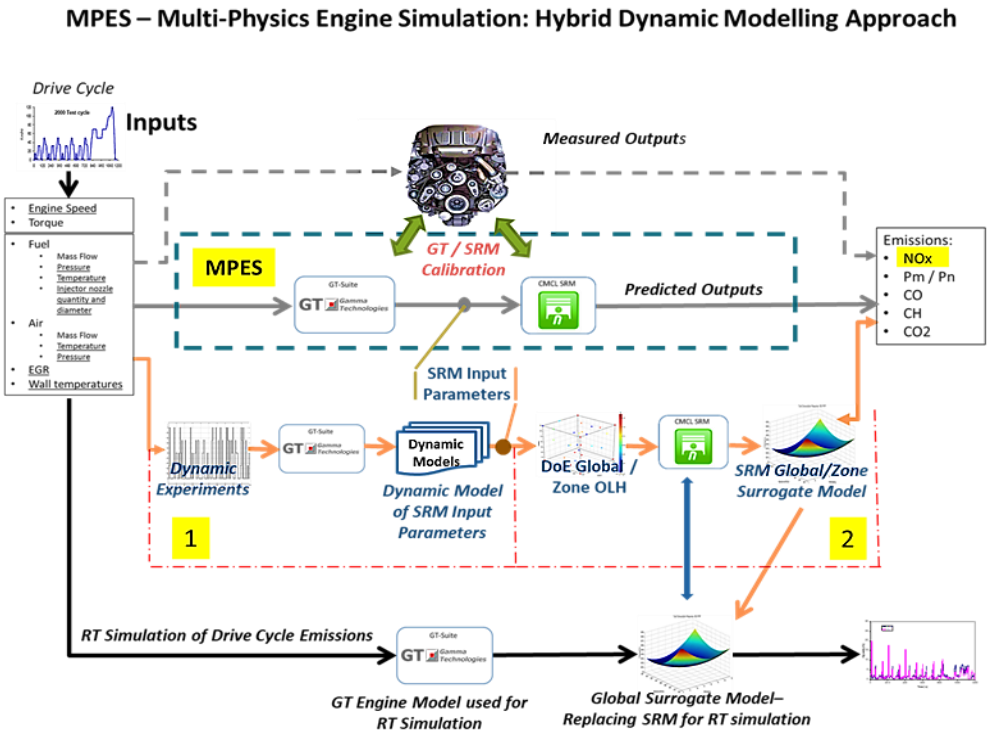

Figure 4.6: Hybrid dynamic modelling approach based on MPES platform.

The fundamental difference between this approach and the steady-state based procedure described in Figure 4.4 is that the aim here is to develop a global meta-model for engine out emissions from the mapping and calibration experiments. The rationale for this is that the global metamodel could have better capability for accurate transient modelling for real-time drive-cycle simulation experiments compared to the look-up table derived from steady-

state experiments suggested in Figure 4.4. A research challenge is to design an efficient experimentation strategy to enable the development of a global metamodel at a cost comparable with the steady state experiments performed to develop the SRM surrogate model. To this end, a hybrid meta-modelling strategy is proposed, which couples two fundamentally different types of metamodeling strategies for the 2 structural parts of the MPES framework:

- A dynamic modelling / identification technique is deployed to develop a surrogate for the GT-Suite dynamic airpath simulation model of the Diesel engine;
- A global exploration DoE experiment, based on space-filling OLH DoEs, to develop a surrogate model for emissions – focussing on NOx engine-out emissions, based on the SRM model.

The integrated combination of the dynamic experimental modelling deployed to the real-time GT airpath model with the global OLH DoE experiment deployed on the SRM individual cycle emissions solver justifies the hybrid nature of the proposed approach. The surrogate model for the dynamic GT airpath model is needed to provide a fast mean value estimate for the inputs required for the SRM model (listed in Table 4.3). This delivers a considerable time saving, as otherwise, the GT model would have to be run for a considerable amount of time (equivalent to reaching stable steady state operation) to deliver a robust input for the global SRM experiments.

The following sections discuss the method employed for the proposed hybrid meta-modelling strategy.

4.4 Research Methodology

The hybrid dynamic modelling approach, illustrated in Figure 4.6, can be separated into two main stages and each stage represent the tasks undertaken for the successful development of the approach. The two stages are as follow:

1) Development of Diesel engine dynamic air path model (labelled as 1 in Figure 4.6)
2) Development of surrogate SRM combustion process model (labelled as 2 in Figure 4.6)

4.4.1 Development of Diesel Engine Dynamic Airpath Model

4.4.1.1 Simulation Experimental Setup

The task of developing the dynamic air path model was approached by partitioning of the operational domain of the drive cycle data, illustrated in Figure 4.3, into smaller sections, zones, based on engine speed. Each zone covered the interval in between steady-state test points (Figure 4.1), i.e. 1000-1250/1250-1500 rpm etc. However, to allow smooth interpolation and gradual transition in between the global models identified at each zone, an overlap between the zones (soft partitioning) was introduced (Johansen and Foss, 1997, 1998). The segmentation of the drive cycle data is illustrated in Figure 4.7. The rationale for this is that the by decomposing modelling problem into zones, compliance to constraints for dynamic experiments can be taken into account more easily (Hametner and Nebel, 2012) and global models at zones could have better accuracy relative to global models generated on a wide

range, as experiments can be planned to suit the needs of a particular zone (Johansen and Foss, 1997).

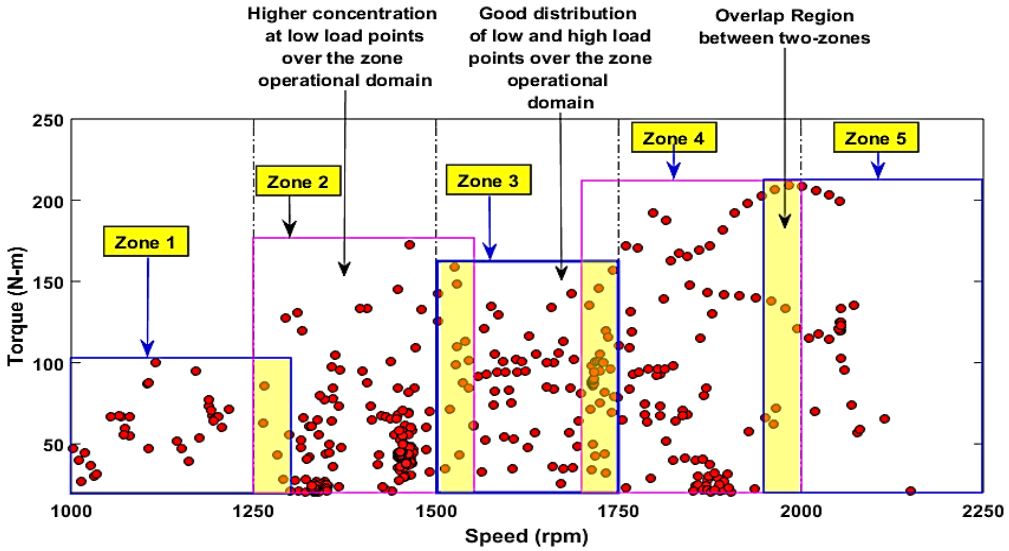

Figure 4.7: Operational domain partition of the drive cycle based on engine speed.

The benefits of segmenting the operating domain to acquire global-zone models, i.e. global models are identified for a zone rather than the entire operating range, are as follow:

- Global-Zone modelling allows consideration of different local noise level or sensitivities in the different operating regime.

- For global modelling, in general, the focus is to reduce the prediction error globally, the model focus would be on those regions of the input space where prediction error is large while other regions are neglected. However, global-zone modelling would overcome this drawback as training data is generated with a focus on the zone operating range.

- This approach can also allow incorporation of inputs which are only active in the certain operating region. However, in this study, this is not applicable as the same number of input parameters are considered across all zones.

- The design of dynamic experiments procedure becomes less complicated when compared to global modelling, as only local interactions are considered.

For the purpose of this study, zone 3 (illustrated in Figure 4.7) was selected. The reasons for specifically choosing zone 3 are as follows:

- An accurate injector model (Jaguar Land Rover, 2017) for the case study was available. The information regarding injection characteristics from this model was communicated by the sponsor company in the form of injection profiles. The injection profiles for speed and load points, covering the range of 1500-1750 rpm (engine speed) and 0-200 Nm (torque), were available.
- Additionally, it can be observed from Figure 4.7, that there is a good distribution of both low and high loads across the operating range of this zone. This would be beneficial to represent the effectiveness of the Hybrid dynamic modelling framework, even though the implementation of the framework is carried out in a smaller region. The operating range of the selected zone is tabulated in Table 4.6.

Although the modelling task for framework was carried out on a narrow range of available drive cycle data, it can be scaled to the entire operating range or

can be applied to any other drive cycle; given an accurate injector model and drive cycle data is available.

Table 4.6: Operating range of case study for dynamic modelling.

Operational Inputs	Units	Range
Speed	rpm	1500-1750
Torque	Nm	20-160.6

4.4.1.2 Design of Dynamic Experiments and Model Architecture selection

The literature review showed, section 2.2, that there are two ways to generate dynamic experiments; model-based approach and model-free approach. The model-based approach is implemented If the model structure is known a priori, and optimal criterion such as D-optimal can be used to generated dynamic experiments. The use of optimality criteria reduces the measurement effort for signal design and has been attempted in (Deflorian and Zaglauer, 2011; Fang, 2012). However, in this study, the knowledge of model structure is not known beforehand, and thus, the model-free approach is utilised.

In regard to the model-free approach, there are three common dynamic signal designs found in literature and have been introduced in section 2.2.2 , PRBS, APRBS, and chirp. All the excitation signal designs introduced, i.e. PRBS, APRBS, and chirp, were generated and their performance was compared for the selected case study. The rationale for this is that in literature, the signal design is generally pre-selected for the modelling application (Guhmann and Riedel, 2011; Burke *et al.*, 2013; Sakushima *et al.*, 2013) but the effect of the

different signal design on different modelling techniques is not reviewed. While in literature there are studies which review the effect of different signal designs, (Röpke *et al.*, 2012; Tietze, 2015) but either the sample size of signal designs was not same to arrive at the conclusive result, or it was implemented on a pre-selected modelling technique.

Accordingly, the research objective of implementing an efficient dynamic experiment is to develop a strategy which takes into consideration effectiveness of the different dynamic signal designs (excitation signals) on the non-linear dynamic modelling techniques, for development of surrogate air path model. Therefore, all three excitation signals were chosen to be implemented during the development of dynamic air path model.

The model structures implemented for the development of dynamic air path are Neural Networks and Local linear neuro-fuzzy models. These model structures were introduced in chapter 3, section 3.3.3 and section 3.3.5 respectively. The model selection was based on the current goal of the industry is to optimise the trade-off between quality, timing, and costs (Atkinson and Mott, 2005; Röpke *et al.*, 2012; Ostrowski *et al.*, 2017). To accomplish this goal and objectives planned for the case study engine modelling techniques with the benefit of speedy evaluation, high accuracy and suitable for real-time applications are needed. As per the review of literature in section 0 and review of the application of modelling techniques in Table 3.2, there are three most common model types available (Röpke *et al.*, 2012): Neural Networks, Volterra series, and Local Linear Neuro Fuzzy models. Volterra series models have been successfully implemented for automotive

applications (Guhmann and Riedel, 2011; Burke *et al.*, 2013; Sakushima *et al.*, 2013). However, the challenge associated with the Volterra series model is that the number of parameters for Volterra kernel functions representations is very large (Cheng *et al.*, 2017). In other words, they have large numbers of terms as a degree of polynomials which results in a higher dynamic order of the model. And for the selected dynamic representation (see section 3.2.2), external dynamic approach, the higher dynamic order increases the dimensionality and number of delayed inputs, which leads to larger regression matrix and increased number of parameters (refer to section 3.2.3). Thus, making the regression process more complex (Burke *et al.*, 2013). Therefore, Neural Networks and Local Linear Neuro Fuzzy models were selected which do not share the disadvantage associated with Volterra series models and have advantages of high accuracy, fast evaluation time, data smoothing ability and high dimensional mapping, refer Table 3.3.

For LLNF modelling, LOLIMOT algorithm was used to identify the dynamic air path model due to its advantages of smooth interpolation, fast parameter estimation, and fast training times. The identification of LLNF could as well be based on HILOMOT algorithm, as it provides a robust estimation of the system. However, it is not selected here due to being computationally expensive when compared to LOLIMOT, owing to nonlinear optimisation of validity function parameters (Klein *et al.*, 2013). The LMN toolbox (Hartmann *et al.*, 2012) was used for developing LOLIMOT models, and it is a script based toolbox which integrates LOLIMOT model objects to the MATLAB

library and allows modelling task to be carried out in the MATLAB software environment.

For Neural Networks, Nonlinear Autoregressive with External (Exogenous) Input (NARX) type of model structure was used. The reason for this is that this model structure is capable of accommodating the dynamics associated with the system by feeding the past values of the network output into the input layer of the network (Hagan and Demuth, 1999; Deng *et al.*, 2013). The Neural Network toolbox in MATLAB has a graphical user interface which allows implementation of NARX model structure for time series prediction or it can also be done through a script-based approach which allows incorporation of more information for modelling task.

4.4.1.3 Dynamic Air Path Modelling Process

Before deploying the dynamic modelling techniques, the dynamic signals were implemented on GT-Suite engine model. A pre-calibrated GT-Suite engine model for the case study engine was available from the sponsor company. This was a Fast Running Model (FRM), i.e. capable of running real time, and was developed based on the one-dimensional fluid dynamics model. The GT-engine model includes physical models to represent the inlet, exhaust, compressor-turbocharger assembly, cylinders etc. These components of the engine are linked together by connection lines, which mirrors the flow path of the engine. The layout of the GT-Suite engine model for the case study engine is illustrated in Figure 4.8.

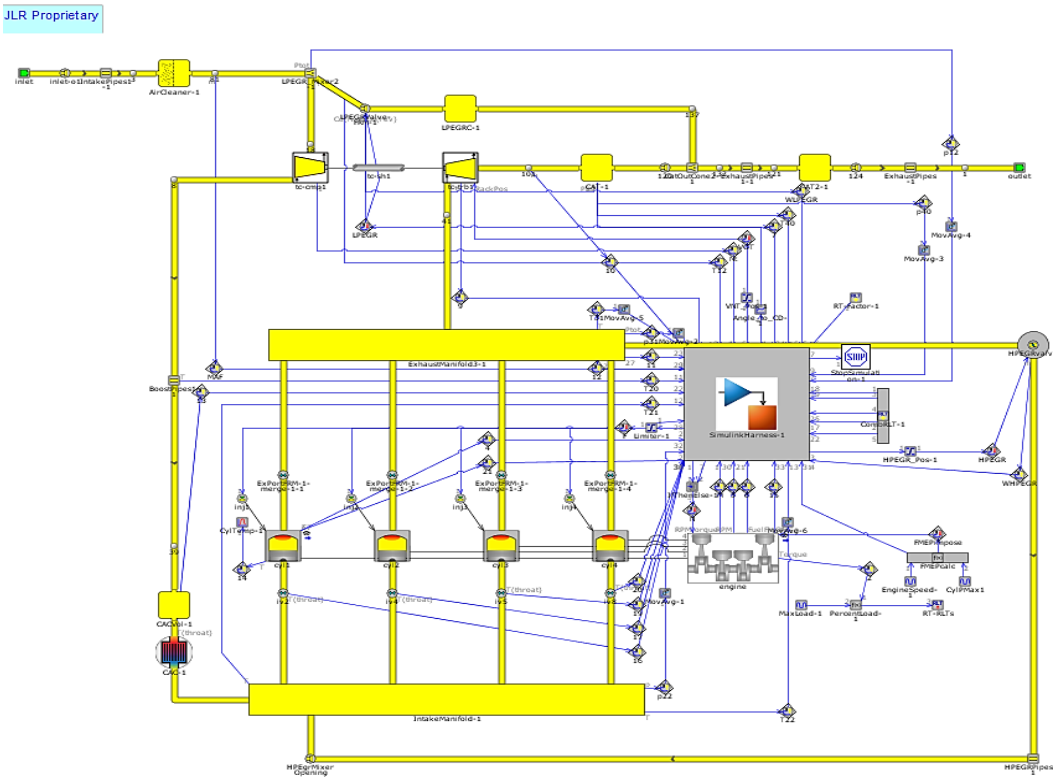

Figure 4.8: GT-Suite Diesel engine model for case study engine.

The simulation of the GT-engine model is controlled through a harness developed by sponsor company in MATLAB/SIMULINK software environment. The harness provides the model with quantities such as desired low/high-pressure EGR valve position (for EGR system), desired VGT Position (for boost control), desired fuel flow, desired engine speed etc., through series of engine maps and controller. The SIMULINK harness only needs the desired engine speed and torque to generate these inputs for GT-engine model. An overview of the harness and ECU is illustrated in Figure 4.9 and Figure 4.10 respectively.

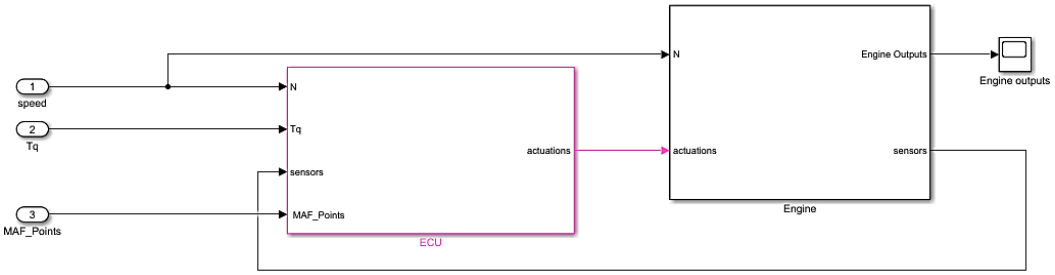

Figure 4.9:Overview of SIMULINK harness.

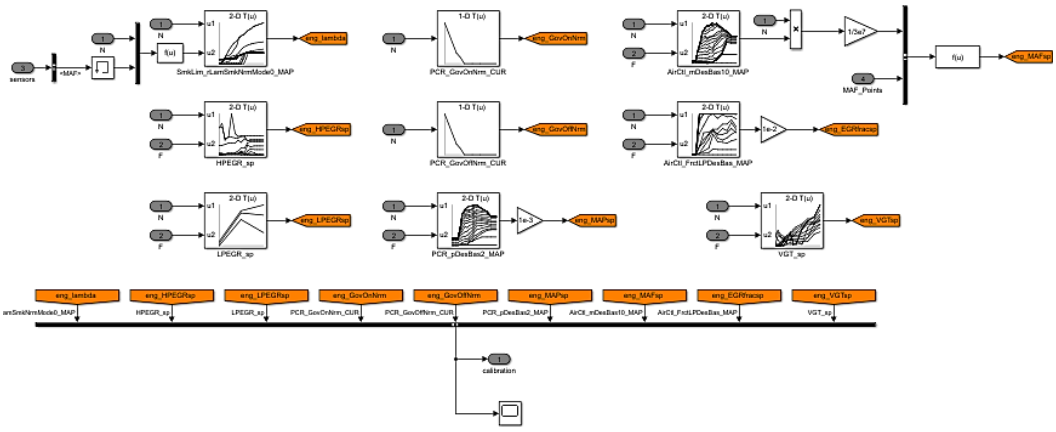

Figure 4.10: Engine control unit in SIMULINK harness to provide input variables to GT-Suite engine model.

The process of identification of dynamic air path for the virtual Diesel engine using the selected model architecture, Local Linear Neuro-Fuzzy Models and Neural Networks, is illustrated in Figure 4.11 and Figure 4.12 respectively. The models developed for the identification of dynamic air path system of the virtual Diesel engine were compared based on their statistical performance and trend analysis. The statistical criteria chosen to compare the results is Root Mean Square Error (refer to section 3.2.5).

Step 1: Define Model Inputs and Outputs

Step 2: Start with the Initial Model

Construct the validity function, if no initial input space partitioning available set number of Local Linear models (LLM), M = 1 with validity function $\phi_1(u) = 1$. Estimate a global linear model $y = w_0 + w_1 x_1 + \cdots + w_n x_n$,.

Step 3: Find Worst LLM

For ***i*** = 1,…,M % LLM

a) Estimate Local Loss Function

$$I_i = \sum_{j=1}^{N} e^2(j)\phi_i(u(j))$$

b) Find the worst performing local model, i.e. $\max(I_i)$, and denote $'k'$ as the index of this worst LLM.

Step 4: Further refine worst LLM $'\boldsymbol{k}'$

a) Cut the hyper-rectangle into two halves, division in all dimension are tried (dim = 1,…,p).
b) Estimate local linear models for each half.
c) Calculate the approximation error (output error) for the model with this cut.
d) Determine which division, in p alternatives dimensions, has led to the smallest approximation error and select that division.

Step 5: Implement Best Division

Perform the division selected in step 3. Place a weighting function within each centre of both hyper-rectangles. Set standard deviations of both weighting functions proportional to the extension of the hyper-rectangle in each dimension. Apply the corresponding estimated local linear models (from 3b). The number of LLM is incremented $\boldsymbol{M \rightarrow M + 1}$

Step 6: Test for Convergence

Convergence: If the termination criterion is met then stop, else go to step 2. Repeat until termination criterion are met.

Figure 4.11: Pseudocode for Local Linear Neuro Fuzzy Modelling technique.

Step 1: Define Input and Target

u = 1: n; % input data for all inputs dimension

t = 1:m; % output data, response to be modelled

Step 2: Define Network

number of hidden layers

input and feedback delays

Training Algorithm

Number of Epochs

Step 3: Training

Loop 1:

for ***i* =** 1: k % k-number of neurons

Randomly Initialise weight vectors and thresholds.

Loop 2:

for j = 1: p % number of training iterations

Initialise network training and train network for 1 iteration

Calculate approximation error = network output – target

$$\mathrm{MSE} = \frac{1}{\mathrm{N}}\sum_{\mathrm{i}=1}^{\mathrm{N}}(\mathrm{y_i} - \hat{\mathrm{y}}_\mathrm{i})^2$$

Error goal achieved, then stop and update the model with calculated weights. If not, proceed to next iteration $\boldsymbol{j \rightarrow j + 1}$

If termination criterion not met after p iterations proceed to loop 1.

End of loop 2

If termination criterion not met after p iterations in loop 2, proceed to next iteration in loop 1, $\boldsymbol{k \rightarrow k + 1}$.

End of loop 1

Step 4: Test for Convergence

If the network does not converge after completion of loop 1 and loop 2, redefine the network in step 2. Repeat until termination criterion met.

If termination criterion met after $\boldsymbol{k \rightarrow k + 1}$, stop and update the model.

Figure 4.12: Pseudocode for Neural Network Modelling technique.

4.4.2 Development of Diesel Engine Surrogate Combustion Model

4.4.2.1 Modelling Methodology

Development of a surrogate model for the combustion process, the second stage of the proposed hybrid dynamic modelling approach, is based on the virtual SRM combustion process model developed for the MPES platform (described in section 4.2.2).

The speed/load specific SRM external parameters, Table 4.3, are provided by the dynamic air path model. To develop a surrogate model global DoEs are planned and run on virtual combustion model, and response surface model is fitted to the collected data. Space-filling OLH DoEs are chosen for the modelling because the virtual combustion system cannot run real time, thus running dynamic experiments would not be possible.

Although steady-state measurements and statistical model structures are employed, they can represent relevant dynamics, given the model inputs are measured dynamically (Sequenz, 2013). As the air path states inputs are provided from the dynamic air path model, the dynamics in engine emission formation will be introduced by the dynamics of the air path.

4.4.2.2 Design of Experiment and Model Fitting

The aim of the design of experiment is to acquire maximum possible information with the least measurement effort. In the case of the combustion model, it is to map the NOx behaviour for the pilot case study, Figure 4.7, with the least possible DoE measurement points.

Given the simulation of SRM combustion process model requires 2-3 minutes per cycle (not capable to run in real time), the approach used in this thesis for the design of experiments is an exploration based sequential DoE framework proposed in (Kianifar et al., 2013). By deploying this framework, the cost associated with the development of surrogate model could be minimised due to its property of terminating introduction of additional test points, once the target accuracy is achieved for the response surface model. Thus, an approximation model can be developed with least possible number of points.

The DoE framework utilised is a Model Building - Model Validation (MB-MV) DoE strategy based on optimal space filling DoEs. The space filling design used is OLH DoEs for both MB and MV experiments. The reason for using OLH design lies in its unique property to cover the entire range of each design variable (Kianifar, 2014). The iterative procedure of this approach is illustrated in Figure 4.13.

This strategy designs both MB and MV DoEs as OLH DoEs, but also ensures that the same space-filling criterion applies for the overall DoE sequence (including all MB and MV test points), i.e. MB+ MV. This is valid through the iterative sequence. This can be explained by using Figure 4.13, for example at start an initial model building experiment (MB1 OLH DoE) of 40 points is planned, followed by a model validation experiment (MV1 OLH DoE) of 10 points. Then a response model is fitted to the MB OLH DoE (40 points), and the quality of the model is evaluated, using certain information criterion, against the MV OLH DoE (10 points). If the model quality is satisfactory, there is no need for further iteration, but if not then the second iteration of DoE is

planned. In the second iteration, a new model validation experiment is generated (MV2), and the model building experiments are the combination of previous model building and model validation experiments (MB1+MV1).

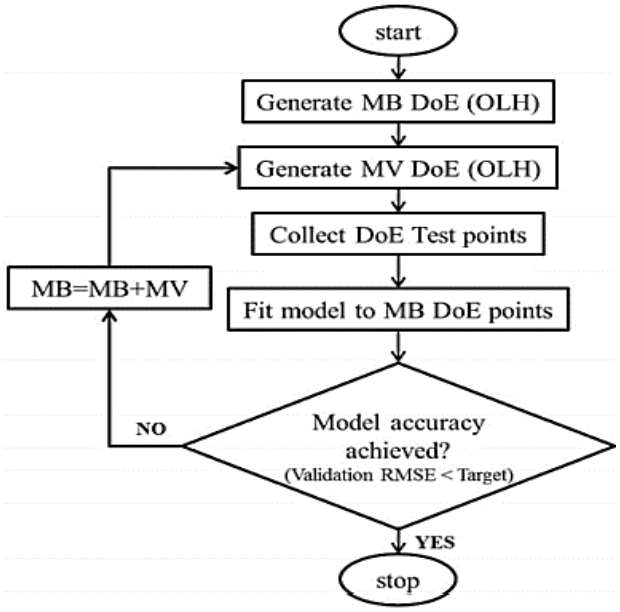

Figure 4.13: MB-MV strategy process description (Kianifar *et al.*, 2013).

The response surface model for combustion model was generated using the Model-Based Calibration Toolbox (MBC) (The Mathworks Inc., 2018). In this research, MBC toolbox was mainly employed as it allows to fit range of statistical models, such as the Gaussian Process model, radial basis function, and hybrid radial basis function to response of interest. These models are available in the toolbox, and due to the fast fitting approximation, multiple models can be fitted before making the decision of the satisfactory model. In addition to this, MBC toolbox provides the functionality of validating the fitted approximation models by employing several statistical metrics such as RMSE, PRESS. The models developed using MBC interface, were compared on their performance by employing a combination of statistical metrics , introduced in

section 3.2.5, such as Root Mean Squared Error (RMSE), Prediction Error Sum of Squares (PRESS), and Validation RMSE, to make the informed decision. Furthermore, the toolbox allows to add boundary constraints to the approximation models such that feasible regions of engine operation can be defined, and it also provides an opportunity to study behaviour of fitted responses over parameters range.

4.4.2.3 Combustion System Surrogate Modelling Process

The process involved in modelling of the surrogate model is described in Table 4.7.

Table 4.7: Modelling Process for Surrogate Combustion Model (Zonal).

1. **Generate a MB-MV OLH DoE for the input parameters if dynamic air path model**
   Generate an initial DoE for parameters as Speed, load, mass air flow.
2. **Process DoE Through Dynamic Air Path Model**
   The dynamic air path model provides the external input required for the combustion model
3. **Simulate Combustion Model**
   Run combustion model to acquire the engine out emission response for both model-building and model-validation DoE.
4. **Fit a Response Surface Model**
   Fit range of statistical model to the response captured for model building DoE.
   Validate the model performance using model validation DoE
   Compare the performance of different models using RMSE, PRESS, and Validation RMSE.
5. **Model Accuracy Not Achieved**
   Proceed with the second iteration of MB-MV OLH DoE, and repeat steps 1-4, until a satisfactory model is acquired.
6. **Model Accuracy Achieved**
   If the satisfactory model is achieved, stop here.

4.5 Evaluation of Hybrid Dynamic Modelling Approach

The final stage in this study was to evaluate hybrid dynamic modelling approach performance and the sensitivity of the model to operating parameters, in terms of effectiveness and efficiency. This was carried out by evaluating the performance of hybrid dynamic modelling approach on the transient drive cycle case study (Zone 3), presented in Figure 4.7.

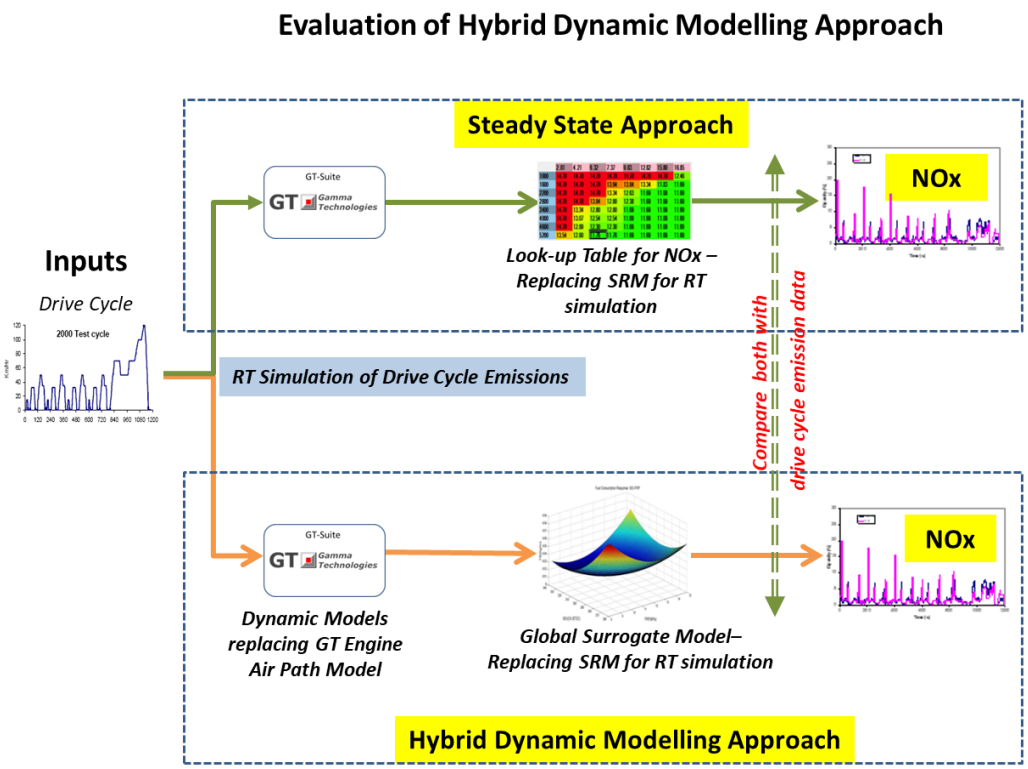

Figure 4.14: Illustration of both steady state and hybrid dynamic modelling approach.

The illustration of the comparison scheme is depicted in Figure 4.14, where on the top of the diagram presents the steady state approach proposed by Korsunovs (2017) which replaces slower SRM model with look-up tables (generated from local surrogate models in relation to the engine speed-load

point tested in the steady-state procedure) for real-time simulation. And the bottom of the illustration presents the hybrid dynamic modelling approach which replaces the slow SRM model with global metamodels.

The performance of the proposed approach will be evaluated in terms of the predictive capability of emissions observed in the drive cycle. The performance will be compared, both with statistical diagnostics and engineering analysis. The comparison in between steady-state approach and hybrid dynamic modelling approach is not intended to establish which approach performs better but is included for comparison in prediction capability with respect to development time.

Indeed, this section examines only one zone of the drive cycle data and is inadequate for comparing the model performance of two approaches (steady state and hybrid dynamic modelling), which should be executed by comparison with experimental data covering a wide range of engine operating conditions. This section adopts a single zone in drive cycle data, as a representative of the possible advantages hybrid dynamic modelling approach could provide regarding the prediction capability and reduction in time for surrogate model development.

4.6 Software Package and Toolbox

Table 4.8: List of software packages and toolboxes utilised during the development process.

Software/Toolbox	Developer	Version	Application
GT- Engine Suite (GT-Suite)	Gamma Technologies	v 2016	• Virtual air path Model • Data Collection
Stochastic Reactor Model (SRM) Engine Suite	Computational Modelling Cambridge Ltd.	v 8.11.2	• Virtual combustion model
MATLAB / Simulink	The MathWorks, Inc.	vR2018a (9.4)	• Model Simulations • Data Processing • Script Designs • Design of Dynamic Experiments
Neural Network (NN) Toolbox	The MathWorks, Inc.	v 11.1	Neural Network Modelling • Training • Validation • Statistical Analysis
Local Model Network (LMN) Toolbox	(Hartmann *et al.*, 2012)	v 1.5.2	Local Linear Neuro Fuzzy Modelling • Training • Validation • Parameter Estimation • Creates Global Models (LMN) from local models
Sequential DoE and Multidisciplinary Optimisation (DoMdo)Toolbox for Engine Experiments	University of Bradford (Kianifar *et al.*, 2013)	NA	• MB-MV sequential Design of Experiments
Model-Based Calibration (MBC) Toolbox	The MathWorks, Inc.	v 5.4	• Fitting approximation models • Defining boundary constraints • Validating approximation models based on statistical metrics. • Engineering analysis based on available visualisation tools.

4.7 Implementation Plan

The implementation of the methodology described in this chapter has been summarised in Figure 4.15 and provides an overview of its application.

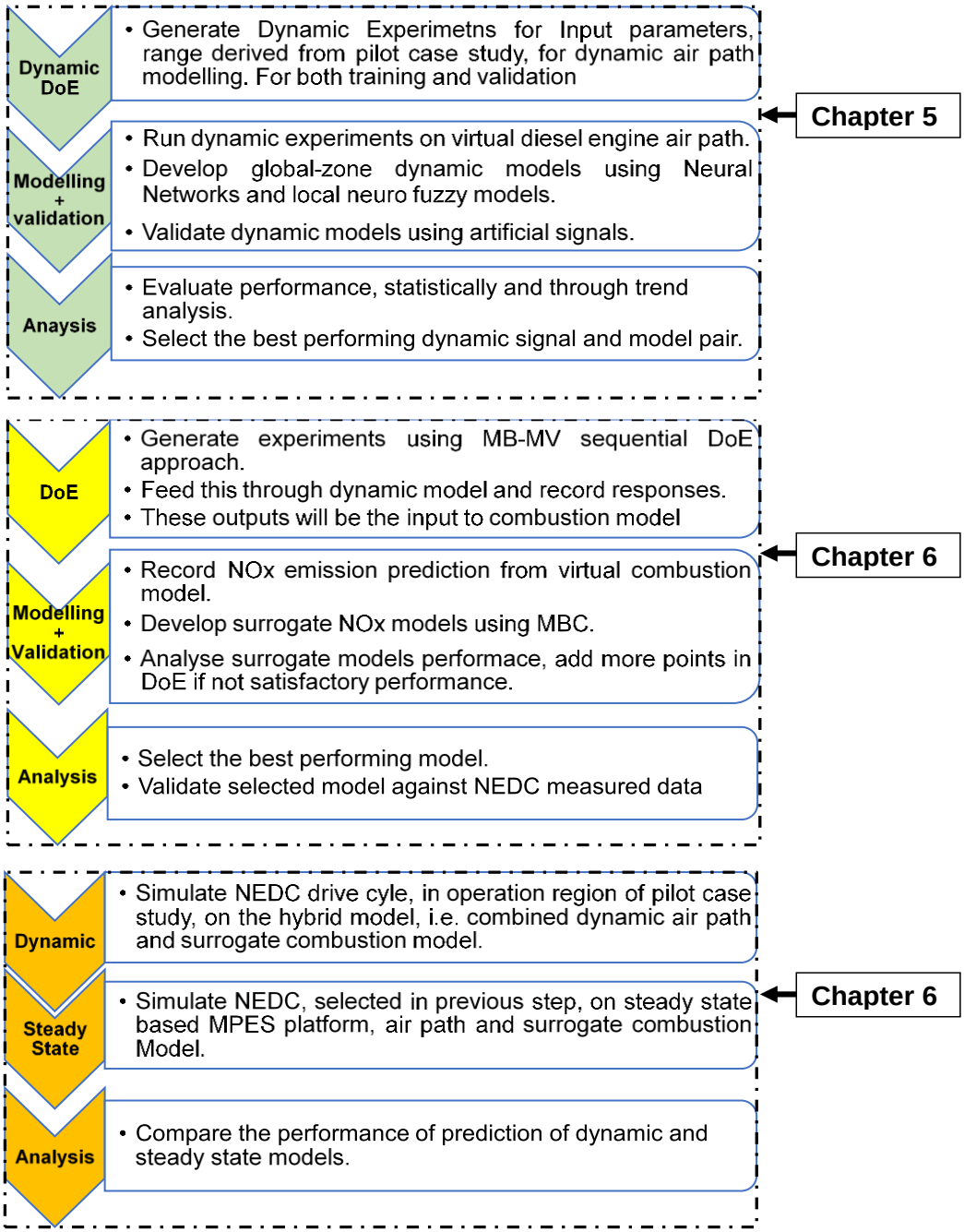

Figure 4.15: Research implementation plan.

Chapter 5 Development of Diesel Engine Dynamic Air Path Model

This chapter presents the implementation of the methodology presented in section 4.4.1 of Chapter 4, in conjunction with the Diesel engine case study. The dynamic air path model is developed to enhance system modelling task during the engine development phase and to capture transient behaviour in the drive cycles. The research was carried, as per the hybrid dynamic modelling framework depicted in Figure 4.6, in the following steps:

- Design of dynamic experiments, generating commonly used excitation signal (PRBS, APRBS, and Chirp), described in section 2.2.2.
- Implementation of nonlinear dynamic modelling techniques (Neural Network and Local Linear Neuro-Fuzzy Models) for developing dynamic air path model based on virtual Diesel engine air path system (MPES).
- Validation of the developed dynamic models.
- Discussion of the results based on statistical criterion and engineering analysis.

5.1 Model Inputs and Outputs

5.1.1 Model Inputs

Three key control variables were selected for the identification of the dynamic air path; engine speed, engine load and Mass Air Flow (MAF). The desired engine speed and load are the quantities required to simulate the GT-suite engine model through Simulink harness, illustrated in Figure 4.9 of section

4.4.1.3. The MAF was selected as an input variable because it controls the EGR valve position in a closed loop, which regulates the amount of exhaust gas entering the engine cylinder.

The excitation range of the engine speed and engine load was defined by the operational limit of the case study tabulated in Table 4.6, presented in section 4.4.1. For MAF, the limit was set to be ± 10% of MAF set position (provided by control maps illustrated in Figure 4.10) to account for the variation in between transient and steady-state modes of operation (Burke *et al.*, 2013). In addition to excitation range, excitation frequency range was defined based on the frequency analysis of the NEDC drive cycle data. For frequency analysis, the measured data was transformed using Discrete Fourier Transformation (Keesman, 2011; Pintelon and Schoukens, 2012), and this was achieved by using Fast Fourier Transformation algorithm (Blahut, 2010; Keesman, 2011). The algorithm was implemented using the functionality provided in the MATLAB programming environment and the code for this can be found in Appendix A.1.

The results of the FFT (Fast Fourier Transformation) algorithm for input signals, speed, load, and MAF, are presented as a power spectrum in Figure 5.1. From frequency analysis upper bound of frequency range was determined, for example in case of torque the upper limit of frequency range was selected to be 0.1Hz (highlighted by the solid line in Figure 5.1). The reason being that when the frequency was higher than 0.1Hz, the power/magnitude became very low, and it is reasonable to assume that these high-frequency components are harmonics/ noise associated with the system,

thus, can be neglected with little effect on the system. The choice of upper limit of frequency is consistent with the one found in literature (Hametner and Nebel, 2012; Burke *et al.*, 2013) where either 0.1 Hz or 10 seconds is used to define the limits. The source of these components with low power could be noise from instruments or engine vibration.

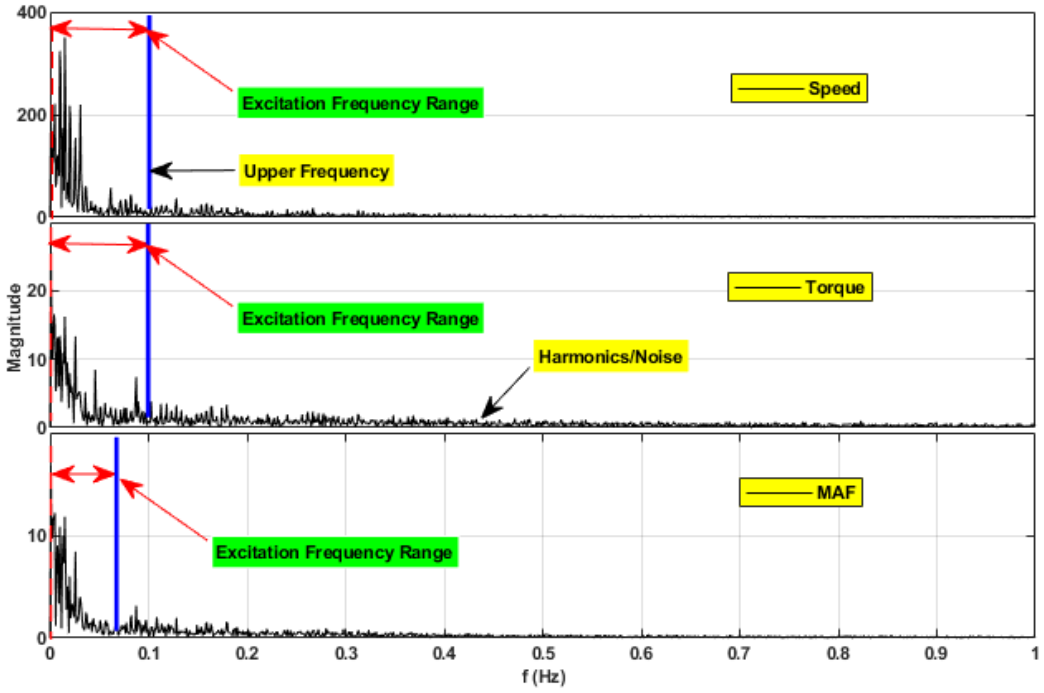

Figure 5.1: Fast Fourier Transformation of NEDC drive cycle data for model inputs.

The lower bound of the frequency should have been zero to cover steady state operation but to remain with dynamic experiments they were defined an order of magnitude lower than upper frequencies. Additionally, the lower frequencies were selected to give the minimum correlation between the input variables (Burke *et al.*, 2013). The findings of the analysis for the frequency range, along with the excitation range have been summarised in Table 5.1.

Table 5.1: Input parameters for dynamic air path model along with their symbols and units.

Input Parameter	Excitation Method	Symbol	Excitation Range	Frequency Range
Engine Speed	Direct control through Simulink harness for 1D model	N	1500-1750 rpm	0.003-0.1Hz
Engine Load	Control through the transformation of torque setpoint to fuel injection quantity via maps	Tq	20-160.6 Nm	0.001-0.1 Hz
Mass Air Flow	Control through mass air flow set point using multiplier function in ECU. This is because EGR is in closed loop control depending on the MAF demand.	MAF	±10%	0.001-0.06Hz

5.1.2 Model Outputs

The three main quantities were recorded as outputs, and they are presented in Table 5.2. The reason to select these quantities, as discussed in Chapter 4, because they are the inputs to the SRM combustion model which are provided by the air path system.

Table 5.2: Model Outputs of the dynamic air path model.

Response	Symbol
Inlet Pressure/ Boost Pressure	P(inl)
Inlet Temperature	T(inl)
Exhaust Gas Recirculation	EGR_mf

5.2 Development of Dynamic Air Path Model

Once the model inputs and outputs have been selected, the next step is to develop a dynamic air path model based on MPES platform, and this process can be divided into two steps:

- Design of Dynamic Experiments
- Identification of dynamic air path model

For dynamic experiments, there are three main types of excitation signals listed in the literature, i.e. PRBS, APRBS, and Chirp. In section 2.2, these signals have been discussed in depth, and their applications have been summarised in Table 2.1. From Table 2.1, it can be observed that either the excitation signals are preselected for the identifications purpose (Guhmann and Riedel, 2011; Burke *et al.*, 2013) or the modelling technique is selected in advance to analyse the effect of different excitation signals on identification process (Röpke *et al.*, 2012; Tietze, 2015). However, the studies which explore the effect of different excitation signals on different modelling techniques- assisting the selection procedure of appropriate excitation signal and modelling technique combination for the identification system of interest- are somewhat limited (Isermann, 2014).

To address this issue, a strategy has been devised in this study which assists in the selection of an appropriate combination of dynamic signal and modelling technique. The developed strategy is illustrated in Figure 5.2 and Figure 5.3, where Figure 5.2 demonstrates the overview of the process involved in the

selection of dynamic signal and modelling technique and Figure 5.3 depicts the training procedure based on MPES platform for dynamic air path model.

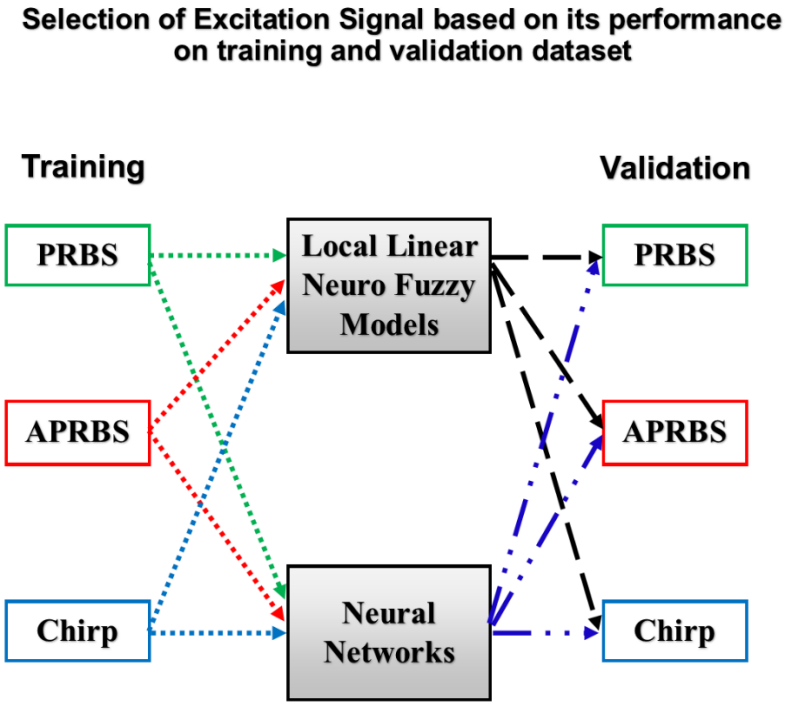

Figure 5.2: Illustration of the selection of the excitation signal for different model architecture.

In Figure 5.2, the dynamic models of Diesel engine air path are developed using a combination of LLNF and NN models with three excitations signals and their performance is validated on three separate validation signals. The process of development is illustrated in Figure 5.3, where excitations signals are fed to virtual Diesel engine air path of MPES platform, and the system responses of interest are captured. The inputs signals along with the outputs are used for training the dynamic models.

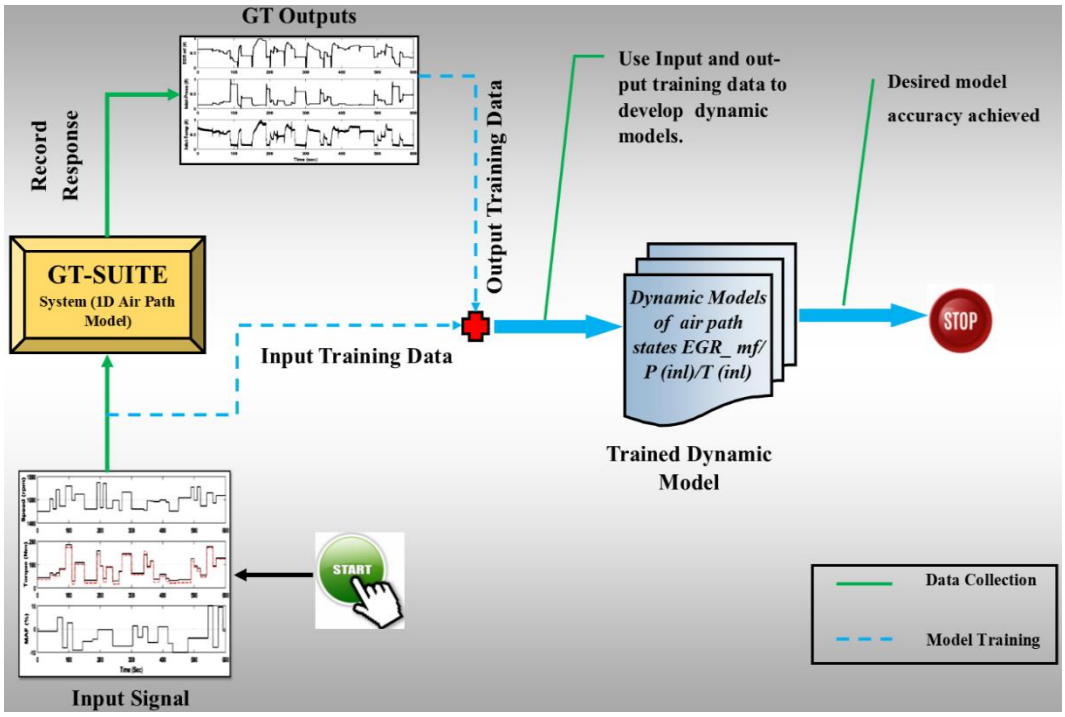

Figure 5.3: Training process during the development of the dynamic air path model.

5.3 Design of Dynamic Experiments

The input excitation signals (PRBS/ APRBS/ Chirp) illustrated in Figure 5.2, were generated using the specification presented in Table 5.1. These signals were implemented on the GT-Suite engine model and two chosen modelling technique, LLNF and Neural Networks, were used to develop the model for responses of interest (Table 5.2). The performance of the developed model was compared for both training and separate validation dataset by using RMSE criteria (refer Equation 3.1).

As a model trained by one type of excitation signal would not be able to simulate the other excitation signal with same capability (Tietze, 2015), therefore, to analyse and compare the performance of a combination of signal

and modelling technique three validation datasets were generated. The validation signals, like training signals, were generated for the three selected signal designs. Thereafter, the signal and modelling technique combination which performs comparatively better on both training and validation signals would be selected to identify dynamic air path.

Both training and validation signals are generated using the System Identification (SYSID) toolbox in MATLAB software environment.

5.3.1 Pseudo Random Binary Signals (PRBS)

The bandwidth or excitation frequency for the PRBS signal is not defined in Hz but by the clock period. The clock period here refers to the time for which signal stays constant before it can change, and it is represented by an inverse of the excitation frequency (MATLAB, 2006). This is generally referred to as hold time, and this is chosen in consideration of expected system dynamics, illustrated in Figure 5.1 and tabulated in Table 5.1.

The script for designing the PRBS signal is presented in Appendix A.2, and the developed training and validation signal is illustrated in Figure 5.4 and Figure 5.5 respectively.

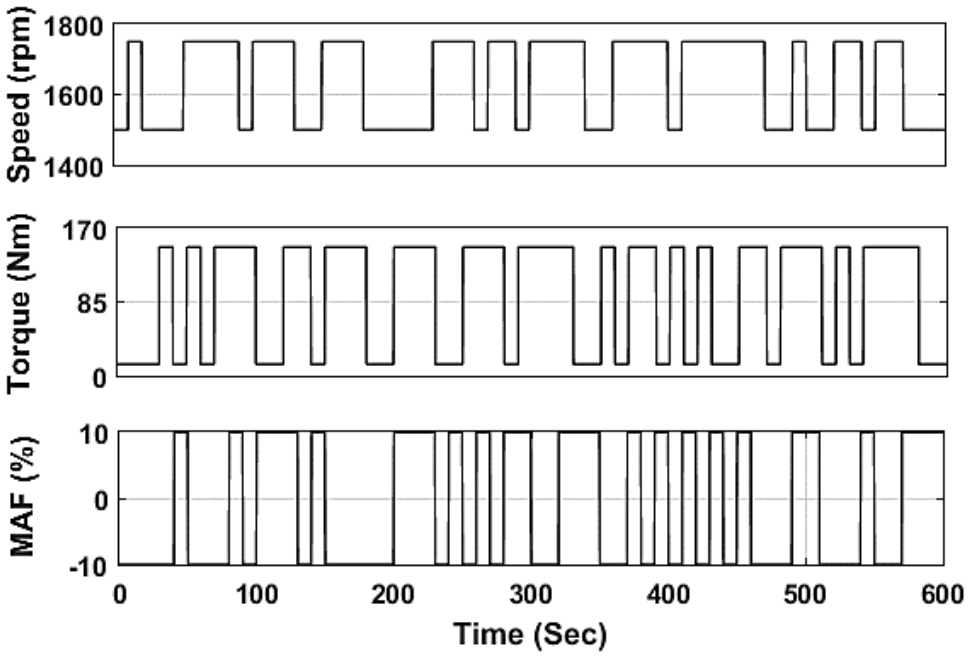

Figure 5.4:PRBS training input signals.

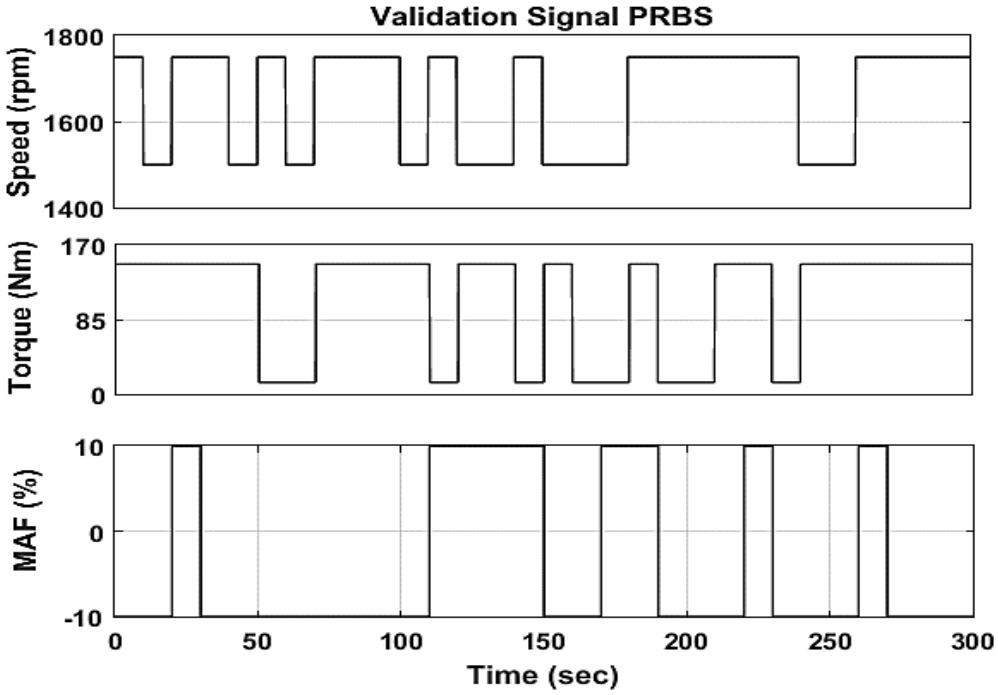

Figure 5.5: PRBS validation input signals.

5.3.2 Amplitude Modulated Pseudo Random Binary Signals (APRBS)

In APRBS signals, like the PRBS signal described above, the frequency content is expressed in terms of the clock period. The main difference between PRBS and APRBS is that unlike PRBS signals which have only two levels(min-max), APRBS are multi-level signals.

The MATLAB based scripts for APRBS signals is presented in Appendix A.3, and the generated signal for training and validation is illustrated in Figure 5.7 and Figure 5.8 respectively.

The signals are designed individually for each input. However, this will result in some operating points that are not achievable in practice because of limitations either in terms of mechanical integrity of the engine or because of operation in unstable conditions. To account for this, the engine torque signal has been continuously scaled as a function of engine speed, and the scaling scheme is illustrated in Figure 5.6. This becomes highly relevant at higher engine speed, as the engine can achieve higher torque level at higher engine speed.

In Figure 5.7, the scaled engine torque is depicted as a solid line and dashed line represents signal before scaling. The MAF did not require scaling as it has been implemented as a percentage factor of the set position in the virtual Diesel engine airpath (GT-Suite) and the scaling is already an inherent part of the engine strategy.

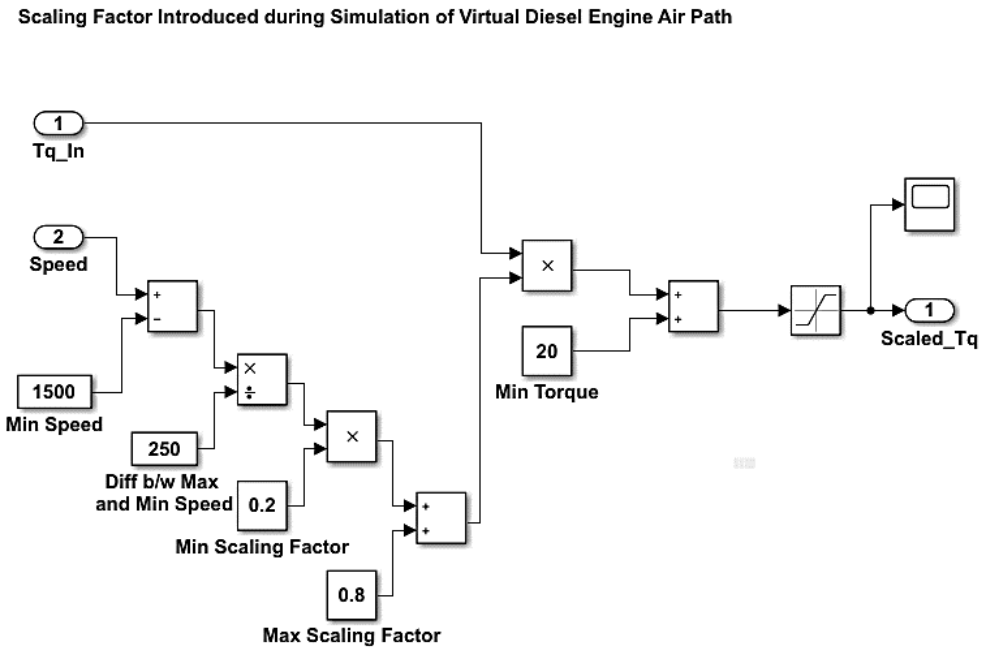

Figure 5.6: Torque scaling as a function of speed.

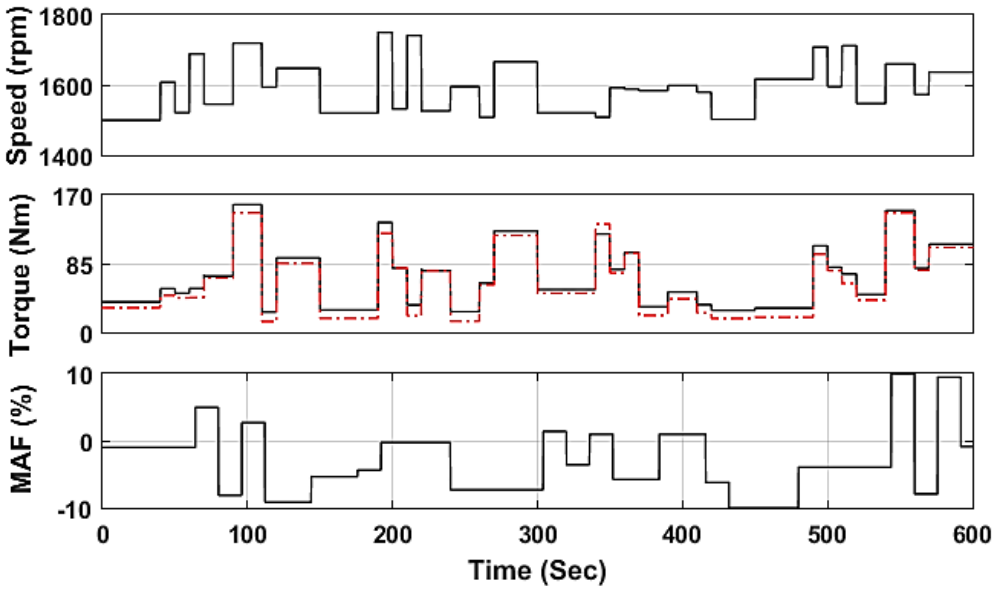

Figure 5.7: APRBS training input signals (dash: original signal & solid: scaled signal).

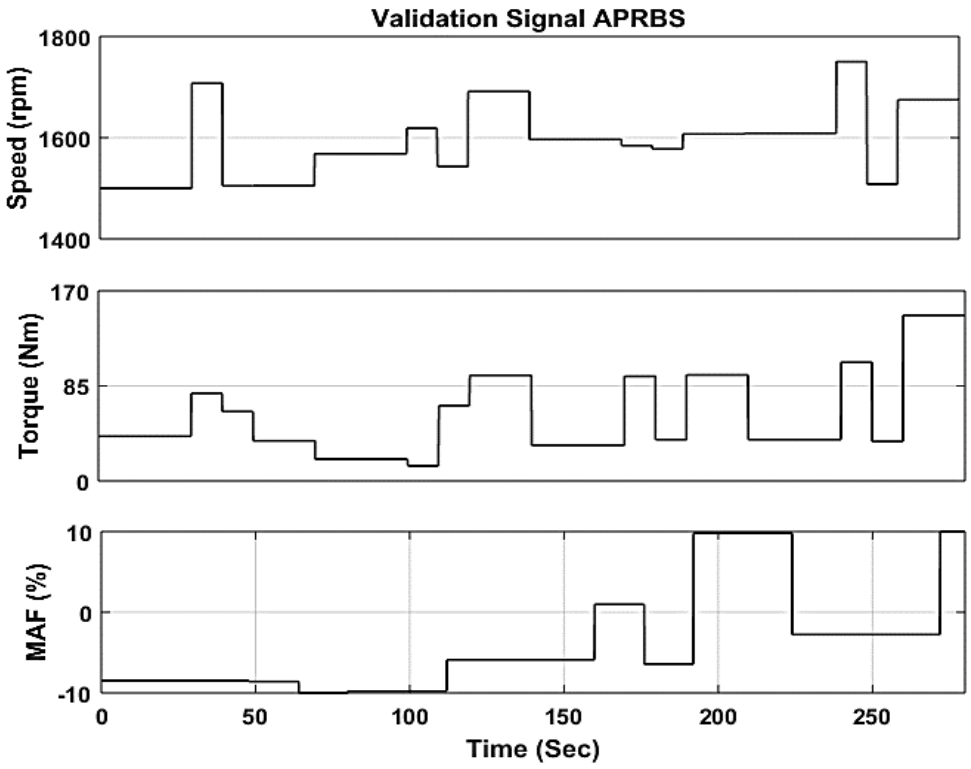

Figure 5.8: APRBS validation input signals.

5.3.3 Chirp Input Signal

The script for generating chirp excitation signal is presented in Appendix A.4, and the signal developed for training and validation is depicted in Figure 5.9 and Figure 5.10 respectively.

The scaling of torque signal was carried out in a similar fashion as APRBS signal, illustrated in Figure 5.6. The scaled torque is represented by the solid line in Figure 5.9 and in the same figure dotted line represents the signal before scaling.

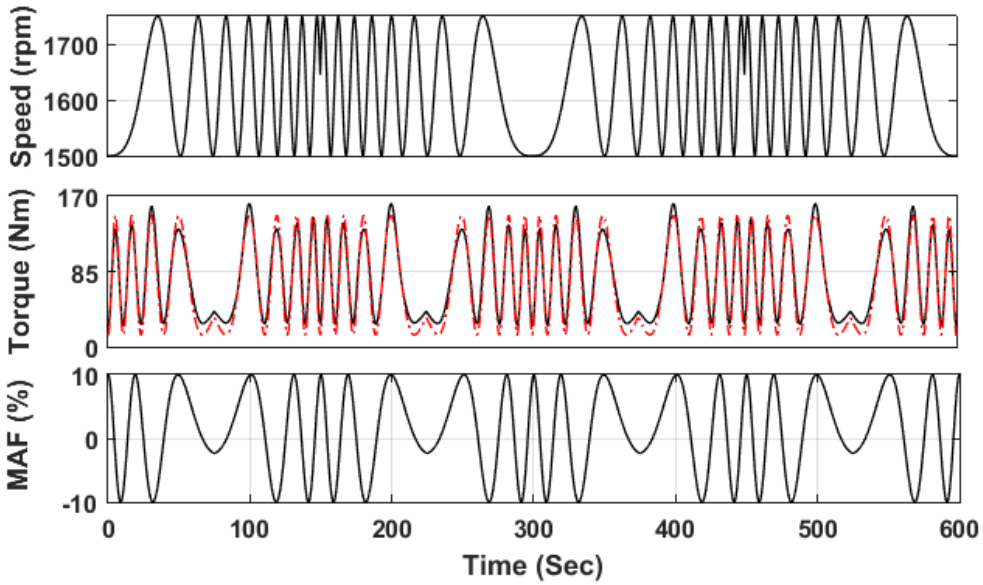

Figure 5.9: Chirp training input Signals: (dotted: original signal & solid: scaled signal).

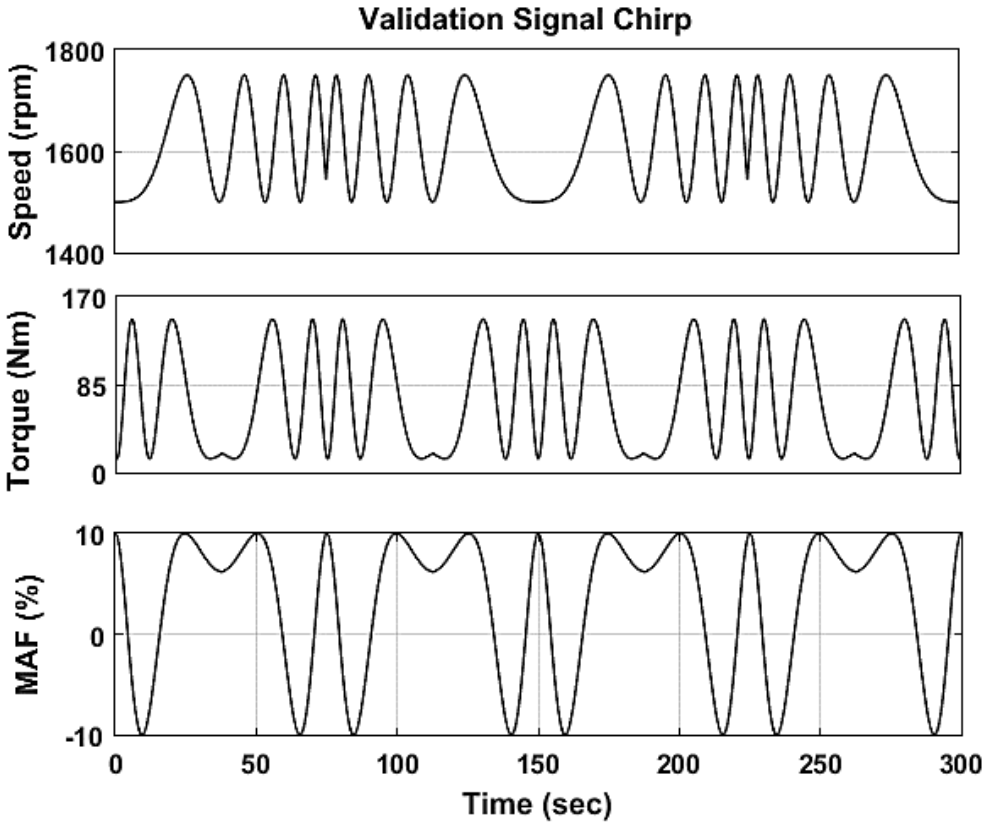

Figure 5.10: Chirp validation input signals.

5.4 Identification of dynamic air path model

Following the proposed framework in Figure 4.6 of section 4.3, the artificial signals generated for the desired inputs (Table 5.1) and were implemented on the virtual Diesel engine air path (GT-Suite Diesel engine model) to generate responses of interest listed in Table 5.2. Thereafter, inputs and outputs were used to create a dynamic air path model by using selected model architectures.

The responses were modelled as multiple inputs and single output (MISO) system, using Neural Network and Local Linear Neuro Fuzzy modelling.

The scripts developed using MATLAB software environment in conjunction with LMN Toolbox (Hartmann *et al.*, 2012) for LLNF model using LOLIMOT algorithm is presented in Appendix A.5 and the scripts for Neural Network model developed using MATLAB Neural Network Toolbox is illustrated in Appendix A.6. A pictorial representation of script run is depicted in Figure 5.11.

A step by step description of the training set-up and training procedure for both LLNF-LOLIMOT model and NN model is depicted in the form of the flow chart in Figure 5.12 and Figure 5.13 respectively.

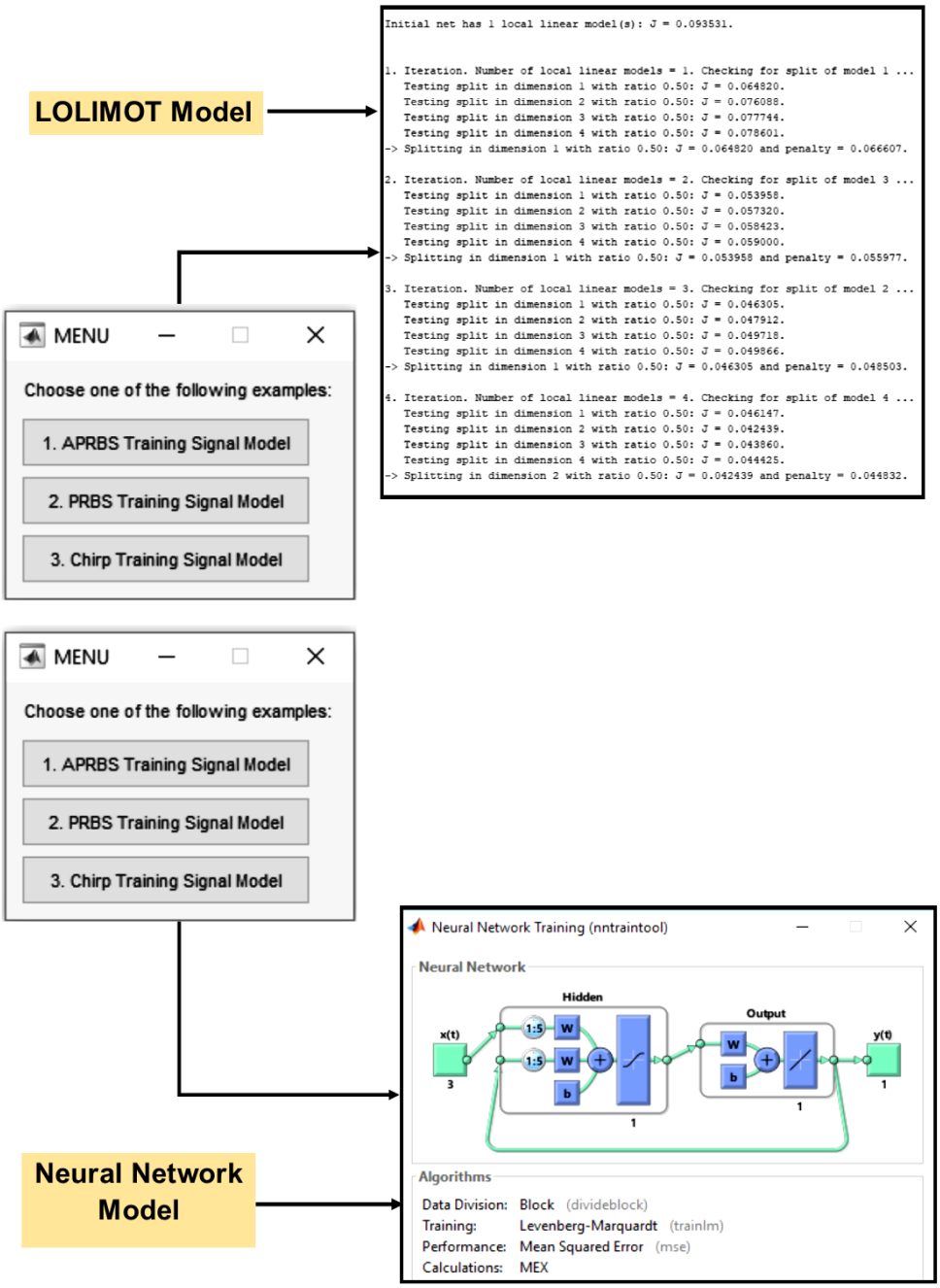

Figure 5.11: An illustration of running script developed for LOLIMOT and Neural Network models.

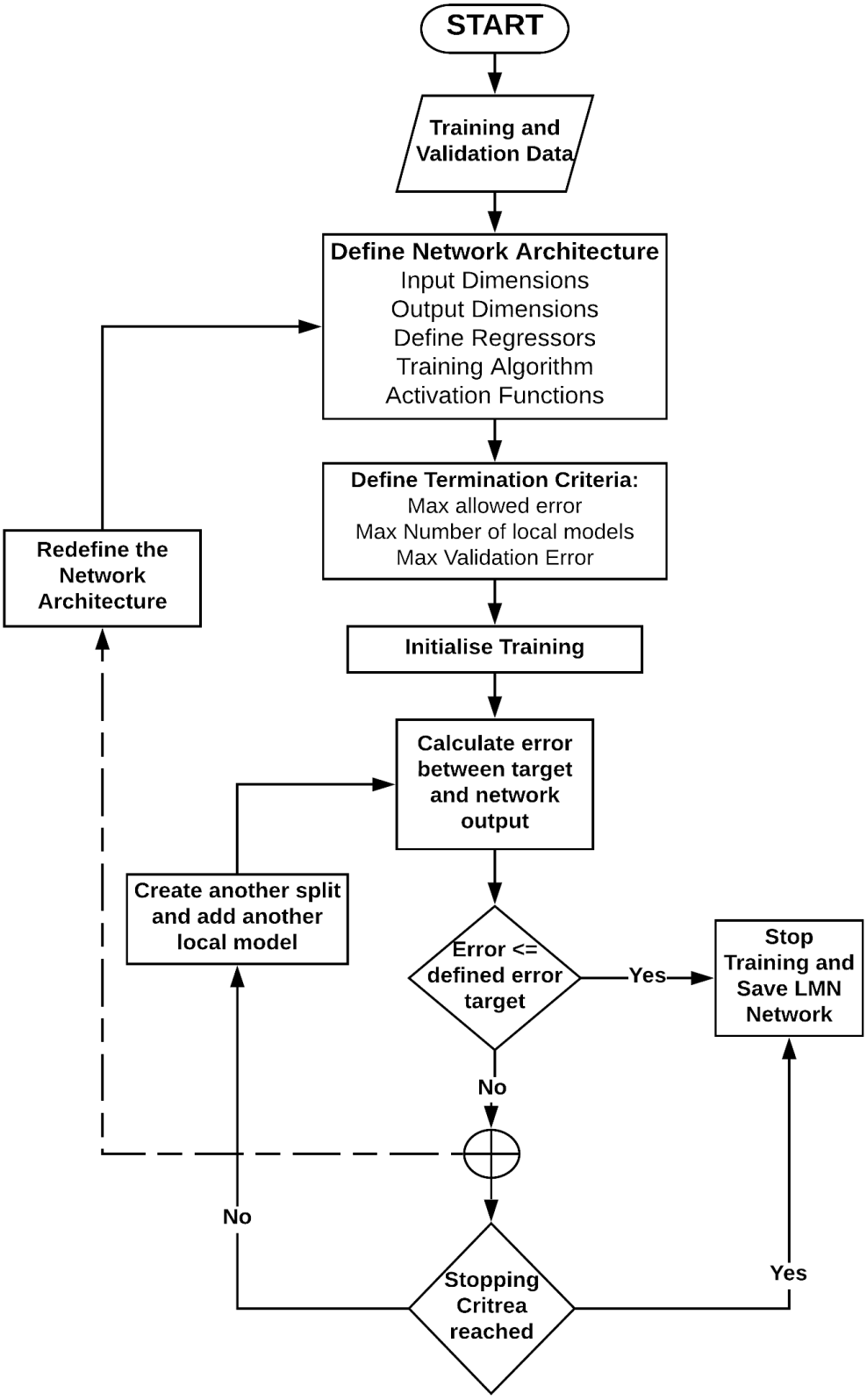

Figure 5.12: Training Process for Local Linear Neuro Fuzzy modelling using LOLIMOT algorithm.

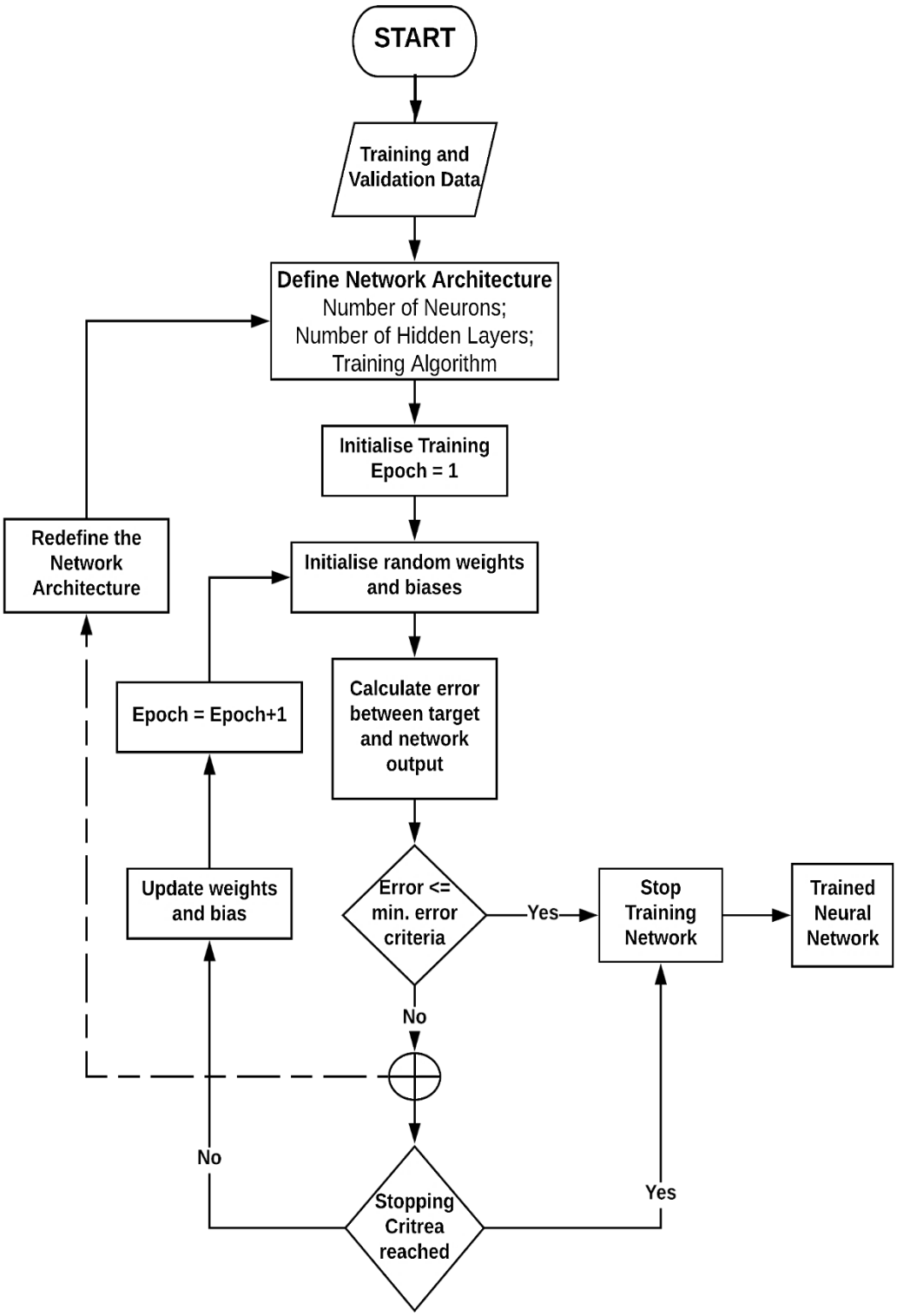

Figure 5.13: Neural Network training process flowchart.

5.5 Dynamic Air Path Model Performance Evaluation

The models developed using the signal designs from section 5.3 and the scripts for modelling techniques (LLNF and NN) in A.5 and A.6, as per the strategy presented in section 5.2, are evaluated in this section. The developed models are evaluated based on the following:

a) Statistical Performance: statistical diagnostic is used to compare the model performance on the training data and validation data. This is carried out as follow:

- Comparing approximation error, using RMSE (refer Equation 3.1), on both training and validation dataset.
- Secondly, by comparing the computational time, the number of effective parameters and number of local models generated to model the system response.

b) Engineering Analysis: analysis of the identified model behaviour by comparing it with the expected system of interest response behaviour, to ensure models are not over or under-fitted.

5.5.1 Analysis of EGR Mass Fraction Response Models

The performance evaluation of dynamic EGR response model based on statistical diagnostic and trend analysis is presented in this section.

5.5.2 Local Linear Neuro Fuzzy- LOLIMOT Air Path Response Model

The design parameter and termination criterion used to develop LOLIMOT model for EGR mass fraction are listed in Table 5.3 and Table 5.4. The inputs and outputs were delayed in order to create a dynamical structure and were chosen by trial and error method. The selected delays represent a third order dynamic system. The same set of parameters and termination criterion was used, for all three types of signal design.

Table 5.3: Design parameters for initial network setting.

Design Parameter	Specification
Input Delays	$u_1(k-1), u_1(k-2), u_2(k-1), u_2(k-2), u_2(k-3), u_3(k-1), u_3(k-2), u_3(k-3)$
Output Delays	$y(k-1), y(k-2)$
Training Algorithm	LOLIMOT
Validity Function Type	Gaussian
K step prediction	Set to infinity, as model generated for simulation purpose

Table 5.4: Termination criterion to evaluate model performance after each iteration.

Termination Criteria	Specification
Number of Local Model Networks (LMN)	50
Minimal Error	0 (default setting)
Minimum Performance Improvement	1.0e-03

A. Statistical Performance

The developed models are compared based on their performance on training and validation using the RMSE information criteria, refer to Equation 3.1. It can be observed in the Figure 5.14, that every model performs better on the type of the validation signal for which it was trained, for example, APRBS LOLIMOT model performs comparatively better for validation signal of APRBS type than for the other two.

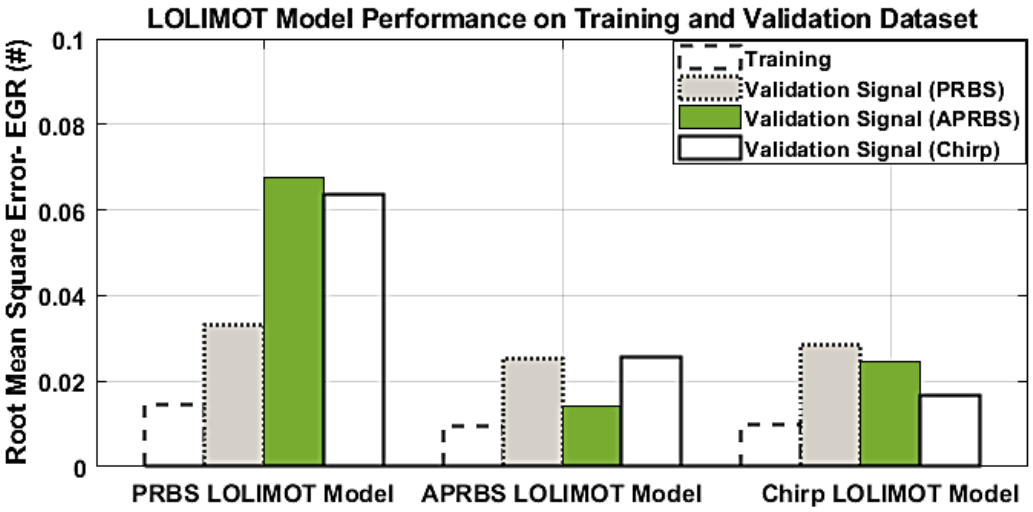

Figure 5.14:RMSE for EGR mass fraction LOLIMOT Model response during training and validation for all signal designs.

The PRBS LOLIMOT model (LOLIMOT model trained on PRBS type signal), in Figure 5.14, provides good performance on training data but the approximation error for the validation dataset increases significantly compared to the training error, indicating overfitting.. Therefore, the PRBS LOLIMOT model is ruled out as a suitable signal-model combination.

The APRBS and Chirp based LOLIMOT models provide better performance when compared to the PRBS based model. It can be noticed in Figure 5.14, that the APRBS and Chirp LOLIMOT model have a similar level of performance for both training and validation dataset. This observation can be strengthened by comparing the values of RMSE for these two models in Table 5.5. In comparison to Chirp based model, APRBS LOLIMOT model performs slightly better.

Table 5.5: Training and Validation RMSE for EGR mass fraction LOLIMOT models.

Excitation Signal	**Training RMSE**	**Validation RMSE (Validation Signal Performance)**		
		PRBS	**APRBS**	**Chirp**
PRBS	0.0145	0.0331	0.0674	0.0637
APRBS	0.0096	0.0254	0.014	0.0255
Chirp	0.0097	0.0286	0.0246	0.0166

Further evaluation of the models based on the number of parameters and training time is presented in Figure 5.15 and Figure 5.16 respectively. The number of parameters associated with APRBS model is less than Chirp based model. Thus, reducing the effort for parameter estimation. Also, it requires a reduced number of models, 21 local models rather than 26 for the chirp-based model, to provide a similar level of performance as a chirp-based model.

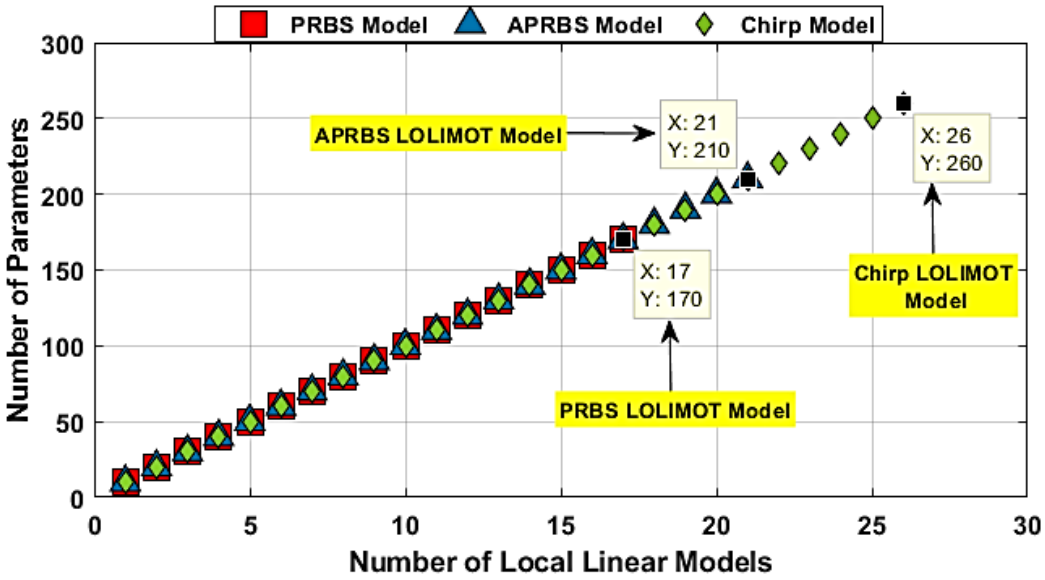

Figure 5.15: Number of parameters for identified EGR LOLIMOT models

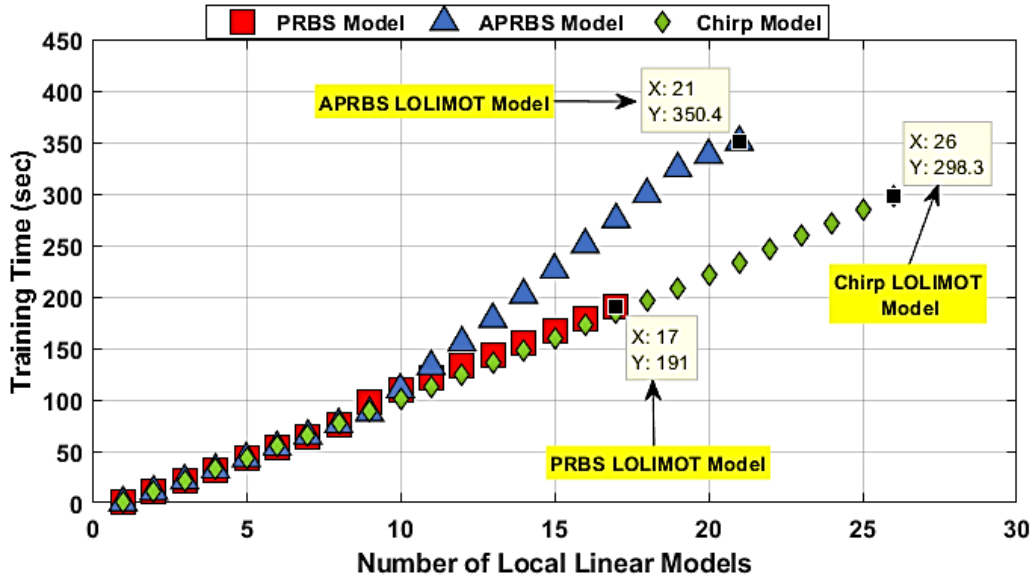

Figure 5.16: Training time associated with the EGR models.

In terms of training time, APRBS based model needs more time to identify the EGR response model than the chirp-based model. However, they are still capable of identifying EGR response model faster than real time, 1.7x times faster. Noteworthy, training time does not include the time spent on

determining the design parameters, they are determined prior to initialising the training process.

B. Engineering Analysis

The results for the training of EGR LOLIMOT models are presented in Figure 5.17, and the solid line in the figure represents the measured EGR mass fraction response (from virtual Diesel engine air path in MPES platform), and the dotted line represents the output of the trained LOLIMOT models.

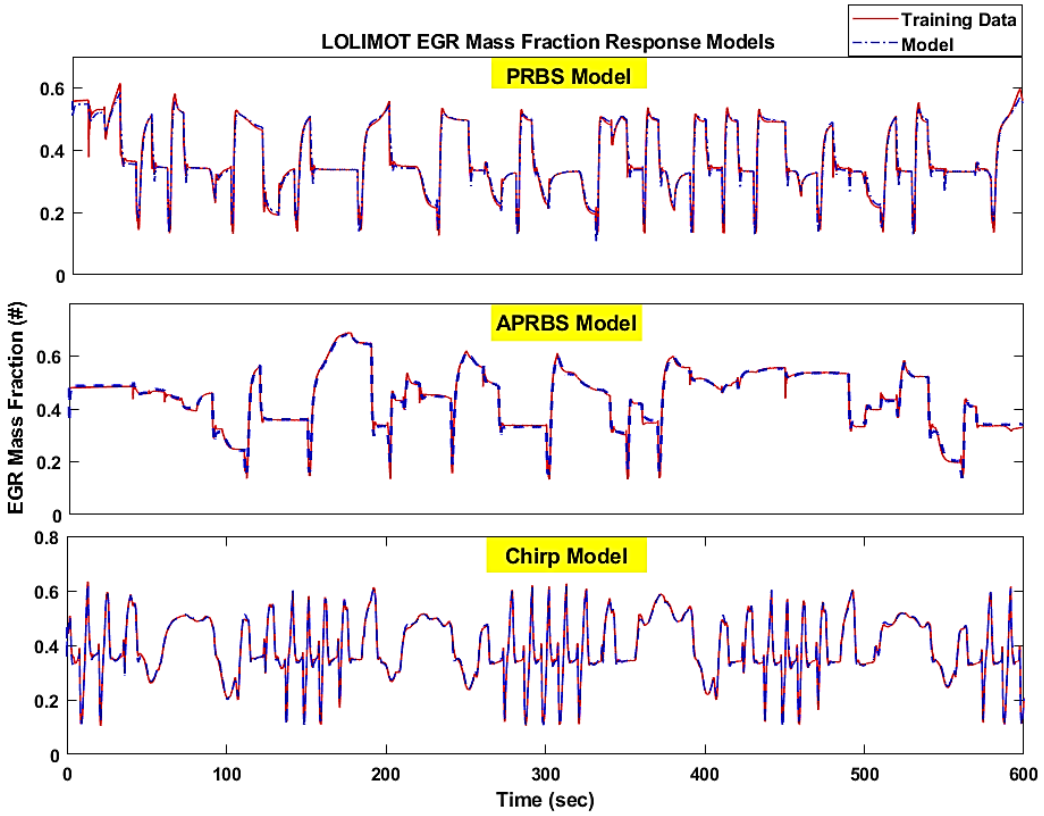

Figure 5.17: LOLIMOT models training performance.

It can be observed, from Figure 5.17 and Table 5.5, that the LOLIMOT models trained with APRBS and chirp signal provide an accurate prediction (error < 0.01 RMSE or 1% EGR_mf) of the measured response during the training

process and LOLIMOT model trained with PRBS signal also provide good prediction (error <0.02 RMSE or 2% EGR_mf). However, during the validation phase, the PRBS model tends to perform poorly (>0.05 RMSE or 5% EGR_mf) when compared to the other two models. As can be seen in Figure 5.18, the LOLIMOT model based on PRBS signal is either over or under predicting the absolute values of the measured response (validation data captured from virtual Diesel engine air path). In case of chirp validation signal, the PRBS model cannot capture the system dynamics and is exhibiting signs of overfitting. For APRBS validation signal, the PRBS model captures the trend in general but with large prediction error.

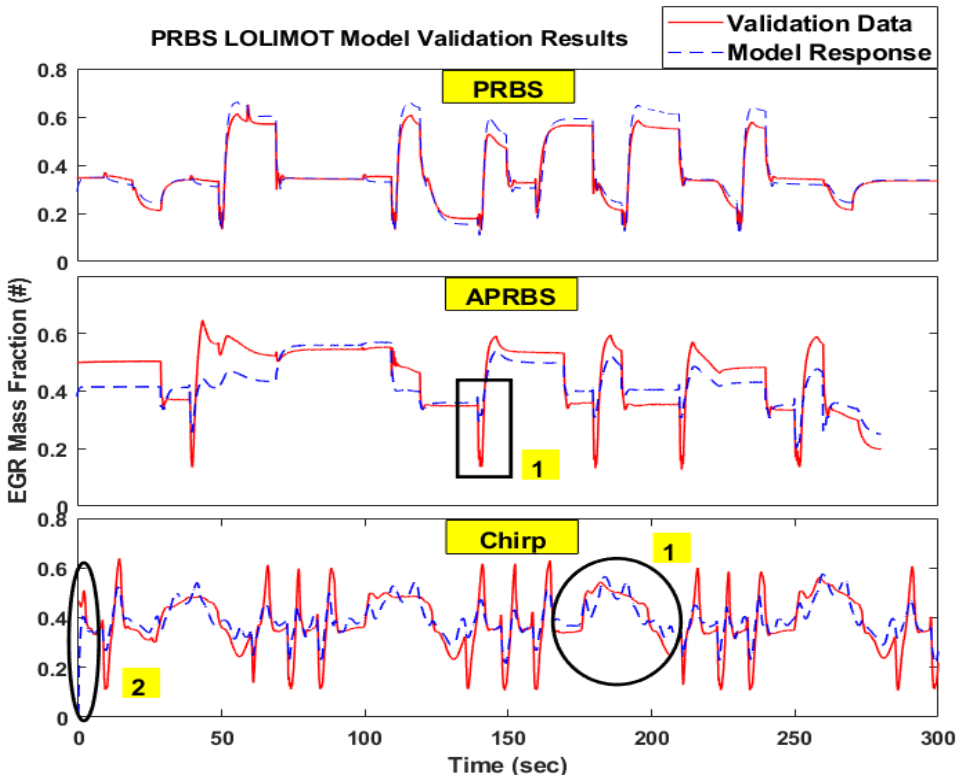

Figure 5.18: Performance of PRBS based LOLIMOT Model on three different validation signals.

The validation results for LOLIMOT model trained with APRBS signal are illustrated in Figure 5.19. The model performs quite well across all three validation signals. For the PRBS validation signal, the model follows the trend in the measured data (from GT-Suite) with some discrepancy in the absolute values.

Although this model is trained on the step-like signal, it predicts the trends in chirp validation signal (sinusoidal nature) reasonably-well (< 0.03 RMSE or 3% EGR_mf). The regions, labelled as 1, where APRBS model is deficient for chirp validation signal is highlighted using the solid circle. In these regions, trends in system dynamics are captured, but the model lacks in estimating the absolute values.

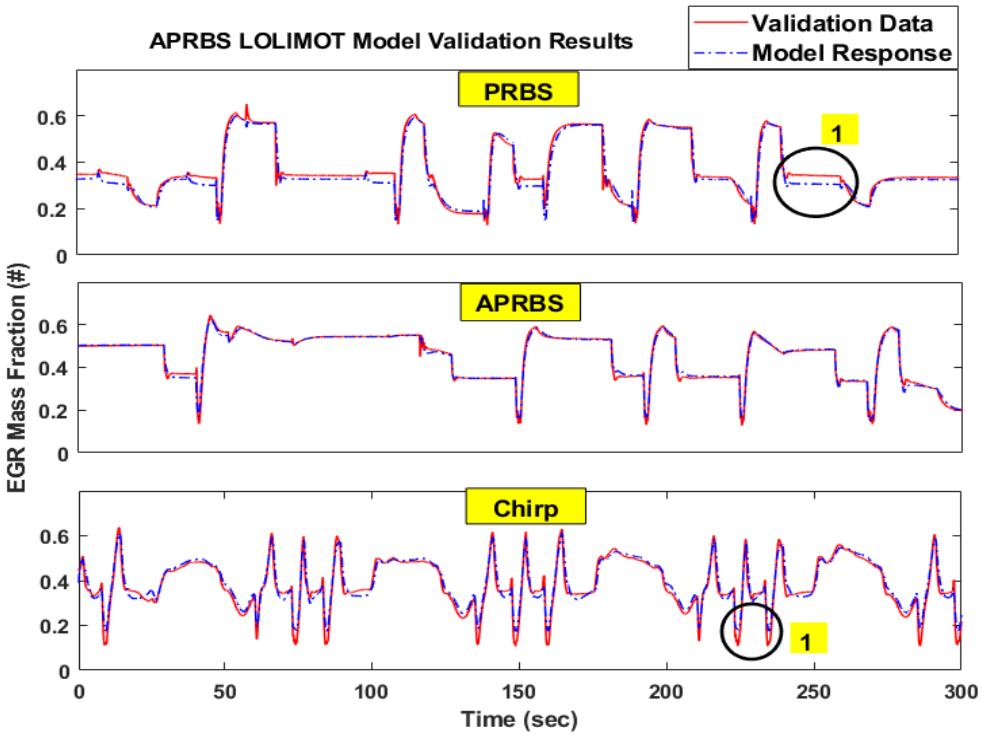

Figure 5.19: Performance of APRBS based LOLIMOT Model on three different validation signals.

The performance of LOLIMOT model based on the chirp signal over the validation signals is depicted in Figure 5.20. The chirp model can capture the system dynamics smoothly, owing to the nature of their training signal which allows slow and smooth amplitude change. However, because of the same effect, it struggles to capture the frequent step changes in the PRBS (labelled as 1 and 2) and APRBS validation signals (labelled as 1). The chirp model extrapolates in these regions and predicts negative EGR mass fraction, which is not possible during engine operation. But for chirp validation signal, as observed in Table 5.5 as well, the model performs extremely well.

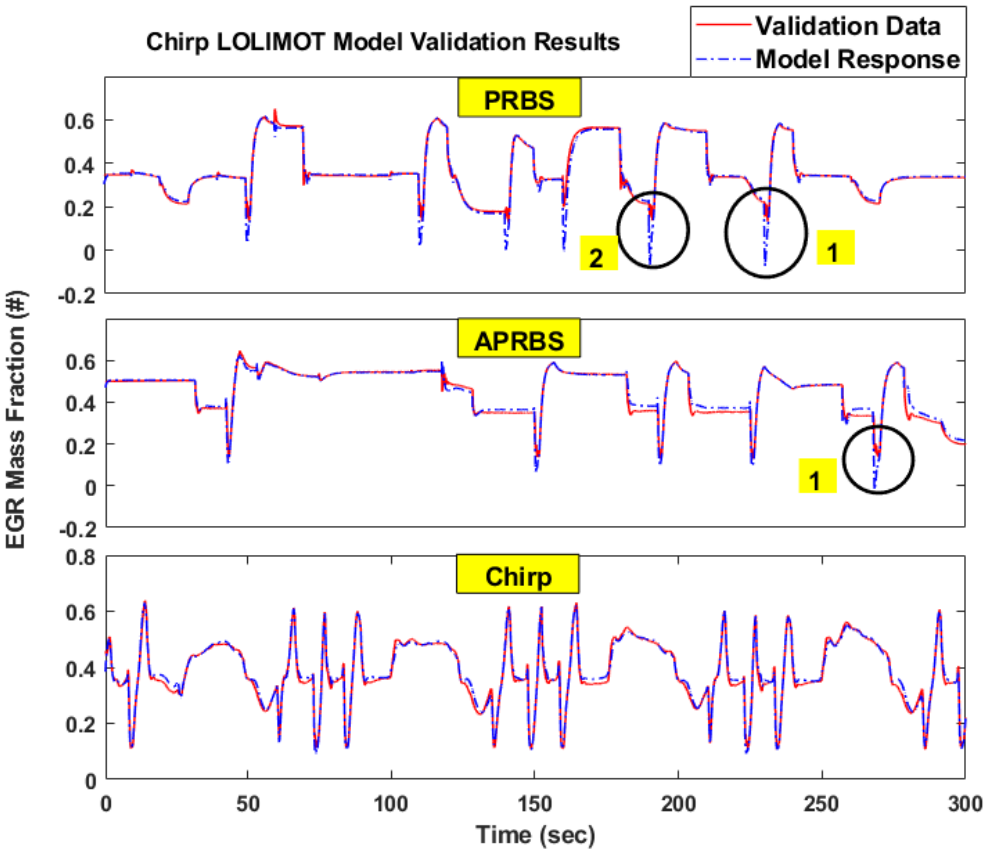

Figure 5.20: Performance of Chirp based LOLIMOT Model on three different validation signals.

On the basis of the statistical and engineering analysis, APRBS signal was selected as a most suitable signal for the LOLIMOT models. Arguably, chirp performance is similar to the APRBS signal, but they require more local models leading to a large number of parameters, and their performance on step-like validation signal was sub-optimal. This is because sinusoidal excitation signals lack steady state excitation phases (Röpke *et al.*, 2012). This disadvantage can be overcome by addition steady state excitation sequence to the chirp signal but would mean longer signal length and increased measurement cost.

5.5.3 Neural Network Air Path Response Model

The parameters define for the training of the Neural Network (NN) models, and the termination criterion are listed in Table 5.6 and Table 5.7 respectively. These parameters were used for training neural networks for all three signal designs.

Table 5.6: Design Parameters define during neural network training.

Design Parameter	**Specification**
Input Delays	$[u_1(k-1),\ u_1(k-2), u_2(k-1), u_2(k-2), u_2(k-3), u_3(k-1), u_3(k-2), u_3(k-3)]$
Output Delays	$[y(k-1), y(k-2)]$
Training Algorithm	Bayesian regularization - 'trainbr'
Activation Function	Hyperbolic Tangent sigmoid – 'tansig'
Hidden Layer	1

Table 5.7: Termination criterion of neural network training

Termination Criteria	Specification
Number of Neurons	50
Maximum Number of Epochs	100
Performance Goal	7.76e-04
Maximum Validation Failures	6

A. Statistical Diagnostics

The performance of neural networks models, developed as per the specification in Table 5.6 and Table 5.7, is depicted in Figure 5.21. In this figure, models are compared based on their performance on training and validation using the RMSE information criteria, refer to Equation 3.1. The PRBS based neural network models are clearly showing signs of overfitting for the APRBS and chirp validation signals.

The APRBS and Chirp based NN models provide better performance when compared to the PRBS based model. The chirp based NN model, as depicted in Figure 5.21, perform slightly better in comparison to APRBS based model. The RMSE error values for Figure 5.21 are listed in Table 5.8 . From the table, it can be observed that the number of neurons required to build the network using a chirp signal is smaller in comparison to APRBS based model.

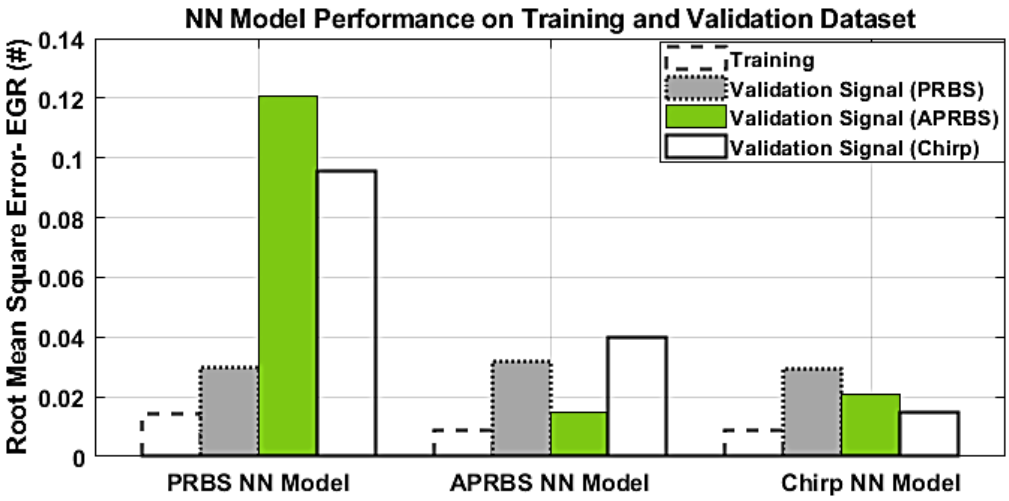

Figure 5.21: RMSE for EGR mass fraction neural network model response during training and validation for all signal designs.

Table 5.8: Training and Validation RMSE for EGR mass fraction neural network models.

Excitation Signal	Number of Neurons	Training RMSE	Validation RMSE (Validation Signal Performance)		
			PRBS	APRBS	Chirp
PRBS	8	0.0151	0.0298	0.1205	0.0954
APRBS	28	0.009	0.0281	0.0150	0.0353
Chirp	23	0.009	0.028	0.0210	0.0150

Additional supporting evidence for the model performance was evaluated based on the model training time, presented in Figure 5.22. The Chirp based model, compared to APRBS based model, require shorter training time. However, the chirp-based model has a higher number of epochs than APRBS

models. The epochs here refer to the number of time whole dataset is fed to the network to optimise network learning.

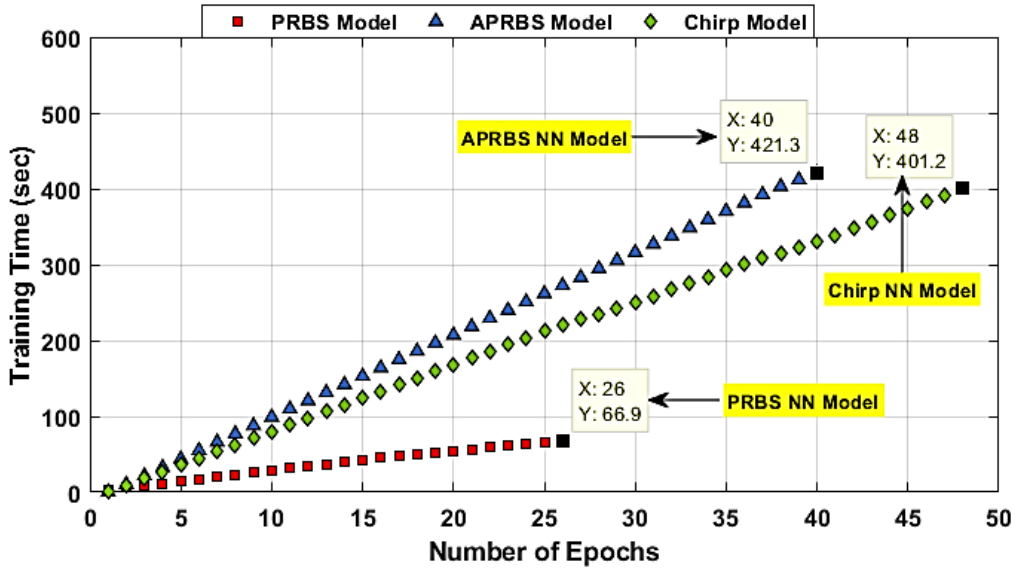

Figure 5.22: Training time associated with the neural network models.

B. Engineering Analysis

To further analyse models' performance and to ensure that they are not overfitted or underfitted, the output of the trained neural network models based on different signal designs are compared with the measured response (from virtual diesel engine air path) for these signals. This comparison is presented in Figure 5.23, and it can be observed that APRBS and Chirp based NN model performs quite well and can capture the trends in the data smoothly. However, the PRBS based model has some overshoots, highlighted in the figure, and can be observed across the whole model response. These overshoots or spikes are not present in the measured response, indicating that the developed PRBS model would not be a suitable choice to represent system dynamics accurately.

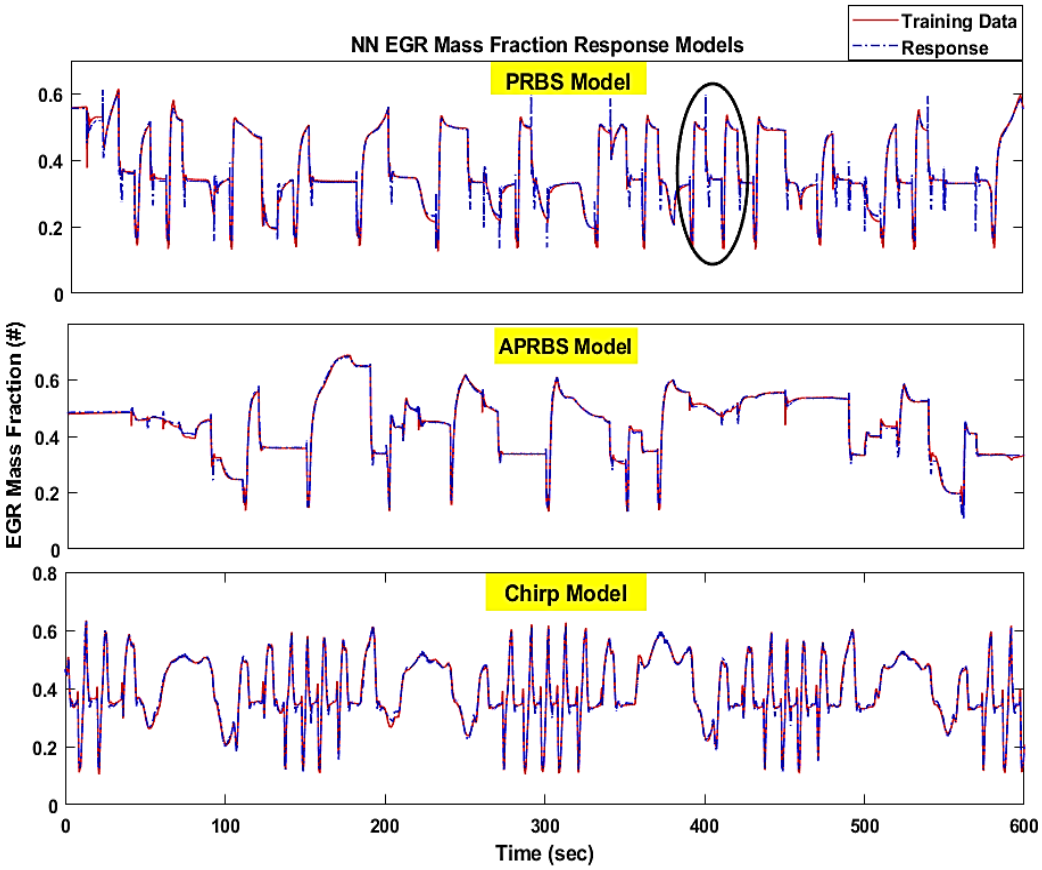

Figure 5.23: Neural Network models training performance.

As expected, based on the statistical analysis, the PRBS based model performs poorly for the new set of data. This becomes significant in the case of chirp validation signal, where the model clearly shows a sign of overfitting. While the performance error for APRBS type validation signal is observed to be worst in the Figure 5.21 and Table 5.8, it seems the model can still predict trends but not across the whole domain and not with reasonable accuracy.

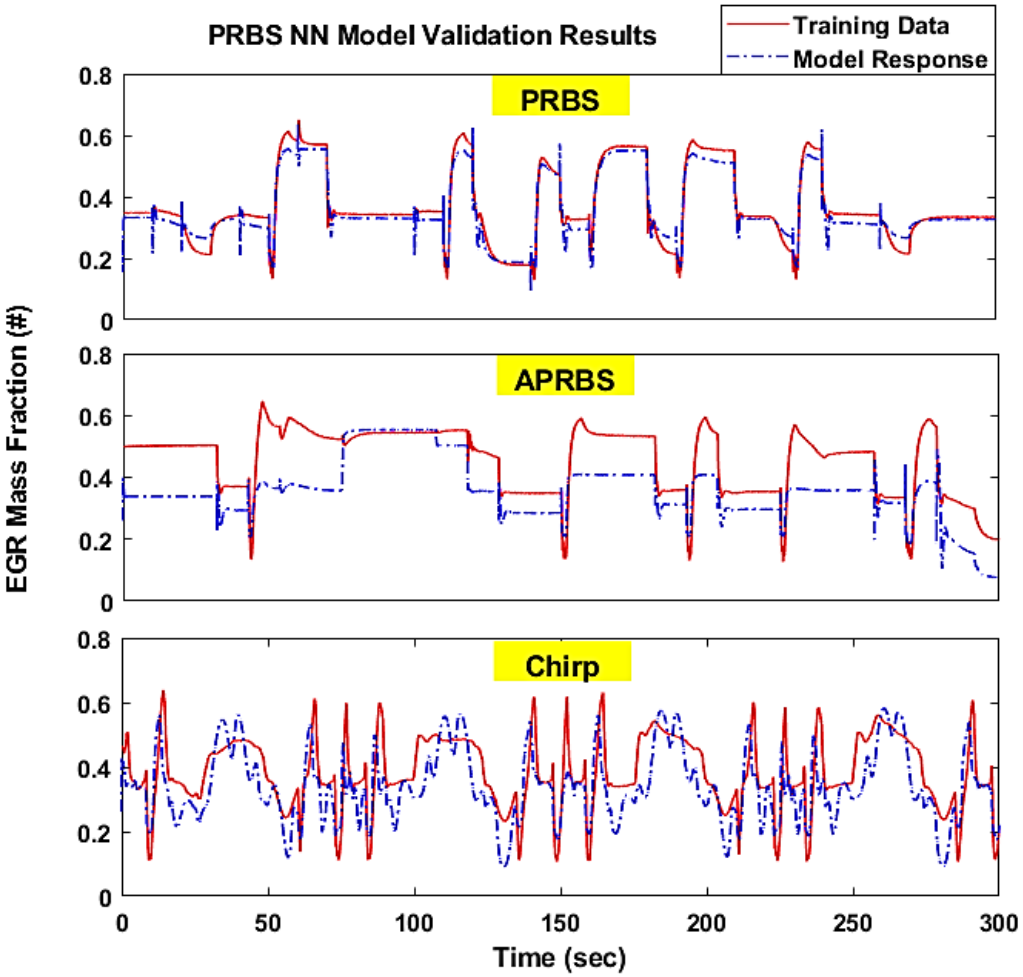

Figure 5.24: Performance of PRBS based NN Model on three different validation signals.

The validation results for NN model based on APRBS signal are illustrated in Figure 5.25. The model performs reasonably well across all three validation signals. For the PRBS validation signal, the model accurately predicts the trend in the data with some discrepancy in the absolute values. This can be observed over the entire PRBS validation signal response, and one of the areas exhibiting this is highlighted as ‘1,’ under PRBS validation signal response of APRBS NN model.

Although this model is trained on the step-like signal, it predicts the trends in chirp validation signal reasonably well. The regions where APRBS model is deficient for chirp validation signal is highlighted as '1'. In these regions, trends in system dynamics are captured, but the model lacks in estimating the absolute values.

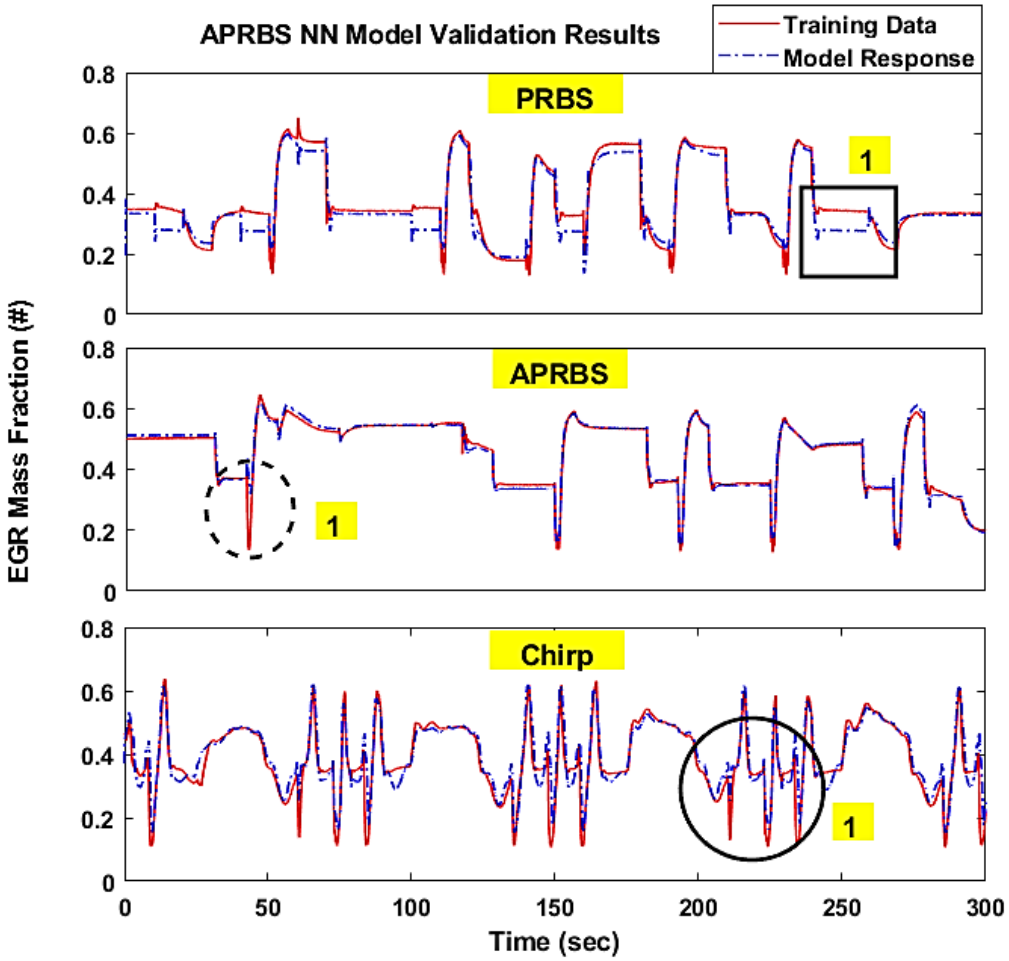

Figure 5.25: Performance of APRBS based NN Model on three different validation signals.

The performance of the NN model based on the chirp signal over the validation signals is depicted in Figure 5.26. The model predicts the response with low prediction error, but it struggles with the frequent step changes in the PRBS and APRBS validation signals, presented in the figure as an enclosed region (labelled 1), and this can be observed across the whole validation dataset. This behaviour of chirp based NN model is more prominent for PRBS type validation signal than for APRBS validation signal. This is because PRBS signal is a 2-level signal with a change in amplitude from minimum to maximum. But for chirp validation signal, the model performs extremely well.

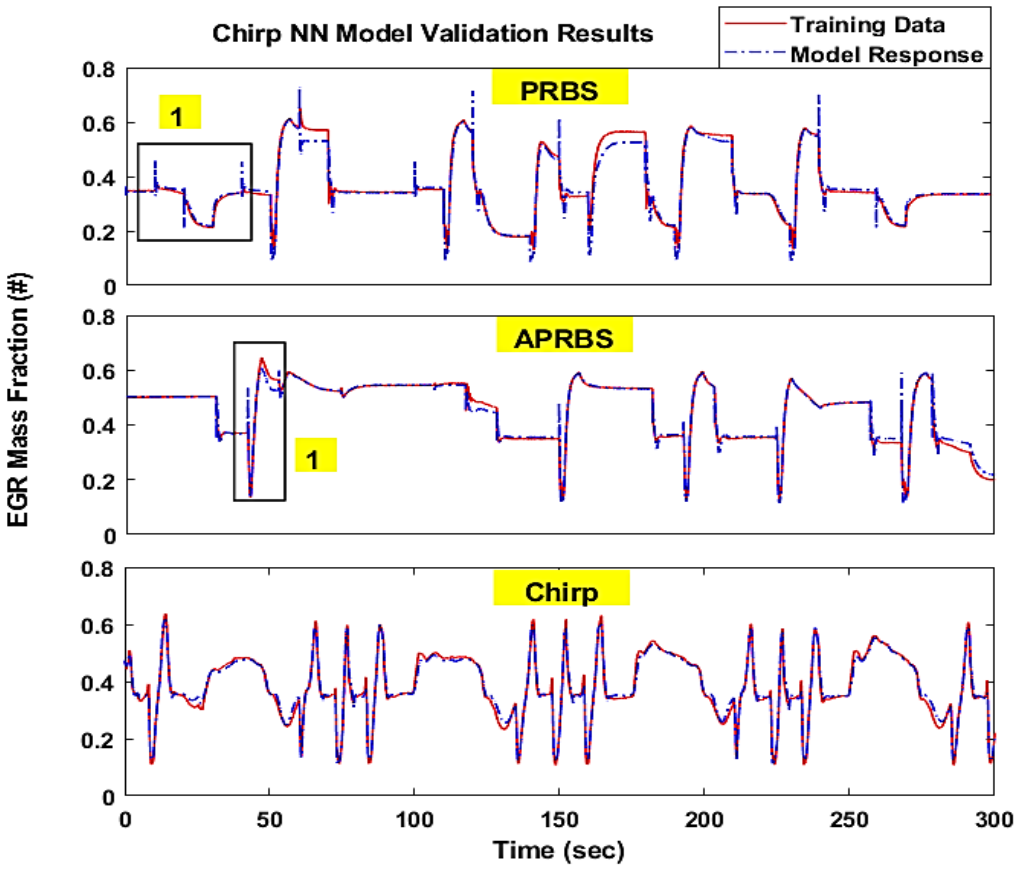

Figure 5.26: Performance of Chirp based NN Model on three different validation signals.

On the basis of the statistical analysis of performance, the chirp signal-based NN model provides better overall performance, and they require shorter training time and provide reasonable accuracy in trends. Therefore, chirp signal was selected as a most suitable signal for the neural network models. Arguably, APRBS based model performance is similar to the chirp based, but they require longer training time and large of number of neurons to identify the EGR response model.

5.6 Selection of Signal Model Combination

In this section previously selected signal model combination, the APRBS based LOLIMOT models and chirp based neural network model, are compared with each other. The best performing combination between the two is selected for modelling the remaining model outputs, inlet pressure and inlet temperature. The recorded statistical performance data, from Table 5.5 and Table 5.8, for the two combinations, is compared and is depicted in Figure 5.27.

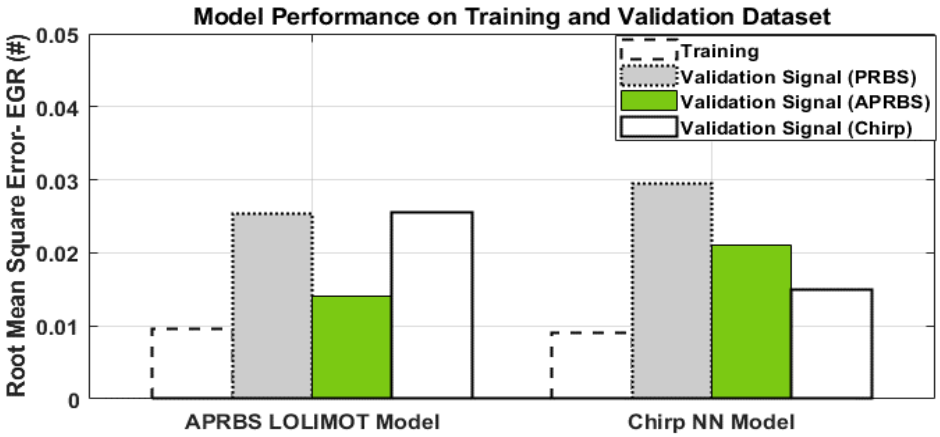

Figure 5.27: Performance of selected LOLIMOT and NN model.

From Figure 5.27, it can be observed that APRBS-LOLIMOT model performs slightly better than the chirp-NN model. Also, APRBS-LOLIMOT model is slightly faster in regards to training time, refer to Figure 5.16 and Figure 5.22.

The major difference between these two models lies in the trend analysis. The APRBS-LOLIMOT model predicts the trends in all three type of validation signals with good accuracy, refer to Figure 5.25. On the other hand, chirp-NN model struggles to capture the step changes, refer to Figure 5.26. Therefore, APRBS-LOLIMOT model is selected as the suitable signal-model combination and is use hereafter for developing dynamic air path model based on MPES platform. Although LOLIMOT type model is selected on the basis of statistical and engineering analysis, the neural network is an equally viable option.

Residual analysis on the selected model, APRBS-LOLIMOT, was carried out to identify that model prediction does not have any bias or trends associated which would violate the constant variance assumption. The residuals are the difference between measured and predicted system response and residual analysis for the selected model is illustrated with the help of three plots in Figure 5.28. The residuals vs time plot (top) confirms the degree of randomisation, as there is no negative serial correlation or other discernible trends present in the error terms. Also, observation of residuals vs fitted value plot (bottom-left) shows residuals are randomly scattered, which indicates that model is correct on average, across the fitted values. Furthermore, normal probability plot (bottom-right) suggest that the distribution of the residuals is approximately linear, this indicates that residuals follow the normal distribution

curve. Based on the three plots presented, the constant variance assumption for the selected model across the observations is a valid assumption.

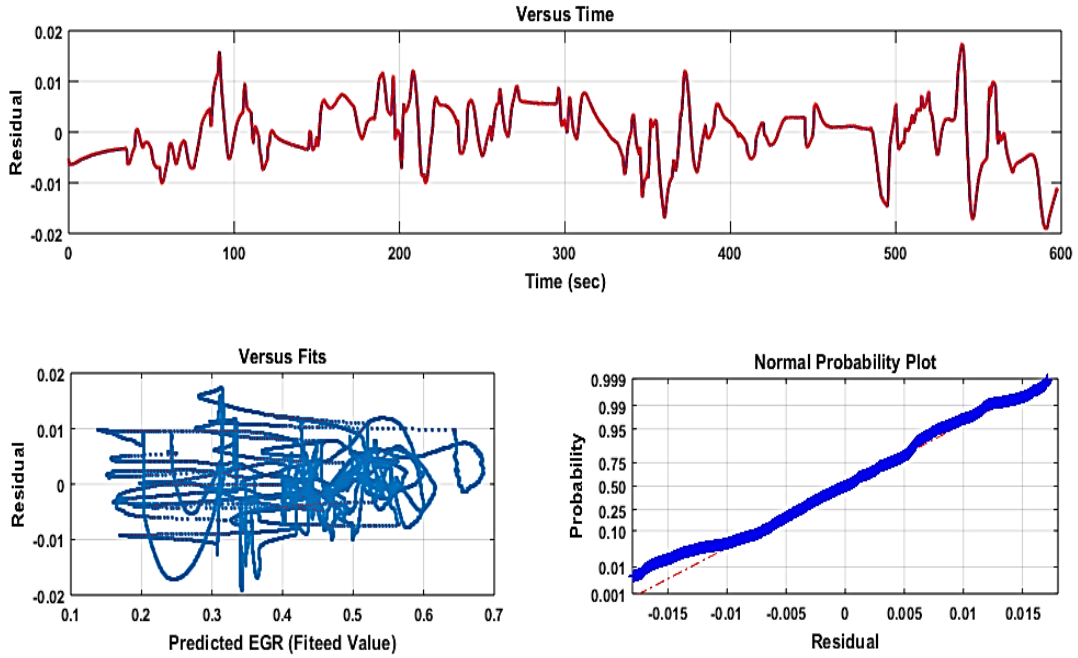

Figure 5.28: Residual plot of selected model (APRBS LOLIMOT).

5.7 Summary

The development of the strategy for dynamic air path model of the hybrid dynamic modelling framework was presented and implemented in this chapter. The process of modelling developing dynamic air path was described in detail along with the selection of excitation signal and modelling architecture. The modelling behaviour associated with different input excitation signal has been illustrated, and their capability has been analysed.

The model selection is done by evaluating training and validation RMSE of the models and by comparing response surface predicted by the model with the response surface of the system (from the simulation models). Based on these

two criterions, the best performing input signal design and modelling architecture is selected. Thereafter, residual analysis of the selected signal and model combination is carried out to ensure the model can capture the system behaviour without any bias. Finally, the selected model is used for development of dynamic air path.

In co-modelling strategy, it was observed that the model trained on a specific signal performs better on validation signal of same type. This is underpinned by signal properties, such as chirp signals, which are slow varying dynamic signals with less significant step changes, not being able to predict the step changes associated with the APRBS signals. Additionally, the chirp signals have sparse coverage in the centre which is not the case for APRBS type signals. However, the continuous nature (slow varying dynamic) of the chirp signals make them less problematic with regards to safe engine operation rather than step disturbances, particularly in case when developing global experiments for whole engine operating envelope. On the other hand, APRBS type of signals cover a broader frequency range (both high and low frequency components) and cover a wide range of amplitude providing best data coverage. If APRBS is implemented in a similar fashion as in this work, global-zone modelling approach, which allows safe engine operation by designing dynamic experiments with less harsh step changes due to local limits and easier compliance of constraints, make APRBS signal types a superior choice of identification purpose. However, if global modelling for entire engine operating envelope is considered, the harsh nature of step changes of these type of signals are not suitable to all engine systems.

Chapter 6 Development of Surrogate Model for SRM Combustion Process Model

This chapter presents the second stage of the hybrid dynamic modelling framework, development of surrogate combustion model, in conjunction with Diesel engine case study. The proposed framework, in section 4.3, combines the dynamic modelling air path strategy (described in the previous chapter) with the statistical modelling of NOx emission, to predict transient emissions in real time. The investigation into surrogate modelling of the combustion process to predict NOx was carried out with the following steps:

- Planning DoE test runs using sequential space filling OLH DoEs.
- Fitting statistical models to the DoE test runs to develop surrogate NOx model.
- Validation of the surrogate NOx model.
- Discussion of the results based on statistical and engineering analysis.
- Evaluation of the hybrid dynamic modelling approach on the transient drive cycle.

6.1 System and Model Parameters

6.1.1 Model Inputs

The model inputs considered for the combustion modelling are the inputs listed in Table 4.3 of Chapter 4. In this thesis, the engine out emission which is being modelled is nitrous oxides (NOx). The model inputs can be classified

into three types depending on the system their point of origin and are as follows:

- **Operation Point Inputs**: these inputs are directed from the engine operational domain. These inputs include engine speed and engine load (Torque), they represent the demand or driver request.
- **Intake Dynamics**: these inputs are directed from the air path model and in this study from the dynamic air path model. In other words, the outputs of the dynamic air path model, listed in Table 5.2.
- **Intake Fuel Dynamics**: the usage of common rail systems enables the variation of rail pressure and a splitting of the injection in the pilot, main and post injections. However, the settling of rail pressure has dynamics associated with it, but it is relatively fast (Sequenz, 2013), and is disregarded in this study. To account for the injection characteristics of the system, injection profiles were provided by the sponsor company, and these profiles were utilised for the combustion process model.

6.1.2 Model Outputs

The pre-validated SRM combustion model provides engine-out emissions as a response to the inputs described above. While the SRM combustion model provides results for all the engine out emissions, such as CO, HC, soot, NOx etc., this work focuses only on the modelling of NOx. This is because the current SRM model is single zone thermodynamic model and prediction of other emissions was problematic (Korsunovs, 2017). And to further improve

prediction capability for other emissions, a multi-zone model is required, therefore, in this study efforts are directed toward modelling of NOx emissions.

6.2 Development of Surrogate Model

The modelling process involved in the development of surrogate combustion model, as described in section 4.4.2 of Chapter 4 is illustrated in Figure 6.1 and summarised in the following few steps:

- Design of Experiment: first step in the modelling process is to generate the design of experiments which would provide information required to develop surrogate models. The DoE test runs carried out on the dynamic air path model to generate inputs for the combustion model.
- Data Collection: run CMCL SRM with operational, air path and fuel system inputs and collect the NOx as output.
- Fit Surrogate Model: utilising inputs and outputs of the CMCL SRM combustion model, fit a set of statistical models and select the best performing model.

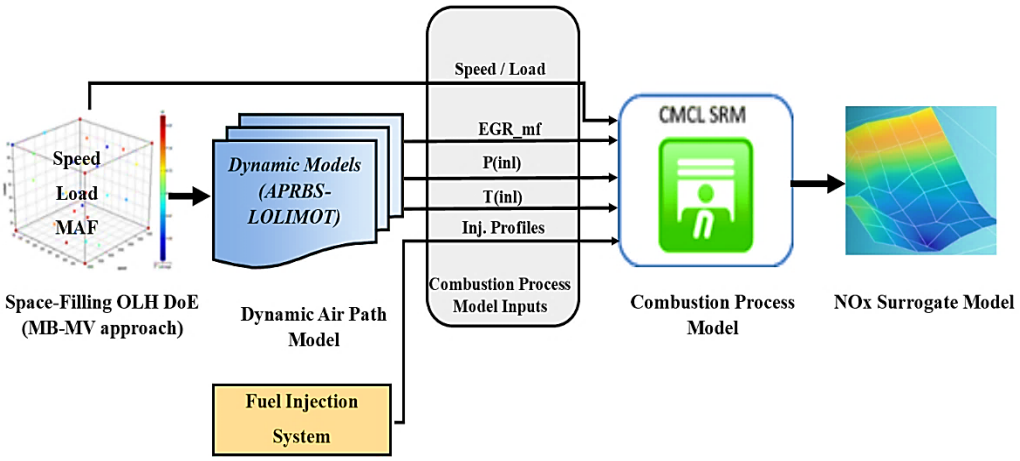

Figure 6.1: Process of developing surrogate NOx model.

The procedure of the development of surrogate combustion model is illustrated in Figure 6.2. The figure depicts the procedure followed and presents the division of the process into stages.

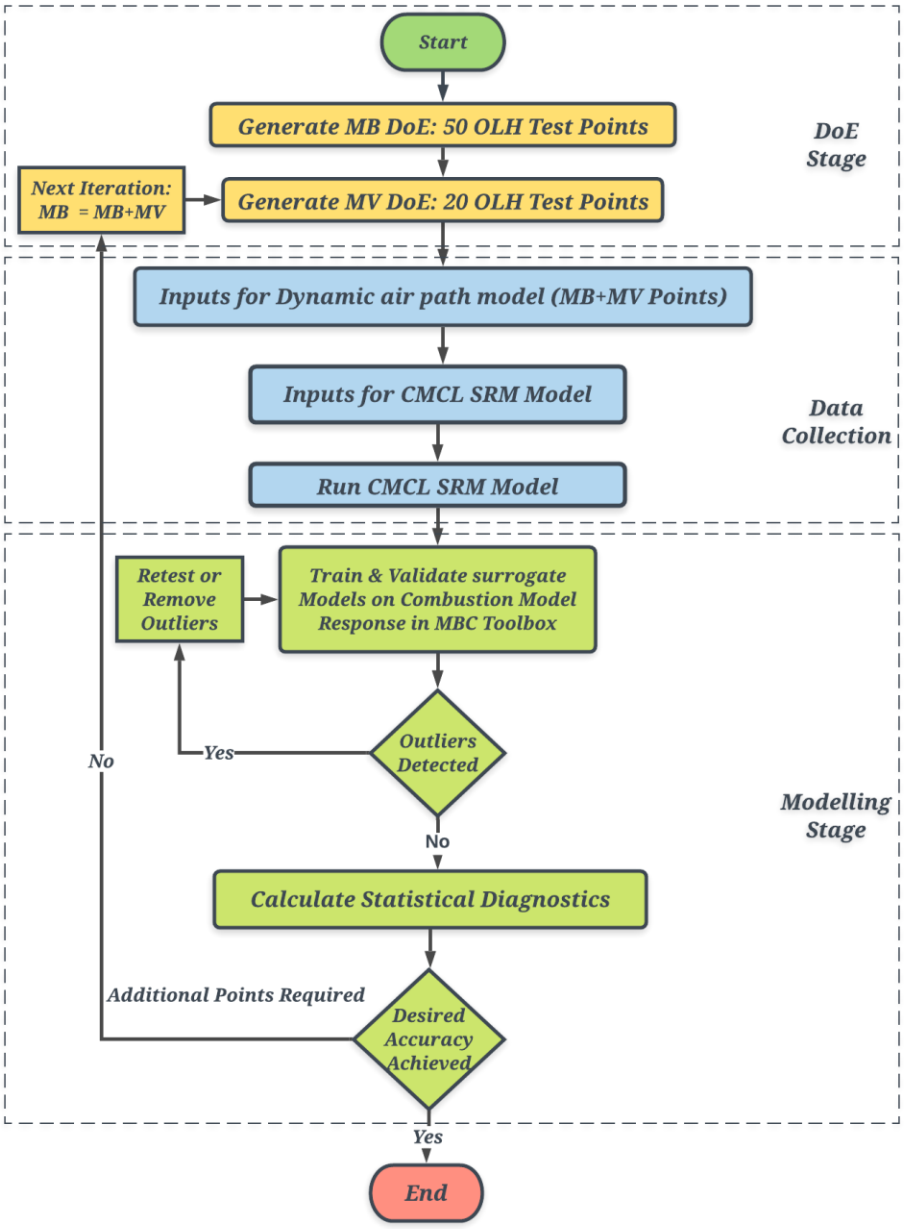

Figure 6.2: The offline DoE and modelling strategy proposed for the metamodeling of combustion model.

6.2.1 Design of Experiments

The method used to generate sequential designs has been described in detail in section 4.4.2.2 of Chapter 4. The OLH based sequential DoE framework is a Model Building - Model Validation (MB-MV) DoE strategy based on optimal space filling DoEs.

In the first step, an MB OLH DoE with 50 points was generated for model inputs (operational and air path system) listed in 6.1.1, (MB). A MV OLH DoE with 20 points was planned as the first model validation design (MV1). The representation of the MB-MV points generated in the first iteration is depicted in Figure 6.3. The figure shows a two-dimensional representation for three-dimensional design space, engine speed, engine load (Torque), and MAF. The distribution of all variable in the design space is illustrated in Figure 6.4.

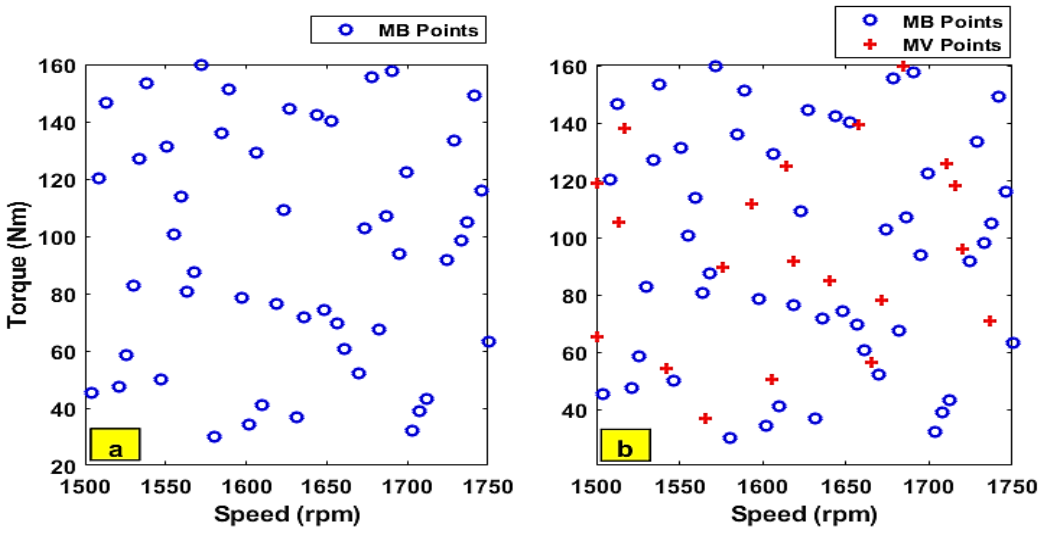

Figure 6.3: MB-MV sequence: a) MB, OLH of 50 points, b) plus points showing the position of validation points (MV1), OLH of 20 points, among MB points.

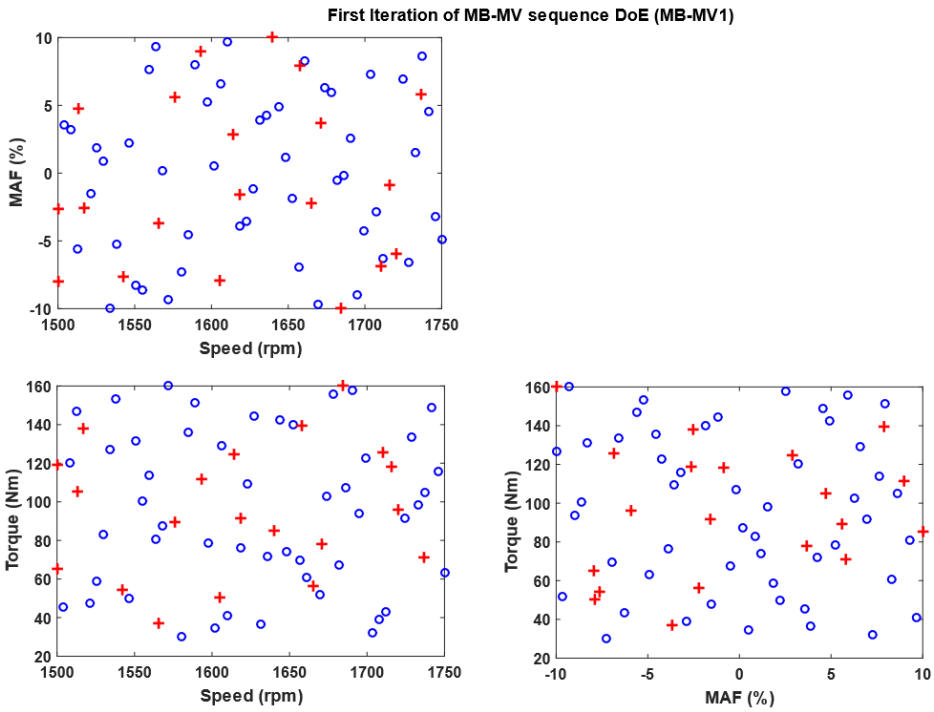

Figure 6.4: MB-MV sequence: design space for all three model inputs.

The quality of DoE generated using MB-MV DoE strategy was evaluated based on the following two criterions:

- **Space-filling property:** The space filling properties of the merged MB-MV1 DoE, is illustrated in Figure 6.5, in terms of the *Euclidean* distance for each of the test points. It can be observed through this figure that the generated test points (for both MB and MV1) are not located too close to each other, thus maintaining space filling property in the design space.
- **Orthogonality:** correlation (r) between the parameters was calculated using Pearson's correlation coefficient (Tietze, 2015), presented in Equation 6.1, which is given as covariance of the two parameters (X_i^k & X_i^j) divided by the product of their standard deviations.

$$r = \frac{\sum_{i=1}^{n}(X_i^k - \overline{X^k})(X_i^j - \overline{X^j})}{\left\{\sum_{i=1}^{n}(X_i^k - \overline{X^k})^2 \sum_{i=1}^{n}(X_i^j - \overline{X^j})^2\right\}^{1/2}} \qquad \text{Equation 6.1}$$

The value of coefficient r = 1 or -1, represent strong positive or negative correlation respectively. To satisfy orthogonality criteria, the value of the correlation coefficient must be zero. It was observed that the correlation between variables for MB-MV1 was negligible, i.e. $-0.05 \leq r \leq 0.05$, thus, design is quasi orthogonal. The values of correlation coefficient observed for the parameters are listed in Table 6.1.

Table 6.1: Correlation coefficient for design variables in MV1 iteration

MB-MV Iteration	Speed-Torque	Speed-MAF	Torque-MAF
MV1	0.01	0.04	-0.03

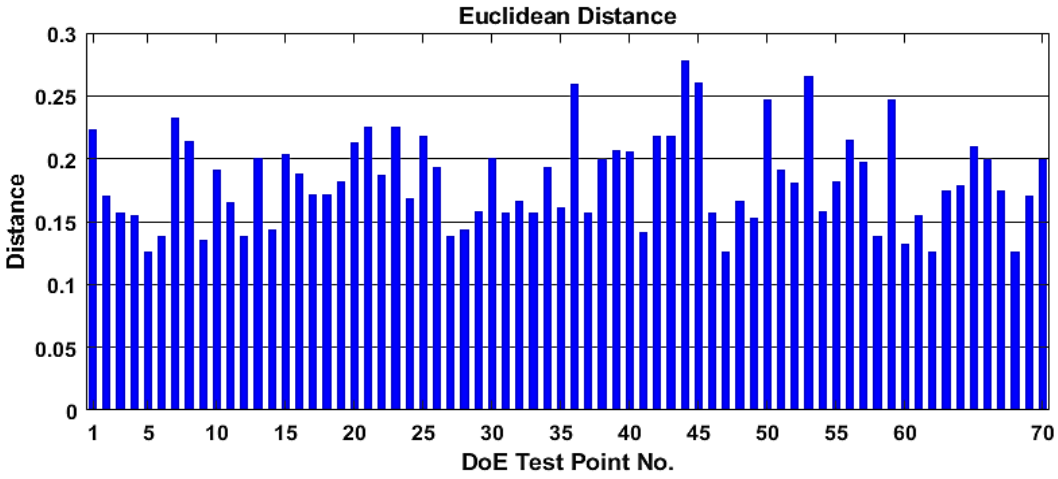

Figure 6.5: Euclidean minimum distance for all MB-MV test points (70 points).

In the process of surrogate NOx modelling, the MB-MV DoE strategy was applied in six iterations. A two-dimensional representation of design space for these iterations is depicted in Figure 6.7. The DoE design quality was again evaluated after the six iterations. The space filling property for the DoE was maintained after 6 iterations, and this can be observed in Figure 6.6, where none of the generated test points (for both MB and MV) is too close to each other.

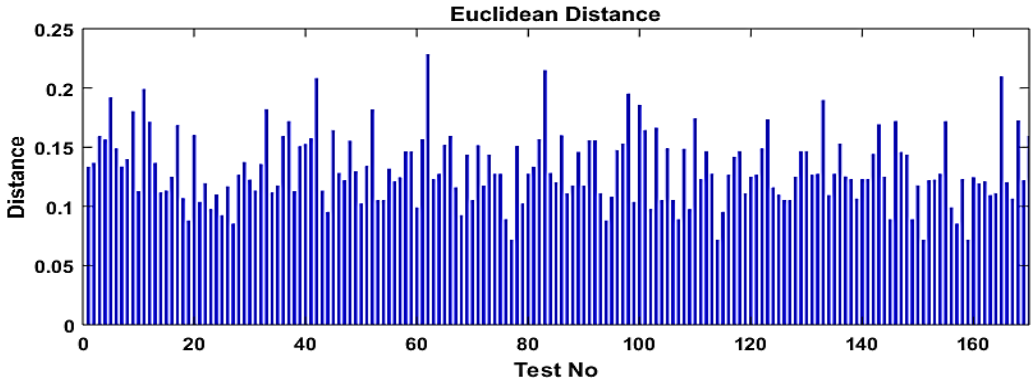

Figure 6.6: Euclidean distance for all MB-MV test points (170 points).

The yielded correlation value between the design variable is presented in Table 6.2, where the correlation coefficient for all the design parameters lies within the range of $-0.04 \leq r \leq 0.04$, thus correlation is negligible. Therefore, the final design is quasi-orthogonal.

Table 6.2: Correlation coefficient value for all design parameter at MV6 iteration.

MB-MV Iteration	Speed-Torque	Speed-MAF	Torque-MAF
MV1	-0.016	0.037	0.028

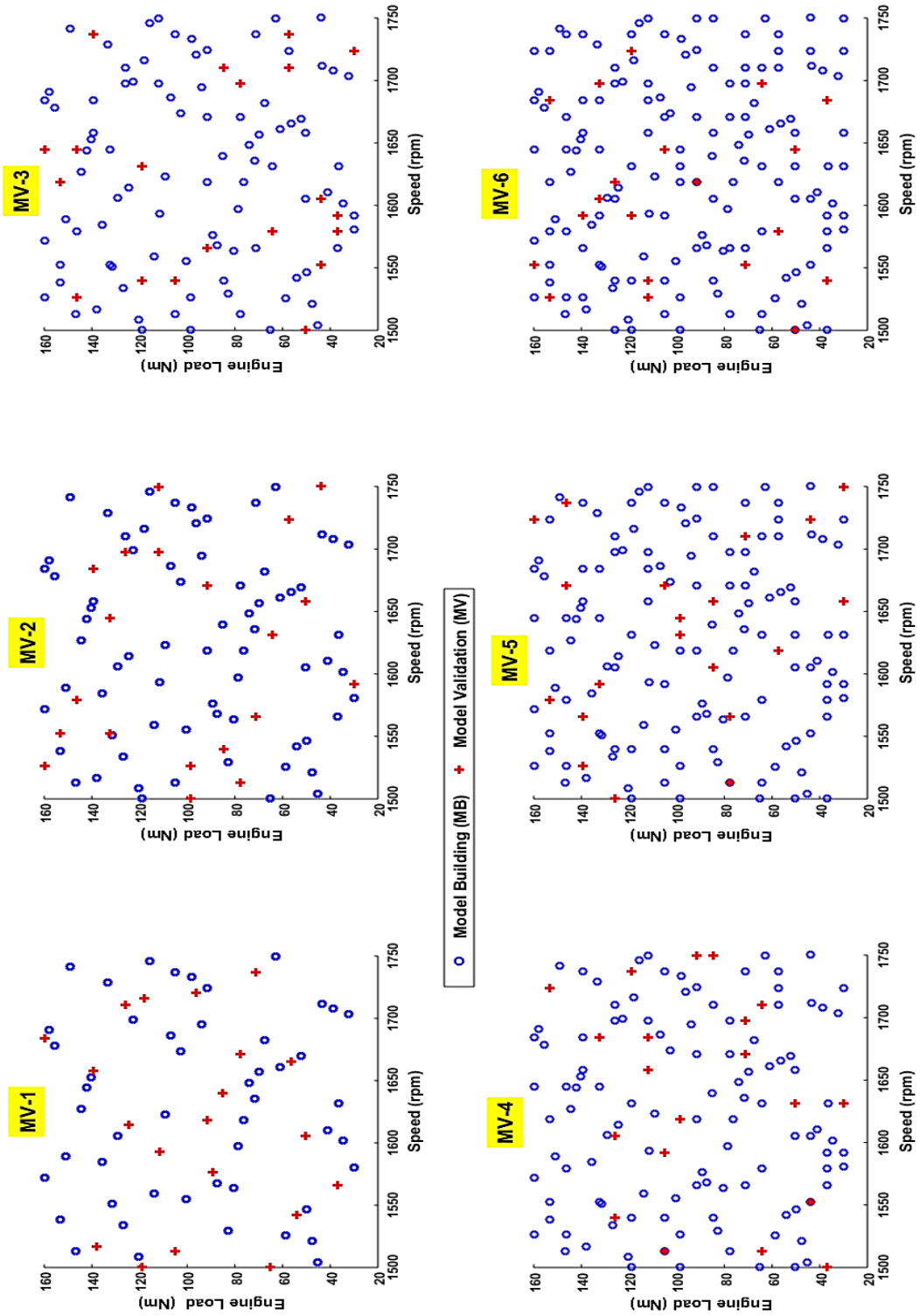

Figure 6.7: MB-MV sequence: 6 iterations generated during the surrogate modelling process of combustion model; plus (+) points show the position of validation points (MV) among the circle (o) MB points.

6.2.2 Analysis of Surrogate Dynamic Air Path Model

Before collecting data for NOx emission by running SRM combustion model, the planned DoE runs were carried out on the dynamic air path model (developed using APRBS-Lolimot signal model combination in section 5.4). The SRM inputs captured by the dynamic air path model are illustrated, along with the response from the GT-Suite Diesel engine model, in Figure 6.8. It can be observed that the model predicts the trends in air path dynamics quite accurately.

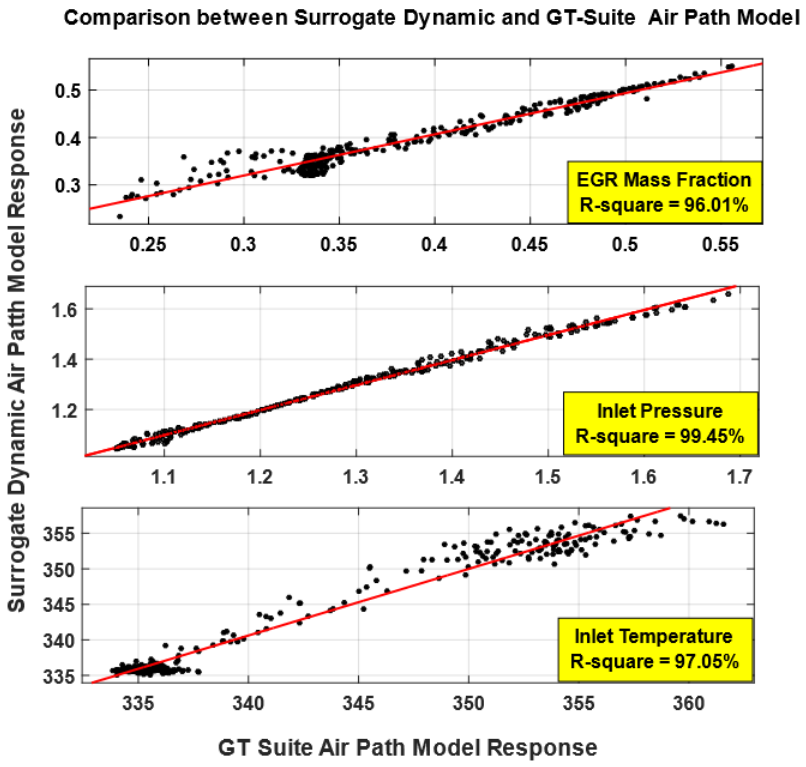

Figure 6.8: Prediction of planned MB-MV DoE by GT-Suite engine model and dynamic air path model.

The R-squared value illustrated in Figure 6.8, indicates that the dynamic model of air path states input account for more than 95% of variance

associated with the response of the system. The fitted line plot above illustrates that the model (dynamic model trained on dynamic signals) accurately (>96% fit for all three air path states input) describes the response for steady state points. In addition to the R-squared value, the statistical analysis of the prediction using validation RMSE (refer Equation 3.2) and relative error (refer Equation 3.3) is listed in Table 6.3. From the table it can be observed that the dynamic models predict accurately for EGR_mf (<0.01 RMSE/1% EGR_mf or ~2% relative error), Inlet pressure (<1% relative error) and temperature (<1% relative error). This analysis illustrates that accuracy of the dynamic models developed earlier is not compromised for the different type of design of experiment approach, i.e. global OLH DoE (steady-state tests).

Table 6.3: Evaluation of performance of surrogate air path model on the DoE for SRM input parameter

Model	**Val_RMSE**	**% Relative Error**
EGR	0.0084	2.1
Inlet Pressure	0.0026	0.20
Inlet Temperature	0.4146	0.12

Noteworthy, it takes GT-Suite Diesel engine model about two and a half hours to generate inputs for the SRM combustion process model on the planned DoE of six iterations. While dynamic air path model was able to do the same task in under 1 minute, that is approximately 210x faster when compared to GT-Suite engine model. This reflects on the benefit of the hybrid dynamic modelling framework which incorporates a dynamic model for system modelling task, allowing quick modelling and fast data capture. The exact

simulation time for both GT Suite engine model and surrogate model is listed in Table 6.4.

Table 6.4: Simulation time to run steady state DoE

Model	Simulation Time (sec)
GT-Suite Diesel Engine Model	**8490**
Surrogate Air Path Model (LOLIMOT-APRBS)	**40**

As depicted in Figure 6.1, the response from the dynamic air path model, operational inputs and the injection profiles are implemented on combustion process model to generate NOx emission response. The surrogate modelling task for the captured NOx response is discussed in the following section.

6.2.3 NOx Model Selection

In this stage of development response surface models are fitted to the NOx emission using MATLAB MBC toolbox. For every new iteration of DoE test plan, i.e. from MV1 to MV6, a new response model was fitted to the update system response. The response model fitting process included the following steps:

6.2.3.1 Fit candidate models

MATLAB MBC toolbox offers a range of statistical models for response surface modelling. Several combinations of response models, Polynomials, RBF with different kernels, Gaussian Process Models with different kernels, were fitted to the NOx emissions response. The advantages of the selected candidate models are as follow:

- **Polynomials:** their advantage lies in their simple structure which makes them easy to interpret and low tendency towards overfitting (Khan, 2011). This makes these models quite common choice and popular in many modelling contexts (Kianifar, 2014). However, given that initial model building DoE only consists of 50 points, they might not be efficient (Kianifar, 2014).

- **Radial Basis Function:** these models types were selected due to their capability of fast and robust modelling (Nelles, 2001)**.** Also, they have superior interpolation behaviour and are capable of providing good generalisation, even for noisy or missing data (Hagan *et al.*, 1995).

- **Gaussian Process Model:** this model type can fit high accuracy global approximation models even with less data (Khan, 2011), thus, making them an ideal candidate for the fitting models to sequential DoE design.

The quality of fit of the candidate models was evaluated using RMSE (see Equation 3.1), and PRESS RMSE (refer section 3.2.5) and any outliers were removed, and the model fit was updated.

6.2.3.2 Model Evaluation and Selection

The model selection criteria employed was minimising PRESS, and during initial iteration, when a small number of test points are available, preference was given to fits with the small number of effective parameters.

The model evaluation was carried out in three phases, and these are as follow:

a) Residual Analysis

this includes analysis of patterns of residuals for model building. Residuals represent the difference observed in the predicted values (by response surface model) and measured values (from the SRM combustion model). Presence of a discernible trend would indicate the inappropriate model for the data, while random appearance would stipulate an appropriate model choice.

b) Statistical Performance

statistical diagnostic is used to compare the response surface model performance on the measured data and to evaluate any improvement in the response surface model with the additional test plan. This is carried out by implementing two performance matrices:

- Internal model validation: based on investigating the model's statistical properties using PRESS RMSE for MB data set, see section 3.2.5.

- External model validation: this validation step investigates the discrepancy between the predicted and the measured values on a new set of data, the validation set (MV), using information criteria Validation RMSE (see Equation 3.2) and Relative Error (see Equation 3.3).

c) Engineering Analysis

Trend analysis was carried out by comparing the fitted model behaviour with the combustion process model response behaviour, to ensure models are not over-fitted or under-fitted.

6.3 NOx Surrogate Model

The process described in the preceding sections for surrogate modelling of NOx is implemented using the MATLAB MBC model browser toolbox.

6.3.1 Fit Candidate Models

The candidate models with various kernel functions were fitted to the first iteration of model building DoE with 50 test points. The comparison of prediction capability (PRESS RMSE) and the number of parameters required by each model are illustrated in Figure 6.9 and Figure 6.10 respectively.

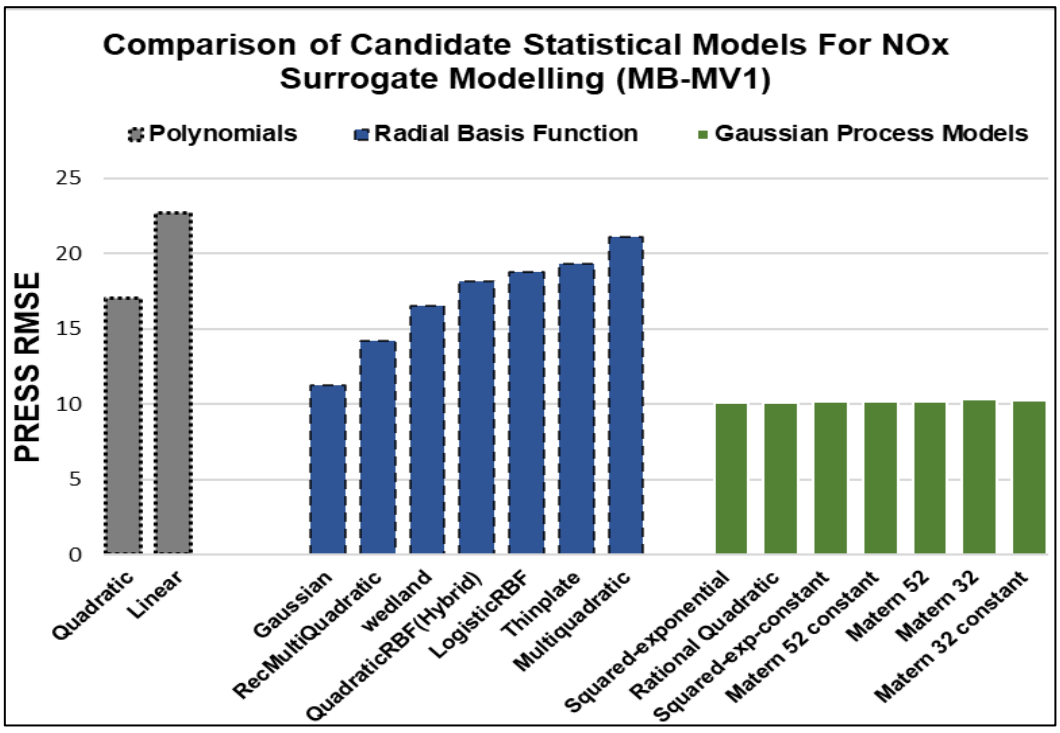

Figure 6.9: Comparison of fitted response surface candidate models based on their prediction capability (PRESS RMSE) at MV1 iteration.

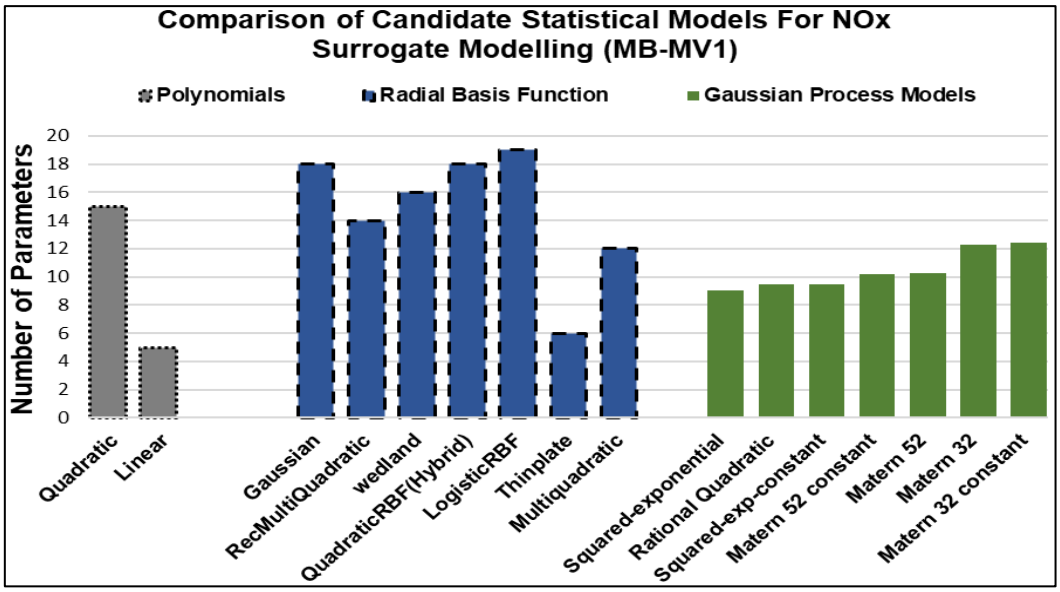

Figure 6.10: Comparison of fitted response surface models based on the number of parameters required for modelling at MV1 iteration.

It can be observed from Figure 6.9, as presumed in section 6.2.3, that polynomials models are not efficient candidate model and have large approximation error associated with them. In respect to the number of parameters, the linear polynomial model has the lowest number of modelling parameters associated with them, but their prediction error is the highest amongst all the other response models. This could be an indicator of under fitted model. Some of the RBF, such as RBF with Gaussian kernel, exhibit good prediction capability but they require a large number of modelling parameters (approximately 1/3rd of test points), thus are not a suitable choice.

The Gaussian Process Model (GPM) with different basis function and kernels, provide both good prediction capability and have a reasonable number of effective parameters. Amongst the GPM models, GPM with squared exponential basis function slightly performs better than the rest, both in terms

of approximation error and number of effective parameters. Therefore, this model was selected for further improvement with additional iterations of MB-MV DoE sequence.

6.3.2 NOx Surrogate Model: Modelling Stage

Once the model was selected, it was improved further to meet the target accuracy through the iterations of sequential DoE plans presented in Figure 6.7. The evaluation of the selected model over these iterations is presented in this section.

A. Residual Analysis

The illustration of residual plots for NOx model at stage 1, MB-MV1, is presented in Figure 6.11. The residual plot is generated using the difference between the measured system response and model-predicted response. In the figure below, residuals are plotted against the observation number, time order in which data was observed. The residuals of a model, approximately, are expected to have the random appearance and no discernible pattern. During the initial observation of the trends in the figure, residuals display either funnelling in and fanning out patterns which are indicators of decrease and increase in error variance. This would lead to a violation of the constant variance assumption (Gonzalez, 2016).

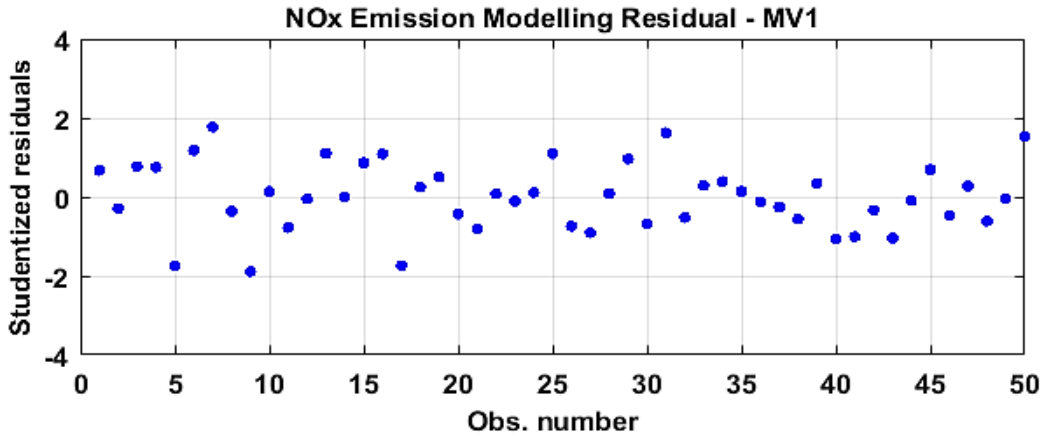

Figure 6.11: Residual plot of GPM squared exponential response surface model for NOx response after the first sequence (MB-MV1).

However, Figure 6.12, the normal probability plot suggests that the distribution of residuals is approximately linear. This would mean that the residuals follow the normal distribution curve (bell curve) and the assumption of constant variance is valid for the fitted models. Also, Figure 6.13 depicts that there is no negative serial correlation or other trends present in the error terms. Thus, constant variance assumption across the observation is a valid assumption.

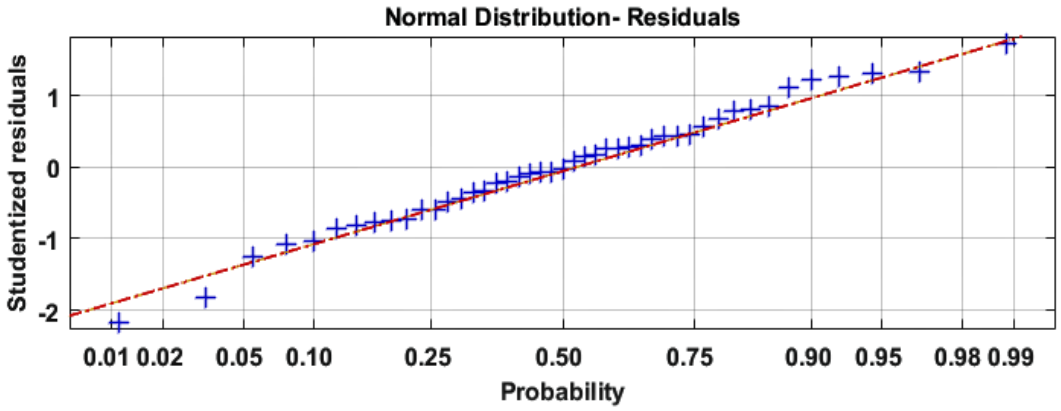

Figure 6.12: Normal probability plot of residuals for GPM NOx surrogate model after the first sequence (MB-MV1).

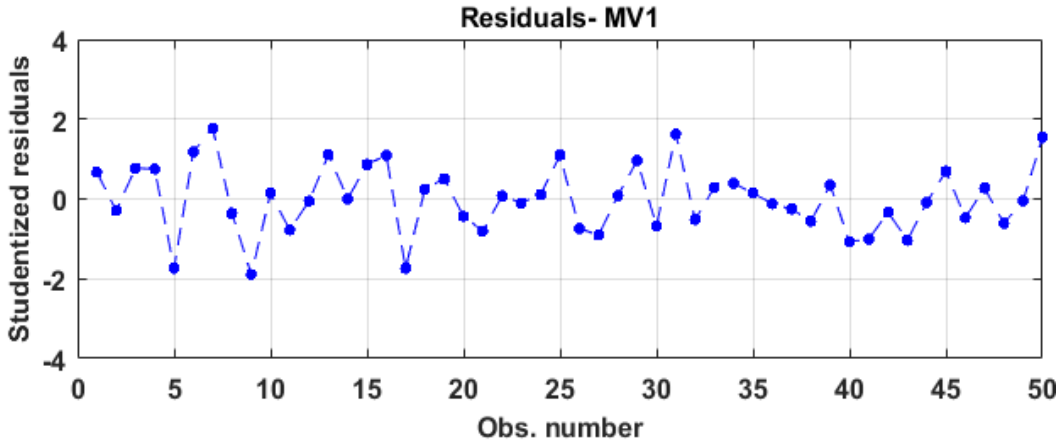

Figure 6.13: Residual plot for GPM NOx surrogate model in MBC toolbox displaying no negative serial correlation after the first sequence (MB-MV1).

B. Statistical Performance

This section presents the evaluation of the response surface model as per the information criterion, PRESS RMSE and Validation RMSE. In Figure 6.14, the PRESS RMSE and the Validation RMSE of the response surface model at every stage have been depicted. It can be observed that the PRESS RMSE and Validation RMSE are decreasing with a subsequent iteration of MB-MV sequential DoE. This indicates that the quality of the response model is improving with every new iteration of the sequential process. The reason for this improvement comes from the fact that there are more infill or test points available for the response models to accurately capture the trends in the modelling data.

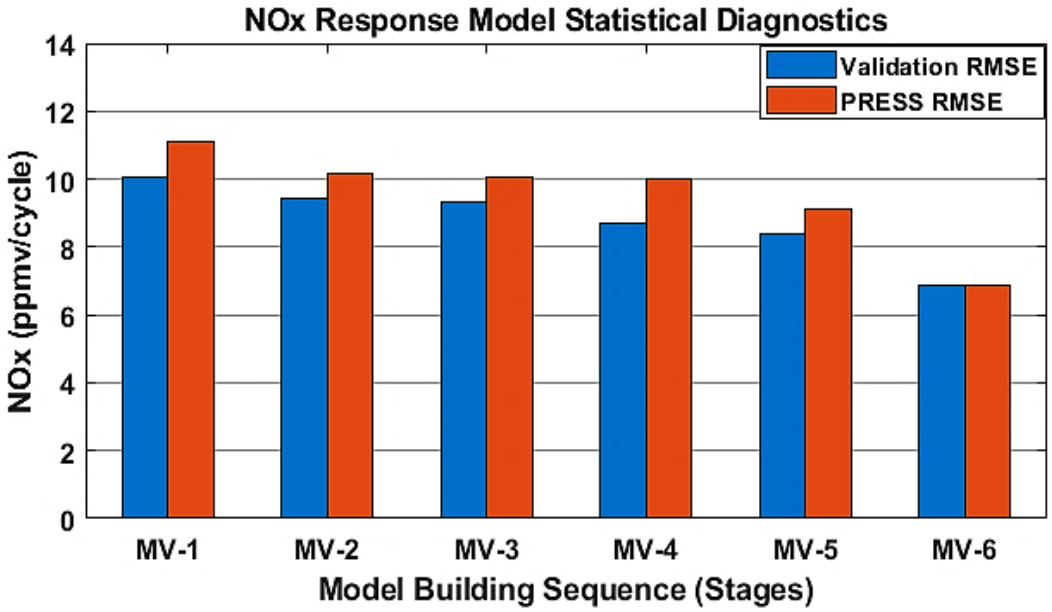

Figure 6.14: PRESS RMSE and Validation RMSE for GPM NOx surrogate model during six different stages/iteration of MB-MV.

In addition to the model improvement observed through the decrease in PRESS RMSE and Validation RMSE, a similar trend was observed for model prediction relative error. The relative error, illustrated in Figure 6.15, is the ratio of validation RMSE to mean response and is expressed as a percentage. The observation of the reduction in the PRESS RMSE, validation RMSE, and relative error (Equation 3.3) with subsequent iterations of DoE represents that response surface is enhanced with every additional stage. The acceptable engineering target for NOx emission modelling lies in between one to ten percent. It can be observed in Figure 6.15, this target was reached at stage 6 (MV-6) with a relative error of 9.4%, and thus, the process was terminated. However, subsequent iterations can be carried, if further improvement is required.

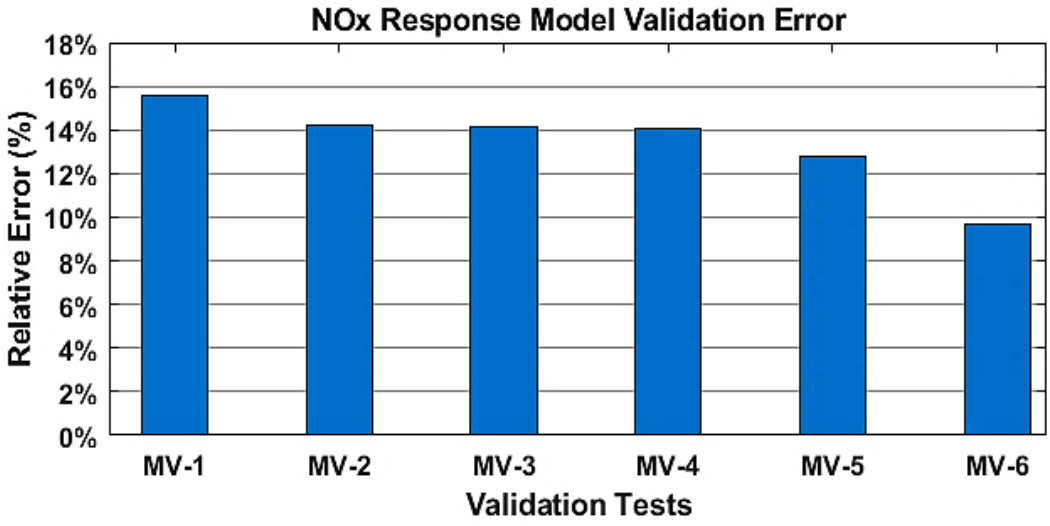

Figure 6.15: NOx prediction relative error for all six stages of MB-MV sequential process.

The identified response surface model at stage 6 was based on a mapping DoE of 150 MB and 20 MV test points. This is significantly less than normal stationary mapping DoEs, which typically use 120-150 (steady state speed and load test points) test points (Yin, 2012). However, the number of points varies and would depend on the number of variables in DoE, and these test points are for a combination of one operational variable, not an entire zone (for example one engine speed and load point). The rule of thumb in the industry is minimum of ten points per variable (three variables in this study). If the constant speed of 1500 rpm is considered with 5 different load points would lead to a minimum of 150 points, while with the methodology presented here; surrogate NOx model was identified for the entire range of the diesel engine case study (1500-1750 rpm) with 150 MB test points. Additionally, combining MB-MV approach provides an advantage of administering target accuracy with each subsequent stage, while for normal mapping DoEs there

is no assurance that target accuracy will be achieved with the pre-determined number of test points.

C. Engineering Analysis

The illustration of NOx emission response surfaces through stage 1 (MV-1), and stage 6 (MV-6) is presented in Figure 6.16 and Figure 6.17 respectively. These figures depict the changes in the response surface, shape and trend, of NOx emission through the iterative process of sequential design of experiments. With the increase in the number of test points, the prediction accuracy of the model improves throughout the design space. The major improvement in between MV-1 and MV-6 response surface can be observed at the extremities of the design space. In Figure 6.16, the design space of stage 1 is deficient at low load region at both low and high engine speed. With the increment in infill points, it can be observed the corners of the design space has extended to cover the low loads, and the prediction accuracy has also improved.

The next step is to analyse if the trends captured by the response surface model compares with the expected trends based on engineering analysis and knowledge available about the system. This last stage in model selection is to check if the trends captured by the response surface model are true characteristics of the system response and not the result of over-fitting or extrapolation among the collected data.

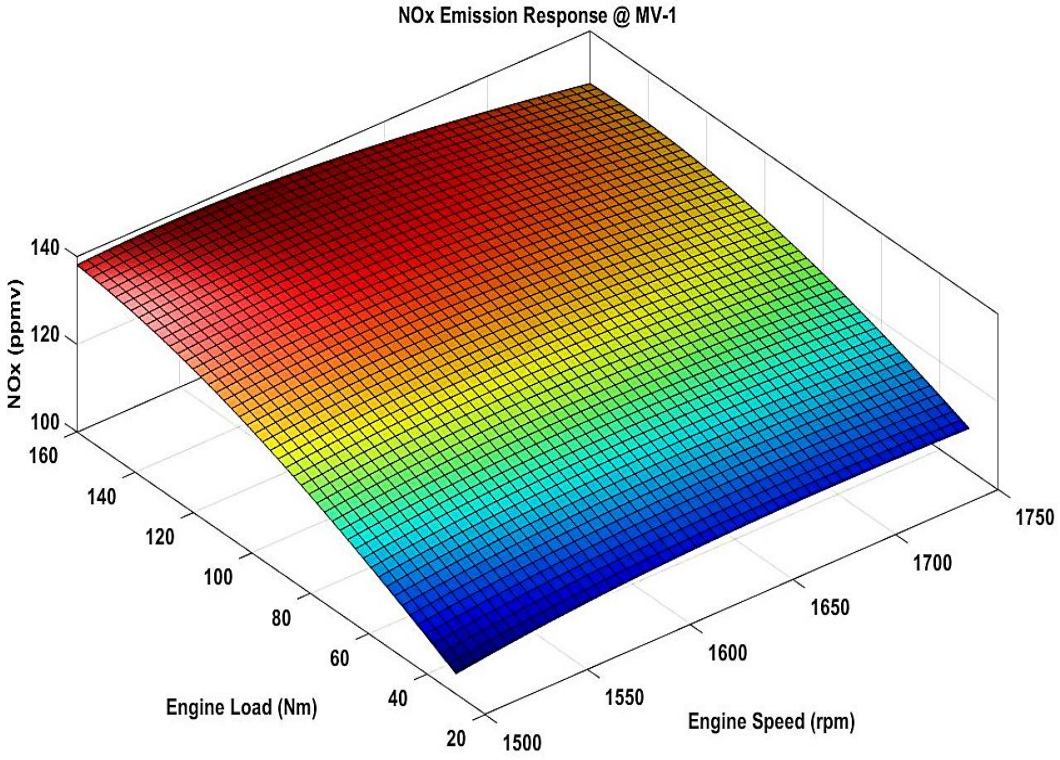

Figure 6.16: GPM NOx surrogate response surface model at MV1 stage.

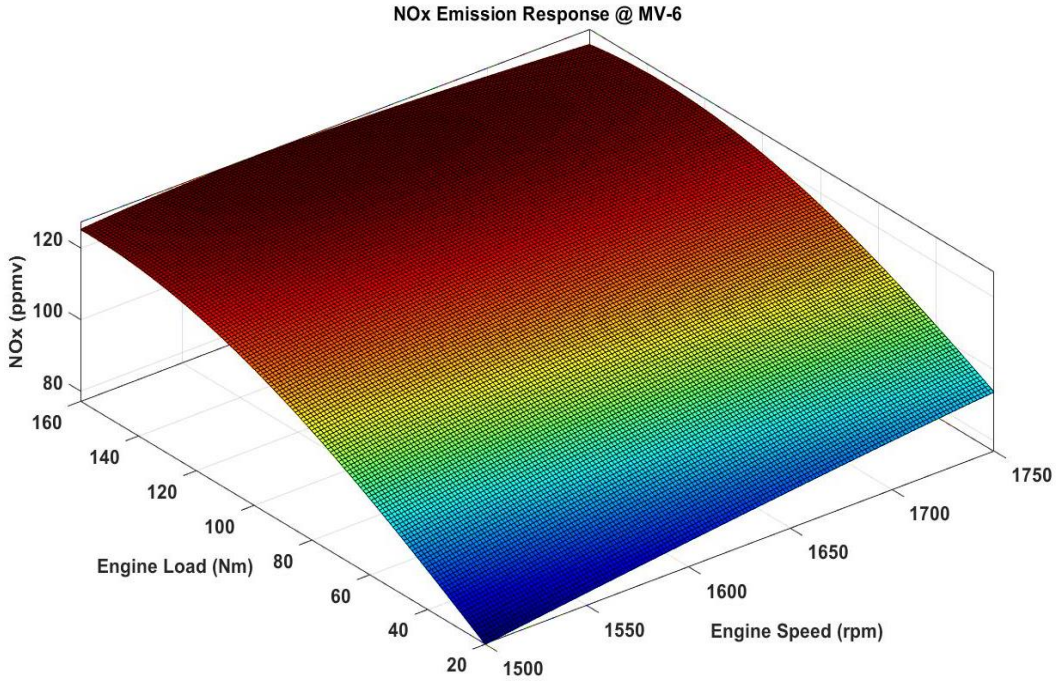

Figure 6.17: GPM NOx surrogate model response surface model at MV6 stage.

In Figure 6.17 for MV-6 stage, there is a clear trend that the concentration of NOx in the engine out emission increases as the load increases. The engine load in this study refers to torque as a set point, which is used to control the injection quantity. Torque being an output of the combustion process does not have a direct effect on the NOx emissions, rather it is an indicator of the change which would be observed in the quantities entering the combustion chamber. The phenomenon observed could be explained with three main factors:

1) The increase in torque is a result of vigorous combustion. To achieve this inlet pressure is increased which causes an increase in the density of air, allowing more air to enter the cylinder, and leading to vigorous combustion. This results in increase in the in-cylinder pressures and temperatures, which causes the increase in NOx.

2) Secondly, high load demand would result in a higher inlet temperature which raises the overall combustion temperature and thus the explainable rise in NOx. However, the effect on NOx from the higher inlet temperature is not as high when compared with an increase in inlet pressure. This is because the increase in inlet temperature decreases the density of air. Hence, less vigorous combustion and lower amount of air mass trapped in the cylinder.

3) Lastly, higher load demand leads to less amount of exhaust gas recirculated by EGR. This is because the purpose of EGR is to reduce NOx by recirculating exhaust gas into the cylinder which results in lower

combustion temperature and reduction in the amount of oxygen available in the cylinder. Hence, leading to less vigorous combustion and lower NOx. Therefore, a reduction in the amount of EGR to meet the high load demand results in an increase in NOx emission. As the sole purpose of EGR is to reduce the NOx formation, it has the most significant contribution to the increase in NOx concentration with the increase in load.

The results of statistical diagnostics for the NOx emission response surface model for the selected model, GPM squared exponential, during all the iterations of DoE are summarised in Table 6.5. The first column in the table represents the stages of the sequential process in terms of model validation (MV) iterations. The 'MB Test Points' column indicates the number of feasible test points used to fit the high-fidelity response models after removing the outliers.

Table 6.5: Summary of Gaussian process models fitted to NOx emissions.

Stage	Model Type	MB Test Points	RMSE	PRESS	Relative Error (%)
MV1	GPM	50	8.48	10.064	15.57
MV2	GPM	68	8.25	9.42	14.23
MV3	GPM	88	8.12	9.32	14.10
MV4	GPM	100	7.47	8.67	14.04
MV5	GPM	118	7.47	8.37	12.75
MV6	GPM	125	6.09	6.86	9.64

6.4 Evaluation of the Hybrid Dynamic Modelling Framework on Transient Drive Cycle

The surrogate model of NOx developed above was validated on the available transient drive cycle data, illustrated in Figure 4.2 in section 4.1. The regions of the drive cycle which are within the boundaries of the operation domain of the diesel engine case study (zone 3) were selected and are presented in Figure 6.18. The selected regions are continuous in time, as extracting points which are not continuous points would lead to distortion of drive cycle and the prediction on such points by NOx model would not be comparable. In total 9 regions were identified, illustrated in Figure 6.19, and these are used to evaluate the performance of NOx surrogate model.

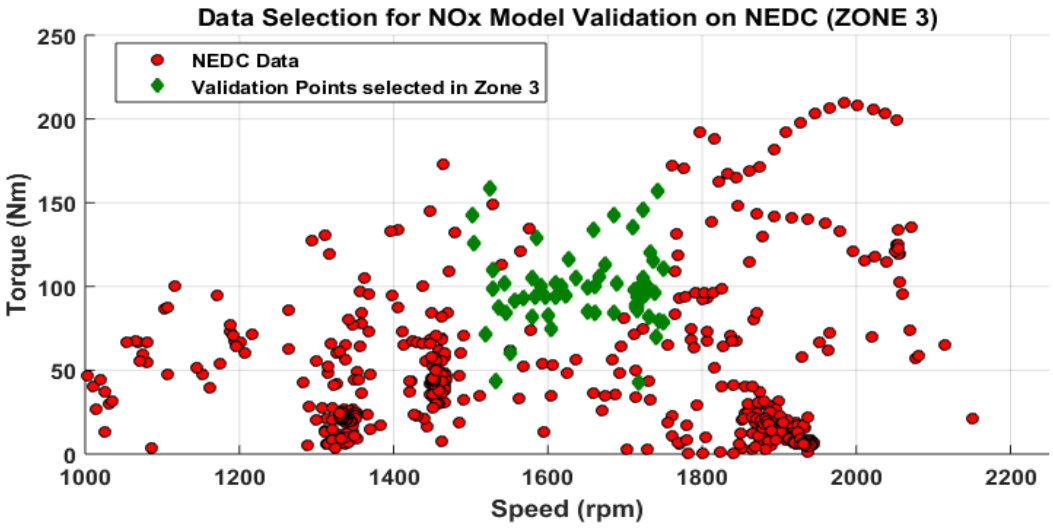

Figure 6.18: Selection of continuous sections in transient drive cycle within the operational limit. The circled point shows drive cycle data, and the diamond represents the points in the extracted regions.

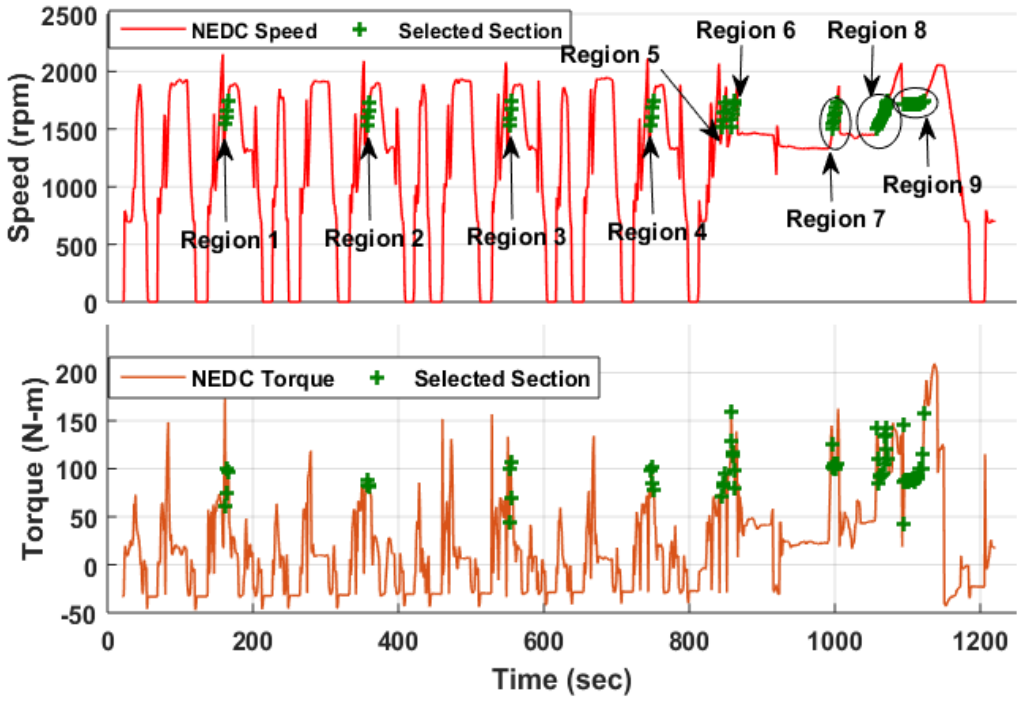

Figure 6.19: Selected regions of the continuous point in NEDC drive cycle within the operational boundaries of zone 3.

The process of evaluating surrogate NOx model based on hybrid dynamic modelling approach and the steady-state based approach was illustrated in Figure 4.14 and described in section 4.5 of Chapter 4. From the figure above, region 9 was selected to present the model performance, as this region had the longest length of the continuous sequence, with 29 data points. The NOx surrogate model performance was compared with the measured drive cycle NOx and steady-state based combustion process surrogate model. A series of pictorial representation to evaluate the model performance has been presented in Figure 6.20, Figure 6.21,Figure 6.22 and Figure 6.23. The evaluation is presented in two section engineering analysis and statistical analysis.

6.4.1 Engineering Analysis

In Figure 6.20, NOx emission prediction for both proposed approach, hybrid dynamic modelling, and steady-state approach have been presented. The prediction of these two modelling approaches is compared against the NOx emission for drive cycle, measured at the test bench (Figure 4.3). The horizontal axis displays the time stamp of the region 9 in the drive cycle data. It can be observed that the first three values in the steady-state approach surrogate model are inconsistent with the overall response of this model. It can be considered as an anomaly of the model and is discounted in Figure 6.21 to be able to analyse the trends in the prediction for both surrogate models.

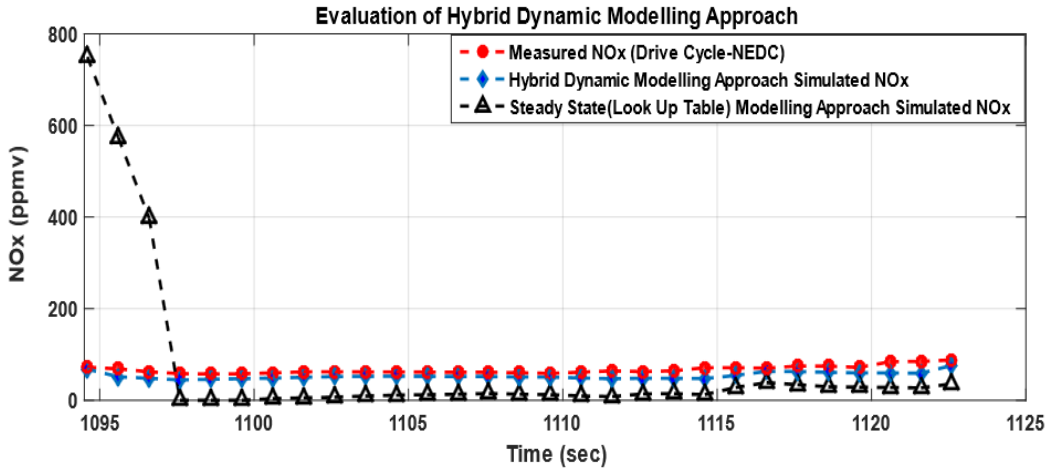

Figure 6.20: NOx emission model performance at region 9 of the NEDC drive cycle.

From Figure 6.21, it can be observed that both steady state and hybrid dynamic modelling approach predicts the trends, associated with the drive cycle NOx emission, reasonably well. The additional advantage of proposed

approach, hybrid dynamic modelling framework, is the required measurement time of only about 40 seconds to generate the inputs for the SRM combustion model to develop surrogate model of zone 3. For both steady state approach and hybrid dynamic modelling approach, the surrogate model struggles to meet the absolute values of NOx emission (when compared to drive cycle NOx emission absolute values), and the effect of this is evaluated in the section.

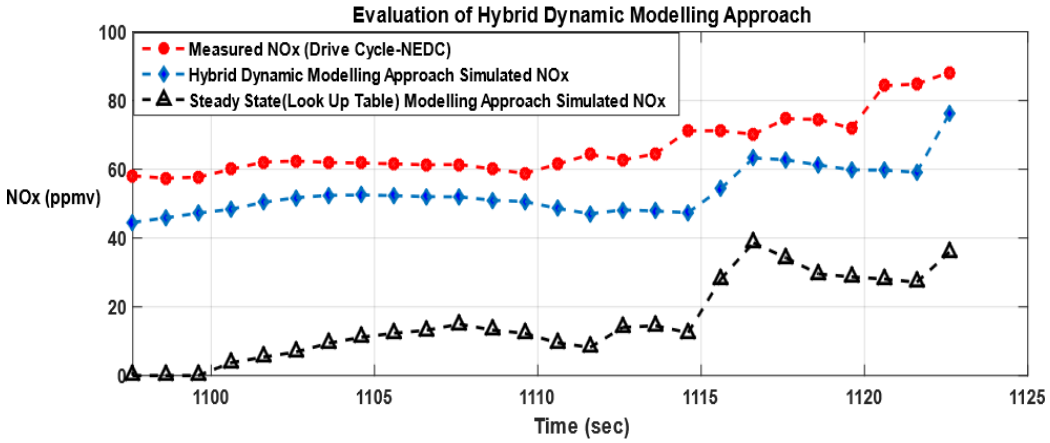

Figure 6.21: NOx emission model performance at region 9 of the NEDC drive cycle (focused view).

6.4.2 Statistical Performance

The criterion used for evaluation of modelling approach against drive cycle data are RMSE (refer Equation 3.1) and relative error (refer Equation 3.3). Table 6.6 shows the evaluation results for both steady state and hybrid dynamic modelling approach. For steady-state based modelling approach, it can be observed from this table that both RMSE and relative error term is extremely high, but this does not provide any conclusive evidence that the

model does not perform well, as the region in which evaluation is carried out is quite narrow. Since, the surrogate model developed (look-up table derived from steady-state experiments) for steady state approach, interpolates to cover the entire operating domain (based on 29 steady state points), it might be extrapolating in this specific region. Also, it can be observed that if the first three points (considered to be abnormal behaviour) are removed, then the model performance improves significantly (compared to when the 3 points are included).

Table 6.6: Evaluation results for both steady state and hybrid dynamic modelling approach.

Modelling Approach	**RMSE (ppmv)**	**% Relative Error**
Hybrid Dynamic Modelling Approach	13.9428	20.93
Steady-State Based Approach	175.578	263.52
Steady-State Based Approach (without first 3 points)	51.0676	76.65

For Hybrid dynamic modelling approach, both the RMSE and relative error is approximately two times the one observed during surrogate modelling, illustrated in Figure 6.14 and Figure 6.15 respectively. This increase in error can be linked to two main factors:

a) As GT suite engine model is a representation of the actual system, it would have an error associated with it. This error is propagated to dynamic models, as the dynamic air path model is developed based on GT-Suite

Diesel engine model. The dynamic air path model provides inputs for combustion model and would explain the discrepancy in between measured and modelled response.

b) Secondly, there will be difference in between the prediction of emissions from SRM combustion model (MPES platform) and measurements on the test bench, and this error will be introduced into the surrogate NOx model. This would also affect the model capability to measure the absolute values accurately.

Although the absolute values of NOx emissions of measured and modelled response are different, it would depend on the development stage if it is acceptable or not. Since, the range of operational domain and number of test points (specifically for steady state, as in dynamic modelling it is a continuous signal) covered by steady state and hybrid dynamic modelling is different, and it is not advisable to compare the numbers, presented in Table 6.6, directly.

A contour plot for the proposed approach is depicted in Figure 6.22, which depicts the percentage error difference between measured (drive cycle data) and simulated (hybrid dynamic modelling surrogate model) NOx emission. The average percentage error for the difference in NOx emission was in the range of around 19 %. For steady-state approach, the same plot is presented in Figure 6.23. The average percentage error associated with the steady-state approach (without the first three points) was found to be 76.65 %.

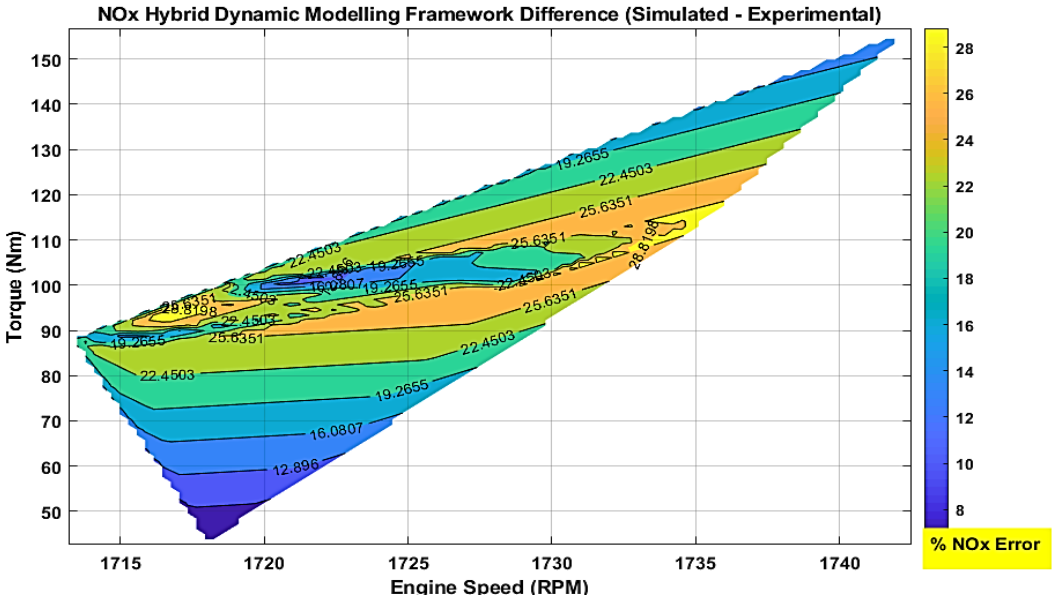

Figure 6.22: NOx error between measured (drive cycle) and surrogate NOx emission model (Hybrid dynamic modelling approach) at region 9.

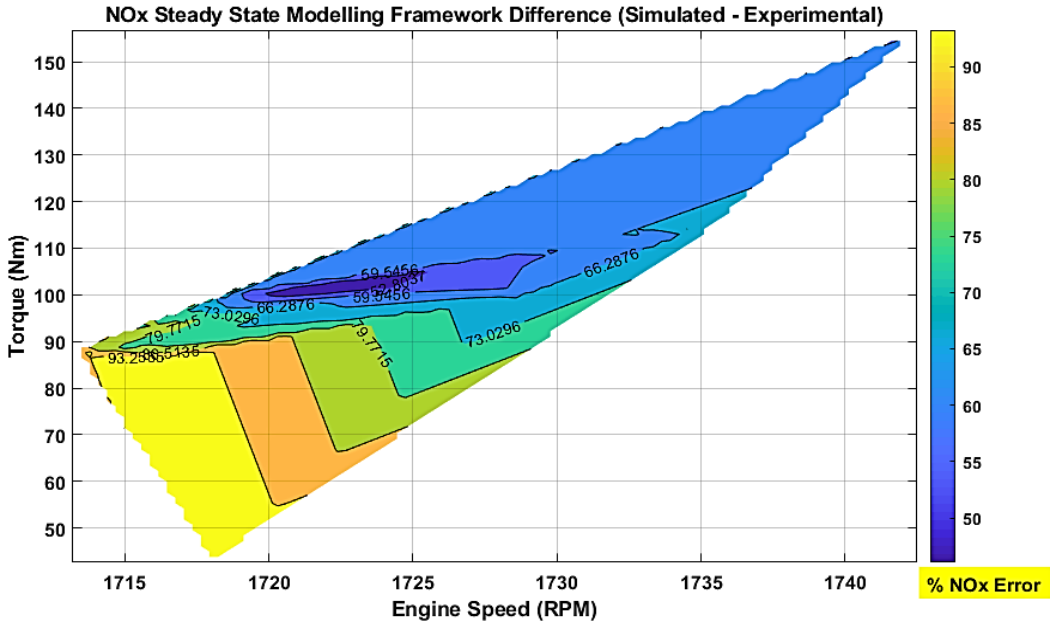

Figure 6.23: NOx error between measured (drive cycle) and surrogate NOx emission model (steady state modelling approach: look-up table) at region 9, without first 3 points.

Although the RMSE error associated with the model prediction of NOx on NEDC drive cycle is high but is still within the reasonable range, and along with its capability to capture the trends accurately makes it an efficient model.

The prediction of all nine extracted regions of the drive cycle is illustrated in Figure 6.24. It can be observed from this figure, that the steady-state based approach surrogate NOx model always overestimates the NOx emission at first few values and then at a later stage it starts to follow the trends associated with measured data quite well. This could be the just the oscillatory behaviour of the model (given sudden start) and might be corrected by adding a pseudo-steady state point at the start of measurement to reduce the oscillations in the model. In the case of the proposed approach, the model predicts the trend in the data quite accurately.

The statistical performance of all the nine regions is presented in Table 6.7, from which it can be observed that average relative error over the nine extracted regions of Zone 3 (illustrated in Figure 4.7) is approximately 11.9%. Although in Region 1, 3, and 9, the error observed is higher, but across all the regions average error is within reasonable limits. Based on the analysis carried out in between hybrid dynamic modelling and steady state approach, the proposed approach provides significant improvement both in terms of capturing trends and accuracy. Although the data on which comparison is carried out is small, the hybrid dynamic modelling framework exhibit enormous potential for simulating drive cycles in real time while providing reasonable accuracy.

Table 6.7: Statistical performance of both surrogate models (hybrid dynamic modelling and steady-state approach) across all the 9 regions.

Region	Hybrid Dynamic Modelling		Steady-State Approach	
	RMSE	%Relative Error	RMSE	%Relative Error
Region 1	13.09	18.01	97.41	133.99
Region 2	1.35	2.30	145.23	247.12
Region 3	13.8	20.35	121.84	179.70
Region 4	3.07	5.66	236.88	437.59
Region 5	9.74	14.99	122.96	189.16
Region 6	5.20	7.05	271.35	367.49
Region 7	4.09	5.87	181.19	260.33
Region 8	8.56	11.480	207.03	277.76
Region 9	13.94	20.93	175.58	263.52
Average	8.09	11.85	173.27	261.85

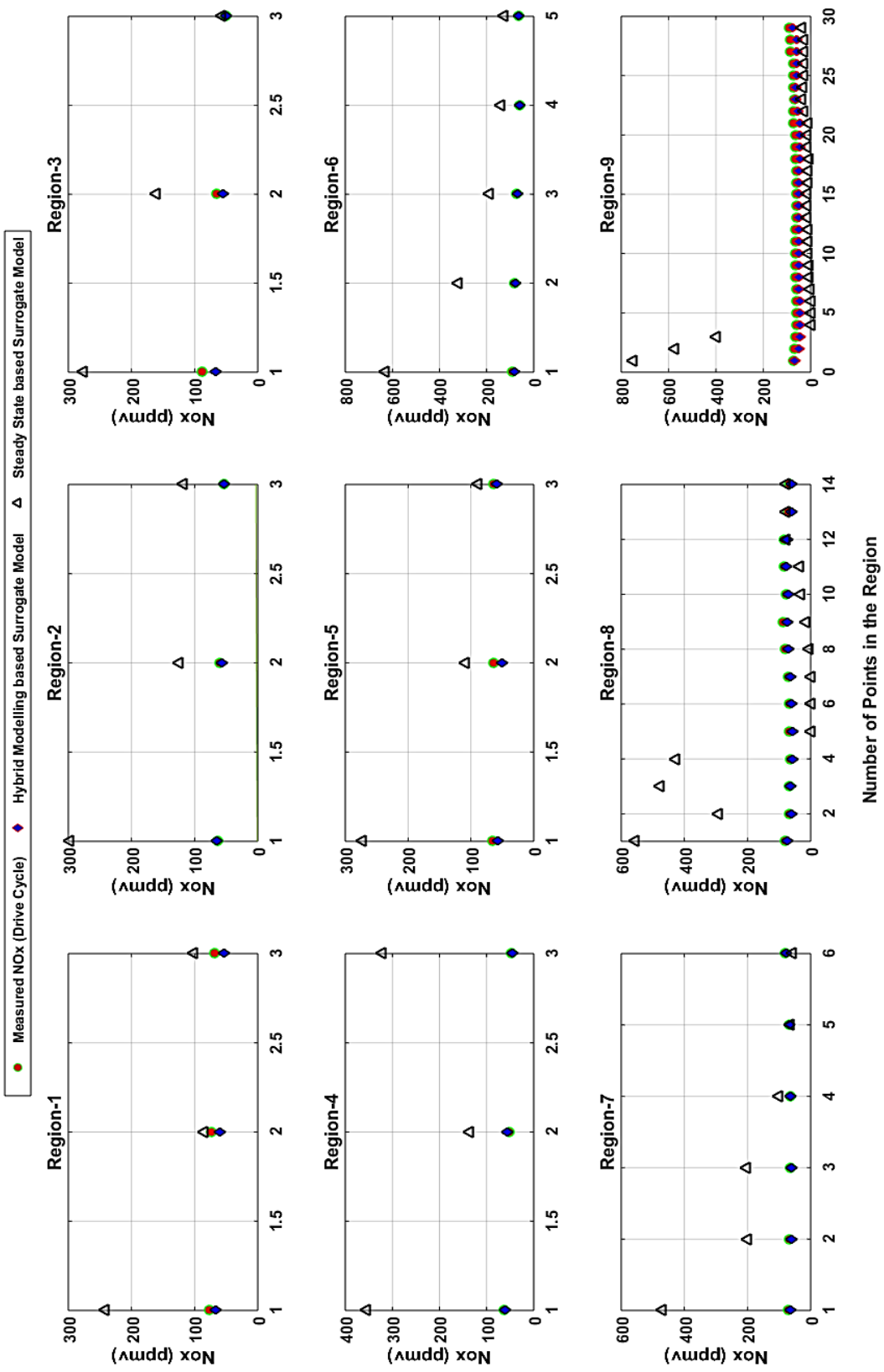

Figure 6.24: Response of NOx model over the 9 regions selected in NEDC drive cycle.

6.5 Summary

The main aim of this chapter was to develop a surrogate model of the combustion model capable of predicting NOx emission in real time and with high fidelity during transients. This was achieved by implementing the modelling framework presented in this thesis which combines dynamic modelling of air path and statistical modelling of combustion model to predict NOx emissions during transients.

The development process of surrogate combustion model presented above was a cyclic process, it starts with the development of the first iteration of DoE, followed by mapping of system response, and thereafter by fitting response surface model to system response recorded by evaluating DoE test plan on the system of interest. These steps were repeated in the loop with every new iteration of DoE until the desired model accuracy was achieved for the system response.

The approach used for the design of experiment was the MB-MV framework, which initialises with the model building DoE of OLH nature and an additional model validation test point of OLH type. The test plan was then iteratively augmented by subsequent model validation point until the desired accuracy was achieved. As the DoE test plan was updated with each iteration, mapping of the system behaviour and modelling of the system response was updated at each new iteration.

The mapping stage was carried out evaluating the DoE test plan on the dynamic air path model, which provided inputs to the combustion model. The

air path states inputs generated by dynamic air path models, operational inputs extracted from the DoE, and the fuel system characteristics provided in the form of injection profile were implemented on the combustion model, and the system response (NOx) was recorded. This was followed by fitting the response surface model, utilising the MATLAB MBC toolbox, to the NOx values at each new iteration. The best response model, which could accurately represent the system response, was selected from a series of candidate models based on the analysis of trends and statistical performance.

The main innovative feature of the approach selected for the development of the combustion model is derived from the combination of dynamic air path model with statistical modelling by MB-MV framework. The dynamic air path model provided the necessary dynamics required for capturing the transients in the system response while reducing the time associated with running GT-Suite engine model to provide inputs to the SRM combustion model. Also, statistical modelling of the combustion process by utilising MB-MV framework for DoE test plan significantly reduced both testing and computational effort. This effect is enhanced in the case of Multi-Physics simulation platform, where the available combustion model is not real time.

Chapter 7 Discussion

7.1 Development of Hybrid Dynamic Modelling Framework on MPES Platform

This research introduced a novel framework to develop a global meta-model for engine out emissions based on a multi-physics engine simulation platform. The rationale for this is that the global metamodel could have better capability for accurate transient modelling for real-time drive-cycle simulation experiments compared to steady-state experiments discussed in Figure 4.5.

The proposed Hybrid Dynamic Framework couples two fundamentally different types of metamodeling strategies for the 2 structural parts of the MPES, refer to section 4.2, framework:

- A dynamic modelling / identification technique is deployed to develop a surrogate for the GT-Suite dynamic airpath simulation model of the Diesel engine.

- A global exploration DoE experiment, based on space-filling OLH DoEs, to develop a surrogate model for emissions – focussing on NOx engine-out emissions, based on the SRM model.

7.1.1 Hybrid Dynamic Modelling Framework: Development of Dynamic Airpath Model

In the development process of the proposed framework, the first stage was the development of the Diesel engine dynamic airpath model. Accordingly, the objective was to develop a surrogate model which would provide fast mean

value estimate for the inputs required for the SRM model (listed in Table 4.3) and would be able to do without loss in accuracy.

The methodology, described in section 4.4 of Chapter 4, adopted to accomplish this objective can be summarised as follow:

- Develop and implement a strategy to select a combination of dynamic experiment and modelling technique, suited to represent the system of interest (section 4.4.1.2).

- Deploy the selected dynamic experiment and modelling technique to develop surrogate model of GT-Suite Diesel engine air path (section 4.4.1.3).

Some of the benefits of employing dynamic modelling techniques for the surrogate model of GT-Suite dynamic airpath model are:

- Reduced amount of measurements need as no settling time is required (Röpke *et al.*, 2012; Fang *et al.*, 2016).

- Capability to reduce simulation time as system response is faster than real time, once trained (Nelles, 2001; Atkinson and Mott, 2005).

- Improvement in model fidelity by incorporating dynamic behaviour of the system (Brahma *et al.*, 2009; Fang *et al.*, 2016)

A strategy was needed to make an informed choice about which dynamic experiment or modelling technique should be deployed for the surrogate modelling purpose. As there are many possible dynamic modelling techniques

and designs of dynamic experiments available in the literature, but either the dynamic experiment is selected beforehand or the modelling technique. There have been efforts made in the literature to compare different types of dynamic experiments (Baumann *et al.*, 2008; Röpke *et al.*, 2012; Tietze, 2015; Belz *et al.*, 2017), but in these studies the modelling technique was pre-selected. There has also been an attempt on designing optimal signal designs rather than using set excitation signal, (Fang and Shenton, 2010; Deflorian and Zaglauer, 2011), but this requires prior knowledge regarding the model structure.

Therefore, a strategy was devised to support the selection of an appropriate dynamic experiment and modelling technique combination without having prior knowledge regarding the system. The dynamic experiments which were considered in this research were PRBS, APRBS, and sinusoidal (chirp) excitation signals, and for the dynamic modelling techniques, Local Linear Neuro Fuzzy models (Nelles, 2001) and Neural Network (Hagan *et al.*, 1995) models were selected.

As described in section 4.4.1.2 and implemented in Chapter 5, the proposed strategy compares the signal and model combination on the basis of statistical performance and engineering analysis. For the development of surrogate air path model, it was found, Figure 5.27 and Table 5.5, that combination of APRBS excitation signal and Local Linear Neuro-Fuzzy (with LOLIMOT algorithm) models perform better than other combinations . This finding was also supported from the literature review, Table 2.1, where LOLIMOT models are generally combined with APRBS signals for identification. Although

APRBS-LOLIMOT combination was selected, chirp-Neural Network combination performed equally well and is a viable option (Guhmann and Riedel, 2011).

The main concern with incorporating dynamic models is the design of dynamic experiments, as care needs to be taken not to violate the operating limits of the system. For this purpose, sinusoidal (for example, chirp) signals have become popular as they allow smooth and slow dynamics when compared to step-like signals (Baumann *et al.*, 2009; Guhmann and Riedel, 2011; Burke *et al.*, 2013; Sakushima *et al.*, 2013). However, step like-signals allow excitation of both low and high-frequency component and provide even coverage of the operating space (including extremities). With this in mind, the modelling task was approached by partitioning the input space into smaller sections, Figure 4.7, which would allow compliance to constraints for dynamic experiments more easily (Hametner and Nebel, 2012). Thereafter, modelling task was based on developing a surrogate model of a GT-Suite simulation model which differs from the approach in the literature. In this work system is represented based on model of a simulation model while in the research quoted above model of a physical system is developed based on the dynamic experiments carried out on the physical system (experimentally measured data). The approach investigated and developed in this work, enables development of virtual engine simulation platform capable of predicting transient drive cycle during preliminary stages of engine development. The strategy investigated also enhances the real time performance of the simulation model by reducing

simulation time required to estimate the mean-value response of the inputs for the combustion process model.

The effectiveness of the strategy and the selected signal model combination was carried out in section 6.2.2. It has been shown in Figure 6.8 and Table 6.3, that the selected model predicts the response (for SRM external input parameters) of GT suite engine model quite accurately with associated error as low as 2.1% for EGR, 0.20% for inlet pressure and 0.12% for inlet temperature. In addition to this, it was also established that the assumption made initially in section 1.3, that dynamic model would provide fast mean value estimate for the inputs required for the SRM combustion model, is justified. This was based on the results presented in Table 6.4, where time to run a planned design of experiment on GT-Suite Diesel engine model and surrogate dynamic air path model was compared. From this table, it was observed that GT-Suite Diesel engine would need about 2.5 hours to generate inputs for the SRM combustion process model while the dynamic surrogate model did the same under one minute (40 seconds). Thus, by incorporating dynamic models to develop the surrogate model of air path model real time performance has been enhanced and this provides about 210x reduction in simulation time. This delivers a considerable time saving, as otherwise, the GT engine model would have to be run for a considerable amount of time (equivalent to reaching stable steady state operation) to deliver a robust input for the global SRM experiments. This was consistent with the findings in literature where incorporation of dynamic models has provided considerable

reduction in measurement or simulation time (Nelles, 2001; Atkinson and Mott, 2005; Röpke *et al.*, 2012).

7.1.2 Hybrid Dynamic Modelling Framework: Development of Surrogate Model for Emissions

The next stage in framework development process was surrogate modelling of SRM combustion process model, procedure presented in section 4.4.2 of Chapter 4. The objective here was to develop a surrogate model of SRM combustion model capable of accurately predicting transient behaviour of the system. This objective was partitioned into the following tasks:

- Plan and implement global exploration Design of experiments using space filling OLH DoEs and evaluate design based on space-filling criteria and orthogonality (refer section 6.2.1).

- Fitting statistical models to the DoE test runs to develop a global meta-model for engine-out emissions, surrogate NOx model (refer section 6.3.2).

- Evaluate the performance of the surrogate model, developed by implementing the proposed approach, on the drive cycle data (refer to section 6.4).

The PDF Stochastic Reactor Model (CMCL Innovations, 2016) was chosen to develop the virtual combustion system, on the basis that it can provide reasonably fast computation using the reduced chemistry mechanism, with a computation time of 2-3 minutes per cycle, while still preserving good

prediction capabilities (Coble *et al.*, 2011). Although being relatively faster compared to the expensive three-dimensional computational fluid dynamics model, the SRM model does not have the capability to run real time. Therefore, to support real-time drive cycle engine simulation a surrogate model for SRM is developed.

To develop the NOx surrogate model, DoEs were planned using exploration based sequential DoE experiment (based on space-filling OLH design of experiment) propose by Kianifar *et al.* (2013). The advantage of using this framework (MB-MV) was:

- It requires no prior knowledge in advance (such as the number of test points required for modelling).

- Based on Figure 6.5 and Figure 6.6, it can be concluded that it provides good space filling property over all the iterations.

- Based on Table 6.1and Table 6.2, it can be established the choice of framework for planning DoE has good orthogonality property (i.e. quasi-orthogonal).

- The iterative process of this framework, allowed to actively monitor the accuracy of the surrogate model being developed, as illustrated in Figure 6.14.

Furthermore, it was shown that by integrating dynamic air path model with MB-MV framework, that the target model accuracy for the diesel engine case study was achieved by fewer test points when compared to common practice

in the industry (steady state set points), illustrated in Figure 6.15 and listed in Table 6.5.

Thereafter, the developed surrogate model was co-simulated with GT-Suite engine model, as illustrated in Figure 4.14, to evaluate its performance on the drive cycle data (Figure 6.19). Considering the results observed in the Figure 6.21 and Figure 6.24, it can be concluded that the surrogate NOx model developed using hybrid dynamic modelling framework can correctly predict the transient trends/ behaviour observed in the drive cycle data (for the case study, zone 3). While the trends were captured quite well, the accuracy of the model is variable across the space. It was observed in Table 6.6, that the developed surrogate model had a worse relative error (in region 9) of approximately 20%. This could be because the MPES platform it was developed on would also have a modelling error term associated with it, and this would be propagated through the developed surrogate models. However, the average error across all the nine regions was observed to be only 11.9%, refer to Table 6.7. In literature, it was found that there are studies (Guhmann and Riedel, 2011; Röpke *et al.*, 2012; Burke *et al.*, 2013), which have been able to estimate NOx emission using dynamic modelling techniques in a range of 5 % -10%. However, in these studies the models were fitted to the test bench data or virtual engine calibration was developed using dynamic modelling techniques based on test bench data. Given that the NOx predictions in this work are based on an engine model, with uncertainty about some important parameters (like the injection profiles, actual EGR etc.), and

that the objective of the work is to provide prediction capability for early engine development stage, the accuracy of predictions can be considered adequate.

Also, the actual measurements (test bench data) used to compare the results against are limited, therefore, the standard of accuracy is not same as those in the literature. However, from Table 6.7, it can be concluded that the proposed approach provides quite a significant improvement over the steady-state based approach, the surrogate NOx emission model developed using hybrid dynamic modelling approach has an average error of only 11.9% compared to 261.85% error form the model based on steady state approach. The prediction error could be further improved with detailed model for air path rather than fast response model, but that would come at the cost of increased computational cost and lack of ability to run real-time.

The main innovative feature of the approach selected for the development of the surrogate combustion model is derived from the combination of dynamic air path model with space -filling OLH DoEs (MB-MV framework). The dynamic air path model provided the necessary dynamics required for capturing the transients in the system response (illustrated in Figure 6.21) while reducing the time associated with running GT-Suite engine model to provide inputs to the SRM combustion model. Also, statistical modelling of the combustion process by utilising MB-MV framework for DoE test plan significantly reduced both testing and computational effort. This effect is enhanced in the case of Multi-Physics simulation platform, where the available combustion model cannot run in real time.

Chapter 8 Conclusion and Recommendations

The main aim of the thesis was to evaluate the Hybrid Dynamic Modelling framework to enable global metamodel of engine emissions and validate it through a case study. The development of framework was based on Multi-Physics Engine Simulation Platform, which replaces the engine testing as the basis for mapping and calibration experiments with virtual engine simulation framework - coupling airpath simulation modelling (GT-Suite) with combustion chemistry solver (SRM).

Accordingly, the specific research objective was to explore a co-modelling strategy for implementing an efficient dynamic experiment in conjunction with dynamic modelling technique to develop a surrogate model of the GT-Suite Diesel engine model, and then, to develop a metamodel for emissions (focusing on NOx) based on the data collected by applying established DoE approach on SRM combustion process model. Furthermore, to integrate two metamodeling strategies (dynamic and statistical) for two main components of MPES platform (GT-Suite + SRM) and to evaluate this hybrid dynamic framework on a diesel engine case study.

The developed framework was studied in context of the 2.0 litre Diesel engine case study. The main objective of the case study was to measure the capability of the proposed framework for accurate transient modelling of real-time drive cycle emissions. The data for hot steady state test and drive cycle was available from the sponsor company.

The dynamic models, LOLIMOT models, have been successfully implemented, in Chapter 5, on the GT-Suite engine model to develop surrogate model of the air path. They provided a considerable reduction in simulation time to estimate inputs to the SRM combustion process model. Thereafter, surrogate model for NOx emissions was also developed in conjunction with dynamic models and has capability to capture the transient behaviour of real-world drive cycle. The prediction capability of surrogate NOx model was evaluated on a drive cycle data, illustrated in Figure 6.19, and it was observed (from Table 6.7) that associated RMSE error for NOx emissions is of 8.09 ppmv (parts per million by volume) which translates to 11.9% relative error (ratio of RMSE to mean of measured NOx). The acceptable error in modelling of NOx emission is from 1% to 10%, however, the 11.9% relative error of surrogate model is acceptable in this work. The reason being it is derived from a metamodel (model of a simulation model) developed without any measurements from a physical system, so it will have an additional error introduced due to discrepancy in between simulation models and actual system.

8.1 Conclusion

The main conclusion based on the research presented in this work can be summarised as follow:

- It was demonstrated that the co-modelling strategy developed for implementing an efficient dynamic experiment and modelling technique enables selection of a combination of experiment and modelling

technique which is best suited to the system of interest. This addresses the gap in the literature, where either the modelling technique or dynamic experiment is selected beforehand and would allow to select an experiment and modelling technique based on the effect of such choice combination on modelling of the system.

- During the evaluation of co-modelling strategy, it was observed that the model trained on a specific excitation signal performs better on validation signal of same type. This is underpinned by signal properties, such as chirp signals, which are slow varying dynamic signals with less significant step changes, not being able to predict the step changes associated with the APRBS signals.

- It was also observed that the purpose of modelling, i.e. global or zonal modelling, would also affect the selection of excitation signal, for an example chirps will be more suited for global modelling due to their continuous nature allowing safe operation. While in zone or region-based modelling, where the step changes are less harsh due to local limits, APRBS will be a superior choice as they cover a broader frequency range (both high and low frequency components) and amplitude range providing best data coverage.

- Considering the results attained from applying co-modelling strategy for generating surrogate models of air path states (EGR-mf, inlet pressure and inlet temperature), it was observed that the proposed strategy performs robustly and also enhances the real time

performance by estimating inputs for SRM combustion process model 210 times faster than it would have taken for GT-Suite Diesel engine model to run to reach stable steady state operation.

- The use of nonlinear dynamic models enabled the development of global metamodel of emission at a comparable cost to steady-state experiments performed to develop the SRM surrogate model by providing fast mean value estimate for the inputs required for SRM combustion process model.

- With the incorporation of global exploration DoEs, the number of measurements required to capture the transient behaviour of the system was considerably reduced when compared to steady-state point-based approach. The surrogate NOx model was fitted using 150 model building test points and validated on additional 20 test points.

- Integration of the dynamic surrogate models for GT-Suite Diesel engine model and statistical models (developed based on data collected using global exploration Doe approach) for SRM combustion process model can enhance the modelling of engine emissions, through delivering high quality models fulfilling the target model accuracy with faster simulation time and reduced number of measurements. As illustrated for the Diesel engine case study (refer to Figure 6.24 and Table 6.7), the NOx surrogate model (developed based on a simulation model) fitted using 150 test points was able to follow the trends observed in the transient drive and was able to do so with associate RMSE of 8.09

ppmv (parts per million by volume) which translates to 11.9% relative error (ratio of RMSE to mean of measured NOx).

8.2 Further Work

The methodologies presented in this research, Chapter 4, provides answers to some of the questions in the literature but it also opens a new line of inquiry and future research opportunities. The hybrid dynamic modelling framework presented here can be further developed in the following aspects:

Development of hybrid dynamic approach for full operating region of engines

The methodology presented here has been implemented on one zone of the operating space (refer to section 4.4) and expansion of the methodology to full operating region can be approached as illustrated in Figure 8.1. The global model is composed of series of local (global-zone) models and weighting functions that are selected according to the current operating point (lies in which operating zone) such that it can accurately represent the system on entire engine envelope based on zonal models. The rationale being that multiple local models may define system non-linearity more accurately than a global model, as they account for local noise level or sensitivities and can have different active inputs in different local regions.

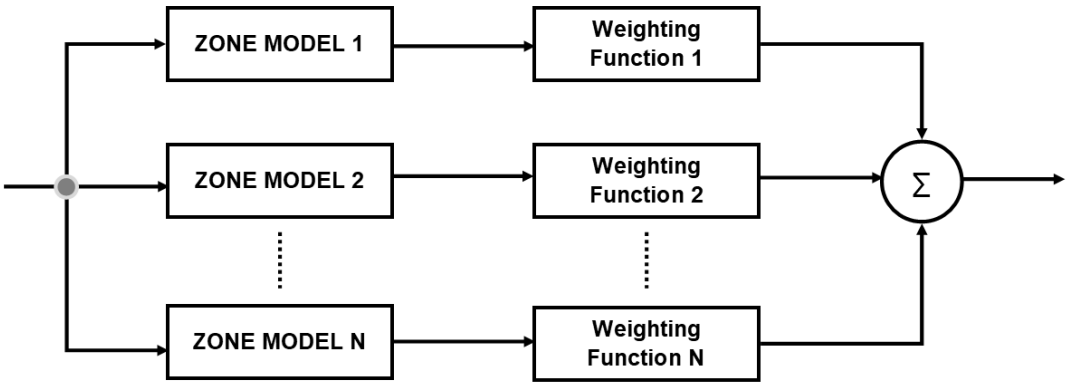

Figure 8.1: A schematic of hybrid dynamic approach for whole engine operating region.

The research objective for developing global model composed of local models can be defined as:

- To explore a strategy which would minimise the approximation error of the model by selecting appropriate local model and weighting function for the current operating point.
- To implement and evaluate the performance of the developed global models on the current legislative transient drive cycles such a WLTP.
- The approach developed here, also offers the possibility to be incorporated into engine calibration, since it allows fast data capture and reduced measurement effort, thus, the less experimental effort required (compared to traditional point-based calibration).
- To consider implementation of hybrid dynamic approach to the gasoline engine.

Design of dynamic Experiments

Further work is needed in design of dynamic experiments to address the issue such as optimal length of excitation signal to identify the underlying dynamics in the system of interest to accurately represent the system response.

- To evaluate optimal dynamic experiment methodology in order to create realistic excitation sequences based on expected / multiple drive cycles. This may enhance the identification process, as by emulating the characteristics (for an example acceleration, braking, constant) of the drive cycles and compressing them into a sequence will allow to train the models on the realistic scenarios. This could provide pragmatic representation of a model performance on the legislative drive cycles.

- To further develop the co-modelling strategy by incorporating the length of the identification signal as an additional factor.

- To further develop dynamic models by incorporating improved methods of order determination.

References

ACEA (2017) *WLTP Facts*. Available at: http://wltpfacts.eu/wltp-benefits/ (Accessed: 5 December 2018).

Adeniran, A. A. and Ferik, S. El (2016) 'Modeling and Identification of Nonlinear Systems : A Review of the Multimodel Approach — Part 1', *IEEE Transactions on Systems, Man, and Cybernetics: Systems*, 47(7), pp. 1149–1159. doi: 10.1109/TSMC.2016.2560129.

Ahmed, F. (2013) *Modeling, simulation and control of the air-path of an internal combustion engine*. Université de Technologie de Belfort-Montbeliard. Available at: https://tel.archives-ouvertes.fr/tel-01002113/document.

Alvarez, L. (2000) *Response Surface Methodology*, *PhD Thesis*. University of Bradord. doi: 10.1080/00401706.1996.10484509.

Arsie, I., Di Genova, F., Pianese, C., *et al.* (2004) 'Development and Identification of Phenomenological Models for Combustion and Emissions of Common-Rail Multi-Jet Diesel Engines', in *2004 SAE Fuels & Lubricants Meeting & Exhibition*. SAE International. doi: https://doi.org/10.4271/2004-01-1877.

Åström, K. J. and Eykhoff, P. (1971) 'System identification—A survey', *Automatica*. Pergamon, 7(2), pp. 123–162. doi: 10.1016/0005-1098(71)90059-8.

Atkinson, A. C. (1996) 'The Usefulness of Optimum Experimental Designs', *Journal of the Royal Statistical Society. Series B (Methodological)*. [Royal

Statistical Society, Wiley], 58(1), pp. 59–76. Available at: http://www.jstor.org/stable/2346165.

Atkinson, A. C., Donev, A. N. and Tobias, R. (2007) *Optimum experimental designs with SAS*. Oxford University Press.

Atkinson, C. and Mott, G. (2005) 'Dynamic Model-Based Calibration Optimization: An Introduction and Application to Diesel Engines', 2005(724). doi: 10.4271/2005-01-0026.

Augasta, M. G. and Kathirvalavakumar, T. (2013) 'Pruning algorithms of neural networks — a comparative study', *Central European Journal of Computer Science*, 3(3), pp. 105–115. doi: 10.2478/s13537-013-0109-x.

Aute, V. C. (2009) *Single and multi-response adaptive design of experiments with application to design optimization of novel heat exchangers*. PhD Thesis, University of Maryland.

Aziz Hairuddin, A., Yusaf, T. and Wandel, A. P. (2016) 'Single-zone zero-dimensional model study for diesel-fuelled homogeneous charge compression ignition (HCCI) engines using Cantera', *International Journal of Automotive and Mechanical Engineering*, 13(2), pp. 3309–3328. doi: 10.15282/ijame.13.2.2016.3.0275.

Bates, S. J., Sienz, J. and Langley, D. S. (2003) 'Formulation of the audze-eglais uniform latin hypercube design of experiments for constrained design spaces', *Advances in Engineering Software*, 34(8), pp. 493–506. doi: 10.1016/S0965-9978(03)00042-5.

Bates, S. J., Sienz, J. and Toropov, V. V (2004) ‘Formulation of the Optimal Latin Hypercube Design of Experiments Using a Permutation Genetic Algorithm Stuart’, *American Institute of Aeronautics and Astronautics*.

Baumann, W., Klug, K., Kohler, B. U. and Röpke, K. (2009) ‘Modelling of Transient Diesel Engine Emissions’, in Röpke, K. (ed.) *Design of Experiments in Engine Development*. Berlin: Expert Verlag, pp. 41–53.

Baumann, W., Schaum, S., Knaak, M. and Röpke, K. (2008) ‘Excitation Signals for Nonlinear Dynamic Modeling of Combustion Engines’, *Proceedings of the 17th World Congress The International Federation of Automatic Control*, pp. 1066–1067.

Bekey, G. A. (1970) ‘System identification- an introduction and a survey’, *SIMULATION*. Sage PublicationsSage CA: Thousand Oaks, CA, 15(4), pp. 151–166. doi: 10.1177/003754977001500403.

Belz, J., Nelles, O., Schwingshackl, D., Rehrl, J. and Horn, M. (2017) ‘Order Determination and Input Selection with Local Model Networks’, *IFAC-PapersOnLine*, 50(1), pp. 7327–7332. doi: 10.1016/j.ifacol.2017.08.1475.

Bernard, G., Lebas, R. and Demoulin, F.-X. (2011) ‘A 0D Phenomenological Model Using Detailed Tabulated Chemistry Methods to Predict Diesel Combustion Heat Release and Pollutant Emissions’, in *SAE 2011 World Congress & Exhibition*. SAE International. doi: https://doi.org/10.4271/2011-01-0847.

Billings, S. A. and Zhu, Q. M. (1994) ‘Nonlinear model validation using

correlation tests', *International Journal of Control*. Taylor & Francis, 60(6), pp. 1107–1120. doi: 10.1080/00207179408921513.

Blahut, R. E. (2010) *Fast Algorithms for Signal Processing*. Cambridge University Press.

Bossley, K. M., Brown, M., Gunn, S. R. and Harris, C. J. (1997) 'Intelligent data modelling using neurofuzzy algorithms', in *IEE Colloquium on Industrial Applications of Intelligent Control (Digest No: 1997/144)*, pp. 7/1-7/6. doi: 10.1049/ic:19970788.

Box, G. E. P., Hunter, W. G. and Hunter, J. S. (1978) *Statistics for experimenters : an introduction to design, data analysis, and model building*. New York : John Wiley & Sons. Available at: https://searchworks.stanford.edu/view/10069393 (Accessed: 22 May 2019).

Box, G. E. P. and Wilson, K. . B. (1951) 'On the Experimental Attainment of Optimum Conditions', *Journal of the Royal Statistical Society*, 13(1), pp. 1–45. Available at: http://www.jstor.org/stable/2983966.

Brahma, I. and Chi, J. N. (2012a) 'Development of a model-based transient calibration process for diesel engine electronic control module tables – Part 1: data requirements, processing, and analysis', *International Journal of Engine Research*, 13(1), pp. 77–96. doi: 10.1177/1468087411424376.

Brahma, I. and Chi, J. N. (2012b) 'Development of a model-based transient calibration process for diesel engine electronic control module tables – Part 2: modelling and optimization', *International Journal of Engine Research*, 13(2),

pp. 147–168. doi: 10.1177/1468087411424377.

Brahma, I., Sharp, M. C. and Frazier, T. R. (2009) ‘Empirical Modeling of Transient Emissions and Transient Response for Transient Optimization’, *SAE International Journal of Engines*, 2(1), pp. 1433–1443. doi: https://doi.org/10.4271/2009-01-1508.

Brahma, I., Sharp, M. C., Richter, I. B. and Frazier, T. R. (2008) ‘Development of the nearest neighbour multivariate localized regression modelling technique for steady state engine calibration and comparison with neural networks and global regression’, *International Journal of Engine Research*, 9(4), pp. 297–323. doi: 10.1243/14680874JER00708.

Breiman, L. (1993) ‘Hinging hyperplanes for regression, classification, and function approximation’, *IEEE Transactions on Information Theory*, 39(3), pp. 999–1013. doi: 10.1109/18.256506.

Burke, R. D., Baumann, W., Akehurst, S. and Brace, C. J. (2013) ‘Dynamic modelling of diesel engine emissions using the parametric Volterra series’, *Proceedings of the Institution of Mechanical Engineers, Part D: Journal of Automobile Engineering*. IMECHE, 228(2), pp. 164–179. doi: 10.1177/0954407013503629.

Cary, M. (2003) *A model based engine calibration methodology for a port fuel injection, spark-ignition engine: the application of non-linear hierarchical statistical modelling and multi-objective optimisation techniques to the solution of real world multi-parameter engin*. PhD Thesis, University of Bradford.

Castric, S., Cherfi, Z., Boudaoud, N. and Schimmerling, P. (2009) ‘A new Bayesian technique for readjusting LOLIMOT models: example with diesel engine emissions’, *International Journal of Design Engineering*, 2(4), p. 472. doi: 10.1504/IJDE.2009.030824.

Chang, J. S., Cheong, J. H., Jo, C. H., Chi, Y. H. and Yoon, K. J. (2007) ‘Feasibility Study on Roboust Calibration by DoE to Minimize the Exhaust Emission Deviations from Injector Flow Rate Scatters’, *Design of Experiments in Engine Development*, pp. 196–210.

Charteris, W. (1992) ‘Taguchi’s system of experimental design and data analysis: a quality engineering technology for the food industry’, *International Journal of Dairy Technology*, 45(2), pp. 33–49. doi: 10.1111/j.1471-0307.1992.tb01723.x.

Cheng, C. M., Peng, Z. K., Zhang, W. M. and Meng, G. (2017) ‘Volterra-series-based nonlinear system modeling and its engineering applications: A state-of-the-art review’, *Mechanical Systems and Signal Processing*. Elsevier, 87(November 2016), pp. 340–364. doi: 10.1016/j.ymssp.2016.10.029.

Chow, A. and Wyszynski, M. L. (1999) ‘Thermodynamic modelling of complete engine systems - a review’, *Proceedings of the Institution of Mechanical Engineers Part D-Journal of Automobile Engineering*, 213(4), pp. 403–415.

Cirak, B. and Demirtas, S. (2014) ‘An Application of Artificial Neural Network for Predicting Engine Torque in a Biodiesel Engine’, *American Journal of Energy Research*, 2(4), pp. 74–80. doi: 10.12691/ajer-2-4-1.

CMCL Innovations (2016) *Kinetics & SRM Engine Suite*.

Coble, A. R., Smallbone, A., Bhave, A., Mosbach, S., Kraft, M., Niven, P. and Amphlett, S. (2011) 'Implementing Detailed Chemistry and In-Cylinder Stratification into 0/1-D IC Engine Cycle Simulation Tools', in *SAE 2011 World Congress & Exhibition*. SAE International. doi: https://doi.org/10.4271/2011-01-0849.

Couckuyt, I., Crombecq, K., Gorissen, D. and Dhaene, T. (2009) 'Automated Response Surface Model Generation with Sequential Design Surrogate modelling', *Proceedings of the First International Conference on Soft Computing Technology in Civil, Structural and Environmental Engineering*. doi: 10.4203/ccp.92.52.

Cox, D. and John, S. (1997) 'SDO: A Statistical Method for Global Optimization', in Alexandrov, N. and Hussaini, M. Y. (eds) *Multidisciplinary Design Optimization: State of the Art*. SIAM, pp. 351–329.

Crombecq, K., Laermans, E. and Dhaene, T. (2011) 'Efficient space-filling and non-collapsing sequential design strategies for simulation-based modeling', *European Journal of Operational Research*, 214(3), pp. 683–696. doi: 10.1016/J.EJOR.2011.05.032.

Crombecq, K., Tommasi, L. D., Gorissen, D. and Dhaene, T. (2009) 'A Novel Sequential Design Strategy for Global Surrogate Modelling', *Proceedings of the Winter Simulation Conference*, pp. 731–742. doi: 10.1109/WSC.2013.6721594.

Deese, J., Deodhar, N. and Vermillion, C. (2017) ‘Nested Plant/Controller Co-Design Using G-Optimal Design and Extremum Seeking: Theoretical Framework and Application to an Airborne Wind Energy System * *This work was supported by NSF grant number 1453912, entitled CAREER: Efficient Experimental Optimiza’, *IFAC-PapersOnLine*. Elsevier, 50(1), pp. 11965–11971. doi: 10.1016/j.ifacol.2017.08.1182.

Deflorian, M. and Klöpper, F. (2009) ‘Design of dynamic experiments’, in *Design of Experiments (DoE) in Engine Development*. Expert Verlag, pp. 31–40.

Deflorian, M. and Zaglauer, S. (2011) ‘Design of Experiments for nonlinear dynamic system identification’, *IFAC Proceedings Volumes*. Elsevier, 44(1), pp. 13179–13184. doi: 10.3182/20110828-6-IT-1002.01502.

Deng, J., Zhong, S. and Ordys, A. (2013) ‘Robustness and Accuracy Test of Particular Matter Prediction Based on Neural Networks’, *Communications and Network*, 05(02), pp. 53–59. doi: 10.4236/cn.2013.52B010.

Dimopoulos, P., Schöni, A., Eggimann, A., Sparti, C., Vaccarino, E. and Operti, C. (1999) ‘Statistical Methods for Solving the Fuel Consumption/Emission Conflict on DI-Diesel Engines’, in *SAE Technical Paper Series*. doi: 10.4271/1999-01-1077.

Ernst, S. (1998) ‘Hinging hyperplane trees for approximation and identification’, in *Proceedings of the 37th IEEE Conference on Decision and Control (Cat. No.98CH36171)*. IEEE, pp. 1266–1271. doi: 10.1109/CDC.1998.758452.

Etheridge, J., Mosbach, S., Kraft, M., Wu, H. and Collings, N. (2009) 'A Detailed Chemistry Multi-cycle Simulation of a Gasoline Fueled HCCI Engine Operated with NVO', *SAE International Journal of Fuels and Lubricants*, 2(1), pp. 2009-01–0130. doi: 10.4271/2009-01-0130.

Fang, H., Rais-Rohani, M., Liu, Z. and Horstemeyer, M. F. (2005) 'A comparative study of metamodeling methods for multiobjective crashworthiness optimization', *Computers & Structures*. Pergamon, 83(25–26), pp. 2121–2136. doi: 10.1016/J.COMPSTRUC.2005.02.025.

Fang, K. (2012) *Optimal Test Signal Design and Estimation for Dynamic Powertrain Calibration and Control*. PhD Thesis, University of Liverpool.

Fang, K., Li, Z., Ostrowski, K., Shenton, A. T., Dowell, P. G. and Sykes, R. M. (2016) 'Optimal-Behavior-Based Dynamic Calibration of the Automotive Diesel Engine', *IEEE Transactions on Control Systems Technology*. IEEE, 24(3), pp. 979–991. doi: 10.1109/TCST.2015.2476781.

Fang, K., Li, Z., Shenton, A., Fuente, D. and Gao, B. (2015) 'Black Box Dynamic Modeling of a Gasoline Engine for Constrained Model-Based Fuel Economy Optimization', in *SAE 2015 World Congress & Exhibition*. SAE International. doi: 10.4271/2015-01-1618.

Fang, K. and Shenton, A. T. (2010) 'Optimal Input Design for Dynamic Engine Mapping', *IFAC Proceedings Volumes*. Elsevier, 43(7), pp. 691–696. doi: 10.3182/20100712-3-DE-2013.00078.

Fischer, M., Nellesa, O. and Isermann, R. (1998) 'Adaptive Predictive Control

of a Heat Exchanger Based on a Fuzzy Model', *Control Engineering Practice*, pp. 259–269.

Flower, J. O. and Hazell, P. A. (1971) 'Sampled-data theory applied to the modelling and control analysis of compression-ignition engines-Part II', *International Journal of Control*. Taylor & Francis, 13(4), pp. 609–623. doi: 10.1080/00207177108931971.

Flower, J. O. and Windett, G. P. (1976a) 'Dynamic measurements of a large diesel engine using p.r.b.s. techniques Part 1. Development of theory for closed-loop sampled systems', *International Journal of Control*. Taylor & Francis, 24(3), pp. 379–392. doi: 10.1080/00207177608932830.

Flower, J. O. and Windett, G. P. (1976b) 'Dynamic measurements of a large diesel engine using p.r.b.s. techniques Part 2. Instrumentation, experimental techniques and results', *International Journal of Control*. Taylor & Francis, 24(3), pp. 393–404. doi: 10.1080/00207177608932831.

Forrester, A., Sobester, D. A. and Keane, A. (2008) *Engineering Design via Surrogate Modelling: A Practical Guide*. Wiley-Blackwell.

Fridriksson, H., Sunden, B., Hajireza, S. and Tuner, M. (2011) 'CFD Investigation of Heat Transfer in a Diesel Engine with Diesel and PPC Combustion Modes', in *SAE International Powertrains, Fuels and Lubricants Meeting*. SAE International. doi: https://doi.org/10.4271/2011-01-1838.

Gamma Technologies Inc (2016) *GT-Power User's Manual*. 2016th edn.

Gautier, P., Albrecht, A., Moulin, P., Chasse, A., Fontvieille, L., Guinois, A.

and Doléac, L. (2008) ‘A New Simulation Step Towards Virtual Bench Through the Challenging Case of Two-Stage Turbocharger Diesel Engine Control Design’, in. doi: 10.4271/2008-01-0355.

Geest, J. De, Dhaene, T. and Fache, N. (1999) ‘Adaptive CAD-model building algorithm for general planar microwave structures’, *IEEE Transactions on Microwave Theory and Techniques*, 47(9), pp. 1801–1809. doi: 10.1109/22.788515.

Georgakis, C. (2013) ‘Design of Dynamic Experiments: A Data-Driven Methodology for the Optimization of Time-Varying Processes’, *Industrial & Engineering Chemistry Research*. American Chemical Society, 52(35), pp. 12369–12382. doi: 10.1021/ie3035114.

Ghosh, R. (2016) *Input Designs for Identification of Ill-conditioned Multivariable Systems*. PhD Thesis, Åbo Akademi University.

Di Gioia, R., Papaleo, D., Vicchi, F. M. and Cavina, N. (2012) ‘Virtual GDI Engine as a Tool for Model-Based Calibration’, in. doi: 10.4271/2012-01-1679.

Gonzalez, R. (2016) *Residual Analysis and Multiple Regression*. Available at: http://www-personal.umich.edu/~gonzo/coursenotes/file7.pdf (Accessed: 6 December 2018).

Gorissen, D., Crombecq, K., Hendrickx, W. and Dhaene, T. (2007) ‘Adaptive Distributed Metamodeling’, *High Performance Computing for Computational Science - VECPAR 2006*, 4395, pp. 579–588. doi: 10.1007/978-3-540-71351-7_45.

Grondin, O., Stobart, R., Chafouk, H. and Maquet, J. (2004) 'Modelling the Compression Ignition Engine for Control: Review and Future Trends.', (724). doi: 10.4271/2004-01-0423.

Grove, D. M. and Davis, T. P. (1992) *Engineering Quality & Experimental Design*. Longman.

Grove, D. M., Woods, D. C. and Lewis, S. M. (2004) 'Multifactor B-Spline Mixed Models in Designed Experiments for the Engine Mapping Problem', *Journal of Quality Technology*, 36(4), pp. 380–391. doi: 10.1080/00224065.2004.11980285.

Guerrier, M. and Cawsey, P. (2004) 'The development of model based methodologies for gasoline IC engine calibration', *SAE Technical Paper 2004-01-1466*, 113(3), pp. 981–1002. doi: 10.4271/2004-01-1466.

Guhmann, C. and Riedel, J. M. (2011) 'Comparison of Identification Methods for Nonlinear Dynamic Systems', in Röpke, K. (ed.) *Design of Experiments (DoE) in Engine Development*. Expert Verlag, pp. 41–53.

Gutjahr, T. (2012) *Dynamic System Identification with Gaussian Processes in Model- Based Engine Development*. PhD Thesis, Universität Ilmenau.

Guzzella, L. and Amstutz, A. (1998) 'Control of diesel engines', *IEEE Control Systems Magazine*, 18(5), pp. 53–71. doi: 10.1109/37.722253.

Hafner, M. and Isermann, R. (2003) 'Multiobjective optimization of feedforward control maps in engine management systems towards low consumption and low emissions', *Transactions of the Institute of Measurement and Control*,

25(1), pp. 57–74. doi: 10.1191/0142331203tm074oa.

Hafner, M., Schüler, M., Nelles, O. and Isermann, R. (2000) ‘Fast neural networks for diesel engine control design’, *Control Engineering Practice*, 8(11), pp. 1211–1221. doi: 10.1016/S0967-0661(00)00057-5.

Hagan, M. T. and Demuth, H. B. (1999) ‘Neural networks for control’, *Proceedings of the 1999 American Control Conference (Cat. No. 99CH36251)*, 3, pp. 1642–1656. doi: 10.1109/ACC.1999.786109.

Hagan, M. T., Demuth, H. B. and Beale, M. H. (1995) *Neural Network Design*. 2nd edn. Boston Massachusetts: PWS. doi: 10.1007/1-84628-303-5.

Hagan, M. T., Demuth, H. B. and Beale, M. H. (2006) *Neural Networks in a Softcomputing Framework*. 2nd edn. London: Springer-Verlag. doi: 10.1007/1-84628-303-5.

Hametner, C. and Nebel, M. (2012) ‘Operating regime based dynamic engine modelling’, *Control Engineering Practice*. Elsevier, 20(4), pp. 397–407. doi: 10.1016/j.conengprac.2011.10.003.

Hametner, C., Stadlbauer, M., Deregnaucourt, M., Jakubek, S. and Winsel, T. (2013) ‘Optimal experiment design based on local model networks and multilayer perceptron networks’, *Engineering Applications of Artificial Intelligence*. Elsevier, 26(1), pp. 251–261. doi: 10.1016/j.engappai.2012.05.016.

Harris, C. J. and Wu, Z. Q. (1997) ‘Neurofuzzy State Estimators and their Applications’, *IFAC Proceedings Volumes*. Elsevier, 30(25), pp. 7–15. doi:

10.1016/S1474-6670(17)41293-6.

Hartmann, B., Baumann, W. and Nelles, O. (2013) ‘Axes-Oblique Partitioning of Local Model Networks for Engine Calibration’, in Röpke, K. (ed.) *Design of Experiments (DoE) in Engine Development*. Expert Verlag, pp. 92–106.

Hartmann, B., Ebert, T., Fischer, T., Belz, J., Kampmann, G. and Nellesa, O. (2012) ‘LMNtool - Toolbox zum automatischen Trainieren lokaler Modellnetze’, *22nd Workshop Computational Intelligence*. Available at: http://www.mb.uni-siegen.de/mrt/lmn-tool/.

Hartmann, B., Moll, J., Nelles, O. and Fritzen, C. P. (2011) ‘Hierarchical Local Model Trees for Design of Experiments in the Framework of Ultrasonic Structural Health Monitoring’, *Proceedings of the IEEE International Conference on Control Applications*, pp. 1163–1170. doi: 10.1109/CCA.2011.6044489.

Hartmann, B. and Nelles, O. (2009a) ‘Automatic Adjustment of the Transition between Local Models in a Hierarchical Structure Identification Algorithm’, in *2009 European Control Conference (ECC)*. IEEE, pp. 1599–1604. doi: 10.23919/ECC.2009.7074635.

Hartmann, B. and Nelles, O. (2009b) ‘On the smoothness in local model networks’, in *2009 American Control Conference*. IEEE, pp. 3573–3578. doi: 10.1109/ACC.2009.5159820.

Hartmann, B. and Nelles, O. (2013) ‘Adaptive Test Planning for the Calibration of Combustion Engines – Methodology’, in *Design of Experiments (DoE) in*

Engine Development. Expert Verlag, pp. 1–16.

Hartmann, B., Nelles, O., Belič, A. and Zupančič–Božič, D. (2009) 'Local Model Networks for the Optimization of a Tablet Production Process BT - Artificial Intelligence and Computational Intelligence', in Deng, H., Wang, L., Wang, F. L., and Lei, J. (eds). Berlin, Heidelberg: Springer Berlin Heidelberg, pp. 241–250.

Hazell, P. A. and Flower, J. O. (1971a) 'Discrete modelling of spark-ignition engines for control purposes', *International Journal of Control*. Taylor & Francis, 13(4), pp. 625–632. doi: 10.1080/00207177108931972.

Hazell, P. A. and Flower, J. O. (1971b) 'Sampled-data theory applied to the modelling and control analysis of compression ignition engines—Part I', *International Journal of Control*. Taylor & Francis Group, 13(3), pp. 549–562. doi: 10.1080/00207177108931964.

He, Y. and Rutland, C. J. (2004) 'Application of artificial neural networks in engine modelling', *Int J Engine Research*, 5(4), pp. 281–296.

Heinz, T. O. and Nelles, O. (2017) 'Iterative Excitation Signal Design for Nonlinear Dynamic Black-Box Models', *Procedia Computer Science*. Elsevier, 112, pp. 1054–1061. doi: 10.1016/J.PROCS.2017.08.112.

Heywood, J. B. (1998) *Internal Combustion Engine Fundamentals*. McGrawHill.

Howlett, R. J., de Zoysa, M. M., Walters, S. D. and Howson, P. a (1999) 'Neural Network Techniques for Monitoring and Control of Internal

Combustion Engines', *International ICSC Symposium on intelligent Industrial Automation,*.

Isermann, R. (2014) *Engine modelling and control*. Springer-Verlag Berlin Heidelberg.

Isermann, R. and Muller, N. (2001) 'Modelling and Adaptive Control of Combustion Engines with Fast Neural Networks', *European Symposium on Intelligent Technologies, Hybrid Systems and their implementation on Smart Adaptive Systems*, pp. 566–582.

Isermann, R. and Münchhof, M. (2011) *Identification of Dynamic Systems*. New York: Springer Heidelberg Dordrecht London.

Jaguar Land Rover (2017) *Private Commnication*.

Jajčević, D. (2011) *CFD-Simulation of High Performance 2-Stroke Engines Applying Multidimensional Coupling Methodologies by Dalibor JAJ Č EVI Ć*. PhD Thesis, Graz University of Technology.

Jakubek, S., Hametner, C. and Keuth, N. (2008) 'Total least squares in fuzzy system identification: An application to an industrial engine', *Engineering Applications of Artificial Intelligence*. Pergamon, 21(8), pp. 1277–1288. doi: 10.1016/J.ENGAPPAI.2008.04.020.

Jia, M., Xie, M. and Peng, Z. (2008) 'A Comparative Study of Multi-zone Combustion Models for HCCI Engines', in *SAE World Congress & Exhibition*. SAE International. doi: https://doi.org/10.4271/2008-01-0064.

Jin, R., Chen, W. and Simpson, T. W. (2001) ‘Comparative studies of metamodelling techniques under multiple modelling criteria’, *Structural and Multidisciplinary Optimization*, 23(1), pp. 1–13. doi: 10.1007/s00158-001-0160-4.

Johansen, T. A. (1994) *Operating Regime based Process Modeling and Identication*, *PhD Thesis*. University of Trondheim. Available at: http://www.noormags.ir/view/fa/articlepage/125267.

Johansen, T. A. and Foss, B. A. (1997) ‘Operating regime based process modeling and identification’, *Computers & Chemical Engineering*. Pergamon, 21(2), pp. 159–176. doi: 10.1016/0098-1354(95)00260-X.

Johansen, T. A. and Foss, B. A. (1998) ‘Orbit - Operating Regime Based Modeling and Identification Toolkit’, *Control Engineering Practice*, 6, pp. 1277–1286.

Johnson, M. E., Moore, L. M. and Ylvisaker, D. (1990) ‘Minimax and maximin distance designs’, *Journal of Statistical Planning and Inference*, 26(2), pp. 131–148. doi: 10.1016/0378-3758(90)90122-B.

Joseph, V. R., Y. and Hung (2008) ‘Orthogonal Maximin Latin Hypercube Designs’, *Statistica Sinica*, 18(1), pp. 171–186.

Jung, M. (2003) *Mean-value modelling and robust control of the airpath of a turbocharged diesel engine*, *PhD Thesis*. University of Cambridge. doi: 10.17863/CAM.11632.

Keesman, K. J. (2011) *System Identification: An Introduction*. London:

Springer-Verlag.

Khan, M. A. Z. (2011) *Transient engine model for calibration using two-stage regression approach*. PhD Thesis, Loughborough University. Available at: https://dspace.lboro.ac.uk/dspace-jspui/handle/2134/8456.

Kianifar, M. R. (2014) *Application of Multidisciplinary Design Optimisation Frameworks for Engine Mapping and Calibration*. PhD Thesis, University of Bradford.

Kianifar, M. R., Campean, L. F. and Richardson, D. (2013) 'Sequential DoE Framework for Steady State Model Based Calibration', *SAE International Journal of Engines*, 6(2), pp. 843–855. doi: https://doi.org/10.4271/2013-01-0972.

Kleijnen, J. P. C. (1987) *Statistical tools for simulation practitioners*. New York: M. Dekker (Statistics, textbooks and monographs ;vol. 76). Available at: file://catalog.hathitrust.org/Record/000486969.

Klein, P., Kirschbaum, F., Hartmann, B., Bogachik, Y. and Nelles, O. (2013) 'Adaptive Test Planning for the Calibration of Combustion Engines - Application', in Röpke, K. (ed.) *Design of Experiments (DoE) in Engine Development*. Expert Verlag, pp. 17–30.

Knaak, M., Schoop, U. and Barzantny, B. (2007) 'Dynamic Modelling and Optimization: The Natural Extension to Classical DoE', in Röpke, K. (ed.) *Design of Experiments (DoE) in Engine Development III*. Berlin: Expert Verlag, pp. 10–21.

Korsunovs, A. (2017) *Multi-Physics Engine Simulation Framework*. Technical Report, University of Bradford.

Korsunovs, A., Campean, F., Pant, G., Garcia-Afonso, O. and Tunc, E. (2019) 'Evaluation of zero-dimensional stochastic reactor modelling for a Diesel engine application', *International Journal of Engine Research*. doi: 10.1177/1468087419845823.

Kruse, T., Kurz, S. and Lang, T. (2010) 'Modern statistical modeling and evolutionary optimization methods for the broad use in ECU calibration', *IFAC Proceedings Volumes (IFAC-PapersOnline)*. IFAC, 43(7), pp. 739–743. doi: 10.3182/20100712-3-DE-2013.00031.

Lacey, R. (2012) 'Off-highway Diesel Engines - Reducing Cost , Improving Quality and Shortening Development Cycles at Caterpillar using Advanced Virtual Validation', in *SIMULIA Community Conference*, pp. 1–15. Available at: http://www.ssanalysis.co.uk/hubfs/KB_NEW_DOCS/Case_Studies/Caterpillar_Diesel_Engine.pdf.

Lam, C. Q. (2008) *Sequential Adaptive Designs In Computer Experiments For Response Surface Model Fit*. PhD Thesis, Ohio State University. Available at: http://rave.ohiolink.edu/etdc/view?acc_num=osu1211911211 (Accessed: 29 August 2018).

Lehmensiek, R., Meyer, P. and Müller, M. (2002) 'Adaptive sampling applied to multivariate, multiple output rational interpolation models with application to microwave circuits', *International Journal of RF and Microwave Computer-*

Aided Engineering, 12(4), pp. 332–340. doi: 10.1002/mmce.10032.

Ljung, L. (1997) *System Identification: Theory for the user*. New Jersey, USA: Prentice--Hall, Inc.

Ljung, L. (2006) 'Some Aspects on Nonlinear System Identification', *IFAC Symposium on System Identificatio*, 39(1), pp. 553–564.

Lumsden, G., Browett, C., Taylor, J. and Kennedy, G. (2004) 'Mapping Complex Engines', in *SAE 2004 World Congress & Exhibition*. SAE International. doi: https://doi.org/10.4271/2004-01-0038.

Marseille, G. J., Fuderer, M., Debeer, R., Mehlkopf, A. F. and Vanormondt, D. (1994) 'Reduction of MRI Scan Time through Nonuniform Sampling and Edge-Distribution Modeling', *Journal of Magnetic Resonance, Series B*. Academic Press, 103(3), pp. 292–295. doi: 10.1006/JMRB.1994.1044.

Martínez-Morales, J. D., Palacios-Hernández, E. R. and Velázquez-Carrillo, G. A. (2013) 'Modeling and multi-objective optimization of a gasoline engine using neural networks and evolutionary algorithms', *Journal of Zhejiang University SCIENCE A*, 14(9), pp. 657–670. doi: 10.1631/jzus.A1300010.

MATLAB (2006) *Generate input signals - MATLAB idinput - MathWorks United Kingdom*. Available at: https://uk.mathworks.com/help/ident/ref/idinput.html#bvkyq33 (Accessed: 26 December 2018).

May, R., Dandy, G. and Maier, H. (2011) 'Review of Input Variable Selection Methods for Artificial Neural Networks', *Artificial Neural Networks -*

Methodological Advances and Biomedical Applications, pp. 19–44.

McKay, M. D., Beckman, R. J. and Conover, W. J. (1979) ‘Comparison of Three Methods for Selecting Values of Input Variables in the Analysis of Output from a Computer Code’, *Technometrics*. Taylor & Francis, 21(2), pp. 239–245. doi: 10.1080/00401706.1979.10489755.

Mohammad Reza Rafimanzelat and Seyed Hossein Iranmanesh (2012) ‘Application of ANFIS and LLNF Models to Automobile Fuel Consumption Prediction: A Comparative Study’, in *International Conference on Information Science, Signal Processing and their Applications (ISSPA)*. IEEE, pp. 734–739. doi: 10.1109/ISSPA.2012.6310650.

Mohile, S. S. (2017) ‘BS VI: Challenges and opportunities for India’s auto industry’, *livemint*, August. Available at: https://www.livemint.com/ (Accessed: 23 May 2019).

Montgomery, D. C., Peck, E. A. and Vining, G. G. (2001) *Introduction to Linear Regression Analysis*. Wiley-Blackwell.

Morris, M. D. and Mitchell, T. J. (1995) ‘Exploratory designs for computational experiments’, *Journal of Statistical Planning and Inference*. North-Holland, 43(3), pp. 381–402. doi: 10.1016/0378-3758(94)00035-T.

Morton, T. M. and Knott, S. (2002) ‘Radial Basis Functions for Engine Modelling’, in *Statistics & Analytical Methods in Automotive Engineering*. Professional Engineering Publishing Ltd, pp. 43–51.

Murray-Smith, R. (1994) *A Local Model Network Approach to Nonlinear*

Modelling. PhD Thesis, University of Strathclyde.

Murray-Smith, R. and Hunt, K. J. (1995) 'Local model architectures for nonlinear modelling and control', *Neural Network Engineering in Dynamic Control Systems*, (1), pp. 61–82.

Myers, R. H., Khuri, A. I. and Carter, W. H. (1989) 'Response Surface Methodology', *Technometrics*. Taylor & Francis, 31(2), pp. 137–157. doi: 10.1080/00401706.1989.10488509.

Narayanan, A., Toropov, V. V., Wood, A. S. and Campean, I. F. (2007) 'Simultaneous model building and validation with uniform designs of experiments', *Engineering Optimization*, 39(5), pp. 497–512. doi: 10.1080/03052150701399978.

Nelles, O. (2001) *Nonlinear System Identification: From Classical Approaches to Neural Networks and Fuzzy Models*. 1st edn. New York: Springer-Verlag Berlin Heidelberg. doi: 10.1007/978-3-662-04323-3.

Nelles, O. (2006) 'Axes-oblique partitioning strategies for local model networks', *in Proc. Int. Symp. Intell. Control*, pp. 2378–2383. doi: 10.1109/ISIC.2006.285656.

Nelles, O., Fink, A. and Isermann, R. (2000) 'Local Linear Model Trees (LOLIMOT) Toolbox for Nonlinear System Identification', *IFAC Proceedings Volumes*, 33(15), pp. 845–850. doi: 10.1016/S1474-6670(17)39858-0.

Nelles, O., Sinsel, S. and Isermann, R. (1996) 'Local basis function networks for identification of a turbocharger', *In Proc. UKACC Int. Conf. Control*, 1(427),

pp. 7–12.

Neumeister, J., Taylor, J. and Gurney, D. (2007) ‘Virtual Air Path Calibration of a Multi Cylinder High Performance GDI Engine Using 1D Cycle Simulation’, in. doi: 10.4271/2007-01-0490.

Ngwaka, U. C., Diyoke, C. and Anosike, N. (2016) ‘Single Zone, Zero Dimensional Model of Diesel Multiple-Injection’, *Energy and Power Engineering*, 08(09), pp. 297–312. doi: 10.4236/epe.2016.89028.

Ostrowski, K., Shenton, A. T. and Neaves, B. (2017) ‘Experimental-based dynamic calibration of the diesel air-path’, *International Journal of Powertrains*, 6(2), p. 169. doi: 10.1504/IJPT.2017.085682.

Parry, O., Dizy, J., Page, V., Bhave, A. and Ooi, D. (2017) ‘Fast Response Surrogates and Sensitivity Analysis Based on Physico-Chemical Engine Simulation Applied to Modern Compression Ignition Engines’, in Röpke, K. and Gühmann, C. (eds) *Automotive Data Analytics, Methods, Design of Experiments (DoE) : Proceedings of the International Calibration Conference*. Berlin: Expert-Verlag GmbH, pp. 233–254. Available at: http://www.cmclinnovations.com/wp-content/uploads/2017-iav-paper.pdf.

Pedram, A., Jamali, M. and Pedram, T. (2008) ‘Local linear model tree (LOLIMOT) reconfigurable parallel hardware’, *Transactions on Engineering, Computing and Technology*, 2(1), pp. 96–101.

Pezouvanis, A. (2009) *Engine modelling for virtual mapping*. PhD Thesis, University of Bradford.

Pintelon, R. and Schoukens, J. (2012) *System Identification: A Frequency Domain Approach*. 2nd edn. Wiley-IEEE Press.

Provost, F., Jensen, D. and Oates, T. (1999) 'Efficient progressive sampling', *Proceedings of the fifth ACM SIGKDD international conference on Knowledge discovery and data mining - KDD '99*, pp. 23–32. doi: 10.1145/312129.312188.

Pucar, P. and Millnert, M. (1995) *Smooth Hinging Hyperplanes - An Alternative to Neural Nets*, *LiTH-ISY-R NV - 1750*. Automatic Control, Department of Electrical Engineering, Linköping University: Linköping University. Available at: http://liu.diva-portal.org/smash/get/diva2:315877/FULLTEXT01.ps.

Rafajłowicz, E. and Schwabe, R. (2006) 'Halton and Hammersley sequences in multivariate nonparametric regression', *Statistics & Probability Letters*, 76(8), pp. 803–812. doi: https://doi.org/10.1016/j.spl.2005.10.014.

Rango, J., Schnorbus, T., Kwee, H., R.Beck, Kinoo, B., Arthozoul, S. and Zhang, M. (2013) 'Comparison of Different Approaches for Global Modelling of Combustion Engines', in Röpke, K. (ed.) *Design of Experiments (DOE) in Engine Development*. Expert Verlag, pp. 70–91.

Reed, R. (1993) 'Pruning algorithms-a survey', *IEEE Transactions on Neural Networks*, 4(5), pp. 740–747. doi: 10.1109/72.248452.

Rehrl, J., Schwingshackl, D. and Horn, M. (2014) 'A Modeling Approach for HVAC Systems based on the LoLiMoT Algorithm', *IFAC Proceedings*

Volumes. Elsevier, 47(3), pp. 10862–10868. doi: 10.3182/20140824-6-ZA-1003.01228.

Ricardo Plc (no date) *Wave [Computer Software]*. Available at: https://software.ricardo.com/products/wave.

Röpke, K. (2009) *Design of Experiments in Engine Development*. Expert Verlag.

Röpke, K. (2014) 'Design of Experiments for Engine Calibration', *Journal of The Society of Instrument and Control Engineers*, 53(4), pp. 322–327. doi: 10.11499/sicejl.53.322.

Röpke, K., Baumann, W., Köhler, B.-U., Schaum, S., Lange, R. and Knaak, M. (2012) 'Engine Calibration Using Nonlinear Dynamic Modeling', in *Lecture Notes in Control and Information Sciences*, pp. 165–182. doi: 10.1007/978-1-4471-2221-0_10.

Roselló, M. D., Serrano, J. R., Margot, X. and Arnau, J. M. (2002) 'Analytic-numerical approach to flow calculation in intake and exhaust systems of internal combustion engines', *Mathematical and Computer Modelling*. Pergamon, 36(1–2), pp. 33–45. doi: 10.1016/S0895-7177(02)00102-4.

Sacks, J., Welch, W. J., Mitchell, T. J. and Wynn, H. P. (1989) 'Design and Analysis of Computer Experiments', *Statistical Science*, 4(4), pp. 409–435.

Sakushima, N., Baumann, W., Röpke, K. and Knaak, M. (2013) 'Transient Modeling of Diesel Engine Emissions', *International Journal of Automotive Engineering*, 4(3), pp. 63–68. doi: 10.20485/jsaeijae.4.3_63.

Sasena, M. J., Papalambros, P. Y. and Goovaerts, P. (2000) ‘Metamodeling sampling criteria in a global optimization framework’, *American Institute of Aeronautics & Astronautics*. Available at: http://hdl.handle.net/2027.42/76903.

Sasena, M., Parkinson, M., Goovaerts, P., Papalambros, P. and Reed, M. (2002) ‘Adaptive experimental design applied to an ergonomics testing’, *Proceedings of the ASME Design Engineering Technical Conferences*. doi: 10.1115/DETC2002/DAC-34091.

Saunders, R. (2004) *Investigation into a Validation Methodology for Non-Parametric Models for Engine Mapping*. MSc Thesis, University of Bradford.

Schaffnit, J., Nelles, O., Isermann, R. and Schmid, W. (2000) ‘Local Linear Model Tree (LOLIMOT) for Nonlinear System Identification of a Turbocharger with Variable Turbine Geometry (VTG)’, *IFAC Proceedings Volumes*. Elsevier, 33(15), pp. 615–620. doi: 10.1016/S1474-6670(17)39819-1.

Schlosser, A., Kinoo, B., Salber, W., Werner, S. and Ademes, N. (2006) ‘Accelerated Powertrain Development Through Model Based Calibration’, in *SAE 2006 World Congress & Exhibition*. SAE International. doi: https://doi.org/10.4271/2006-01-0858.

Schmiechen, P., Baumann, W. and Konstanz, R. (2013) ‘Identification of a data-driven dynamic model from virtual test bench results: an extended Hammerstein approach’, *IFAC Proceedings Volumes*. Elsevier, 46(21), pp. 786–788. doi: 10.3182/20130904-4-JP-2042.00052.

Schögl, O., Schmidt, S., Abart, M., Kirchberger, R., Fitl, M. and Gschwantner,

P. (2009) ‘Early stage development of a 4-stroke gas exchange process by the use of a coupled 1D / 3D simulation strategy’, in *Small Engine Technology Conference & Exposition*. Society of Automotive Engineers of Japan.

Seabrook, J., Collins, J. and Edwards, S. (2005) ‘Application of Advanced Modelling techniques to the calibration of Gasoline Engines with Direct Injection and variable Valve Timing’, in Röpke, K. (ed.) *Design of Experiments (DoE) in Engine Development*. Berlin: Expert Verlag, pp. 235–245.

Seabrook, J., Salamon, T., Edwards, S. and Noell, I. (2003) ‘A comparison of Neural Networks, Stochastic Process Methods and Radial Basis Function for the Optimization of Engine Control Parameters’, in *Design of Experiments in Engine Development*.

Sequenz, H. (2013) *Emission Modelling and Model-Based Optimisation of the Engine Control*. Düsseldorf: VDI Verlag (VDI Fortschrittsberichte). Available at: http://tuprints.ulb.tu-darmstadt.de/3948/.

Sequenz, H. and Isermann, R. (2011) ‘Emission Model Structures for an Implementation on Engine Control Units’, *IFAC Proceedings Volumes*. Elsevier, 44(1), pp. 11851–11856. doi: 10.3182/20110828-6-IT-1002.03131.

Serikov, S. A. (2010) ‘Neural network model of internal combustion engine’, *Cybernetics and Systems Analysis*, 46(6), pp. 998–1007. doi: 10.1007/s10559-010-9281-3.

Siemens (2012) *Siemens helps Detroit-based manufacturer of diesel engines reduce energy costs and slash CO2 emissions*. Detroit. Available at:

www.usa.siemens.com/motioncontrol (Accessed: 23 May 2019).

Simpson, T., Allen, J. and Mistree, F. (1998) 'Spatial correlation metamodels for global approximation in structural design optimization', *Proceedings of ASME 1998 Design Engineering Technical Conferences*, (January). Available at: http://citeseerx.ist.psu.edu/viewdoc/download?doi=10.1.1.455.2810&rep=rep1&type=pdf.

Simpson, T. W., Peplinski, J. D., Koch, P. N. and Allen, J. K. (2001) 'Metamodels for computer-based engineering design: Survey and recommendations', *Engineering with Computers*, 17(2), pp. 129–150. doi: 10.1007/PL00007198.

Singh, R., Campean, F., Seale, B., Grove, D. and Cary, M. (2007) 'Evaluation of Camshaft Control Strategies using a Multi-Evolutionary Genetic Algorithm', *Design of Experiments in Engine Development*, pp. 165–183.

Sjöberg, J., Zhang, Q., Ljung, L., *et al.* (1995) 'Nonlinear black-box modeling in system identification: a unified overview', *Automatica*. Pergamon, 31(12), pp. 1691–1724. doi: 10.1016/0005-1098(95)00120-8.

Skogtjarn, P. (2002) *Modelling of the Exhaust Gas Temperature for Diesel Engines*, *PhD Thesis*. Linkopings universitet.

Smallbone, A., Bhave, A., Coble, A. R., Mosbach, S., Kraft, M. and McDavid, R. (2011) 'Identifying Optimal Operating Points in Terms of Engineering Constraints and Regulated Emissions in Modern Diesel Engines', in *SAE 2011*

World Congress & Exhibition. SAE International. doi: https://doi.org/10.4271/2011-01-1388.

Smallbone, A. and Coble, A. (2011) 'A "Physics-Based" Combustion and Emissions Tool for Transient Simulations', in Sens, M. and Wiedemann, B. (eds) *Motorprozesssimulation und Aufladung, III: Engine Process Simulation and Supercharging*. Expert-Verlag GmbH, pp. 17–24. Available at: https://www.expertverlag.de/index.php?i=3073&m=expert+service&p=service-i.

Steidten, T., Adomeit, P., Kircher, B. and Wedowski, S. (2005) 'Automated Gas Exchange Model Calibration Using an Online Optimizer Tool', *in Design of Experiments in Engine Development*, pp. 184–200.

Stinstra, E., Stehouwer, P., Den Hertog, D. and Vestjens, A. (2003) 'Constrained maximin designs for computer experiments', *Technometrics*, 45(4), pp. 340–346. doi: 10.1198/004017003000000168.

Takagi, T. and Sugeno, M. (1985) 'Fuzzy identification of systems and its applications to modeling and control', *IEEE Transactions on Systems, Man, and Cybernetics*, SMC-15(1), pp. 116–132. doi: 10.1109/TSMC.1985.6313399.

Tan, A. H. and Godfrey, K. R. (2002) 'The generation of binary and near-binary pseudorandom signals: an overview', *IEEE Trans. Instrumentation and Measurement*, 51, pp. 583–588.

The Mathworks Inc. (2018) *Model-Based Calibration Toolbox - MATLAB*.

Available at: https://uk.mathworks.com/products/mbc.html (Accessed: 3 October 2018).

Themi, V. (2016) *Multi-Physics Co-Simulation of Engine Combustion and Exhaust Aftertreatment System*. PhD Thesis, University of Bradford.

Tietze, N. (2015) *Model-based Calibration of Engine Control Units Using Gaussian Process Regression*. PhD Thesis, Technischen Universität Darmstadt.

Tietze, N., Konigorski, U., Fleck, C. and Nguyen-Tuong, D. (2014) 'Model-based calibration of engine controller using automated transient design of experiment', in Bargende, M., Reuss, H.-C., and Wiedemann, J. (eds) *14. Internationales Stuttgarter Symposium*. Wiesbaden: Springer Fachmedien Wiesbaden, pp. 1587–1605.

Toropov, V. V, Schramm, U., Sahai, A., Jones, R. D. and Zeguer, T. (2005) 'Design Optimization and Stochastic Analysis based on the Moving Least Squares Method', *6th World Congresses of Structural and Multidisciplinary Optimization Design Optimization and Stochastic Analysis based on the Moving Least Squares Method*, (June).

Turkson, R. F., Yan, F., Ali, M. K. A. and Hu, J. (2016) 'Artificial neural network applications in the calibration of spark-ignition engines: An overview', *Engineering Science and Technology, an International Journal*, 19(3), pp. 1346–1359. doi: https://doi.org/10.1016/j.jestch.2016.03.003.

Unver, B., Koyuncuoglu, Y., Gokasan, M. and Bogosyan, S. (2016) 'Modeling

and validation of turbocharged diesel engine airpath and combustion systems', *International Journal of Automotive Technology*. The Korean Society of Automotive Engineers, 17(1), pp. 13–34. doi: 10.1007/s12239-016-0002-4.

Van-Dam, E. R., Husslage, B., den Hertog, D. and Melissen, H. (2007) 'Maximin Latin Hypercube Designs in Two Dimensions', *Operations Research*, 55(1), pp. 158–169. doi: 10.1287/opre.1060.0317.

Verhelst, S. and Sheppard, C. G. W. (2009) 'Multi-zone thermodynamic modelling of spark-ignition engine combustion - An overview', *Energy Conversion and Management*, 50(5), pp. 1326–1335. doi: 10.1016/j.enconman.2009.01.002.

Wahlström, J. and Eriksson, L. (2011) 'Modelling diesel engines with a variable-geometry turbocharger and exhaust gas recirculation by optimization of model parameters for capturing non-linear system dynamics', *Proceedings of the Institution of Mechanical Engineers, Part D: Journal of Automobile Engineering*.IMECHE,225(7),pp. 960–986. doi: 10.1177/0954407011398177.

Wellstead, P. E., Thiruarooran, C. and Winterbone, D. E. (1978) 'Identification of a Turbo-Charged Diesel Engine', *IFAC Proceedings Volumes*. Elsevier, 11(1), pp. 361–367. doi: 10.1016/S1474-6670(17)65963-9.

Winterbone, D. E. and Yoshitomi, M. (1990) 'The Accuracy of Calculating Wave Action in Engine Intake Manifolds', in *SAE Technical Paper 900677*. doi: 10.4271/900677.

Wu, H., Wang, X., Winsor, R. and Baumgard, K. (2011) ‘Mean Value Engine Modeling for a Diesel Engine with GT-Power 1D Detail Model’, in *SAE Technical Paper 2011-01-1294*. doi: 10.4271/2011-01-1294.

Xu, K., Xie, M., Tang, L. C. and Ho, S. L. (2003) ‘Application of neural networks in forecasting engine systems reliability’, *Applied Soft Computing*, 2(4), pp. 255–268. doi: https://doi.org/10.1016/S1568-4946(02)00059-5.

Yates, F. (1964) ‘Sir Ronald Fisher and the Design of Experiments’, *International Biometric Society*, 20(2), pp. 307–321. doi: doi:10.2307/2528399.

Ye, K. Q., Li, W. and Sudjianto, A. (2000) ‘Algorithmic construction of optimal symmetric Latin hypercube designs’, *Journal of Statistical Planning and Inference*, 90(1), pp. 145–159. doi: 10.1016/S0378-3758(00)00105-1.

Yin, X. F. (2012) *Application of Multidisciplinary Design Optimisation to Engine Calibration Optimisation*. University of Bradford.

Zheng, J. and Caton, J. A. (2012) ‘Use of a single-zone thermodynamic model with detailed chemistry to study a natural gas fueled homogeneous charge compression ignition engine’, *Energy Conversion and Management*. Pergamon, 53(1), pp. 298–304. doi: 10.1016/J.ENCONMAN.2011.09.005.

Appendices

A.1 Fast Fourier Transformation

```
clc
clearvars
filename = uigetfile;
load(filename)
Fs = 100; %Sampling Frequency
L = length(filename); % Number of Samples

% Assigning label to the data coloumns
Label = {'Torque'; 'Speed'; 'MAF'; 'EGR'; 'Temperature';...
    'Pressure'; 'InjCtl'};

for i = 2:8
    Y = fft(Data11(:,i)-mean(Data11(:,i)));
    P2 = abs(Y/L);
    P1 = P2(1:L/2+1);
    P1(2:end-1) = 2*P1(2:end-1);
    f = Fs*(0:(L/2))/L;

    figure
    plot(f,P1)
    title(Label(i-1))
    xlabel('f (Hz)')
    ylabel('|P1(f)|')
end
%
% Same as above, repreated for second data set
filename = uigetfile;
load(filename)
L = length(filename);

Labe2 = {'Torque-2'; 'Speed-2'; 'MAF-2'; 'EGR-2'; 'Temperature-2';...
    'Pressure-2'; 'InjCtl-2'};


for i = 2:8
    Y = fft(Data12(:,i)-mean(Data12(:,i)));
    P2 = abs(Y/L);
    P1 = P2(1:L/2+1);
    P1(2:end-1) = 2*P1(2:end-1);
    f = Fs*(0:(L/2))/L;

    figure
    plot(f,P1)
    title(Labe2(i-1))
    xlabel('f (Hz)')
    ylabel('|P1(f)|')
end
```

Published with MATLAB® R2018a

A.2 Excitation Signal Design: Pseudo Random Binary Sequence

```
clear all
close all
clc

%%Speed

sd = randi(1e3);
seq = ltePRBS(sd,60);

time1 = 0:10:length(seq)*10-10;

time = 0:1/100:60000/100-1/100;
speed = zeros(size(time));
for i = 1:length(time)
    speed(i) = seq(find(time1<=time(i),1,'last'));
end
speed = (speed*250)+1500;

figure
plot(time,speed)

%%Torque

sd = randi(1e3);
seq = ltePRBS(sd,60);

time1 = 0:10:length(seq)*10-10;

time = 0:1/100:60000/100-1/100;
torque = zeros(size(time));
for i = 1:length(time)
   torque(i) = seq(find(time1<=time(i),1,'last'));
end
torque = (torque*(180.6-2*20))+20;

figure
plot(time,torque)

%%MAF

sd = randi(1e3);
seq = ltePRBS(sd,60);

time1 = 0:10:length(seq)*10-10;

time = 0:1/100:60000/100-1/100;
MAF = zeros(size(time));
for i = 1:length(time)
   MAF(i) = seq(find(time1<=time(i),1,'last'));
end
MAF = (MAF*20)-10;
figure
plot(time,MAF)

%%Preparing data for simulation
Cycle_dataPRBS = [time', speed', torque', MAF'];)
```

Published with MATLAB® R2018a

A.3 Excitation Signal Design: Amplitude Modulated Pseudo Random Binary Sequence (APRBS)

```
clear all
close all
clc

%%Speed

Range = [1,2];
Band = [1/25 1/1000]; % Excitation Frequency
speed = idinput([15000,1,4],'prbs',Band,Range); %Generating random dataset

% Locating the step changes
in1 = find(diff(speed)>0);
in2 = [0; find(diff(speed)<0); length(speed)];

% Scaling Signal to the required amplitude
for i = 1:length(in1)
    amp = rand;
    speed(in2(i)+1:in1(i)) = amp*speed(in2(i)+1:in1(i));

    amp = rand;
    speed(in1(i)+1:in2(i+1)) = amp*speed(in1(i)+1:in2(i+1));
end

speed = (speed-min(speed));
speed = (speed*250)/max(speed)+1500;

time = 0:1/100:length(speed)/100-1/100;

figure
plot(time,speed)

%%Torque

Range = [1,2];
Band = [1/25 1/1000]; %Excitation Frequency
torque = idinput([15000,1,4],'prbs',Band,Range);

% Locating the step changes
in1 = find(diff(torque)>0);
in2 = [0; find(diff(torque)<0); length(torque)];

% Scaling Signal to the required amplitude
for i = 1:length(in1)
    amp = rand;
    torque(in2(i)+1:in1(i)) = amp*torque(in2(i)+1:in1(i));

    amp = rand;
    torque(in1(i)+1:in2(i+1)) = amp*torque(in1(i)+1:in2(i+1));
end

torque = (torque-min(torque));
torque = (torque*(180.6-2*20))/max(torque)+20;

figure
plot(time,torque)

%%MAF

Range = [1,2];
Band = [1/25 1/1600]; %Excitation Frequency
MAF = idinput([24000,1,4],'prbs',Band,Range);

MAF = MAF(1:length(time));

% Locating the step changes
```

```
in1 = find(diff(MAF)>0);
in2 = [0; find(diff(MAF)<0); length(MAF)];

% Scaling Signal to the required amplitude
for i = 1:length(in1)
    amp = rand;
    MAF(in2(i)+1:in1(i)) = amp*MAF(in2(i)+1:in1(i));

    amp = rand;
    MAF(in1(i)+1:in2(i+1)) = amp*MAF(in1(i)+1:in2(i+1));
end

MAF = (MAF-min(MAF));
MAF = (MAF*20)/max(MAF)-10;

figure
plot(time,MAF)

%%Preparing data for simulation
Cycle_dataAPRBS = [time', speed, torque, MAF];
figure; scatter(speed,torque)
```

Published with MATLAB® R2018a

A.4 Excitation Signal Design: Chirp

```
clearvars
close all
clc
%%Speed
hchirp = dsp.Chirp( ...
    'InitialFrequency', 0.003,...
    'TargetFrequency', 0.1, ...
    'TargetTime', 150, ...
    'SweepTime', 1000, ...
    'SampleRate', 100, ...
    'SamplesPerFrame', 15000);

chirpData = (step(hchirp))';

speed = [chirpData chirpData(end:-1:1)];
speed = [speed speed(end:-1:1)];
speed = (-speed + 1)*250/2+1500;

time = 0:1/100:600-1/100;
% Plot the chirp signal
figure
plot(time,speed);

%%Torque
hchirp = dsp.Chirp( ...
    'InitialFrequency', 0.1,...
    'TargetFrequency', 0.01, ...
    'TargetTime', 75, ...
    'SweepTime', 500, ...
    'SampleRate', 100, ...
    'SamplesPerFrame', 7500);

chirpData = (step(hchirp))';

torque = [chirpData chirpData(end:-1:1)];
torque = [torque torque(end:-1:1)];
torque = [torque torque(end:-1:1)];
torque = (-torque + 1)*(180.6-2*20)/2+20;

% Plot the chirp signal
figure
plot(time,torque);

%%MAF
hchirp = dsp.Chirp( ...
    'InitialFrequency', 0.06,...
    'TargetFrequency', 0.001, ...
    'TargetTime', 75, ...
    'SweepTime', 500, ...
    'SampleRate', 100, ...
    'SamplesPerFrame', 7500);

chirpData = (step(hchirp))';

MAF = [chirpData chirpData(end:-1:1)];
MAF = [MAF MAF(end:-1:1)];
MAF = [MAF MAF(end:-1:1)];
MAF = MAF*10;

% Plot the chirp signal
figure
plot(time,MAF);

%%Prepare data for simulation
Cycle_dataChirp = [time', speed', torque', MAF'];
```

Published with MATLAB® R2018a

A.5 LOLIMOT Training Algorithm

– Script to select which training signal model to run.

```
%   Available Neural Network Modelling Process:
%       Model 1: APRBS Training Signal Model.
%       Model 2: PRBS Training Signal Model.
%       Model 3: Chirp Training Signal Model.

clear;
clearvars;
close all;
clc

% Menu
i = menu('Choose one of the following examples:',...
    '1. APRBS Training Signal Model', ...
    '2. PRBS Training Signal Model', ...
    '3. Chirp Training Signal Model');


% Add Neural Network Model examples directory to MATLAB search path
LMNDirectory = fileparts(which(mfilename));
LMNmodelsDirectory = [LMNDirectory '/LMN'];
addpath(LMNDirectory);
addpath(LMNmodelsDirectory);

% Execute demo program
if i == 1
    LMNAPRBS
elseif i == 2
   LMNPRBS
elseif i == 3
    LMNChirp
end

% Clear variables
clear i LMNDirectory LMNmodelsDirectory
```

– Generic Script compiled to show training algorithm for all excitation training signals

```
% This script serves as an example of generating
% Local Linear Neuro Fuzzy Model using Lolimot algorithm.
% In here a generic form of script for EGR Lolimot Model is presented.     %
The script can be modified to system of interest.
% This script is generated using the toolbox (Hartmann et al., 2012)

%   LoLiMoT - Nonlinear System Identification Toolbox
%   Torsten Fischer, 17-February-2012
%   Institute of Mechanics & Automatic Control, University of Siegen,
%   Germany
%   Copyright (c) 2012 by Prof. Dr.-Ing. Oliver Nelles
```

Pre-Start

```
clearvars;
close all
```

```
clc
tic
```

Training Data

```
LMN = lolimot;          % initialize lolimot object

filename=uigetfile;
load(filename);
%load('PRBS_Processed_Data.mat')
%load('APRBS_Processed_Data.mat')
%load('Chirp_Processed_Data.mat')

% Assign the training Data
LMN.input = APRBS_Inputs(:,2:4);
LMN.output = EGR_mf;

% % Assign the training Data
% LMN.input = PRBS_Inputs(:,2:4);
% LMN.output = EGR_mf;

% % Assign the training Data
% LMN.input = Chirp_Inputs(:,2:4);
% LMN.output = EGR_mf;
```

Validation Data

```
% Validation PRBS Signal_P1
filename=uigetfile;
load(filename);
load('Val_PRBS_data.mat')

%Assigning Validation Data
LMN.validationInput = Val_PRBS_Inputs(:,1:3);
LMN.validationOutput = Val_PRBS_Inputs(:,5);

% Validation APRBS Signal_A1
filename=uigetfile;
load(filename);
load('Val_APRBS_data.mat')

%Assigning Validation Data
LMN.validationInput = Val_APRBS_Inputs(:,1:3);
LMN.validationOutput = Val_APRBS_Inputs(:,5);

%Validation Chirp Signal_C1
filename=uigetfile;
load(filename);
load('Val_Chirp_data.mat')

%Assigning Testing Data
LMN.testInput = Val_Chirp_Inputs(:,1:3);
LMN.testOutput = Val_Chirp_Inputs(:,5);
```

Internal Parameters of the Modelling (Hyper Parameters)

```
% Se feedback  delays
LMN.xInputDelay = cell(3,1); LMN.xOutputDelay = cell(1,1);
LMN.zInputDelay = cell(3,1); LMN.zOutputDelay = cell(1,1);
LMN.xInputDelay{1} = [1 2]; LMN.xInputDelay{2} = [1:3]; LMN.xInputDelay{3} =
[1:3];
LMN.xOutputDelay{1} = [1 2];
LMN.zInputDelay{1} = [1 2]; LMN.zInputDelay{2} = [1:3]; LMN.zInputDelay{3} =
[1:3];
LMN.zOutputDelay{1} = [1:2];
```

Options for training

```
% Option to adjust the transition steepness of the validity functions
LMN.smoothness = 1;

% Termination criterion for maximal number of LLMs
LMN.maxNumberOfLM = 50;
```

```
%  Termination criterion for minimal error
LMN.minError = 1.0e-7;

% Defines min perfomance improvement before assigning new split
LMN.minPerformanceImprovement = 1e-3;

% Simulation not one-step-ahead prediction
LMN.kStepPrediction = inf;  % one step ahead predcition k = 1; simulation k
=inf

% display information
LMN.history.displayMode = true;

%  Split direction is optimized - axes oblique splits are possible
LMN.oblique = true;   % (default: true)

% Determines if the analytical gradient is used or not

LMN.GradObj = true;
```

Initiate Training of the Local Model Network

```
 LMN = LMN.train; % trains the network based on the hyperparameters defined
                                    %above
```

Generalisation

```
load('Val_APRBS_Processed_Data.mat')

yGModel = calculateModelOutput(LMN, Val_APRBS_Inputs(:,1:3),...
    Val_APRBS_Inputs(:,4));

JG = calcGlobalLossFunction(LMN, Val_APRBS_Inputs(:,4), yGModel)
```

Visualization

```
% Model Plot
figure
LMN.plotModel

% Validation_ P1
figure
plot(calculateModelOutput(LMN, Val_PRBS_Inputs(:,1:3),...
    Val_PRBS_Inputs(3,5)*ones(size(Val_PRBS_Inputs(:,5)))))
hold on
plot(Val_PRBS_Inputs(3:end,5))

% Validation_ A1
figure
plot(calculateModelOutput(LMN, Val_APRBS_Inputs(:,1:3),...
    Val_APRBS_Inputs(3,5)*ones(size(Val_APRBS_Inputs(:,5)))))
hold on
plot(Val_APRBS_Inputs(3:end,5))

% Validation_ C1
figure
plot(calculateModelOutput(LMN, Val_Chirp_Inputs(:,1:3),...
    Val_Chirp_Inputs(3,5)*ones(size(Val_APRBS_Inputs(:,5)))))
hold on
plot(Val_Chirp_Inputs(3:end,5))
```

Miscellaneous Operations

```
[outputModel] = calcYhat(LMN.xRegressor,LMN.MSFValue,LMN.MSFValue);

Simulation_check = simulateParallel(LMN,Val_APRBS(:,1:3),Val_APRBS(1,4)...
    *ones(size(Val_APRBS(:,4))),LMN.localModels,LMN.leafModels);
toc
```

Published with MATLAB® R2018

A.6 Neural Network Training Algorithm

Script to select which training signal model to run.

```
%   Available Neural Network Modelling Process:
%       Model 1: APRBS Training Signal Model.
%       Model 2: PRBS Training Signal Model.
%       Model 3: Chirp Training Signal Model.


clear;
clearvars;
close all;
clc

% Menu
i = menu('Choose one of the following examples:',...
    '1. APRBS Training Signal Model', ...
    '2. PRBS Training Signal Model', ...
    '3. Chirp Training Signal Model');


% Add Neural Network Model examples directory to MATLAB search path
NNDirectory = fileparts(which(mfilename));
NNmodelsDirectory = [NNDirectory '/NeuralNetwork'];
addpath(NNDirectory);
addpath(NNmodelsDirectory);

% Execute demo program
if i == 1
    NNAPRBS
elseif i == 2
   NNPRBS
elseif i == 3
    NNChirp
end


% Clear variables
clear i NNDirectory NNmodelsDirectory
```

Published with MATLAB® R2018a

Generic Script compiled to show training algorithm for all training signals.

```
clc
clearvars;

%Recording time start
tic
```

Check Directory available for saving network, if not create one

```
% %For APRBS
% if isdir('network_APRB')==0
%     mkdir('network_APRB');
% end
% if ~isempty(gcp('nocreate'))
%  delete(gcp)
```

```
% end

% % For PRBS
% if isdir('network_PRB')==0
%     mkdir('network_PRB');
% end
% if ~isempty(gcp('nocreate'))
%  delete(gcp)
% end

% For Chirp
if isdir('network_Chirp')==0
    mkdir('network_Chirp');
end
if ~isempty(gcp('nocreate'))
 delete(gcp)
end
```

Load Necessary Data files

```
load('NN_data.mat')

%%Define Inputs and Outputs
%Choose the training signal for which you need to create the network

% %FOR APRBS Signals
% X = tonndata(APRBS_Inputs (:,1:3),false,false);
% T = tonndata(EGR_A,false,false);

% %For PRBS Signals
% X = tonndata(PRBS_Inputs (:,1:3),false,false);
% T = tonndata(EGR_P,false,false);

%FOR CHIRP Signals
X = tonndata(Chirp_Inputs (:,1:3),false,false);
T = tonndata(EGR_C,false,false);
```

Choose Training Function

```
trainFCN = 'trainbr'; % Bayesian Regularisation backpropogation, as per
%                       %Matlab performs better than early stopping %
% trainFCN = 'trainlm'; % fast training algorithm

%
% trainFCN = 'trainscg'; % Scaled conjugate gradient backpropagation
```

Create a Nonlinear Autoregressive Network with External Input

```
for k = 1:25
    inputDelays = 1:3;
    feedbackDelays = 1:2;
    hiddenLayerSize = k;
    net = narxnet(inputDelays,feedbackDelays,hiddenLayerSize,...
        'closed',trainFCN);

    %Input and Feedback Pre/Post-Processing Functions
    net.inputs{1}.processFcns =...
        {'removeconstantrows','mapminmax'}; % Customise Input Paramaters
    %net.inputs{2}.processFcns ={'removeconstantrows','mapminmax'};%
Customise Output Paramters

    %Prepare Data for Training and Simulation
    [x,xi,ai,t] = preparets(net,X,{},T);
```

```
    %Divide Data for Training/ cross-validation/ and test performance
    %(only if large data sample is available)
    net.divideFcn = 'divideblock'; % Divides data in block, training first,
                                   %followed by validation and at last test
    net.divideParam.trainRatio = 75/100; % Training data
    net.divideParam.valRatio = 15/100; % validation data fro cross val.
    net.divideParam.testRatio = 15/100;% separate data used after training

    %%Choose a performance function
    net.performFCN = 'mse'; % Mean Squared Error
    net.trainParam.epochs= 100;

    %%Choose Plot Functions
    net.plotFcns = {'plotperform','plottrainstate', 'ploterrhist', ...
        'plotregression', 'plotresponse', 'ploterrcorr', 'plotinerrcorr'};

    %Train the Network
    [net, tr] = train(net,x,t,xi,ai);

    %Test the Network
    y = net(x,xi,ai);
    e = gsubtract(t,y);
    performance(k) = perform(net,t,y);

    %Plots
    figure, plotperform(tr)
    figure, plottrainstate(tr)
    figure, ploterrhist(e)
    figure, plotregression(t,y)
    figure, plotresponse(t,y)
    figure, ploterrcorr(e)
    figure, plotinerrcorr(x,e)

    %Save network at every iteration
%     save(['network_APRB\net' num2str(k)],'net');%save the network
%     save(['network_PRB\net' num2str(k)],'net');%save the network
    save(['network_Chirp\net' num2str(k)],'net');%save the network
end
```

Save the Performance

```
% fid=fopen('mse_APRB_lm.txt', 'wt');
% fprintf(fid, 'Nh\t Performance\n');
% fprintf(fid, '%4.0f\t %f\n', [1:25;performance]);
% fclose all;

% fid=fopen('mse_PRB_lm.txt', 'wt');
% fprintf(fid, 'Nh\t Performance\n');
% fprintf(fid, '%4.0f\t %f\n', [1:25;performance]);
% fclose all;

fid=fopen('mse_Chirp_lm.txt', 'wt');
fprintf(fid, 'Nh\t Performance\n');
fprintf(fid, '%4.0f\t %f\n', [1:25;performance]);
fclose all;

%Plot the Perfomance
figure; hold on
plot(1:25, performance, 'b*-'); hold on;
legend('Training_Error'); xlabel('Number of hidden layer neurons');
ylabel('MSE');

toc
```

Published with MATLAB® R2018a